Clinical and Radiological Studies in PSP and Related Conditions

Submitted for the degree of

Doctor in Philosophy

LA Massey

Sara Koe PSP Research Centre

UCL Institute of Neurology

August 2013

I, Luke Aidan Massey, confirm that the work presented in this thesis is my own. Where information has been derived from other sources, I confirm that this has been indicated in the thesis.

Signed:

Date:

Table of Contents

Abstract

This thesis examines clinical and radiological aspects of Progressive Supranuclear Palsy (PSP) and related conditions.

- Significant milestones occur sooner in pathologically confirmed PSP than multiple system atrophy (MSA); older age of onset and shorter duration to first milestone are associated with worse prognosis in both; in PSP, the Richardson's syndrome phenotype and male gender and in MSA, early autonomic failure and the female gender are also predictive of poorer prognosis.
- Using objective measurements of bradykinesia we found progressive bradykinesia and hypokinesia in Parkinson's disease (PD) which correlates with disability and responds to levodopa but hypokinesia without decrement in PSP.
- Using conventional MRI 72.7% of PSP and 76.9% of MSA are correctly identified. The 'hummingbird sign' was highly specific for PSP, but sensitvity was 68.4%.
- A simple measurement of the midbrain < 9.35mm had 100% specificity for a pathological diagnosis of PSP. In a clinically diagnosed PSP 90.5% had a measurement of < 9.35mm.
- Using high field 9.4 Tesla MRI, the anatomy of the subthalamic nucleus is clearly defined when compared to histology in post mortem material. The anteromedial portion was hypointense in correlation with Perls stain and there was variability in the volume, shape and location of its borders. The nigrosomes within the substantia nigra were visibile as high intensity bands which correlated with calbindin poor zones on immunohistochemical stains. The volume and anatomy were preserved in PD but not PSP.
- Multimodal 3 Telsla MRI during life revealed distinct patterns of atrophy in PSP and MSA using voxel-based morphometry. Tract-based spatial statistics revealed abnormalities in the frontal and parieto-occipital white matter changes in PSP more than MSA. Midbrain atrophy and frontal white matter increased mean diffusivity were associated with increasing PSP rating scale score, and frontal white matter reduced fractional anisotropy with disease duration.

Author Roles

Chapter 2:

This study was jointly conceived, planned and the data collected with Dr Sean O'Sullivan. Dr O'Sullivan performed the statistical analysis.

Chapter 3:

This study was jointly conceived, planned, participants were recruited, pilot studies performed and the data collected including clinimetric scoring and video recording with Dr Helen Ling. Dr Helen Ling performed the statistical analysis with supervision from Professor Brian Day.

Chapter 4:

This study was conceived, planned, participants were recruited from the QSBB and data collected with input from Dr Dominic Paviour, Dr Caroline Micallef, Dr Rolf Jager and Professor Nick Fox. Philip England in Newcastle, and Adrienne Wallis from London were instrumental in locating many of the hard copy images. Statistical analysis was performed with input from a statistician, Dr. Costantinos Kallis.

Chapter 5:

This study was conceived, planned, participants were recruited from the QSBB and data were collected with input from Dr Dominic Paviour, Dr Caroline Micallef, Dr Rolf Jager and Professor Nick Fox. Statistical analysis was performed with input from a statistician, Dr. Costantinos Kallis.

Chapters 7&8:

This study was conceived and planned with Dr Mario Miranda and Professor Tarek Yousry. Participants were recruited from the QSBB and tissue blocks prepared by Professor Tamas Revesz and Dr Janice Holton. Dr Catherine Stand cut and stained the slides. Dr Harry Parkers and Dr. Po-Wah So helped to develop the protocol for imaging and performed the set up including manual shimming. Dr John Thornton and Professor Xavier Golay provided expert advice on imaging procotols and techniques and data processing/analysis.

Chapter 9:

This study was conceived and planned with input from Dr Enrico de Vita, Dr Chris Sinclair, Dr Mark White, Dr John Thornton, Dr Laura Mancini and Dr Rolf Jager. Patients were recruited from clinics at the National hospital for Neurology (Professor Andrew Lees, Professor Kailash Bhatia, Professor Christopher Matthias, Professor Claire Fowler, Dr Pras Korlipara, Dr Michael Lunn) and through adverts in the PSP (Europe) association and Sara Matheson Trust publications. Pilot studies and data analysis were devised with input from all of the above but particularly Dr Enrico Devita with regards to volumetric analysis including VBM and TBSS.

This thesis was performed under the supervision of Professor Andrew Lees (clinical neurology), Professor Tarek Yoursy (neuroradiology) and Professor Tamas Revesz (neuropathology).

Publications arising from the Thesis

Publications

Clinical outcomes of progressive supranuclear palsy and multiple system atrophy.
O'Sullivan SS, **Massey LA**, Williams DR, Silveira-Moriyama L, Kempster PA, Holton JL, Revesz T, Lees AJ.
Brain. 2008 May;131(Pt 5):1362-72

Hypokinesia without decrement distinguishes progressive supranuclear palsy from Parkinson's disease.
Ling H, **Massey LA**, Lees AJ, Brown P, Day BL.
Brain. 2012 Apr;135(Pt 4):1141-53

Conventional magnetic resonance imaging in confirmed progressive supranuclear palsy and multiple system atrophy.
Massey LA, Micallef C, Paviour DC, O'Sullivan SS, Ling H, Williams DR, Kallis C, Holton JL, Revesz T, Burn DJ, Yousry T, Lees AJ, Fox NC, Jäger HR.
Mov Disord. 2012 Dec;27(14):1754-62

The midbrain to pons ratio: a simple and specific MRI sign of progressive supranuclear palsy.
Massey LA, Jäger HR, Paviour DC, O'Sullivan SS, Ling H, Williams DR, Kallis C, Holton J, Revesz T, Burn DJ, Yousry T, Lees AJ, Fox NC, Micallef C.
Neurology. 2013 May 14;80(20):1856-61.

Targeting of the pedunculopontine nucleus by an MRI-guided approach: a cadaver study.
Zrinzo L, Zrinzo LV, **Massey LA**, Thornton J, Parkes HG, White M, Yousry TA, Strand C, Revesz T, Limousin P, Hariz MI, Holton JL.
J Neural Transm. 2011 Oct;118(10):1487-95

High resolution MR anatomy of the subthalamic nucleus: imaging at 9.4 T with histological validation.
Massey LA, Miranda MA, Zrinzo L, Al-Helli O, Parkes HG, Thornton JS, So PW, White MJ, Mancini L, Strand C, Holton JL, Hariz MI, Lees AJ, Revesz T, Yousry TA.
Neuroimage. 2012 Feb 1;59(3):2035-44.

Papers Submitted

White matter disease in Progressive Supranuclear Palsy and Multiple System Atrophy using TBSS at 3T.

LA Massey, E DeVita, JS Thornton, MJ White, CDJ Sinclair, AJ Lees, T Yousry & HR Jäger.

Papers in Preparation

Histologically validated nigral anatomy in controls and parkinsonism using spin echo MR Microscopy at 9.4T

LA Massey, MA Miranda, O Al-Helli, HG Parkes, J Thornton, P-W So, M White, L Mancini, C Strand, J Holton, AJ Lees, T Revesz & TA Yousry.

Reviews

Anatomy of the substantia nigra and subthalamic nucleus on MR imaging.

Massey LA, Yousry TA.

Neuroimaging Clin N Am. 2010 Feb;20(1):7-27.

Book Chapters

Chapter 46 Neurodegeneration: Cerebellum and Brainstem

Massey LA, Yousry TA.

Imaging of the Brain. Expert Radiology Series. Eds Naidich, Castillo, Cha and Smirniotopoulos. Elsevier. 2013

Imaging in CBS and CBD (in press)

Massey LA, O'Sullivan SS

Imaging in Neurodegenerative Disorders. Ed Saba. OUP (in press expected 2014)

List of Tables

Chapter 4

Chapter 5

Chapter 6

Chapter 7

Chapter 8

Chapter 9

List of Figures

Chapter 5

Chapter 6

Chapter 7

Chapter 8

Chapter 9

Abbreviations

3D MPRAGE	three dimensional magnetization prepared rapid acquisition gradient echo
A	Anterior
AC	Anterior commissure
AD	Axial diffusivity
AL	Ansa lenticularis
ANOVA	Analaysis of variance
CB	Calbindin immunohistochemistry
CBD	Corticobasal degeneration
CBS	Corticobasal syndrome
CC	Crus cerebri
CM	Centromedian nucleus of the thalamus
cMRI	conventional MRI
CV	Coefficient of variation
DARTEL	Diffeomorphic anatomical registration through exponential lie algebra
DTI	Diffusion tensor imaging
DTT	Dorsal tegmental tract
DWI	Diffusion weigthed imaging
F	Fornix
FA	Fractional anisotropy
FAB	Frontal assessment battery
FMT	Fornix-mammillothalamic tract
FNIRT	FSL's non linear registation tool
FOV	Field of view
FR	Fasciculus retroflexus
FSL	FMRIB software library
FSL-BET	FSL's brain extraction tool
FSL-FDT	FSL's diffusion toolbox
GE	Gradient echo
GM	grey matter
GP	Globus pallidus
GPi	Globus pallidus internal segment
H	H field of Forel

H1	H1 field of Forel
H2	H2 field of Forel
Hab	Habenular nucleus
HabC	Commissure of the habenular nucleus
HB sign	Hummingbird sign
HCB sign	Hot cross bun sign
Hyp	Hypothalamus
I	Inferior
IC	Internal capsule
III	Third ventricle
IML	Internal medullary lamina
LF	Lenticular fasciculus
LFB/CV	Luxol fast blue / cresyl violet
LGB	Lateral geniculate body
MB	Mammillary body
MCP	Middle cerebellar peduncle
MCP sign	Middle cerebellar peduncle sign
MD	Mean diffusivity
MGB	Medial geniculate body
MGF sign	Morning glory flower sign
ML	Medial lemniscus
MMSE	Minimental state examination
MSA	Multiple system atrophy
MSA-C	MSA with predominant cerebellar features
MSA-EAS	MSA with early autonomic symptoms
MSA-P	MSA with predominant parkinsonism
MTT	Mammillothalamic tract
NPV	Negative predictive value
OPCA	Olivopontocerebellar atrophy
OT	Optic tract
P	Posterior
PC	Posterior commissure
PD	Parkinson's disease
PD-OFF	PD off levodopa (overnight)
PD-ON	PD on levodopa
PPV	Positive predictive value

PSP	Progressive supranuclear palsy
PSP-P	PSP with parkinsonism phenotype
PSP-RS	PSP with Richardson's syndrome phenotype
PSPRS	PSP rating scale
PT	Pyramidal tract
Pulv	Pulvinar
Q	Pallidoreticular bundle Q of Sano
QSBB	Queen square brain bank for neurological disorders
RCTF	Rubro-cerebello-thalamic fascicles
RD	Radial diffusivity
RN	Red nucleus
S	Superior
SCP	Superior cerebellar peduncle
SE	Spin echo
SF	Subthalamic fasciculus
SN	Substantia nigra
SND	Striatonigral degeneration
SP	Substance P immunohistochemistry
SPM8	Statistical parametric mapping version 8
STN	Subthalamic nucleus
STT	Spinothalamic tract
SupC	Superior colliculus
T	Tesla
TBSS	Tract based spatial statistics
TE	Echo time
TF	Thalamic fasciculus
TFCE	Threshold free cluster enhancement
Th	Thalamus
TR	Repetition time
UMSARS	Unified MSA rating scale
UPDRS	Unified PD rating scale
VBM	Voxel-based morphometry
WM	White matter
ZI	Zona incerta

Chapter 1: Overview and Background of the thesis

A. Overview and Aims

The aim was to study clinical and radiological aspects in progressive supranuclear palsy (PSP) and related conditions.

This thesis has four sections.

1. In the first clinical section the natural history of PSP and multiple system atrophy (MSA) in pathologically confirmed disease are studied and bradykinesia as manifest in finger taps and micrographia in PSP and Parkinson's disease (PD) are studied objectively.

2. In the second section the accuracy of conventional MRI (cMRI) is studied in pathologically confirmed disease - both subjective assessment and the development of a simple linear measurement based on the pathological topography of disease.

3. In the third section the importance of anatomical accuracy using MRI is studied after a literature review focusing on the subthalamic nucleus (STN) and substantia nigra (SN) - key structures in PSP and PD in particular both from a pathological point of view, and also increasingly from a therapeutic standpoint given the development of deep brain stimulation (DBS) of the STN in PD.

4. In the fourth section high field multimodal MRI techniques are used to study the brain voxel-wise i.e. without a priori assumptions about the regions of the brain which are affected in PSP and MSA.

By way of background this introductory chapter describes the key clinical and pathological features of PSP and related conditions and diagnostic accuracy rates from clinicopathological series.

B. Background

1. Progressive Supranuclear Palsy

Progressive Supranuclear Palsy (PSP) is a primary tauopathy characterised by degeneration in the brainstem, basal ganglia and cerebellum and presenting clinically with a vertical supranuclear gaze palsy, pseudobulbar palsy, axial rigidity and dementia (Steele, Richardson et al. 1964). It is also referred to in the literature as Steele-Richardson-Olsewski syndrome (SROS) and SRO disease.

a) Epidemiology

Epidemiological studies give an estimated prevalence of 5.0 – 6.4 / 100 000 in the UK (Schrag, Ben-Shlomo et al. 1999; Nath, Ben-Shlomo et al. 2001).

b) Clinical presentation

Classically PSP presents in the seventh and eighth decades and no cases have been described below the age of 40. Disease duration is about six years from first symptom to death. It is equally present in men and women. The mean time to diagnosis is 4-5 years from symptom onset (Burn and Lees 2002). There are now known to be at least five well-defined clinical subtypes.

The classical PSP presentation has been referred to as 'Richardson's syndrome' (PSP-RS): these patients present with postural instability and early falls , dysarthria, a supranuclear downgaze palsy, hypokinesia which does not respond well to levodopa, and a dysexecutive syndrome with bradyphrenia, apathy, reduced verbal fluency, utilization or imitation behaviour and frontal release signs (Steele, Richardson et al. 1964; Litvan, Agid et al. 1996). Although not described until the Steele et al paper, Charles Dickens and Wilkie Collins may have been describing PSP when they wrote '*The Lazy Tour of Two Idle Apprentices*' and described meeting

> ".....A chilled, slow, earthy, fixed old man. A cadaverous man of measured speech. An old man who seemed as unable to wink, as if his eyelids had been nailed to his forehead. An old man whose eyes—two spots of fire—had no more motion that [sic] if

> they had been connected with the back of his skull by screws driven through it, and rivetted and bolted outside, among his grey hair."
>
> "He had come in and shut the door, and he now sat down. He did not bend himself to sit, as other people do, but seemed to sink bolt upright, as if in water, until the chair stopped him." (Larner 2002).

The gait is wide based, erect with a characteristic tendency to fall backwards. They may exhibit motor recklessness, the 'rocket sign' on standing up and sit 'en bloc'. Non-specific visual complaints including diplopia, difficulty reading, and photophobia are superceded by the development of a supranuclear gaze palsy with particular difficulty looking down which may be manifest as messy eating and the 'messy tie sign' (Steele, Richardson et al. 1964; Litvan, Agid et al. 1996; Burn and Lees 2002). The first eye sign may be reduced speed of vertical saccadic movements and there may be difficulties suppressing blinking to a bright light stimulus (Litvan, Agid et al. 1996). There is a severely reduced blink frequency and eyelid opening dyspraxia with associated overactivity of the frontalis muscle giving rise to the impression of a constantly surprised or worried expression. Symmetrical parkinsonism with axial rigidity, and bulbar features characteristed by a distinctive growling dysarthria and dysphagia with risk of aspiration pneumonia (Litvan, Agid et al. 1996; Williams and Lees 2009) and cognitive and behavioural features are seen early in the disease progression when compared to Parkinson's disease. The 'subcortical dementia' of PSP includes cognitive slowing (bradyphrenia), dysexecutive function as demonstrated in reduced verbal fluency, and in tests of initiation and set shifting, and impaired memory characterised by recall but not recognition deficits, grasping and utilization behaviour, perseveration, apathy and depression and irritability (Albert, Feldman et al. 1974; Magherini and Litvan 2005).

In the original description of PSP the authors felt that clinical confusion with PD would be unlikely. However, subsequently most neurologists now class PSP in the category of 'Parkinson's plus' syndromes due to prominent akinetic-rigid features, although response to levodopa is not usually as pronounced as in PD. Clinicopathological studies have revealed that there are other clinical presentations of PSP than the classical Richardson's syndrome (Williams and Lees 2009) and we now know that atypical presentations of PSP with a more striking levodopa-unresponsive bradykinetic-rigid syndrome (Morris, Gibb et al. 2002) or an asymmetric syndrome with a typical pill rolling tremor which is moderately responsive to

levodopa and difficult to distinguish from PD and multiple system atrophy with predominant parkinsonism (MSA-P), which is now termed PSP-Parkinsonism (PSP-P), are associated with PSP pathology at post mortem, with PSP-P accounting for around a third of pathologically confirmed cases (Morris, Gibb et al. 2002; Williams, de Silva et al. 2005). The absence of postural instability, cognitive impairment and eye movement abnormalities mean a diagnosis of PSP is difficult particularly early in the disease, however, visual hallucinations, drug-induced dyskinesias and autonomic dysfunction are very uncommon in PSP-P and support a diagnosis of PD (Williams and Lees 2010).

Pure akinesia with gait freezing (PSP-PAGF) is associated with PSP pathology in a clinicopathological study in 6/7 cases - the other case having Lewy bodies (Williams, Holton et al. 2007). These patients present with progressive gait akinesia with start hesitation and freezing of gait, speech or writing but without rigidity, tremor, cognitive impairment or eye movement abnormalities during the first five years although these may develop later in the disease course (Williams, Holton et al. 2007; Williams and Lees 2009). The disease course is longer with a mean duration of 11 years.

PSP presenting with a corticobasal syndrome (PSP-CBS) - with markedly asymmetric levodopa-unresponsive parkinsonism, dystonia, myoclonus, dyspraxia, cortical sensory loss and the alien limb phenomenon without early postural instability and falls, bulbar failure or axial rigidity - is a rarer presentation of PSP pathology (4% at the QSBB) and is difficult to distinguish from corticobasal degeneration (CBD) (Tsuboi, Josephs et al. 2005; Williams and Lees 2009; Ling, O'Sullivan et al. 2010). At post mortem the burden of pathology is different to PSP-RS with more tau in cortical and less in the basal ganglia in PSP-CBS (Ling, de Silva et al. 2013).

PSP can also present with progressive apraxia of speech evolving into progressive non-fluent aphasia with effortful, non-fluent, agrammatic speech with phonemic paraphasias (PSP-PNFA) (Josephs, Boeve et al. 2005)(Boeve, Dickson et al. 2003), late onset frontotemporal dementia (Rippon, Boeve et al. 2005), late onset cerebellar ataxia (PSP-C) (Kanazawa, Tada et al. 2013) or with a pyramidal presentation and a primary lateral sclerosis phenotype (Nagao, Yokota et al. 2012).

Imaging studies to date have included cases which fulfil criteria similar to the NINDS-SPSP criteria [Table 1.1] (Litvan, Agid et al. 1996) which identifies cases of PSP-RS with high

specificity but excludes these other subtypes which have subtle differences in pathological burden.

In addition to the variable clinical presentation of PSP, there is a differential diagnosis for patients presenting with a PSP syndrome including parkinsonism, postural instability and falls, and eye movement abnormalities. This includes the other neurodegenerative parkinsonian syndromes (PD, MSA and CBD), but also prion disease (Petrovic, Martin-Bastida et al. 2012) and dementia with Lewy bodies (Fearnley, Revesz et al. 1991; Josephs and Dickson 2003; Haug, Boyer et al. 2013). There is an association of atypical parkinsonism in Guadeloupe including a PSP-like syndrome with soursop consumption (Lannuzel, Hoglinger et al. 2007). A PSP phenotype has also been reported in vascular disease (Winikates and Jankovic 1994), infectious diseases (Whipple's disease (Amarenco, Roullet et al. 1991; Magherini, Pentore et al. 2007), HIV (Jang, Kim et al. 2012), Neurosyphilis (Murialdo, Marchese et al. 2000)), lead toxicity (Sanz, Nogue et al. 2007), as a paraneoplastic syndrome with B-cell lymphoma (Tan, Goh et al. 2005) and in antiphospholipid antibody syndrome (Reitblat, Polishchuk et al. 2003). Metabolic conditions associated with a supranuclear gaze palsy include adult onset Nieman Pick type C (Godeiro-Junior, Inaoka et al. 2006) and Gaucher's disease with mutations in glucocerebrosidase (Alonso-Canovas, Katschnig et al. 2010). PSP phenotypes have been described in association with mutations of Microtubule associated protein tau (MAPT) (Borroni, Agosti et al. 2011), progranulin (PRGN) (Tremolizzo, Bertola et al. 2011), chromosome 9 open reading frame 72 expansions (c9orf72) (Lesage, Le Ber et al. 2013), dynactin (DCTN1) (Aji, Medley et al. 2013), Kufor Rakeb / PARK 9 (ATP1382) (Williams, Hadeed et al. 2005) and the prion protein (PRNP) (Matej, Kovacs et al. 2012).

c) Molecular Biology

PSP along with CBD is associated with the deposition of insoluble fibrillary deposits containing the microtubule-associated protein, tau (Williams 2006). There are six isoforms of tau: in normal brain 3 repeat and 4 repeat tau are approximately equally abundant; in Alzheimer's disease there is preponderance of 3 repeat tau whereas PSP and CBD are associated with predominantly four microtubule binding domains (Arai, Ikeda et al. 2001). Tau is involved in stabilisation of the cell cytoskeleton: in PSP insoluble and resistant tau is deposited in tangles and threads in specific brain regions. PSP and CBD are associated with a common tau haplotype, H1 (Houlden, Baker et al. 2001). The microtubule associated protein tau (MAPT) gene is located on chromosome 17.

d) Histology and Macroscopic Pathology

Atrophy of the globus pallidus, subthalamic nucleus and brainstem, dilatation of the third and fourth ventricles and cerebral aqueduct, hypopigmentation of the substantia nigra and locus coeruleus and mild atrophy of Brodman's area 4 may be seen on macroscopic examination (Hauw, Daniel et al. 1994).

Tau immunoreactive neurofibrillary tangles, neuropil threads and tufted astrocytes in the brainstem and basal ganglia associated with variable neuronal loss and astrogliosis with tau positive glial inclusions called coiled bodies are the histological hallmarks of PSP (Hauw, Daniel et al. 1994). Particulary affected regions include the globus pallidus, subthalamic nucleus, substantia nigra and pontine nuclei and other regions usually affected include the striatum, oculomotor compex, medulla and dentate nucleus (Hauw, Daniel et al. 1994).

There are differences in the regional distribution and severity of tau accumulation in the different clinical subtypes with the most heavy deposition in PSP-RS (Williams, de Silva et al. 2005; Williams, Holton et al. 2007; Williams, Holton et al. 2007).

Figure 1.1: Distribution of severe tau pathology in mid sagittal plane (Williams, Holton et al. 2007)

1. **Inclusion Criteria**
    - Gradually progressive disorder
    - Age at onset > 40 or later
    - ***Possible PSP***: *either* vertical supranuclear gaze palsy *or* both slowing of vertical saccades and postural instability with falls within 1 year
    - ***Probable PSP***: vertical supranuclear gaze palsy and prominent postural instability and falls within 1 year
    - ***D*efinite PSP***:* criteria for possible or probable PSP are met plus histopathological confirmation

2. **Exclusion criteria**
    - Recent history of encephalitis
    - Alien limb phenomenon
    - Cortical sensory deficit
    - Focal frontal or temporoparietal atrophy
    - Hallucinations or delusions unrelated to dopaminergic therapy
    - Cortical dementia of Alzheimer type
    - Prominent early cerebellar symptoms or unexplained dysautonomia
    - Evidence that other diseases could explain the clinical features

3. **Supportive Features**
    - Symmetric akinesia or rigidity proximal more than distal
    - Abnormal neck posture particularly retrocollis
    - Poor or absent response of parkinsonism to levodopa
    - Early dysphagia or dysarthria
    - Early onset cognitive impairment including > 2 of apathy, impairment in abstract thought, decreased verbal fluency, utilization or imitation behaviour, or frontal release signs

Table 1.1: NINDS-SPSP Clinical Criteria for the Diagnosis of PSP (Litvan, Agid et al. 1996)

2. Parkinson's Disease

Parkinson's disease (PD) is a neurodegenerative disorder characterized by loss of pigmented dopaminergic cells in the substantia nigra pars compacta (SNc) associated with the presence of alpha synuclein immunoreactive Lewy bodies.

a) Epidemiology

PD occurs in all ethnic groups and affects male and female in equal proportion. The estimated incidence of PD is 20/100 000 and prevalence increases exponentially between ages of 65 and 90 and the estimated true prevalence is 200/100 000 (Schapira 1999; Schrag, Ben-Shlomo et al. 2000).

b) Clinical Presentation

Parkinson's disease presents with characteristically asymmetrical bradykinesia, rigidity and tremor, and also postural instability (Gibb and Lees 1991) [Table 1.2].

It is important to exclude secondary causes of parkinsonism including iatrogenic drug-induced parkinsonism associated with dopaminergic antagonists including antiemetics and major tranquilizers, post encephalitic parkinsonism, head injury (including boxing), normal pressure hydrocephalus and structural lesions such as stroke and other space occupying lesions which may cause hemiparkinsonian syndromes. Other degenerative diseases causing parkinsonism may masquerade as PD including PSP, MSA and CBD.

1. Diagnosis of a Parkinsonian Syndrome:

a. Bradykinesia: slowness of initiation of voluntary movment with progressive reduction in speed and amplitude of repetitive actions

b. Plus at least one of:

   i. Muscular rigidity

   ii. 4-6 Hz Rest tremor

   iii. postural instability not caused by primary visual, vestibular, cerebellar or proprioceptive dysfunction

2. Exclusion Criteria:

a. History of repeated strokes or stepwise progression of Parkinsonian features

b. History of repeated head injury

c. History of definite encephalitis

d. Oculogyric crises

e. Neuroleptic treatment at onset of symptoms

f. More than one affected relative

g. Sustained remission

h. Strictly unilateral features after 3 years

i. Supranuclear gaze palsy

j. Cerebellar signs

k. Early severe autonomic involvement

l. Early severe dementia with disturbances of memory, language and praxis

m. Babinski sign

n. Presence of cerebral tumour or communicating hydrocephalus on CT scan

Table 1.2: Queen Square Brain Bank Clinical Diagnostic Criteria for the Diagnosis of Parkinson's Disease (Gibb and Lees 1991).

Post Mortem series have shown that around a quarter of those clinically diagnosed with PD during life will turn out to have an alternative diagnosis (Hughes, Daniel et al. 1992), although more recently this figure was found to be less than 10% in specialist hands (Hughes, Daniel et al. 2002). It is likely that non-specialist diagnostic accuracy rates are lower.

Bradykinesia may manifest as slowness in manual tasks, difficulty doing up buttons, using a key board etc, reduction in arm swing when walking, masking of facial expression and micrographia. The tremor is classically a 4-6 Hz resting tremor, although it is not unusual to have an additional postural tremor. Up to 25% do not have tremor. The gait is described as shuffling or festinant and there may be postural instability and falls. There is a good clinical response to levodopa in more than 90% of patients (Lees, Hardy et al. 2009). Increasingly non-motor features are being recognized. This includes hyposmia which may predate motor symptoms by some time, neuropsychiatric features including depression and dementia, sleep disorders such as REM sleep behaviour disorder which may also pre-date the motor features, autonomic features including urinary incontinence, disorders of sweating, orthostatic hypotension and erectile impotence, disorders of the gastrointestinal tract (constipation) and sensory disturbances amongst other symptoms (Chaudhuri, Healy et al. 2006).

Typically medical treatment is required within the first few years of disease and currently there are many symptomatic treatments available which act to replace the dopamine deficit found in PD. Despite being the first medical treatment for PD levodopa remains the most efficacious although it is associated with motor complications in the longer term including a reduction in the duration of action leading to a 'wearing off' effect, choreiform dyskinesias and unpredictable off periods. Other medications which stimulate dopaminergic receptors (dopamine agonists) or act to reduce the rate of dopaminergic breakdown (COMT inhibitors, MAOB inhibitors) and others (amantadine) are used to control these complications and it is often possible to control symptoms adequately without significant adverse reactions for many years. Some patients however require infusions (duodopa enteral infusions, apomorphine subcutaneous infusions) and deep brain surgery to the pallidum and subthalamic nucleus (lesioning or electrode stimulation). These therapies are most efficacious for symptoms of parkinsonism responding to levodopa.

However as the disease progresses axial and levodopa unresponsive features including abnormalities of postural stability, speech and cognitive decline become more evident and form the most disabling symptoms after around 15 years of disease (Hely, Morris et al. 2005). By 20 years 74% of patients have died, and 84% of those still alive have dementia (Hely, Reid et al. 2008).

c) Pathophysiology

Degeneration of the dopaminergic neurons in the SNc leads to a reduction in striatal dopamine. Through the basal ganglia thalamocortical circuitry this ultimately results in an increased activity in the subthalamic nucleus (STN) and an ensuing increase in GABAergic activity in the output nuclei of the basal ganglia (the substantia nigra pars reticulata (SNr) and internal segment of the globus pallidus (GPi)) and inhibition of the thalamus and brainstem outflow nuclei. This in turn causes inhibition of cortical motor areas. Although there are inconsistencies in this simplified theory of the pathophysiology of parkinsonism it has enabled the development of targeted surgical interventions including stimulation of the subthalamic nucleus which is an effective symptomatic therapy for PD in some patients (Limousin, Pollak et al. 1995; Limousin, Pollak et al. 1995).

d) Molecular Biology

Although the vast majority of Parkinson's disease is sporadic there are now well-characterised genetic forms of the disease (PARK1-12). The autosomal dominant forms include mutations of alpha-synuclein SNCA (PARK1/4) and dardarin LRRK2 (PARK8) although this condition has a variable penetrance. Autosomal recessive forms include parkin PRKN (PARK2), PINK1 (PARK6) and DJ-1 (PARK7) (Hardy, Cai et al. 2006).

e) Macroscopic pathology and Histopathology

The pathological hallmark of PD is the round eosinophilic intracytoplasmic inclusion (the Lewy body) and dystrophic neurite (Lewy neurite) (Forno 1996). The Lewy body has a distinctive dense core from which can be seen radiating microfilaments on electron microscopy. Lewy bodies contain alpha synuclein – a protein whose function is currently unclear but it is expressed throughout the brain and particularly found in presynaptic nerve terminals. Mutations of alpha synuclein (point mutations or triplications) are known genetic causes of PD. Knowledge gleaned from studying genetic PD indicates that degeneration of dopaminergic neurons involves mitochondrial dysfunction, oxidative stress and impairment of the ubiquitin proteasomal system all of which interact at several levels. In sporadic PD this ultimately leads to the deposition of alpha synuclein and formation of Lewy bodies although these are not necessarily found in genetic forms of PD (Forno 1996; Moore, West et al. 2005).

PD typically affects the substantia nigra pars compacta and locus coeruleus. This is evident macroscopically as pallor of these usually darkly stained nuclei visible to the naked eye. Loss of pigmented neurons in the SN at the rate of 4.7% per decade is found in normal aging and 45% in the first decade in PD (Fearnley and Lees 1991). Neuronal loss is selective – in normal aging the most severely affected region is the medial ventral and dorsal tiers; in PD the loss is greatest in the lateral ventral tier (Fearnley and Lees 1991; Gibb 1992). This leads to selective loss of dopaminergic innervation of the striatum and explains the pattern of reduced presynaptic nigrostriatal loss seen in PET and SPECT studies. The progression of pathology in PD progresses from the caudal ventrolateral SNpc rostrally, medially and dorsally (Damier, Hirsch et al. 1999).

Not only the SN is affected and the recent pathological staging of PD suggests that the disease starts in the dorsal motor nucleus of the vagus and olfactory areas and progresses through the brainstem towards the cortex with the SN becoming involved only at an intermediate stage (Braak, Del Tredici et al. 2003) [Table 1.3].

Stage	Region	Nuclei affected
1	Medulla oblongata	IX, X cranial nerve motor nuclei and intermediate reticular zone
2	Medulla oblongata & pontine tegmentum	Caudal raphe nuclei, coeruleus-subcoeruleus complex and gigantocellular reticular nucleus
3	midbrain	Particularly the pars compacta of the substantia nigra
4	Basal prosencephalon & temporal mesocortex	Temporal mesocortex and allocortex
5	Neocortex	Higher order sensory areas of neocortex and prefrontal neocortex
6	Neocortex	First order sensory association areas of neocortex and premotor areas

Table 1.3: Braak Staging System for the Pathology of PD (Braak, Del Tredici et al. 2003)

3. Multiple System Atrophy

Multiple system atrophy (MSA) encompases illnesses previously referred to as olivo-ponto-cerebellar atrophy (OPCA), striatonigral degeneration (SND) and Shy Drager syndrome (SDS).

a) Epidemiology

The age-adjusted prevalence of MSA is 4.4 / 100 000 (Schrag, Ben-Shlomo et al. 1999). It is equally prevalent in men and women.

b) Clinical Presentation

MSA presents in the 6th decade and lasts up to 9 years from first symptom. The clinical features of MSA include the autonomic, cerebellar, parkinsonian and pyramidal systems. MSA is subdivided depending on the dominant clinical phenotype: a parkinsonian subtype (MSA-P) occurs in approximately 80% and a cerebellar (MSA-C) subtype in 20% (Wenning, Colosimo et al. 2004).

Autonomic features include erectile impotence, urinary incontinence, constipation and orthostatic hypotension. Some patients present with syncope. Parkinsonism may initially respond to levodopa to some degree but classically this wanes; patients may develop characteristic orofacial dyskinesias and dystonia. There is also axial dystonia manifest as antecollis, a 'Pisa syndrome' or camptocormia. Tremor, if present, is jerky. Gait and limb ataxia and oculomotor abnormalities indicate cerebellar involvement (Litvan, Bhatia et al. 2003; Wenning, Colosimo et al. 2004).

Depending on the mode of presentation and relative distribution of pathology in the nigrostriatal or olivo-ponto-cerebellar pathways MSA can be clinically confused with PD, or other cerebellar degenerations. MSA-C accounts up for a around 1/4 of sporadic cerebellar ataxia (Gilman, Little et al. 2000); MSA-P accounts for 8% of those presenting with parkinsonism (Schwarz et al., 1998).

Clinical red flags for a diagnosis of MSA include early postural instability, early use of a wheelchair, the Pisa syndrome or camptocormia, early bulbar or respiratory involvement and emotional incontinence [Table 1.4] (Kollensperger, Geser et al. 2008).

1. Early postural instability
2. Rapid progression – the wheelchair sign
3. Abnormal postures including the Pisa syndrome and camptocormia
4. Bulbar dysfunction: characteristic

Table 1.4: Red Flags for a Clinical Diagnosis of Multiple System Atrophy (Kollensperger et al., 2008)

The use of clinical diagnostic criteria are highly specific but less sensitive [Tables 1.5 & 1.6]. Early in the disease there is still significant difficulty in making an accurate diagnosis.

Clinical Domain	Features	Criterion
Autonomic and urinary dysfunction	Orthostatic hypotension Urinary incontinence incomplete bladder emptying	Orthostatic fall in blood pressure, and/or urinary incontinence
Parkinsonism	Bradykinesia Rigidity Tremor Postural instability	Bradykinesia plus one of the other three
Cerebellar dysfunction	Gait ataxia Ataxic dysarthria Limb ataxia Sustained gaze-evoked nystagmus	Gait ataxia plus one of the other three
Corticospinal tract dysfunction	Extensor plantar responses with hyper-reflexia	Not a requirement

Table 1.5: Clinical Consensus Criteria for diagnosis of MSA (Gilman, Low et al. 1999)

Diagnostic Category	Inclusion Criteria	Exclusion Criteria
Possible MSA	One criterion plus two other features or poor response to levodopa if criterion is parkinsonism	1. Symptom onset < 30 yrs 2. Family history 3. Systemic features or other causes for features present 4. Hallucinations off medication 5. Dementia 6. Prominent slowing of vertical saccades or supranuclear gaze palsy 7. Evidence of focal cortical dysfunction 8. Metabolic, genetic or imaging evidence of alterative cause for features
Probable MSA	One criterion for autonomic dysfunction plus poorly levodopa responsive parkinsonism or cerebellar dysfunction	
Definite MSA	Pathologically confirmed with glial cytoplasmic inclusions in nigrostriatal and olivopontocerebellar pathways	

Table 1.6: Categorisation of MSA (Gilman, Low et al. 1999).

c) Molecular Biology

MSA is characterised by apha-synuclein positive glial cytoplasmic inclusions and along with PD and dementia with Lewy bodies forms the group of proteinopathies called the 'synucleinopathies' (Spillantini 1999). It is not clear whether the aggregration of alpha-synuclein is causal or a bystander effect in the pathogenesis of MSA (Wenning, Colosimo et al. 2004).

d) Macroscopic pathology and Histology

There is putaminal atrophy with grey-green discolouration particularly in the dorsolateral and posterior two thirds (Fearnley and Lees 1990; Kume, Takahashi et al. 1993) and atrophy of the pons and pontocerebellar fibres, the middle cerebellar peduncle, and cerebellum. There is pallor of the SN and LC (Lantos 1998).

Glial Cytoplasmic inclusions (GCI) with astrogliosis neuronal loss and demyelination are the hallmarks of MSA and occur in a characteristic distribution in the striatonigral and olivopontocerebellar pathways (Papp, Kahn et al. 1989; Ozawa, Paviour et al. 2004). GCI are half-moon/oval/sickle shaped oligodendroglial argyrophilic inclusions which are made up of tubular filaments (Lantos 1998). The most severe lesions in MSA are found in the SN, LC, putamen, inferior olives, the pontine nuclei, the Purkinje cells and the intermediolateral columns (Lantos 1998). Neuronal cytoplasmic inclusions also occur. Pathologically both the nigrostriatal and olivopontocerebellar pathways may be affected although the pontocerebellar pathway is more affected in MSA-C and nigrostriatal pathway in MSA-P (Ozawa, Paviour et al. 2004). The topography of disease is typically in the dorsolateral posterior 2/3 of the putamen in MSA-P, and the lateral SNc. Loss of neurons in the SNc is relatively less significant than the putaminal loss which may help explain the lack of response to levodopa due to a postsynaptic dopaminergic deficit (Fearnley and Lees 1990; Kume, Takahashi et al. 1993; Ozawa, Paviour et al. 2004).

4. Corticobasal degeneration and corticobasal syndrome

Corticobasal degeneration (CBD) was first described in 1968 by Rebeiz et al as 'corticodentatonigral degeneration with neuronal achromasia' (Rebeiz, Kolodny et al. 1968). CBD has gone by a variety of other names including corticonigral degeneration with neuronal achromasia (1993), cortical degeneration with swollen chromatolytic neurons (Clark, Manz et al. 1986), cortical basal ganglionic degeneration (Riley, Lang et al. 1990), and corticobasal degeneration which is the most common term now used (Gibb, Luthert et al. 1989).

a) Epidemiology

CBD is onset in the 7th decade (61-66 yrs (Rinne, Lee et al. 1994)(Wenning, Litvan et al. 1998)(Ling, O'Sullivan et al. 2010)) with no cases identified under 45 yrs (Wenning, Litvan et al. 1998). There is no gender predisposition (Rinne, Lee et al. 1994; Ling, O'Sullivan et al. 2010).

True incidence is unknown and in a UK community based study no cases were identified (Schrag, Ben-Shlomo et al. 2000). At the Queen Square Brain Bank for Neurological disorders 19/1440 cases in the archive had a pathological diagnosis of CBD which was much less common than PD (608), PSP (179) and MSA (117) (Ling, O'Sullivan et al. 2010). However, it has been estimated to be less than 1 in 100 000 (Williams 2006) and in a Russian population the age standarized incidence rate was 0.02 per 100 000/yr for CBD, with figures for PD of 9.03, 0.11 for MSA and 0.14 for PSP (Winter, Bezdolnyy et al. 2010).

b) Clinical Presentation

The features found in CBD's classic presentation are known as the corticobasal syndrome (CBS) (Boeve, Lang et al. 2003). This is a multisystem syndrome with extrapyramidal, cortical, oculomotor, cognitive and neuropsychiatric features.

Domain	Feature	Comments
Extrapyramidal	Rigidity	Characteristically progressive and asymmetric
	Akinesia	
	poor levodopa response	may have transient mild response
	myoclonus	usually associated with dystonia
	dystonia	including blepharospasm
	postural instability	usually later
Cortical / cognitive	dyspraxia	limbs, speech, gait, eye movements, eyelid opening
	alien limb	more than limb levitation alone
	cortical sensory loss	
	dysphasia visuospatial deficits dysexecutive / frontal deficits	increasingly recognised as a common feature particularly non fluent dysphasia
Neuropsychiatric	depression	
	apathy	
	irritability	
	sleep inversion	
	obsessive compulsive behaviours	
Others	frontal release signs	dyphagia and dysarthria are usually late
	bulbar symptoms	
	chorea	

Table 1.7: Clinical Features of a corticobasal syndrome

The typical features include a markedly asymmetric progressive akinesia and rigidity which does not response to levodopa therapy (Gibb, Luthert et al. 1989; Wenning, Litvan et al. 1998; Ling, O'Sullivan et al. 2010). This can start in the arm or leg with associated manifestations. There may be a mild non-sustained levodopa response which is unusual to

be significant enough to lead to confusion with levodopa responsive idiopathic PD (Lang 2005), although this has been described (Ling, O'Sullivan et al. 2010). Parkinsonism was an early prominent feature seen in 9/19 (47%) pathologically confirmed CBD patients (Ling, O'Sullivan et al. 2010). Myoclonus is also found in approximately 50% of corticobasal presentations of CBD, and in approximately 37% of all pathologically-confirmed CBD cases (Stamelou, Alonso-Canovas et al. 2012). Often there is a jerky tremor but this is not characteristic of PD and likely related to myoclonus with action and postural components.

Apraxia commonly co-exists with the parkinsonian features and is found in 80-90% of corticobasal syndromes (Leiguarda, Lees et al. 1994) and 72% of patients with pathologically-proven CBD (Stamelou, Alonso-Canovas et al. 2012). Cortical sensory loss is seen in less than a quarter of cases, and visual neglect is also reported (Armstrong, Litvan et al. 2013). Patients report that the limb is acting on its own and they feel dissociated from it - the limb may rise up on its own ('levitation') and other features such as forced grasping or reaching for objects in the immediate environment and inter-manual conflict are reported (Boeve, Lang et al. 2003).

The presence of delayed saccadic latency supports the diagnosis of CBD (Gibb, Luthert et al. 1989; Rinne, Lee et al. 1994) whereas abnormalities of saccadic speed and in the vertical plane are more predictive of PSP although abnormalities in the vertical plane may be seen later in the disease but are likely to be milder than in PSP (Rivaud-Pechoux, Vidailhet et al. 2000). Oculomotor apraxia and a late supranuclear gaze palsy have also been described (Boeve, Lang et al. 2003). Axial signs including bulbar (dysarthria and dysphagia) and gait disturbance, pyramidal signs and ataxia and chorea are also reported but are less discriminating from other diseases (Boeve, Lang et al. 2003; Armstrong, Litvan et al. 2013).

Although dementia was felt to be an exclusion criterion for the diagnosis of CBD in the early literature more recently dementia has been described as in all likelihood the most common presentation of CBD.

Clinicopathological studies recently published indicate that there are two angles from which this clinical conundrum can be approached. Determining the pathology associated with a corticobasal syndrome, and identifying the presentations of those who turn out to have CBD.

Clinical Corticobasal Syndrome (CBS)
Neurodegenerative disease: •Corticobasal Degeneration (<47%) •Alzheimer's disease (<50%) •Progressive supranuclear palsy (Richardson's syndrome) (<29%) •Frontotemporal dementia with TDP43 pathology (<13%) •Pick's disease •Dementia with Lewy Bodies •Creutzfeld-Jakob Disease •Neurofilament inclusion body disease / Frontotemporal dementia with FUS pathology •Argyrophilic Grain Disease •Mixed pathology
Vascular disease: •Carotid stenosis •Stroke
Genetic disease: •MAPT mutations •Progranulin mutations •TDP43 mutations •FUS mutations •C9ORF72 mutations

Table 1.8: Aetiology of CBS

In a report from a primarily movement disorders setting at the Queen Square Brain Bank for Neurological Disorders, of 19 cases with a pathological diagnosis of CBD, only 5 had a CBS diagnosis at time of death i.e. approximately a quarter of cases of CBD were accurately diagnosed during life (sensitivity 26.3%). On the other hand, of 21 corticobasal syndrome presentations only 5 were associated with CBD pathology i.e. approximately one quarter of cases of corticobasal syndrome turn out to have corticobasal degeneration at post mortem and another diagnosis is more likely although the figure is almost 50% if a movement disorders specialist is the attending physician (Ling, O'Sullivan et al. 2010).

Confirmed Corticobasal Degeneration (CBD)
Presenting clinical Phenotype •Corticobasal Syndrome •Progressive nonfluent aphasia •Progressive supranuclear Palsy or 'executive-motor phenotype' •Frontotemporal dementia (FTD) including the behavioural variant (bvFTD) •Posterior cortical atrophy (AD) •Parkinson's disease •Pick's disease •Progressive quadriparesis with myoclonus' •Apraxia of speech •Incidental •'Symmetric'

Table 1.9: clinical presentation of CBD

In another series from a primarily cognitive centre 18 cases with CBD pathology were associated with an executive motor presentation (containing both features of CBS and being PSP-like but not fulfilling clinical research criteria for the diagnosis) in 7/18 . At post mortem examination of 40 patients with corticobasal syndrome, 14 had a pathological diagnoses of CBD (35%) (Lee, Rabinovici et al. 2011).

This has led to the development of more complicated clinical research diagnostic criteria (Armstrong, Litvan et al. 2013).

Lang 1994	Boeve 2003	Armstrong 2013
Inclusion criteria: Rigidity and one cortical sign: 1. apraxia 2. cortical sensory loss 3. alien limb Asymmetric rigidity, dystonia and focal reflex myoclonus **Exclusion criteria:** •early dementia •early vertical gaze palsy •rest tremor •severe autonomic disturbance •sustained levodopa response •imaging abnormalities supportive of another diagnosis	**Core features:** Insidious onset and progressive course no identifiable cause cortical dysfunction with at least one of: • focal or asymmetric idiomotor apraxia • alien limb phenomenon • cortical sensory loss • visual or sensory neglect • constructional apraxia • focal or asymmetric myoclonus • apraxia or speech or non fluent aphasia Extrapyramidal dysfunction: • focal or asymmetric appendicular rigidty lacking sustained or prominent levodopa respnonse • focal or asymmetric dystonia **Supportive features:** •cognitive dysfunction with relative preservation of learning and memory •focal or asymmetric perifrontal cortex atrophy on structural imaging or hypoperfusion on SPECT or PET	**Probable CBS:** asymmetric presentation with 2 of: •limb rigidity/akinesia, •limb dystonia •myoclonus plus 2 of: •orobuccal or limb dyspraxia cortical sensory deficit •alien limb **Frontal behavioural spatial syndrome:** •executive dysfunction •behavioural or personality change •visuospatial deficit **Nonfluent variant of primary progressive aphasia:** •impaired grammar with preserved single word comprehension •apraxia of speech **Progressive supranuclear palsy syndrome:** •axial/limb rigidiy/akinesia •postural instability/falls •urinary incontinence •behavioural changes •supranuclear gaze palsy or slowing of vertical saccades

Table 1.8: diagnostic criteria for CBD. Lang 1994, Boeve 2003 (Boeve, Lang et al. 2003) and Armstrong 2003 (Armstrong, Litvan et al. 2013). Using the Armstong criteria for possible CBS only one feature from the extrapyramidal and cortical domains are needed; for probable CBD the onset must be insidious with gradual progression, duration greater than one year, age greater than 50 years, no family history in more than one relative, no MAPT mutation and the phenotype must be one of the first three with at least one CBS feature. Possible sporadic CBD criteria are less stringent (Armstrong, Litvan et al. 2013).

c) Molecular biology in CBD

CBD is classified as a four repeat tauopathy along with PSP. Mirroring the clinical diagnostic uncertainties surrounding CBS and CBD it was not until 2002 that standardised neuropathological criteria were agreed for the diagnosis of CBD (Dickson, Bergeron et al. 2002). Although there is general consensus that CBD is a distinct entity, there is ongoing nosological debate about whether PSP and CBD form part of a spectrum of the same disease given (1) their clinical and pathological overlap, (2) that they both are associated with 4 microtubule binding repeat tau deposition and a H1 haplotype and (3) that both clinical syndromes have been reported in presentations of MAPT mutations which cannot be pathologically differentiated from CBD (Mizuno, Shiga et al. 2005)(Scaravilli, Tolosa et al. 2005). Others have suggested that CBD, PSP and FTD should be grouped together as part of the "Pick complex of diseases" (Kertesz, Martinez-Lage et al. 2000).

d) Macroscopic Pathology and Histology in CBD

Typically there is cortical atrophy in frontal lobes with lateral ventricle dilatation (Massey, Micallef et al. 2012) and characteristically parasagittal cortical gyri narrowing is seen in a peri-Rolandic distribution with the posterior superior frontal gyrus more affected than the middle or inferior frontal gyri (Dickson, Bergeron et al. 2002). Atrophy may be asymmetric and in cases with aphasia inferior frontal and temporal lobe involvement is seen. Loss of associated white matter is seen (Massey, Micallef et al. 2012) with thinning of the corpus callosum. The thalamus may be atrophic and the caudate head flattened. The substantia nigra is pale (Massey, Micallef et al. 2012) but the locus coeruleus is preserved (Dickson, Bergeron et al. 2002) or pale (Massey, Micallef et al. 2012).

Neuronal loss and astrogliosis are found in affected areas with spongiosis and microvacuolation in affected regions of cortex with underlying white matter myelin loss (Dickson, Bergeron et al. 2002). In the 3rd, 5th and 6th cortical layers 'swollen', 'achromatic' or 'ballooned' neurons (BN) (Rebeiz, Kolodny et al. 1968) are seen which are immunoractive for neurofilaments but with different immunoreactivity to Pick bodies of Pick's disease and if in characteristic cortical areas are relatively specific for CBD (Dickson, Bergeron et al. 2002). Tau immunohistochemistry reveals pretangles, or small neurofibrillary tangles in the cortex and substantia nigra and locus coeruleus. The neuropil also contains tau-immunoreactive cell processes and the location in cell processes is characteristic of CBD. Tau-immunoreactive alphasynuclein negative coiled bodies are found in oligodendroglia

(Dickson, Bergeron et al. 2002). In the neocortex tau-immunoreactive astrocytic lesions are characterised by an annular cluster of processes named 'astrocytic plaques' and are the most specific finding in CBD. There is lateral substantia nigra cell loss and astrogliosis (Gibb, Luthert et al. 1989).

	Feature
Macroscopic findings	(asymmetric) posterior frontal atrophy with associated white matter atrophy and callosal thinning atrophy of caudate and thalamus nigral pallor
Microscopic findings	focal neuronal loss and astrogliosis in affected cortex and substantia nigra white matter myelin loss *ballooned neurons* in affected cortical areas tau immunoreactive neuronal inclusions in affected cortex, lentiform, thalamus, subthalamus, substantia nigra and locus coeruleus *astrocytic plaques* in affected cortex and basal ganglia tau positive threads and coiled bodies in centrum semiovale, corticospinal tracts, lentiform nucleus, pontine base and gray matter of affected cortex, basal ganglia, thalamus and brainstem

Table 1.11: macroscopic and microscopic findings in corticobasal degeneration adapted from Dickson et al Office of Rare Diseases Criteria for CBD (Dickson, Bergeron et al. 2002)

C. Accuracy of the clinical diagnosis

As can be seen accurate clinical diagnosis of these parkinsonian conditions, even in experienced hands, can be difficult. The clinico-pathological literature has taught us that these conditions overlap in clinical presentation and that particularly in CBD, for example, the ability to predict the underlying diagnosis is very inexact.

In a series of 100 patients with a clinical diagnosis of Parkinson's disease 76 had Lewy bodies consistent with pathologically confirmed disease, 6 had PSP pathology, 5 MSA, 3 Alzheimer's disease, 3 Alzheimer-type pathology, 3 vascular disease, 2 nigral pathology without Lewy bodies, 1 post-encephalitic parkinsonsim and 1 was normal (Hughes, Daniel et al. 1992). Likely due to improved awareness in the neurological community 10 years later the diagnostic accuracy was approximately 90% for PD with PSP and MSA the most commonly identified pathologies masquerading as PD clinically (Hughes, Daniel et al. 2001). The positive predictive value of a clinical diagnosis by a movement disorder neurologist of MSA is 85.7% and PSP 80% with sensitivity of 88.2% in MSA and 84.2% in PSP (Hughes, Daniel et al. 2002), which is greater than the accuracy of the clinical research criteria for in PSP (probable PSP sensitivity 50%, PPV 100%; possible PSP sensitivity 83%, PPV 83% (Litvan, Agid et al. 1996)). More recent data indicate that these diagnostic difficulties persist.

Disease	Sensitivity of clinical diagnosis	Positive predictive value of clinical diagnosis
PSP	73.2%	69%
PD	92.8%	82.7%
MSA	70.1%	70.1%
CBD	26.3%	23.8%

Table 1.12: Diagnostic acumen in parkinsonian syndromes from 1440 cases at the Queen Square Brain Bank (Ling, O'Sullivan et al. 2010).

Thus, although improvements in clinical diagnosis have certainly been made over the last 20 years, the heterogeneity of clinical features of these diseases and in CBD particularly the

inexact correlation between clinical phenotype and pathology indicate that further work is needed both to better classify clinically these diseases and to identify ways in which these diseases can be identified more accurately during life.

Chapter 2: Clinical Outcomes of Progressive Supranuclear Palsy and Multiple System Atrophy

A. Introduction

Progressive Supranuclear Palsy (PSP) and Multiple System Atrophy (MSA) are the most common causes of neurodegenerative-parkinsonism after Parkinson's disease, with an estimated prevalence for PSP of 6·4 per 100 000 and for MSA of 4·4 per 100 000 (Schrag, Ben-Shlomo et al. 1999). MSA may be divided into clinical subtypes, according to whether cerebellar (MSA-C) or parkinsonian (MSA-P) symptoms predominate (Gilman, Low et al. 1999) and a recent study has demonstrated that early autonomic dysfunction may also be a prognostic indicator in MSA (Tada, Onodera et al. 2007). PSP may also be classified into two clinical subtypes, 'Richardson's syndrome' (PSP-RS) and 'PSP-parkinsonism' (PSP-P) (Williams, de Silva et al. 2005).

Currently, there is little data available comparing the clinical progression of the clinical subtypes of MSA and PSP. There have been two published studies of the natural history of PSP with over 100 cases but with only a minority of cases with pathological confirmation (Nath, Ben-Shlomo et al. 2001; Golbe and Ohman-Strickland 2007). Similarly, with the exception of a meta-analysis (Wenning, Tison et al. 1997) the few large natural history studies in MSA lack pathological confirmation, with only 22 of the 230 patients described by Watanabe undergoing autopsy (Watanabe, Saito et al. 2002).

Accurate natural history data is essential for clinicians to be able to provide prognostic information to patients and their families. Furthermore this information could serve as a source of historical controls for use in future interventional studies. However, because clinical diagnosis is difficult in these conditions (Hughes, Daniel et al. 2002) prospective natural history studies are limited by diagnostic inaccuracy and selection bias, making analysis of disease progression and the factors that predict prognosis often difficult.

B. Aims

We attempted to overcome these difficulties by investigating the clinical features in a series of pathologically confirmed cases of PSP and MSA. In particular, we sought to determine

the disease progression through significant clinical milestones, and compare these between the disease subtypes seen in MSA and PSP.

C. Materials and Methods

1. Participant Selection

Patients with a pathologically proven diagnosis of PSP and MSA were identified from the records of donors to the Queen Square Brain Bank for Neurological Disorders that were autopsied between 1987 and 2007 where tissue is donated according to ethically approved protocols and is stored under a licence from the Human Tissue Authority.

The diagnosis of PSP was made according to the National Institute for Neurological Diseases and Stroke-Society for PSP (NINDS-SPSP) neuropathological criteria (Hauw, Daniel et al. 1994; Litvan, Hauw et al. 1996) and the diagnosis of MSA was made according to established consensus criteria (Gilman, Low et al. 1999) and neuropathological criteria (Papp, Kahn et al. 1989; Lowe and Leigh 1997).

2. Medical Record Review

We performed a systematic review of the case files, including the comprehensive case notes of the family doctor and all of the correspondence between the family doctor and the medical specialist. All patients had been assessed by hospital specialists (neurologists or geriatricians) who were blinded to the pathological diagnosis. Cases were excluded if the medical records did not contain regular and well-documented reports of clinical developments.

A clinical data sheet was designed to record the presence or absence of clinical features either early in the disease course (within 2 years of first symptom onset) or at any time during the disease, as described previously (Williams, de Silva et al. 2005). Symptoms were recorded as being absent if not reported and clinical signs were recorded separately as unknown if they were not specifically mentioned in the notes. Where conflicting clinical features were reported, the findings of the neurologist were used.

Definitions were as follows:

(i) Age of onset: age at the time of the first reported symptom considered to be attributable to MSA or PSP.

(ii) Duration: time between the age of onset and the age at death.

(iii) Bradykinesia: the presence of any mention of bradykinesia or motor slowing.

(iv) Asymmetric onset: if there was a clear difference between the signs on the left and the right, asymmetry was recorded as being present. This included asymmetry of tremor, rigidity, bradykinesia or functional decline. It did not include specific tasks such as writing and using tools.

(v) Tremor: the recording of any tremor.

(vi) Rigidity: the recording of axial or peripheral muscle rigidity; extrapyramidal and pyramidal rigidity were not differentiated.

(vii) Impaired postural reflexes: the presence of this sign was recorded only if specifically mentioned in the clinical notes.

(viii) Supranuclear gaze palsy: the specific recording of restricted range of eye movement in the vertical plane.

(ix) Impaired saccadic or pursuit movements: the specific recording of abnormal saccadic or smooth pursuit eye movements.

(x) Extra axial-dystonia: the presence of dystonia in any body part apart from trunk and neck.

(xi) Pyramidal signs: pathologically brisk reflexes and/or extensor plantar response(s).

(xii) Autonomic dysfunction: either abnormal autonomic function testing or documentation of any two of urinary urgency, frequency and nocturia without hesitancy; chronic constipation; postural hypotension; sweating abnormalities; or erectile dysfunction.

(xiii) Response to levodopa: the patient's and clinician's interpretation of improvement were assessed from the case notes and in some cases from the completed Parkinson's Disease Society Brain Bank Annual Assessment (PDSBB) Forms. A self-reported improvement of >30% coincident with the introduction of levodopa was recorded as being a positive response. This degree of response was graded by a 4-point scale modified from the PDSBB annual assessment forms: 1 = nil, or slight response (<30% improvement); 2 = moderate response (30–50% improvement); 3 = good response (51–70% improvement); and 4 = excellent response (71–100% improvement).

(xiv) Cerebellar signs: the recording of axial or peripheral ataxia.

Seven milestones of disease advancement were selected on the basis that each was clinically important and therefore likely to require additional medical attention and to be well recorded in the case notes. These were:

(i) Frequent falling (defined as falls occurring more than twice per year, or the documentation of "frequent" or "regular" falls).

(ii) Cognitive disability.

(iii) Unintelligible speech or the requirement of communication aids.

(iv) Severe dysphagia or the offering of percutaneous endoscopic gastrostomy (PEG) tube placement for feeding.

(v) Dependence on wheelchair for mobility.

(vi) The use of urinary catheters.

(vii) Placement in residential or nursing home care.

The year of onset or occurrence of each was recorded. When the onset of a symptom was not documented, we recorded the time that the symptom was first documented. Judgments about onset of cognitive disability were the most difficult to make as confusion was often initially episodic (Kempster, Williams et al. 2007). Substantial and apparently permanent impairment of ability to perform tasks of daily living because of cognitive disability was the criterion used (severity criterion for dementia) (DSM-IV 1995). In cases where the presence of a milestone or the timing of reaching a milestone was unclear, these were decided by a joint review.

3. Clinical sub-division of PSP and MSA cases

The confirmed cases of PSP were subdivided when possible according to the two clinical phenotypes: 'Richardson's syndrome' (PSP-RS) and 'PSP-parkinsonism' (PSP-P) (Williams, de Silva et al. 2005). These groups were assigned according to the number of clinical features present in the first two years of disease. When falls, cognitive dysfunction, supranuclear gaze palsy, abnormalities of saccadic eye movements and postural instability were the predominant clinical features, patients were grouped as PSP-RS. However, PSP-P was designated if these features were absent in the first two years of disease in the presence of bradykinesia or tremor, levodopa response, asymmetric onset and limb dystonia (Williams, de Silva et al. 2005). When features of both groups were equal in the first two years patients were grouped as 'unclassifiable'.

In MSA, we compared patients presenting with symptoms and signs of autonomic dysfunction within the first two years from disease onset (early autonomic dysfunction - EAD). Because of referral bias to the Queen Square Brain Bank, which specialises in parkinsonian disorders, the vast majority of MSA cases were of the MSA-P subtype. Therefore comparisons between MSA-P and MSA-C were not possible.

4. Statistical Analysis

Clinical details including age at disease onset, age at death, disease duration were compared between patient groups. Mean results and comparisons for each milestone of advanced disease refer only to those patients in whom one of these event occurred. Univariable analyses using χ^2 for categorical and two-tailed t-test or the Mann–Whitney U-test, as appropriate, for continuous variables were applied. The interval in years from first symptom onset to each key motor impairment or death was graphically assessed using Kaplan-Meier curves, and curves from each patient subgroup were compared with the log rank test. Cox multiple stepwise regression analysis was performed in MSA and PSP for disease duration, using clinical factors present around disease onset (within the first two years) and gender as categorical covariates and age at onset as a continuous variable. Statistical analyses of data were performed with SPSS version 12.0 (SPSS, Chicago, IL).

D. Results

1. Clinical Features

A total of 123 cases of pathologically confirmed PSP were identified, of which 13 were excluded; 93 cases of pathologically confirmed MSA were identified, of which 10 were excluded. Cases were excluded because of incomplete data. Approximately 5% of included cases did not have adequate data to establish whether all clinical milestones were or were not reached.

Of the 110 cases of PSP, 69 (62.7%) were classified as RS and 29 (26.4%) as PSP-P. Twelve (10.9%) of the PSP cases were unclassifiable because of incomplete documentation of the defining symptoms, or equal numbers of symptoms in the "RS" and "PSP-P" criteria.

Of the 83 cases of MSA included, 42 (53.2%) had documented autonomic dysfunction within two years of disease onset.

A higher proportion of those patients with RS (86%) than PSP-P (41%) were diagnosed during life with PSP (χ^2, p<0.001). Patients with MSA and EAD were more likely to be diagnosed during life with MSA (χ^2, p=0.001). A higher proportion of males had EAD (male:female 1.5:1.0) than in the group of patients without EAD (0.4:1.0, χ^2, p=0.0012).

Clinical features were compared between cases with MSA or PSP in addition to comparisons between clinical subgroups of MSA and PSP [Table 2.1].

	PSP vs MSA			PSP subtypes			MSA subtypes		
	PSP	MSA	p	RS	PSP-P	p	With EAD	Without EAD	p
n	110	83		69	29		42	37	
Female (%)	41 (37%)	46 (55%)	0.013*	21 (32%)	14 (54%)	ns	17 (40%)	26 (70%)	0.012*
Age at onset (mean ± SD)	65.6 ± 8.4	56.8 ± 10.2	< 0.001**	66.5 ± 7.4	63.2 ± 9.9	ns	54.7 ± 9.5	58.1 ± 10.2	ns
Time from onset to diagnosis (mean ± SD)	3.5 ±2.6	3.7 ±2.5	ns	3.1 ± 2.0	4.0 ± 3.7	ns	3.7 ± 2.3	4.0 ± 2.7	ns
Disease duration (mean ± SD)	8.0 ± 4.1	7.9 ± 2.8	ns	6.3 ± 2.4	11.7 ± 4.9	<0.001**	7.2 ± 2.7	8.8 ± 2.7	0.014**
Age at death (mean ± SD)	73.8 ± 8.1	64.7 ± 9.0	< 0.001**	72.8 ± 7.1	74.9 ± 9.3	ns	61.9 ± 8.0	66.9 ± 8.9	0.01**
Clinical diagnosis correct	79 (72%)	58 (70%)	ns	59 (86%)	12 (41%)	<0.001*	37 (88%)	20 (54%)	0.001*
L-dopa responsive	28 (33.7%)	44 (62.9%)	0.001*	8 (17%)	19 (65.5%)	<0.001**	20 (62.5%)	22 (61.1%)	ns
L-dopa response (mean ± SD)	1.2 ± 0.9	1.9 ± 1.0	<0.001	0.9 ± 0.6	2.0 ± 0.9	<0.001**	1.7 ± 1.0	2.1 ± 1.0	ns
L-dopa responsive > 2 years	18 (27.7%)	24 (34.3%)	ns	5 (10.6%)	12 (41.1%)	0.004	12 (37.5%)	10 (27.8%)	ns

Table 2.1: Clinical features of included cases, according to disease (MSA or PSP) and disease subtypes. ns = not significant. EAD = Early Autonomic Dysfunction. * = Chi squared test. ** = Student's t-test

2. Survival comparisons between patient groups

Patients with PSP had an older age of onset than those with MSA (t-test, p<0.001), but disease duration was similar in both conditions [Table 1, Figure 1A-1E].

RS and PSP-P groups had similar mean ages of disease onset; however patients with RS had a shorter disease duration than those with PSP-P (t-test p<0.001, Log Rank (Mantel-Cox), p<0.001).

Patients with MSA with and without EAD had similar mean ages of disease onset, but those with EAD had a shorter disease duration (t-test, p=0.0014, Log Rank (Mantel-Cox), p=0.037) than those patients without EAD. Figures 2.1D – 2.1E describe survival curves in PSP and MSA according to the age of disease onset.

Figure 2.1 (overleaf): Kaplan-Meier survival curves from symptom onset according to clinical subtypes.

(A) Interval from disease onset to death in PSP and MSA (years). Log Rank (Mantel-Cox) df = 1, P = 0.5. PSP, green; MSA, blue.

(B) Interval from disease onset to death in PSP subtypes (years). Log Rank (Mantel-Cox), df = 2, P = 0.000. PSP-RS green; PSP-P blue; Unclassified yellow.

(C) Interval from disease onset to death in MSA subtype (years). Log Rank (Mantel-Cox), df = 1, P = 0.037. EAD green; no EAD blue.

(D) Interval from disease onset to death in PSP subtype (years) according to the age of symptom onset. Log Rank (Mantel-Cox), df=2, P=0.011 < 60 yrs old, blue; 60-69.9 yrs old, green; >70 yrs old yellow.

(E) Interval from disease onset to death in MSA subtype (years) according to the age of symptom onset. Log Rank (Mantel-Cox), df = 2, P = 0.000. <50yrs old, blue; 50-59.9 yrs old, green; >60 yrs old, yellow.

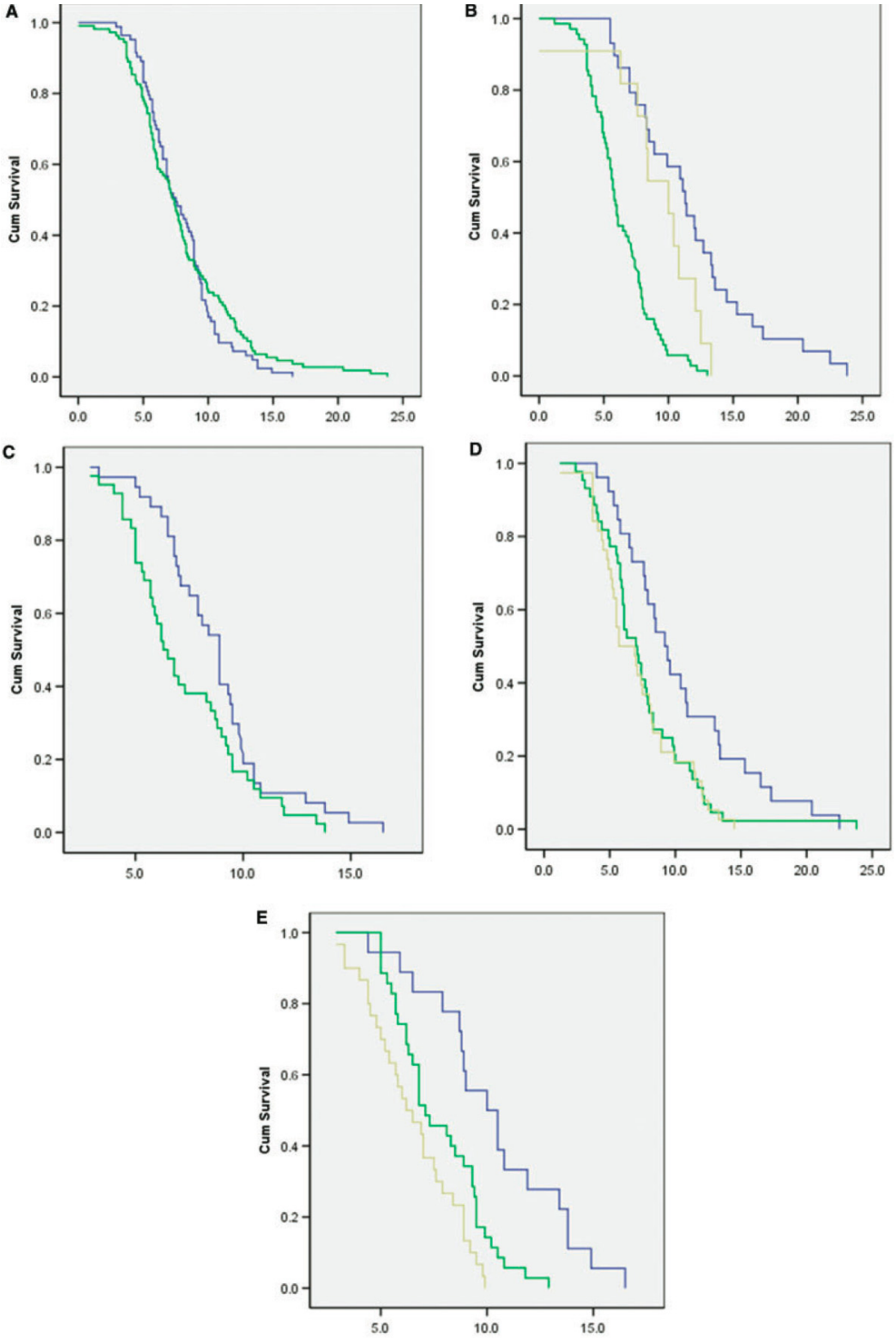
A
B
C
D
E
Cum Survival
1.0
0.8
0.6
0.4
0.2
0.0
0.0
5.0
10.0
15.0
20.0
25.0

3. Predictors of disease duration

Multivariate analyses performed using the Cox multiple stepwise regression model on early clinical features, age, and gender identified several clinical factors which independently influence disease duration.

In PSP, a PSP-RS phenotype, male gender, older age of onset, and a short interval from disease onset to reaching the first clinical milestone were all independent predictors of shorter disease duration until death. In MSA, EAD, female gender, older age of onset, a short interval from disease onset to reaching the first clinical milestone, and not being admitted to residential care were independent factors predicting shorter disease duration until death [Table 2.2].

	Independent Predictors	HR	95% CI	p
PSP	RS phenotype	2.37	1.21-4.64	0.01
	Age of onset	1.05	1.02 -1.1	0.005
	Male gender	1.7	1.03-2.91	0.038
	Interval between disease onset and reaching first clinical milestone	0.8	0.71 – 0.9	<0.001
MSA	Not admitted to residential care	2.8	1.45 – 5.46	0.002
	Early Autonomic dysfunction	6.0	3.1 -11.7	<0.001
	Age of onset	1.05	1.02 – 1.1	0.003
	Female gender	3.0	1.7-5.4	<0.001
	Interval between disease onset and reaching first clinical milestone	0.58	0.49 – 0.68	<0.001

Table 2.2: Factors affecting disease duration in PSP and MSA: independent predictors from Cox multiple regression analysis on early clinical features, age and sex

4. Clinical milestones reached - PSP vs MSA

Overall, 93% of patients had at least one clinical milestone documented prior to death. Fifty four patients with PSP and 33 patients with MSA reached ≥3 clinical milestones before death [Figure 2.2].

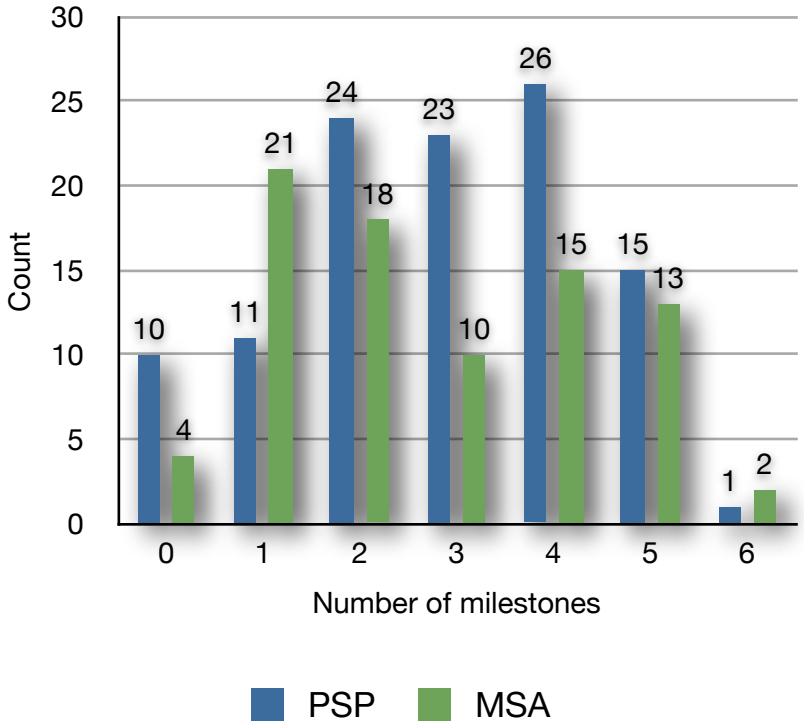

Figure 2.2: Number of clinical milestones per patient prior to death according to diagnosis.

Frequent falling was the most common first milestone reached in PSP (63.6%) and MSA (39.3%). The next most frequent first milestone in PSP was cognitive impairment (15.4%); in MSA the next most frequent first milestone reached was requiring urinary catheterization (29.4%). Approximately 10% of patients in both groups reached more than one 'first milestone' simultaneously. Patients with PSP reached their first clinical milestone earlier in the disease course, after a mean of 3.9 ± 2.7 years from disease onset, compared to patients with MSA at 5.3 ± 2.2 years (t-test, $p < 0.001$, Log Rank (Mantel-Cox), p=0.004) [Figure 2.3A]. Of the patients documented as having frequent falls, 53% of patients with PSP became wheelchair dependent (χ^2, p=0.001), and 50% of those with MSA became wheelchair dependent (χ^2, p=0.6). See table 2.3 for the proportion of patients in each clinical subgroup reaching individual clinical milestones, the mean intervals from disease onset to developing clinical milestones, and the mean intervals from developing a clinical milestone to death.

Comparing those patients reaching particular clinical milestones with either PSP or MSA, the following occurred after a shorter mean interval in the PSP group: regular falls (t-test, p= 0.000), unintelligible speech (t-test, p= 0.04), cognitive impairment (t-test, p= 0.03). A higher proportion of patients with PSP developed frequent falls (χ^2, p=0.001) and significant

cognitive impairment (χ^2, p=0.000) than patients with MSA. A higher proportion of patients with MSA required urinary catheterization (χ^2, p=0.000) [Table 2.3].

Milestone	Frequency and onset	PSP vs MSA			PSP subtypes			MSA subtypes		
		PSP	MSA	p	RS	PSP-P	p	With EAD	Without EAD	p
Frequent falls	n (%)	84 (82%)	47 (59%)	0.001*	60 (92%)	15 (60%)	0.001*	22 (55%)	23 (64%)	ns
	Time from onset (mean ± SD)	3.9 ± 2.5	5.5 ± 2.2	< 0.001 **	2.9 ± 1.5	6.0 ± 3.0	0.002**	5.7 ± 2.2	5.4 ± 2.4	ns
	Time to death (mean ± SD)	3.8 ± 2.4	2.8 ± 2.0	0.01**	3.1 ± 2.5	2.5 ± 3.2	ns	1.9 ± 1.5	3.8 ± 2.0	0.002 **
Wheelchair dependent	n (%)	48 (46%)	43 (54%)	ns	32 (47%)	13 (50%)	ns	23 (55%)	19 (56%)	ns
	Time from onset (mean ± SD)	6.4 ± 2.7	6.7 ± 2.2	ns	5.2 ± 1.9	9.1 ± 2.6	<0.001* *	6.6 ± 2.5	6.9 ± 1.8	ns
	Time to death (mean ± SD)	1.6 ± 1.2	1.4 ± 1.3	ns	0.7 ± 1.1	0.8 ± 1.3	ns	1.1 ± 1.1	1.9 ± 1.4	0.04* *
Unintelligible speech	n (%)	39 (38%)	34 (41%)	ns	28 (44%)	6 (23%)	ns	14 (33%)	19 (53%)	ns
	Time from onset (mean ± SD)	6.0 ± 2.5	7.2 ± 2.0	0.04**	5.7 ± 2.3	7.0 ± 3.9	ns	6.7 ± 2.0	7.6 ± 2.0	ns
	Time to death (mean ± SD)	1.5 ± 1.5	1.7 ± 1.6	ns	0.5± 0.9	0.7 ± 1.7	ns	1.7 ± 1.4	1.8 ± 1.7	ns
Severe dysphagia	n (%)	35 (33%)	26 (32%)	ns	28 (42%)	4 (15%)	0.02*	13 (32%)	12 (33%)	ns
	Time from onset (mean ± SD)	6.4 ± 2.4	7.2 ± 2.3	ns	5.9 ± 1.9	9.4 ± 3.8	ns	7.1 ± 2.4	7.6 ± 2.3	ns
	Time to death (mean ± SD)	1.0 ± 1.1	1.4 ± 1.2	ns	0.4 ± 0.7	0.2 ± 0.9	ns	0.9 ± 0.8	2.0 ± 1.3	0.02* *
Urinary catheter	n (%)	27 (26%)	49 (60%)	0.000*	18 (27%)	6 (23%)	ns	29 (71%)	18 (50%)	ns
	Time from onset (mean ± SD)	6.3 ± 3.1	6.1 ± 2.6	ns	5.4 ± 2.7	8.3 ± 3.2	ns	5.8 ± 2.7	6.9 ± 2.3	ns
	Time to death (mean ± SD)	1.2 ± 1.1	1.9 ± 1.7	0.02**	0.3 ± 0.8	0.2 ± 0.6	ns	1.9 ± 1.5	2.1 ± 2.0	ns
Cognitive impairment	n (%)	54 (52%)	11 (14%)	<0.001*	41 (62%)	7 (28%)	0.005*	5 (13%)	5 (14%)	ns
	Time from onset (mean ± SD)	4.2 ± 2.9	6.2 ± 2.4	0.03**	3.7 ± 2.4	6.5 ± 4.7	ns	6.6 ± 2.5	6.6 ± 2.0	ns
	Time to death (mean ± SD)	2.4 ± 1.8	1.1 ± 1.1	0.005**	1.4 ± 1.9	0.5 ± 1.0	0.001**	0.9 ± 0.5	0.8 ± 1.2	ns
Residential care	n (%)	27 (26%)	14 (18%)	ns	19 (28%)	5 (19%)	ns	5 (12%)	9 (25%)	ns
	Time from onset (mean ± SD)	6.1 ± 3.0	7.9 ± 3.3	ns	4.8 ± 2.0	9.9 ± 2.2	0.003**	9.0 ± 2.0	7.3 ± 3.8	ns
	Time to death (mean ± SD)	1.8 ± 1.3	2.1 ± 1.8	ns	0.4 ± 0.7	0.5 ± 1.3	ns	0.8 ± 0.6	2.7 ± 1.9	0.02* *
First milestone	n (%)	100 (91%)	79 (95%)	ns	68 (99%)	20 (69%)	<0.001*	40 (95%)	35 (95%)	ns
	Time from onset (mean ± SD)	3.9 ± 2.7	5.3 ± 2.2	0.000**	2.8 ± 1.7	6.2 ± 2.9	<0.001* *	5.4 ± 2.4	5.4 ± 2.1	ns
	Time to death (mean ± SD)	3.7 ± 2.2	2.6 ± 1.9	0.001**	3.5 ± 2.1	4.4 ± 2.8	ns	2.0 ± 1.5	3.4 ± 2.2	0.002 **

Table 2.3: Milestones of disease advancement according to disease (MSA or PSP) and disease sub-categories (RS v PSP-P, and MSA with v without early autonomic symptoms). *Chi squared test. ** Student's t-test.

See figures 2.3A-2.3H for Kaplan-Meier curves of the intervals to reaching clinical milestones.

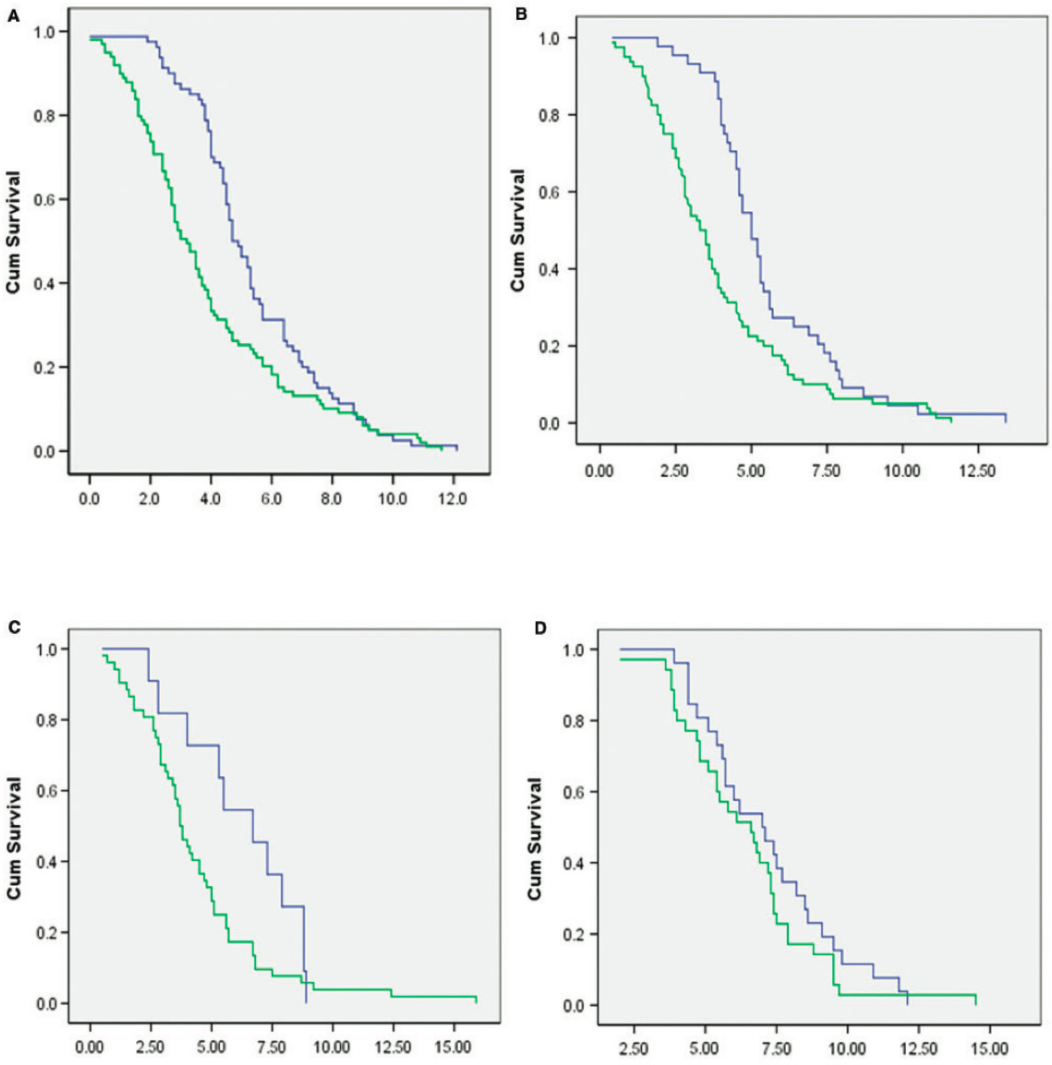

Fig.2.3 A-D: Comparison between PSP and MSA of interval from disease onset to reaching clinical milestones. PSP, green; MSA, blue.

(A) Interval in years from disease onset to the first clinical milestone reached. Log Rank (Mantel-Cox), df = 1, P = 0.004.

(B) Interval in years from disease onset to developing frequent falls. Log Rank (Mantel-Cox), df = 1, P = 0.003.

(C) Interval in years from disease onset to developing significant cognitive impairment. Log Rank (Mantel-Cox), df = 1, P = 0.07.

(D) Interval in years from disease onset to developing significant dysphagia. Log Rank (Mantel-Cox), df = 1, P = 0.29.

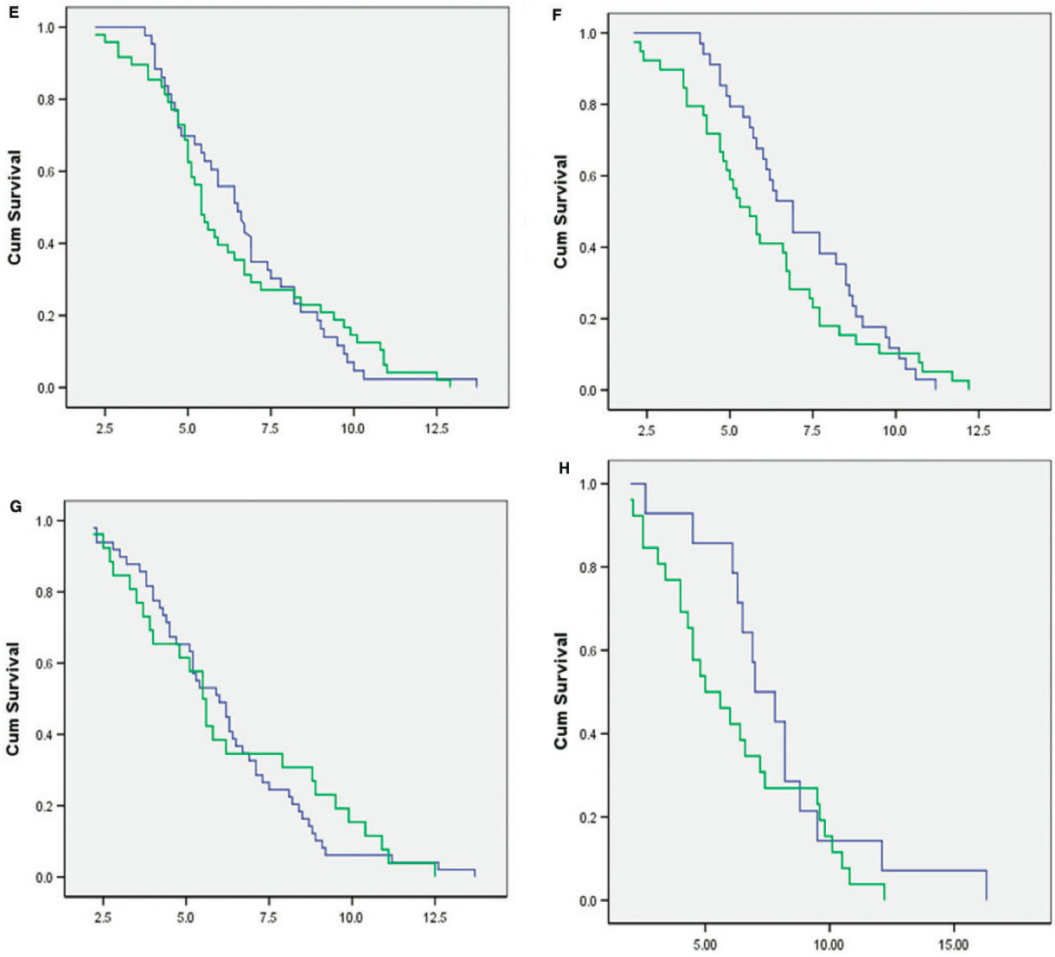

Fig.2.3 E-H: Comparison between PSP and MSA of interval from disease onset to reaching clinical milestones. PSP, green; MSA, blue.

(E) Interval in years from disease onset to developing wheelchair dependence. Log Rank (Mantel-Cox), df = 1, P = 0.95.

(F) Interval in years from disease onset to developing unintelligible speech. Log Rank (Mantel-Cox), df = 1, P = 0.28.

(G) Interval in years from disease onset to requiring urinary catheterization. Log Rank (Mantel-Cox), df = 1, P = 0.79.

(H) Interval in years from disease onset to requiring residential care. Log Rank (Mantel-Cox), df = 1, P = 0.23.

After reaching their first clinical milestone, patients with PSP had longer disease duration until death at 3.7 ± 2.2 years, than those with MSA at 2.6 ± 1.9 years (t-test, p = 0.001). Patients with PSP who develop regular falls (Log Rank (Mantel-Cox), df = 1, p=0.016) or significant cognitive impairment (Log Rank (Mantel-Cox), df = 1, p=0.015) have a longer disease duration from developing these milestones than patients with MSA who develop these milestones. Patients with MSA who require urinary catheterization live longer from reaching this milestone than patients with PSP (Log Rank (Mantel-Cox), df = 1, p=0.049). No other differences were seen between the PSP and MSA groups when comparing the intervals from reaching clinical milestones to death.

5. Clinical milestones reached: PSP-RS vs PSP-P

Patients with PSP-RS reached their first clinical milestone after a shorter interval from disease onset compared to patients with PSP-P (t-test, p< 0.001 Log Rank (Mantel-Cox), p<0.001). A higher proportion of patients with PSP-RS developed frequent falls (χ^2, p=0.001), significant cognitive impairment (χ^2, p=0.005) and severe dysphagia (χ^2, p=0.02) than patients with PSP-P. A similar proportion of patients with PSP-RS and PSP-P were documented as having the other clinical milestones, however these occur earlier in the disease progression in PSP-RS for the following: wheelchair dependence (t-test, p<0.001), requiring residential care (t-test, p= 0.003) [Table 2.3]. No differences between PSP-RS and PSP-P were seen comparing the interval following the development of particular milestones to death, apart from a longer survival from developing cognitive impairment in the PSP-RS group (t-test, p= 0.001).

6. Clinical milestones reached: MSA with EAD vs MSA without EAD

No difference was seen in the proportion of patients with MSA reaching clinical milestones or interval from disease onset to reaching a clinical milestone when this group was divided according to the presence of early autonomic dysfunction. However, the interval from developing the first clinical milestone and the following milestones, to the patients' deaths was shorter in those with EAD: frequent falls (t-test, p= 0.002), wheelchair dependence (t-test, p= 0.04), severe dysphagia (t-test, p= 0.02), and requiring residential care (t-test, p= 0.02) [Table 2.3].

E. Discussion

We have described the natural history of disease in pathologically confirmed PSP and MSA and compared the disease course according to sub-groups based on early presenting features. Progression of disease was measured using clinically significant milestones relevant to independence. We have identified early clinical features in PSP and MSA that are associated with a worse prognosis and found that a more rapid development of the first clinical milestone in both PSP and MSA is associated with a more rapid disease progression and shorter survival duration.

1. Comparison of the natural history in PSP vs MSA

a) Age at onset and disease duration

Patients with PSP were older at disease onset than those with MSA, consistent with previous studies describing the onset of PSP in the 7th decade (Nath, Ben-Shlomo et al. 2003; Papapetropoulos, Gonzalez et al. 2005; Golbe and Ohman-Strickland 2007) and MSA in the 6th decade (Wenning, Ben Shlomo et al. 1994). In both conditions the interval between disease onset to final clinical diagnosis was around 3.5-4.0 years, consistent with results seen in a comparison of non-pathologically confirmed cases of PSP and MSA (Testa, Monza et al. 2001).

The mean PSP disease duration of 8.0 ± 4.1 years in our study is similar to other clinical studies, showing a duration of between 6 and 10 years (Maher and Lees 1986; Golbe, Davis et al. 1988; Golbe and Ohman-Strickland 2007). The mean survival of patients with MSA of 7.9 ± 2.8 years in our study is consistent with previous data showing a survival duration of between 6 and 9 years (Ben-Shlomo, Wenning et al. 1997; Testa, Monza et al. 2001; Watanabe, Saito et al. 2002). We observed a predominance of males in PSP, when compared to MSA.

b) Diagnostic accuracy

Similar rates of diagnostic accuracy were seen between groups (70-72%), which are lower than those in a similar study which found a diagnostic sensitivity of 84-88% for PSP and MSA (Hughes, Daniel et al. 2002). A higher proportion of those with PSP-RS than PSP-P were correctly diagnosed with PSP during life which would be expected given that RS is the

classic PSP presentation and PSP-P often mistaken for PD (Williams, de Silva et al. 2005). MSA with EAD was more likely to be correctly diagnosed during life, when compared to those patients without EAD.

c) Clinical progression

Patients with PSP reach the majority of the milestones after a significantly shorter interval from disease onset, with only the requirement for urinary catheterization tending to occur later than in the course of MSA. This suggests that although survival figures in these two conditions are similar, the clinical burden of PSP which occurs in an older patient group is more significant. Although formal quality of life measures are not available in our study, given the degree of dependence for the activities of daily living seen in patients with PSP, quality of life may be more impaired in this condition.

2. Clinical factors predicting disease progression in PSP

We found that male gender, a short interval from disease onset to the development of the first clinical milestone, and older age of onset were associated with shorter disease duration. Previous studies on smaller numbers of pathologically-confirmed PSP cases have suggested early falls and dementia (Papapetropoulos, Gonzalez et al. 2005) and early dysphagia and incontinence (Litvan, Mangone et al. 1996) as poor prognostic indicators for disease progression and survival. In non-pathologically confirmed PSP, Nath and Golbe describe older age of disease onset, but not gender, being associated with a significantly higher relative mortality (Davis, Golbe et al. 1988; Nath, Ben-Shlomo et al. 2003).

However, the most significant predictor of a decreased survival in PSP that we identified is the RS clinical subtype of PSP (HR = 2.37, 95% CI = 1.21-4.64) which is based on the clinical phenotype seen within the first two years of disease onset. This subgroup has more severe tau pathology at post mortem (Williams, Holton et al. 2007).

3. Comparison of PSP-RS and PSP-P

PSP-RS patients had a similar age at disease onset but a more rapid disease progression than those patients with PSP-P as shown by the shorter disease course in RS and in the increased frequency of clinical milestones reached, and the development of frequent falls and wheelchair dependence at an earlier stage. Although it is important to note that early

falling in PSP-RS may influence these 'ambulatory milestones', there is also a trend for patients with RS to reach other milestones not always associated with mobility at an earlier stage including severe dysphagia, unintelligible speech, significant cognitive impairment, requirement for urinary catheterization, and admission to residential care.

4. Clinical factors predicting disease progression in MSA

Female gender, an older age of onset, a short interval from disease onset to the development of the first clinical milestone, and not being admitted to residential care were independent factors predicting shorter disease duration until death in MSA. Older age of MSA onset was seen to be associated with increased risk of death and wheelchair dependence in a study by Watanabe and colleagues, although gender was not found to be associated with difference in prognosis (Watanabe, Saito et al. 2002). Klockgether and colleagues found older age of disease onset to be associated with decreased survival, and also demonstrated an increased risk of wheelchair dependence in females, but no gender differences regarding survival (Klockgether, Ludtke et al. 1998).

Our finding of a potential beneficial effect on survival associated with admission to nursing home is interesting, when we consider that factors like severe dysphagia, which may benefit from nursing home care, are seen in a similar proportion of patients with PSP.

The most important early clinical prognostic feature regarding survival that we identified in MSA was that of EAD (HR = 6.0, 95% CI = 3.1 -11.7). In non-pathologically confirmed cases, MSA-P patients have been shown to have more rapid functional deterioration than MSA-C patients (Schulz, Klockgether et al. 1994; Watanabe, Saito et al. 2002) although this finding was not replicated in a study of 49 pathologically-proven MSA cases (Tada, Onodera et al. 2007). Instead, Tada and colleagues described a poor prognosis in patients presenting with EAD within 2.5 years of the onset of MSA symptoms (Tada, Onodera et al. 2007) which has previously been suggested as a prognostic factor (Watanabe, Saito et al. 2002).

In our study, patients with MSA with or without EAD had a similar age of disease onset but those with EAD had shorter disease duration. The higher proportion of males in the EAD group may reflect the frequency of documentation of erectile failure as an early symptom of autonomic failure in men, in comparison to the lack of documentation of secondary anorgasmia as a symptom of sexual dysfunction in women, a finding noted in previous studies (Wenning, Ben Shlomo et al. 1994). Although we did not find differences between

MSA sub-groups when analyzing the interval from disease onset to the development of other clinical milestones, we show that when patients with EAD reach the following clinical milestones, there is a shorter interval from this point to death – frequent falling, wheelchair dependence, severe dysphagia and requirement for residential care. These findings may also suggest an accelerated later stage of disease progression in this patient subgroup [Figure 2.4].

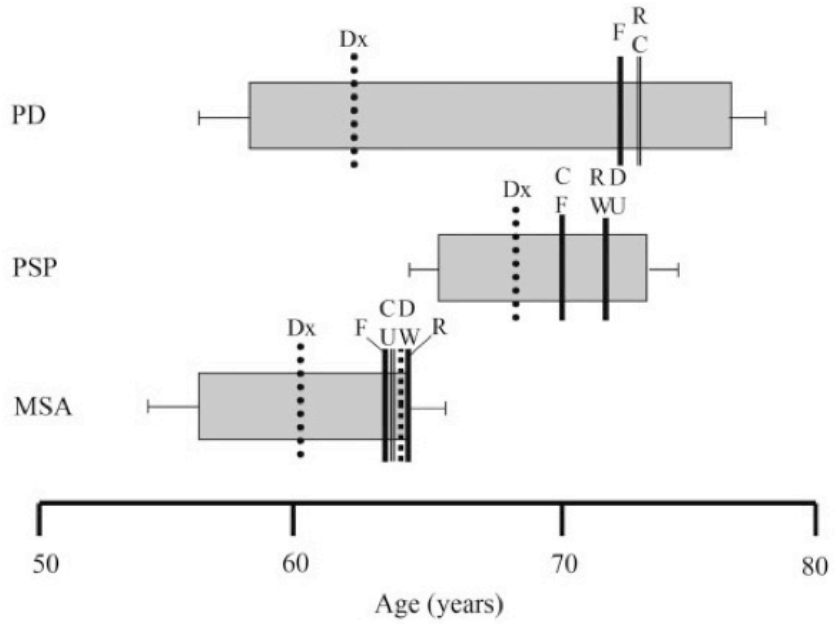

Figure 2.4: Milestones of disease advancement and total disease course. The grey rectangles represent disease duration, commencing with the time point of first symptoms. The vertical lines denote time of clinical diagnosis (Dx) and time of documentation of milestones (Residential care, R; Cognitive disability, C; Dysarthria/dysphagia, D; Frequent falls, F; Wheelchair dependent, W; Urinary catheter, U). Error bars for standard error of the mean.

5. Limitations

The retrospective data collection methodology and the selection bias that is expected in a brain bank post mortem series may account for the differences with previous studies (Maraganore, Anderson et al. 1999). As our data was obtained from different sources, without using a systematic history-taking method, it is likely that there is variability in the degree of documentation of various clinical milestones. For example, the number of patients (approximately 50%) who are documented as being wheelchair dependent may be an underestimate, given the proportion of patients with frequent falls (approximately 70%).

The fact that the milestones often were reached some time before a clinic visit may have reduced the accuracy of the timing of these determinations, particularly if patients were not reviewed on a frequent basis. The large number of patients, and the inclusion of patients who otherwise might not have been included in a prospective clinical study are relative strengths of this study.

F. Conclusions

We describe the natural history of pathologically-proven cases of PSP and MSA, and compare important clinical milestones according to disease sub-groups. These sub-groups are based upon early clinical features and may serve to improve the prognostic accuracy of clinicians. Further prospective studies with subsequent pathologically-confirmed diagnoses will be required to confirm validity of these early prognostic markers.

Chapter 3: Hypokinesia without decrement distinguishes progressive supranuclear palsy from Parkinson's disease

A. Introduction

1. Definition of Bradykinesia

Bradykinesia is key for the diagnosis of Parkinson's disease (PD) [Figure 1.2] (Gibb and Lees 1988). The term bradykinesia is often used interchangeably with the terms akinesia and hypokinesia. However, bradykinesia literally describes slowness in movements, akinesia means absence of expected spontaneous voluntary movement including slow reaction time (Hallett 2011), and hypokinesia refers to small amplitude movements. Bradykinesia, akinesia and hypokinesia are closely related but not necessarily correlated in individual patients. Each component of motor abnormality probably has a different underlying mechanism (Berardelli, Rothwell et al. 2001).

2. Bradykinesia in PD

Bradykinesia is explicitly defined in the Queen Square Brain Bank (QSBB) criteria for the diagnosis of Parkinson's disease as 'slowness of initiation of voluntary movement with progressive reduction in speed and amplitude of repetitive action' (Gibb and Lees 1988). Both bradykinesia and hypokinesia in PD improve with levodopa therapy whereas reaction time is thought to be related to non-dopaminergic deficit (Velasco and Velasco, 1973, Berardelli *et al.* , 1986, Jahanshahi *et al.* , 1992). The term 'sequence effect' is used to describe progressive reduction in amplitude and speed in sequential movements and is a key feature of PD (Berardelli, Rothwell et al. 2001; Iansek, Huxham et al. 2006). If the amplitude and speed on sequential movements progressively decline until the movement ceases, this is known as motor arrest (Marsden, 1989, Kim *et al.* , 1998, Iansek *et al.* , 2006). The pathophysiology and levodopa response of the sequence effect are unclear.

3. Bradykinesia in PSP

PSP is characterized by vertical supranuclear gaze palsy, early gait instability with falls characteristically in a backwards direction, axial rigidity and bulbar dysfunction. In the original description, elements of bradykinesia were seen in only two cases, one of whom had slowness in walking and the other had awkwardness in performing rapid repetitive movements (Steele, Richardson et al. 1964). In fact the authors were thoroughly convinced that clinically these were clinically distinct, as summarised in the following excerpt from the original description:

'….Though perhaps unnecessary, it is emphasised that none of these cases presented a clinical neurological picture which has been considered as parkinsonism by any of the numerous neurologists who have examined them. In earlier stages there have been features leading one to wonder if the case would progress to parkinsonism, but in all cases the fully developed clinical picture has differed widely from any acceptable definition of "parkinsonism". Aside from the absence of tremor there has not been any flexion of attitude, not has there been any parkinsonian posturing of hands. The gait has differed and there has been a preservation of associated movements unlike paralysis agitans. Of course the ophthalmolplegia has been much greater and different from the pseudo-ophthalmoplegia occurring in some cases…. The immobile facies of these cases is superficially similar to that of parkinsonism, but there are deeper lining and more frequent blinking… In later stages the rigidity of limbs and trunk in these cases does not present features similar to advanced stages of parkinsonism and other basal ganglion diseases…' (Steele, Richardson et al. 1964)

However current opinion considers PSP to be an example of 'atypical parkinsonism' and PSP to be one of the 'Parkinson's plus syndromes'. In support of this in post-mortem series of PSP early bradykinesia was reported in 75-88% of patients with pathologically confirmed PSP (Litvan, Agid et al. 1996; Williams, de Silva et al. 2005). Furthermore, up to 6% of cases with a clinical diagnosis of Parkinson's disease turn out to have tau pathology compatible with PSP at post-mortem examination (Hughes, Daniel et al. 2002). These and other findings have led to the delineation of two common clinical phenotypes: classical PSP, termed Richardson's syndrome (PSP-RS) and PSP-Parkinsonism (PSP-P) (Morris, Gibb et al. 2002; Williams, de Silva et al. 2005). In accordance with the original description of Steele et al, our clinical observations over the last ten years suggest that most PSP patients do not

exhibit slowness or progressive reduction in amplitude and speed during finger tapping or handwriting.

4. Micrographia in PD and PSP

Micrographia or small handwriting has been associated with focal cerebral lesions (Scolding and Lees 1994; Derkinderen, Dupont et al. 2002; Kim, Lee et al. 2005; Kuoppamaki, Rothwell et al. 2005), post-encephalitic parkinsonism (Froment, 1921), PD (McLennan, Nakano et al. 1972) and Huntington's disease (Iwasaki, Ikeda et al. 1999). Micrographia characterised by small handwriting with further progressive reduction in size can be observed in 15% of patients with PD (McLennan, Nakano et al. 1972). The relationship between micrographia and bradykinesia remains controversial (McLennan, Nakano et al. 1972). It is also not known if handwriting in PD differs from that in PSP.

B. Aims

Using objective measurements we assessed performance of repetitive finger tapping movements and handwriting in PD and PSP to determine whether there are any quantitative differences that may be of clinical utility. Repetitive finger tapping was selected as it is more severely impaired in PD patients than either the hand opening and closing or the hand pronation and supination elements of the motor section of Part III of the UPDRS (Agostino, Berardelli et al. 1998; Agostino, Curra et al. 2003).

C. Materials and Methods

1. Participants

Fifteen patients with PD, 9 with PSP and 16 healthy controls of similar age and gender ratio participated in this study. Patients fulfilled the United Kingdom Queen Square Brain Bank diagnostic criteria for PD (Gibb and Lees 1988), the Neurological Disorders and Stroke (NINDS) Society for PSP diagnostic criteria (Litvan, Agid et al. 1996) and were recruited from the movement disorder clinics in the National Hospital for Neurology and Neurosurgery, Queen Square, London, United Kingdom. PD patients were included if they were taking levodopa treatment with predictable motor fluctuations but were excluded if they had hand dystonia or if their tremor or dyskinesia were severe enough to interfere with their motor performance in the experiments.

Exclusion criteria included significant medical co-morbidity, cognitive impairment (Mini Mental State Examination score < 28) (Folstein, Folstein et al. 1975), depression (Beck depression score ≥ 21) (Beck, Ward et al. 1961) and disabilities that might restrict finger movements. All participants were assessed by the Edinburgh Handedness Inventory (Oldfield 1971). The UPDRS was performed in all patients (Fahn, Elton et al. 1987). The PSP Rating Scale (Golbe and Ohman-Strickland 2007) and the Frontal Assessment Battery (FAB) (Dubois, Slachevsky et al. 2000) were performed in patients with PSP. Patients' daily intake of anti-parkinsonian medications including levodopa, dopamine agonist, monoamine oxidase type B inhibitor, catechol-O-methyl transferase inhibitor and amantadine was recorded. Total daily levodopa equivalent dose (LED) was calculated for each patient according to published conversion formulae (Tomlinson, Stowe et al. 2010). The study was conducted with the understanding and written consent of all participants and was approved by the Camden and Islington Community Research Ethics Committee of the National Research Ethics Service.

2. Experimental Method

Participants were instructed to repeatedly tap their index finger and thumb as rapidly and as widely as possible for 15 seconds. The participants were instructed to relax the 3rd, 4th and

5th digits in a semi-extended position so that the index finger-thumb movements are not restricted. The beginning and the end of the 15-second each finger tapping trial were signalled by a buzzer. Infrared-emitting diodes were fixed to 8 designated regions on digits and the back of the hand, and motion was recorded in 3D (Coda Cx1, Charnwood Dynamics, Rothley, UK) [Figure 3.1]. Three 15-second trials were performed consecutively by each hand with 60 seconds rest in between. Hand order was pseudo-randomised across participants.

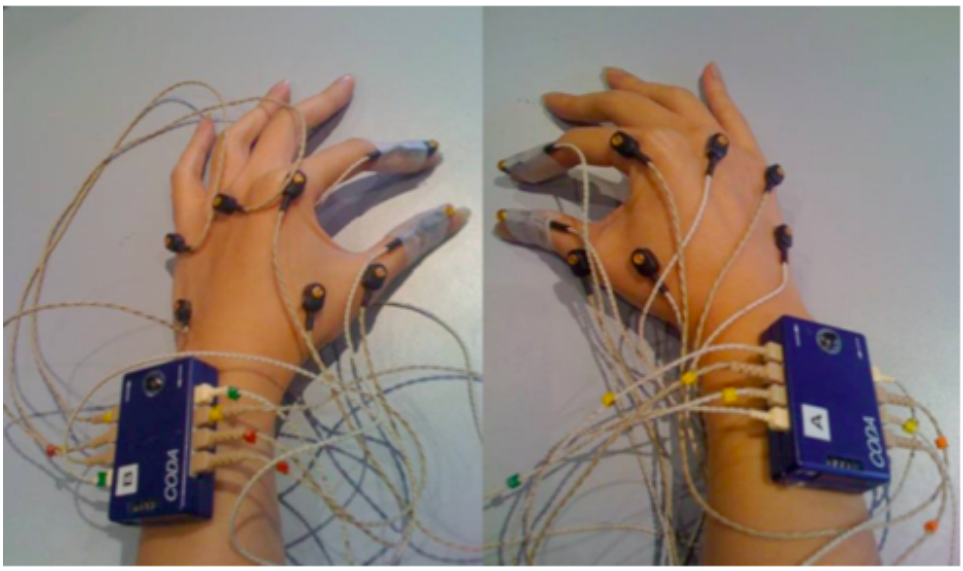

Figure 3.1: Light-emitting diodes fixed to 8 designated spots

PD patients were tested during 'OFF' in the morning after 12 hours of overnight withdrawal of levodopa therapy, followed by a second experiment during 'ON' in the afternoon one hour after taking levodopa. Only two PSP patients were receiving levodopa treatment and both underwent overnight withdrawal of medication for 12 hours prior to testing.

The handwriting task was performed after the tapping experiments by all participants and was repeated during 'ON' by PD patients. The participant was asked to copy three times a standardised print of an eleven-word sentence in Times New Roman, 34 font size, on unlined paper. No instructions were provided to the participants regarding the required size or speed of their script. The letters 'a' in the third (W3) and eleventh words (W11) were selected and measurements were obtained using Microsoft Paint® programme. The script size (cm^2) of the selected letter was determined by the product of height and width outlined by the upper, lower, left and right margins of the loop in the letter. The size of W3 and W11 were plotted separately against successive sentence trials (1 to 3). Progressive reduction in

size was represented by two slopes of the fitted linear regression line across the scatter-plots: script slope 1 from W3 and script slope 2 from W11.

3. Determining kinematic parameters

Amplitude (mm), cycle duration (ms) and mean speed (mm/s) were measured for each cycle from one finger-thumb separation to the next using custom scripts written in Matlab [Figure 3.2]. Mean speed, designed to be sensitive to both amplitude and cycle duration, was the mean rate of change in aperture regardless of whether the aperture was opening or closing. Thus, mean speed decreased when the cycle duration increased independently of amplitude, when amplitude decreased independently of duration, and when both occurred simultaneously. If amplitude increased at the expense of cycle duration, or vice versa, the mean speed tended to stay constant. Close and open velocities (mm/s) were the peak velocities of aperture closure and opening within a cycle. To eliminate potential confounding factors of different hand size and finger length across participants, distance (mm) measured was converted into the degree (deg) of angle separation between index finger and thumb. The conversion was obtained by the product of distance (mm) and k-value (deg/mm), calculated by the linear regression slope of maximum finger-thumb separation angle against maximum finger-thumb separation distance of each hand of the participant.

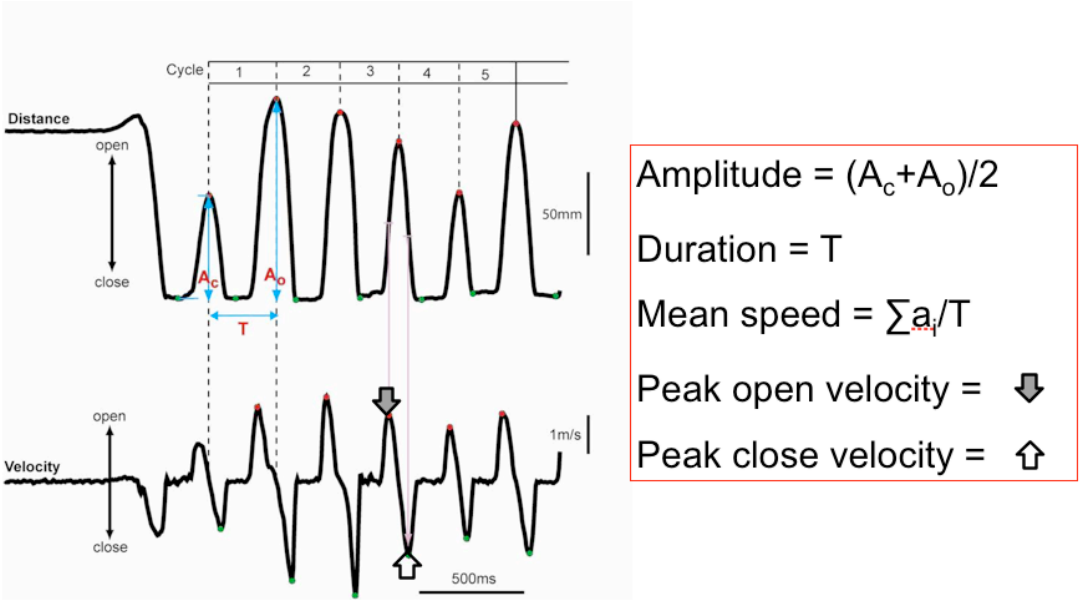

Figure 3.2: Finger-thumb separation parameters

Progressive changes in amplitude, duration and speed across a 15-second finger tap trial were represented by the slope of the fitted linear regression line across the scatter-plot of the kinematic parameter against the tap cycle. The slope of change in amplitude was used to assess progressive hypokinesia or 'decrement'. The slope of change in speed which encompassed both amplitude and duration was used to assess progressive slowing of movement or 'fatigue' [Figure 3.3]. Measurement of regularity of amplitude and speed across a tap trial was represented by the coefficient of variation (CV), which was computed by the residual standard deviation about the linear regression line divided by the mean value. High amplitude or speed CV values represent irregularities of these kinematic parameters.

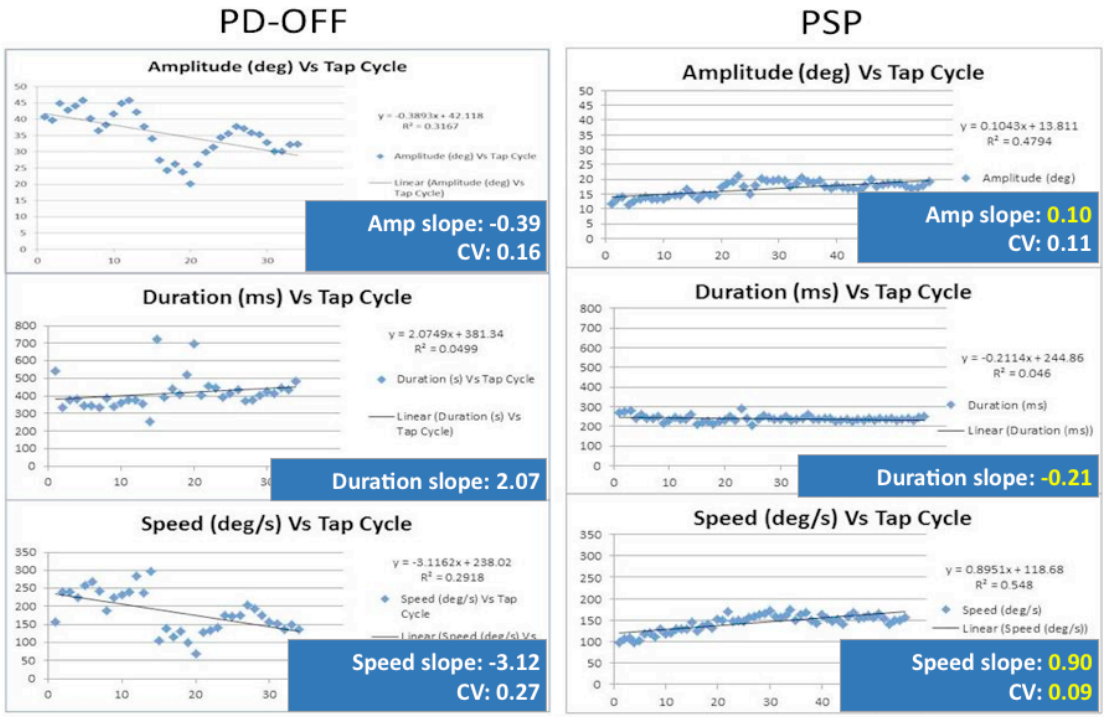

Figure 3.3: Kinematic parameters during the first 15s right finger tap trial in a Parkinson's disease patient when OFF (left) and PSP patient (right). Slopes for amplitude, duration and speed, and coefficient of variation for speed are shown. Lack of decrement and fatigue in PSP is shown by positive amplitude and speed slopes. The speed coefficient of variation is 0.27 in PD vs 0.09 in PSP indicating high speed irregularity in PD.

Group parameters including amplitude, cycle duration, maximum close velocity, maximum open velocity, mean speed, slopes and CVs were summarized by computing the mean parameter value for all tap cycles across three finger tap trials of both hands for all subjects.

4. Statistical analysis

Comparisons of continuous variables were carried out by univariate Analysis of Variance (ANOVA) with gender, age and disease duration as covariates to ensure comparisons were adjusted for any gender, age and disease duration differences across subjects. Student's t-test was used to compare disease duration and total daily levodopa equivalent dose between two patient groups. Tukey HSD post-hoc analysis was used to determine differences between groups (controls, PD-OFF and PSP). Paired t-tests were used to compare variables of PD patients in ON vs. OFF states. χ^2 test was used for discrete variables. Spearman's correlation was used to study correlation between group parameters and clinimetric scores. Statistical significance was determined when $p \leq 0.05$. SPSS version 17.0 was used for statistical analysis.

D. Results

1. Demographic and clinimetric features

	Controls (N=16)	PSP Patients (N=9)	PD Patients (N=15)	p-values
Age (years)	68.9 ± 4.5	70.9 ± 8.3	65.0 ± 9.2	0.14**
Gender	9M : 7F	5M : 4F	9M : 6F	0.97#
Handedness	13R : 3L	7R : 2L	14R : 1L	0.51#
Edinburgh Handedness Inventory	61.9 ± 56.4	55.6 ± 77.3	78.0 ± 50.9	0.62**
Disease duration (years)	NA	4.5 ± 3.3 (1.0-12.0)	10.8 ± 7.5 (2.0 – 26.0)	0.01*
Total daily levodopa equivalent dose (mg/day)	NA	255.6 ± 194.4	874.8 ± 323.9	<0.001*
UPDRS				
I	NA	NA	3.1 ± 2.5	
II-ON	NA	NA	7.7 ± 3.9	
II-OFF	NA	NA	17.2 ± 8.7	
III-ON	NA	NA	24.4 ± 9.3	
III-OFF	NA	41.6 ± 14.1	36.3 ± 9.7	
IV	NA	NA	6.7 ± 4.3	
H&Y				
ON	NA	NA	2.1 ± 0.4	
OFF	NA	NA	2.8 ± 0.6	
PSP Rating Scale	NA	39.4 ± 2.4	NA	
FAB	NA	14.4 ± 2.4	NA	

Table 3.1: Demographic and Clinical data. Mean ±SD. * Student's t-test. ** ANOVA. # Pearson Chi square test. NA not applicable.

The demographic features and clinimetric scores are listed in table 3.1. Age was closely matched between groups. There were slightly more male participants than female in each group and the majority of participants were right-handed.

All PD patients were receiving dopamine replacement therapies and all of them had derived good or excellent sustained therapeutic benefit. In PD there were significant improvements in the UPDRS II, III, H&Y scores one hour after taking levodopa (OFF Vs. ON; $p<0.001$ for all). The mean total daily levodopa equivalent dose in PD was greater than that of PSP (t-test, $p<0.001$). Eight PSP patients were taking amantadine but only two were receiving levodopa therapy. The PSP patients who were not receiving levodopa had failed to respond to levodopa and had a negative therapeutic response to an acute levodopa challenge (Steiger and Quinn 1992). The mean bradykinesia subscore, which included the sum of UPDRS motor scores for finger tap, hand opening and pronation/supination movements, also improved after levodopa therapy (OFF: 2.06±0.54; ON: 1.76±0.66; paired t-test, $p=0.009$).

Five of 9 PSP patients had evidence of midbrain atrophy on their most recent MRI. One PSP patient died six months after participating in this study and his pathological diagnosis was confirmed to be PSP at post-mortem. The mean disease duration in PD was longer than in PSP (t-test, $p=0.01$).

2. Repetitive finger tap movements

Amplitude, duration, peak velocities, and mean speed were measured for each tap cycle and used to calculate mean performance, progressive changes in performance (slope of linear regression line of variable against cycle number), and regularity of performance (coefficient of variation; CV) achieved over a 15-s trial. One-way ANOVA revealed significant differences between the three groups for all measures apart from slope of cycle duration [Table 3.2].

		Controls (N=16)	PSP (N=9)	PD-OFF (N=15)	F(1,19)	p values
Average number of tap cycles/15s		50.04 (10.7)	52.22 (10.3)	41.54 (9.7)	8.53	0.009*
Average parameters	Amplitude (deg)	45.91 (8.7)	18.65 (6.3)	37.82 (16.0)	18.53	<0.001*
	Duration (ms)	295.80 (65.6)	288.34 (67.7)	356.51 (80.6)	7.80	0.012*
	Close velocity (deg/s)	-928.22 (215.2)	-386.28 (134.4)	-737.46 (385.0)	11.39	0.003*
	Open velocity (deg/s)	788.91 (167.9)	327.72 (106.1)	584.40 (297.0)	10.34	0.005*
	Speed (deg/s)	330.13 (64.6)	142.90 (49.8)	224.08 (93.1)	8.33	0.009*
Average CVs	Amplitude CV	0.09 (0.03)	0.27 (0.13)	0.14 (0.08)	9.69	0.006*
	Duration CV	0.09 (0.03)	0.28 (0.18)	0.17 (0.10)	4.26	<0.001*
	Speed CV	0.09 (0.02)	0.236 (0.9)	0.167 (0.06)	6.88	0.017*
Average slopes values	Amplitude slope (deg/cycle)	-0.12 (0.12)	0.01 (0.17)	-0.20 (0.21)	4.45	0.048*
	Duration slope (s/cycle)	0.77 (0.75)	1.86 (2.58)	1.49 (2.39)	0.16	0.70
	Speed slope (deg/s/cycle)	-1.52 (0.81)	-0.39 (0.79)	-1.71 (1.59)	7.81	0.012*

Table 3.2: Mean measurements (SD) for control, PD-OFF and PSP with ANOVA adjusting for age, gender and duration of disease. CV coefficient of variation.

3. Healthy subjects

Linear regression analysis did not show a significant correlation of any variable with age or gender. Mean cycle duration was longer for the non-dominant hand (dominant hand: 289.38±64.6ms; non-dominant hand: 302.23±67.5ms; p=0.003) but no other performance parameters differed between the two hands.

The slope of the dominant hand's mean speed was significantly more negative in the third trial compared to the first (trial 1 speed slope=-1.03 deg/s/cycle; trial 3 speed slope=-1.46

deg/s/cycle; p=0.043), indicating an increase in physiological fatigue. All other parameters showed a similar, but non-significant, slight decline in performance in progressive trials.

4. PSP patients

In PSP small amplitudes of finger-thumb separation distance with a lack of decrement and with excessive variability of performance between cycles were seen.

The small mean amplitude in PSP (mean=18.65deg) was less than half that of healthy subjects (mean=45.91deg) and PD-OFF (mean=37.82deg) (p<0.001 in both cases) [Table 3.2 & Figure 3.4a]. The amplitude slope in PSP had a positive value of 0.01, indicating a lack of amplitude decrement. This value differed significantly from the negative slope in PD-OFF (p=0.002) [table 3.2 & figure 3.4b]. After adjusting for the low mean amplitude in PSP, there was no difference in mean amplitude slope between PSP and controls, indicating an absence of decrement in PSP [p=0.36, table 3.3].

A greater number of tap cycles were achieved by PSP patients (mean=52.22 cycles/15s) when compared to PD-OFF (mean=41.54 cycles/15s; p=0.046), but not controls (50.03 cycles/15s) [table 3.2].

Although the cycle duration was normal in PSP, the markedly reduced amplitude led to an overall reduction in close and open velocities and mean speed in PSP when compared to PD-OFF (close velocity: p=0.01; open velocity: p=0.02; mean speed: p=0.04) and controls (p<0.001 in all) [table 3.2 & figure 3.4a]. This probably does not indicate an intrinsic slowing of movement as such, but simply stems from the digits moving through a smaller distance in approximately the same time.

	PD-OFF vs. Controls		PSP vs. Controls		PSP vs. PD-OFF	
	F(1,26)	p values	F(1,20)	p values	F(1,18)	p values
Amplitude slope (adjusted for mean amplitude)	4.41	0.046*	0.88	0.36	4.45	0.048*
Duration slope (adjusted for mean duration)	0.47	0.501	3.75	0.067#	3.20	0.09#
Speed slope (adjusted for mean speed)	2.89	0.070#	1.70	0.208	3.33	0.085#

Table 3.3: p values for the comparisons of slope values between PD-OFF, PSP and controls after adjusting for mean amplitude, duration and speed respectively. General linear model univariate analysis (*significant, p<0.05, # borderline significant, p=0.05-0.10). Covariates appearing in the model PD-OFF vs. controls are evaluated at the following values: gender = 0.58, age = 66.99, mean amplitude for amplitude slope model = 42.34, mean duration for duration slope model = 325.18, mean speed for speed slope model = 278.81. Covariates appearing in the model PSP vs controls are evaluated at the following values: gender = 0.56, age = 69.6, mean amplitude for amplitude slope model = 36.09, mean duration for duration slope model = 293.12, mean speed for speed slope model = 262.73. Covariates appearing in the model PSP vs. PD-OFF are evaluated at the following values: gender = 0.58, age = 67.19, disease duration = 8.43, mean amplitude for amplitude slope model = 31.08, mean duration for duration slope model = 330.95, mean speed for speed slope model = 193.64; *F*(degrees of freedom) = f value from univariate analysis of variance

In PSP there was greater variability of performance from one cycle to the next as reflected in the highest CV values. They were greater than control for amplitude CV, cycle duration CV and mean speed CV (p<0.001 in all cases) and were also greater than PD-OFF for amplitude CV (p=0.001) and mean speed CV (p=0.009).

Among the PSP group, there was no correlation between mean amplitude and clinical markers of disease severity including disease duration, total daily levodopa equivalent dose, UPDRS motor score, H&Y, PSP staging or Frontal Assessment Battery scores (p>0.05 for all). There was a positive correlation between the number of tap cycles/15-s and the Frontal Assessment Battery score in PSP (Spearman's coefficients: 0.64; p=0.04).

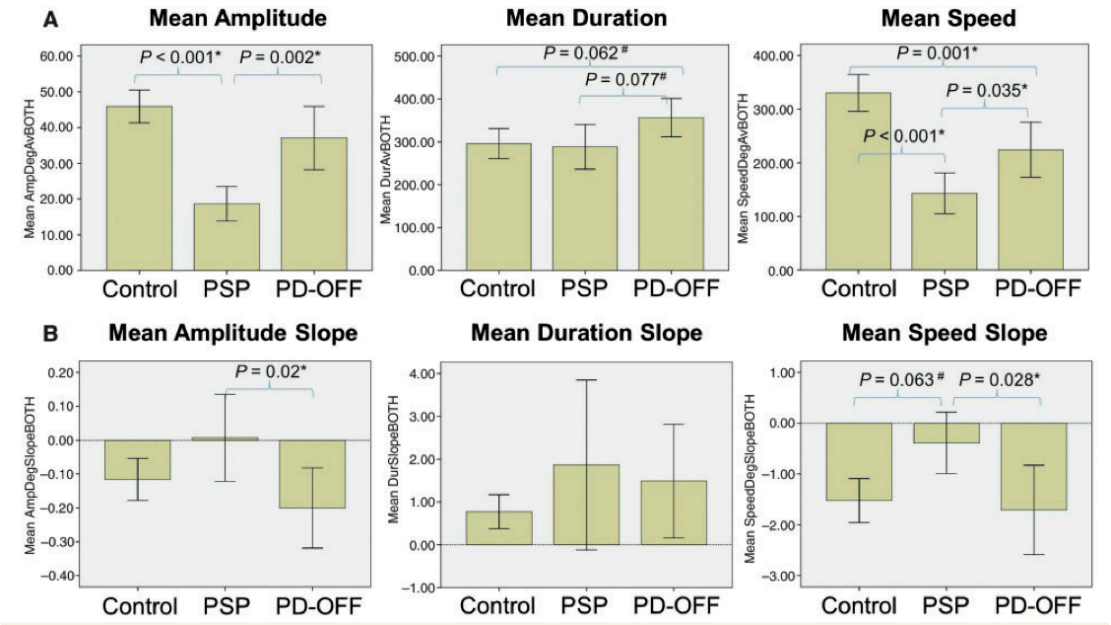

Figure 3.4:

(A) Mean amplitude, duration and speed of control, PSP and PD-OFF groups and p-values by post hoc analysis. Error bars represent 95% confidence intervals. *P < 0.05 indicates statistical significance and #P = 0.05–0.10 indicates borderline significance by Tukey HSD post hoc analysis.

(B) Mean slope values for amplitude, duration and speed of control, PSP and PD-OFF groups and P-values by post hoc analysis. Error bars represent 95% confidence intervals. Dotted reference lines represent zero, values below which represent progressive downward negative slope across the 15-s finger tap trial. *P < 0.05 indicates statistical significance and #P = 0.05–0.10 indicates borderline significance by Tukey HSD post hoc analysis.

4. PD patients

When compared with controls, the main finding in PD-OFF was slowness of movement with greater variability of speed between tap cycles. When compared with PSP, PD-OFF exhibited larger amplitude movements, a smaller number of tap cycles, and greater decrement of performance during a trial.

PD-OFF amplitude tended to be smaller than that in healthy subjects (p=0.10) while cycle duration tended to be more prolonged (p=0.06), but only with borderline significance.

However, the combination of both these trends led to a highly significant lower mean speed of PD-OFF compared with controls (p=0.001) [figure 3.4]. Similarly, peak open velocity of PD-OFF was less than controls (p=0.033), although there was no difference in peak close velocity between the two groups. In addition, CV of mean speed in PD-OFF was significantly greater than that of controls (p=0.004), suggesting proportionally greater irregularities between cycles.

Both amplitude and speed slopes in PD-OFF, reflecting the progressive decrement in performance, were more strongly negative when compared to those of PSP (amplitude: p=0.002; mean speed: p=0.028). However, the negative amplitude and speed slopes of PD-OFF, were numerically, but not significantly, greater than in healthy subjects. In PD patients with severe parkinsonism, slope measurements may be underestimated due to poor performance during the tap trial, which would render their slope values lower than patients with milder disease severity who do not exhibit a 'floor' effect. After adjusting for differences in mean amplitude, the amplitude slope in PD-OFF became significantly more strongly negative than PSP and healthy controls (PD-OFF vs PSP, p = 0.048; PD-OFF vs controls, p=0.046) [table 3.3]. There was a trend for a more negative speed slope in PD-OFF when compared to controls after adjusting for mean speed (p=0.07) [table 3.3]. These findings demonstrate progressive decrement in performance in PD-OFF and represents sequence effect in PD.

The UPDRSIII-OFF score was correlated with small amplitude (Spearman's coefficient: -0.79, p<0.001), slow mean speed (Spearman's coefficient: -0.68, p=0.005) and high irregularities in speed (Spearman's coefficient: 0.75, p=0.001). There was no correlation between performance decrement, i.e. slopes for amplitude and speed, and disease duration, total daily levodopa equivalent dose, UPDRS motor scores or H&Y (p>0.05 in all cases).

Levodopa therapy improved the total number of tap cycles (OFF: 41.5±9.7; ON: 45.9±9.5, p=0.04), peak open velocity (OFF: 584.4±297.0; ON: 639.9±269.0; p=0.04), mean speed (OFF: 224.1±93.1; ON: 255.6±86.4; p=0.006) and speed CV (OFF: 0.167±0.07; ON: 0.150±0.08; p=0.014). However, levodopa therapy did not significantly improve

performance decrement (amplitude slope: OFF=-0.20±2.1; ON=-0.17±2.1; speed slope: OFF=-1.71±1.6; ON=-1.78±1.4).

When analysis of the effect of levodopa was limited to the PD patients' more affected hand, more robust ON vs OFF differences were observed. In addition to the improvements described above, improvement was also observed in mean cycle duration (OFF: 370.8±103.6; ON: 321.1±93.2; p=0.005) and there was a trend towards improvement in performance decrement (amplitude slope: OFF: -0.20; ON: -0.15; p=0.07).

5. Hypokinesia without decrement

Hypokinesia was defined as a mean amplitude of less than 23deg, i.e. 50% of the mean amplitude in the control group. Hypokinesia was observed in 70% of the finger tap trials in the PSP group, 24% of the PD-OFF group and 2% of the control group. The remaining 30% of finger tap trials in the PSP group had a small mean amplitude of 27.8 ±3.7 deg and a positive mean amplitude slope of 0.05deg/cycle. The 24% of the PD-OFF group with hypokinesia were performed by 4 patients who had severe parkinsonism with a mean UPDRSIII-OFF score of 46.4 and a long mean disease duration of 17.5 years. All 4 patients had good levodopa response and an average improvement in UPDRS motors score by 14.3 one hour after intake of levodopa therapy. Despite severe hypokinesia with a mean amplitude of 11.4 ±5.6 deg, decrement was still evident with a negative mean amplitude slope of -0.037 ±0.1 deg/cycle (vs control, p=0.05). When lack of decrement, defined as a positive amplitude slope, was combined with hypokinesia, 87% of finger tap trials in the PSP group, 12% in the PD-OFF group and none in the control group exhibited these features.

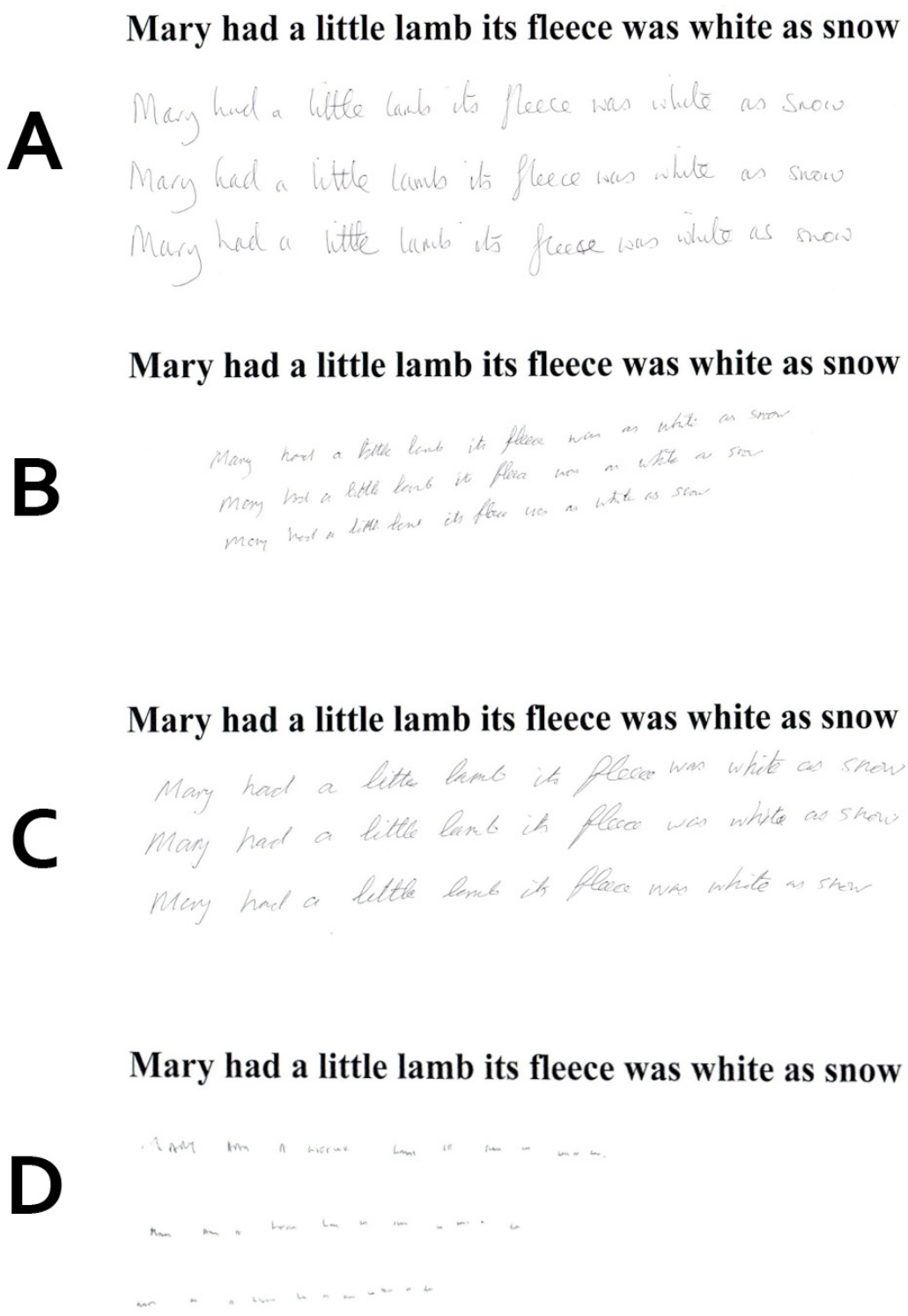

Figure 3.5: Handwriting examples. [A] healthy 65 yr old female; [B] 58 yr old PD-OFF; [C] the same 58 yr old PD-ON; [D] PSP

6. Handwriting in PD and PSP

The scripts by 1 PSP and 2 PD patients were discarded from the analysis as they were written in capital letters. The mean script size of PSP (0.50cm^2±0.42) was numerically, but not statistically, smaller than PD-OFF (0.76cm^2±0.37) and controls (0.75cm^2±0.19)(p=0.25) [Figure 3.5]. In all groups, there was less progressive reduction in the letter 'a' of the third word (script slope 1) than the tenth word (script slope 2) in successive sentences. The mean script slope 2 was significantly different between PSP (2.33±3.22) and PD-OFF (-3.24±11.15) after adjusting for age, gender, disease duration and mean script size (p=0.01). A similar trend was found in the mean script slope 1 (PSP: -0.15±7.76; PD-OFF: (-3.84±7.69; p=0.16).

Micrographia was determined as present when the mean script size was less than 0.40cm^2, i.e. half the mean script size of the control group, and the lack of progressive micrographia was represented by a positive mean script slope. Micrographia was more frequent in PSP (N=6, 75%) than in PD-OFF (N=2, 15.4%) and control (N=1, 6.3%) (p=0.003). Micrographia persisted in the same PD patients after levodopa therapy; their mean script size slightly improved but did not make the cut-off of 0.40cm^2. Positive script slope 2 was more frequent in PSP (N=5, 62.5%) than in control (N=1, 6.3%) and PD-OFF (N=2, 15.4%)(χ^2, p=0.005). A similar trend was noted in script slope 1 (PSP: N=6, 75%, PD-OFF: N=3, 23.1%, Control: N=8, 50%; χ^2, p=0.06). The smallest script size (mean=0.14cm^2) was observed in a patient with advanced PSP.

A positive script slope 1 was more frequent in PSP (n = 6, 75%) than in PD-OFF patients (n = 3, 23.1%; P = 0.03), but it did not differ from control subjects (n = 8, 50%; P = 0.23). The patients with the smallest script size in the PSP and PD-OFF groups were also noted to have the most severe UPDRSIII score in their group (minimum script size in PSP = 0.14 cm2, UPDRSIII = 69; minimum script size in PD-OFF = 0.11 cm2, UPDRSII I = 50).

There were more patients with PSP (n = 5, 62.5%) who had both hypokinesia (<23deg) and micrographia (50.40cm^2) than the control (0; P = 0.001) and the PD-OFF (n = 1, 7.7%; P = 0.014) groups. In PSP, the finger tap amplitude slope was strongly correlated with script

slope 2 (Spearman's coefficient = 0.88, P = 0.004). No correlation was found between script findings and markers of disease severity in either Parkinson's disease or PSP groups.

E. Discussion

1. Bradykinesia in Parkinson's disease

We have made objective recordings during repetitive finger tap movements and found that progressive decrements in amplitude were present in PD but not in PSP. The characteristic finger tap pattern in PD consists of slowness with variability in speed and progressive decrement in performance, as demonstrated here and in previous studies (Agostino, Berardelli et al. 1994; Agostino, Berardelli et al. 1998). Although levodopa improved most tapping parameters in PD, it did not improve the sequence effect of progressive deterioration in cycle duration and speed. However, there was a borderline improvement in decrement in treated PD when only the more affected hand was studied. We conclude that the sequence effect in PD may be relatively independent of dopaminergic regulation.

This is supported by a recent study using a Modified Purdue Pegboard Test showed that the sequence effect in PD did not respond to levodopa medication (Kang, Wasaka et al. 2010). Furthermore, gait freezing may be a consequence of a combination of hypokinesia and the sequence effect, and in another study, reduced stride length (hypokinesia) improved with either levodopa or visual cues, but the progressive reduction of stride length (the sequence effect) only improved with cueing (Iansek et al. , 2006). We found that the variability of speed was significantly greater in PD-OFF when compared to controls, and that it improved with levodopa therapy, suggesting that the mechanisms underlying the temporal regularity of movements and the sequence effect are likely to be different.

2. Hypokinesia without decrement in PSP

In PSP the index finger-to-thumb separation amplitude during repetitive finger tapping was markedly reduced. The average amplitude of finger separation in PSP was less than half of that in controls and PD-OFF. PSP patients also had a greater number of tap cycles and higher variability in amplitude and speed when compared to PD-OFF. The greater number of tap cycles was likely related to the small amplitude as the digits were moving through a smaller distance and more cycles were performed within a given time.

While small amplitude in the PD-OFF group was correlated with more severe UPDRS motor score, there was no correlation between the amplitude and markers for disease severity in the PSP group. Hence, the differences in disease duration between PD and PSP could not account for the reduced mean amplitude in PSP. Also, the finding of severe hypokinesia in PSP in relation to PD-OFF was not dependent on medication state because all PD and PSP patients were tested after 12 hour-withdrawal of anti-parkinsonian medication.

In the PSP group there was no evidence for progressive reduction in amplitude. It is compatible with our clinical observations that most PSP patients do not exhibit progressive reduction in performance during repetitive finger tapping. The positive amplitude slope of 0.01 in PSP was similar to controls but differed significantly from the negative slope of -0.2 in PD-OFF. The possibility that lack of decrement in PSP might be due to a floor effect caused by severe hypokinesia would seem unlikely, as even among the subgroup of PD patients with severe hypokinesia (amplitude<23deg), we noted a mean amplitude slope of -0.037deg/cycle (vs controls, p=0.051), and furthermore when comparisons between amplitude slopes of the patient groups and controls were performed after adjustment for any differences in mean amplitudes between groups the amplitude slope in PD-OFF was more negative than in PSP and controls [Table 3.3], while there was no difference between PSP and controls. These findings support the notion of minimal or lack of performance decrement and sequence effect in PSP which would not fulfil the QSBB criteria for bradykinesia (Gibb and Lees 1988).

3. Implications for bedside finger tap assessments

'Hypokinesia without decrement' was identified in 87% of finger tap trials in the PSP group and only 12% of the PD-OFF group. This finding might be particularly useful in patients with PSP-Parkinsonism (PSP-P), of which the clinical symptoms can mimic PD. The remaining PSP finger tap trials also had a small mean amplitude of 27.8deg, but not quite making the cut-off value of 23deg for hypokinesia. Small finger tap amplitudes can be easily recognized by careful bedside examination. Small degrees of decrement may however be difficult to detect in patients with Parkinson's disease with severe motor impairment who have small

amplitude finger movements on initiation of finger movements. These patients are readily differentiated from PSP by their sustained levodopa response and relatively long disease duration.

The PD patients with severe hypokinesia in the present study had a mean disease duration of 17.5years, whereas the mean disease duration from diagnosis to death in PSP is 7 years (Williams, de Silva et al. 2005). In addition to decrement, delayed initiation of voluntary movements and motor arrests during repetitive finger tapping were other findings in PD which may also have clinical usefulness (Fahn, Elton et al. 1987; Marsden 1989).

The average number of tap cycles performed in 15 seconds was 50 in controls, 52 in PSP, 42 in PD-OFF and 46 in PD-ON. Therefore, to detect the differences reported above would require a tap trial of approximately 50 finger-thumb tap cycles. The modified MDS-UPDRS (Goetz, Tilley et al. 2008) proposed a 10-tap trial, which would take an average of 3.8 seconds (15s/42taps x 10taps) for PD-OFF subjects to perform, as estimated by data in the present study. We postulated that a tap trial consisting of only 10 taps would be too brief for the sequence effect to emerge in either treated or untreated PD. To investigate this, we have performed an additional analysis on our data by arbitrarily assessing only the initial 20 taps of the first trials performed by both hands after adjusting for disease duration, age and gender.

With a 20-tap trial, PSP can still be differentiated from both PD-OFF and controls by having amplitudes of less than half the expected size. Mean speed in PD-OFF was slower than controls ($p=0.007$). However, after 20 taps, the amplitude slope (mean=+0.04) and speed slope (mean=+0.21) in PD-OFF group were both positive, indicating the lack of decrement and fatigue at that time point and the slope values did not differ between PD-OFF, PSP and control groups. This analysis indicated that 20-tap trials were not adequate in detecting decrement or fatigue in PD. We propose that repetitive finger tapping with 50 tap cycles is required to detect criteria-defined bradykinesia in treated and untreated PD patients. Patients with hypokinesia and absence of progressive reduction in amplitude during a 50-tap trial are more likely to have a diagnosis of PSP.

	Controls (*N* = 16)	PD-OFF (*N* = 15)	PSP (*N* = 9)	F values (1, 19)	*P* values (ANOVA)	*p* values from Tukey HSD post hoc analysis (< 0.05)
Amplitude (deg)	49.12 (8.8)	41.19 (18.1)	18.82 (7.8)	19.35	<0.001*	Controls Vs PSP (< 0.001); PD-OFF Vs PSP (= 0.001)
Duration (ms)	279.80 (65.7)	342.13 (82.1)	285.18 (58.2)	4.40	0.05	NA
Speed (deg/s)	346.51 (85.7)	247.29 (99.5)	143.0 (52.6)	11.41	0.003	Controls Vs PSP (< 0.001); PD-OFF Vs PSP (= 0.017); Controls Vs PD-OFF (= 0.007)
Amplitude slope (deg/ cycle)	-0.08 (6.4)	0.04 (0.3)	0.13 (0.3)	0.80	0.38	NA
Duration slope (s/cycle)	-0.37 (1.7)	1.27 (3.8)	1.80 (6.9)	0.54	0.47	NA
Speed slope (deg/s/cycle)	-0.10 (2.1)	0.21 (1.2)	0.45 (2.8)	1.19	0.29	NA

Table 3.6: Parameter measurements of the initial 20 taps of the first trials performed by both hands. Mean (Standard Deviation); Covariates appearing in the model above are evaluated at the following values: gender = 0.58 (0-female; 1-male), age = 67.87years, disease duration = 8.43years; *F* (degrees of freedom) = f value from one-way ANOVA; NA = not applicable with $p \geq 0.05$; * $p < 0.05$ by one-way ANOVA

4. Handwriting in PD and PSP

Micrographia was more common in PSP (75%) than in PD (15%). There was also less progressive reduction in script size in PSP than in PD-OFF. These findings in handwriting were equivalent to hypokinesia with lack of decrement in repetitive finger tapping in PSP and might share common underlying mechanisms. Five of the 6 patients with PSP who had micrographia also manifested hypokinesia on repetitive finger tapping. 'Fast micrographia' characterised by small size handwriting performed at a normal or slightly faster than normal speed may indicate underlying pallidal dysfunction (Kuoppamaki, Rothwell et al. 2005). This phenomenon has been linked with PSP. The 'fast' speed might simply represent a shorter performance time due to the reduced stroke size rather than an intrinsic increase

in speed. However, the present study did not time the handwriting task and was unable to study this feature.

Our finding of a small number of PD patients with micrographia is similar to a previous study (McLennan, Nakano et al. 1972). A copying task, as in the present study, writing on parallel lines and with a verbal reminder to write 'big' can serve as external clues to prevent reduction in script size (Oliveira, Gurd et al. 1997; Kim, Lee et al. 2005; Bryant, Rintala et al. 2010). Abnormally increased dependence on external visual feedback has been noted in patients with PD (Demirci, Grill et al. 1997). The mechanism of micrographia is poorly understood but the hypothesis of a 'tuned-down' sensorimotor apparatus might explain the reduction in motor scaling during sequential motor tasks such as finger tapping and handwriting (Demirci, Grill et al. 1997). Levodopa therapy does not improve script size in PD except in a small group of patients (McLennan, Nakano et al. 1972). In 4 of our PD patients script size was numerically improved but such improvement did not achieve statistical significance. Previous work has shown that there is a lack of correlation between micrographia and parkinsonism (McLennan, Nakano et al. 1972), which is supported by our study as no correlation was found between micrographia and clinimetric scores.

5. Strengths and limitations of present study

The 3-dimensional motion assessment used in this study to objectively measure repetitive finger tapping proved particularly useful in tremulous patients who would have had difficulties maintaining their finger separation in a 2-dimensional plane. Pilot studies were conducted on healthy volunteers and it was determined that healthy elderly participants become tired after prolonged tap sequences of more than 15-20 seconds. In order to minimise the confounding factor of physiological fatigue, the trial duration was, therefore, limited to 15 seconds. Not all of these measurements are practical at the bedside and further studies are warranted to apply our findings in such a setting. However, very small finger tapping amplitudes should be easily identified during neurological examination. The relative persistence of the sequence effect despite levodopa therapy in PD makes it an especially useful physical sign to help distinguish PD and PSP. Future prospective studies on patients with early PSP or PSP-Parkinsonism subtype will determine if this specific finger tap pattern can be used as a reliable early diagnostic clue in these clinical conundrums.

The inherent limitation of clinical studies of this kind is the lack of pathological confirmation of diagnosis given that about 20% of suspected PSP cases and 10% of suspected PD cases are found at post-mortem to have a different pathology (Ling, O'Sullivan et al. 2010). Finally, it should be noted that patients with prominent tremor were excluded from our study. In tremor-predominant PD, motor flurries can potentially interrupt normal self-paced movements, possibly confounding bedside interpretations (Bajaj, Gontu et al. 2010).

F. Conclusion

Patients with PSP have small finger separation amplitude without progressive decrement on repetitive finger tapping and do not have "true" bradykinesia. The severe hypokinesia irrespective of disease severity and the lack of a sequence effect help distinguish these patients from those with PD. Micrographia is more common in PSP than in PD and a lack of progressive reduction in script size was observed in PSP.

Chapter 4: Conventional Magnetic Resonance Imaging in Confirmed Progressive Supranuclear Palsy and Multiple System Atrophy

A. Introduction

Progressive Supranuclear Palsy (PSP), Multiple System Atrophy (MSA), Parkinson's disease (PD) and Corticobasal degeneration (CBD) may be difficult to diagnose in the early stages of disease, particularly if, as is not uncommon, the clinical presentation has atypical features. In addition to the need for accurate diagnostic and prognostic information for patients, the promise of disease-modifying treatments in these neurodegenerative disorders means that reliable biomarkers are badly needed. Despite some similarities - particularly that all affect the substantia nigra - the topography of these diseases is different:

•PSP affects the midbrain, subthalamic nucleus, globus pallidus, dentate nucleus and frontal lobes (Williams, Holton et al. 2007).
•MSA affects the corpus striatum, globus pallidus, the olivopontocerebellar structures, the intermediolateral column of the spinal cord and Onuf's nucleus (Wenning, Colosimo et al. 2004).
•PD affects the locus coeruleus, dorsal motor nucleus of the vagus, the pedunculopontine nucleus and nucleus basalis of Meynert (Braak, Del Tredici et al. 2003).
•CBD affects perirolandic cortical areas which may be asymmetric and some subcortical regions (Mahapatra, Edwards et al. 2004).

These topographical differences should be amenable to assessment during life with conventional MRI (cMRI).

There are no reliable specific abnormalities on cMRI in PD (Savoiardo 2003; Seppi and Schocke 2005) although appearances may not be completely normal (Kraft, Schwarz et al. 1999; Savoiardo 2003; Yekhlef, Ballan et al. 2003) [table 4.1].

In PSP cMRI may show midbrain atrophy, atrophy of the quadrigeminal plate, dilatation of the third ventricle or atrophy of the superior cerebellar peduncle (Rutledge, Hilal et al. 1987; Drayer 1988; Savoiardo, Strada et al. 1989; Yagishita and Oda 1996; Aiba, Hashizume et al. 1997; Schrag, Good et al. 2000; Savoiardo 2003; Paviour, Price et al. 2005; Slowinski, Imamura et al. 2008), midbrain signal hyperintensity on T2 (Drayer, Olanow et al. 1986;

Savoiardo, Strada et al. 1989; Savoiardo, Girotti et al. 1994; Yagishita and Oda 1996) or proton density weighted images (Oka, Katayama et al. 2001) and fluid attenuated inversion recovery (FLAIR) images (Kataoka, Tonomura et al. 2008). A concave appearance of the superior profile of the midbrain (Righini, Antonini et al. 2004), a characteristic 'hummingbird' (the HB sign) (Kato, Arai et al. 2003) or 'giant penguin' (Oba, Yagishita et al. 2005) appearance, or in the axial images a 'morning glory flower' (the MGF sign) (Adachi, Kawanami et al. 2004; Mori, Aoki et al. 2004) are highly suggestive in the context of a Parkinsonian syndrome. An 'eye of the tiger sign' has also been reported in PSP (Davie, Barker et al. 1997). [Table 4.1; Figure 4.1]

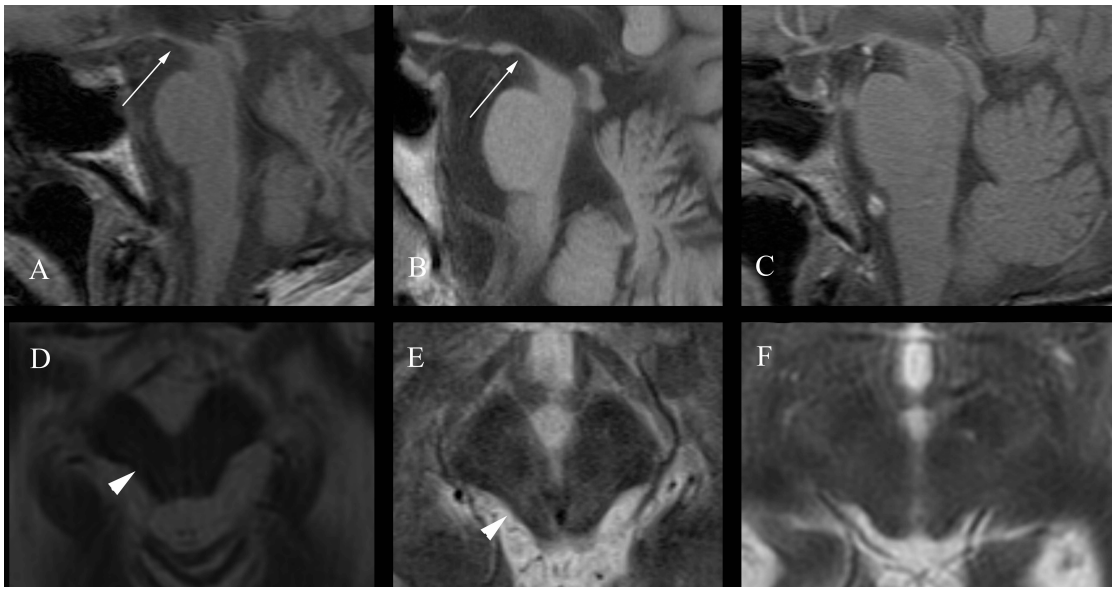

Figure 4.1: Hummingbird (HB) and morning glory flower (MGF) signs in PSP. Sagittal T1 [A-C] sand axial T2 [D-F] images in pathologically confirmed disease. [A] HB (arrow) & [D] MGF in PSP 1.5 yrs after onset; [B] HB (arrow) & [D] MGF in PSP 4 yrs after onset; [C] & [F] normal appearances of the midbrain in PD. Axial images were screened for the presence of the MGF sign by the published method which detects a concave profile of the midbrain tegmentum in PSP (arrow heads) (Adachi, Kawanami et al. 2004).

Putaminal atrophy and signal abnormalities are seen in MSA (Drayer, Olanow et al. 1986; Pastakia, Polinsky et al. 1986; Drayer 1988; Savoiardo, Strada et al. 1989; Stern, Braffman et al. 1989; Savoiardo, Girotti et al. 1994; Schrag, Kingsley et al. 1998; Schrag, Good et al. 2000; Bhattacharya, Saadia et al. 2002; Yekhlef, Ballan et al. 2003; Seppi, Schocke et al. 2006), and a hyperintense putaminal rim is characteristic (Savoiardo, Strada et al. 1989; Savoiardo, Strada et al. 1990; Yagishita and Oda 1996; Bhattacharya, Saadia et al. 2002; Savoiardo 2003; Yekhlef, Ballan et al. 2003) although this has been occasionally seen in PD

and PSP (Kraft, Schwarz et al. 1999; Bhattacharya, Saadia et al. 2002; Schocke, Seppi et al. 2002). Also in MSA, atrophy of the pons, cerebellum and middle cerebellar peduncles (MCP) is seen (Drayer, Olanow et al. 1986; Pastakia, Polinsky et al. 1986; Rutledge, Hilal et al. 1987; Drayer 1988; Savoiardo, Strada et al. 1990; Savoiardo, Girotti et al. 1994; Yagishita and Oda 1996; Schrag, Kingsley et al. 1998; Schrag, Good et al. 2000; Savoiardo 2003; Seppi and Schocke 2005). The pons can take on the appearance of a 'hot cross bun' (HCB sign) in the axial plane (Schrag, Kingsley et al. 1998; Schrag, Good et al. 2000; Bhattacharya, Saadia et al. 2002; Seppi and Schocke 2005) and T2 hyperintensity in the MCP has been termed 'the MCP sign' [Figure 2] (Uchino, Sawada et al. 2004). [Table 4.1; Figure 4.2]

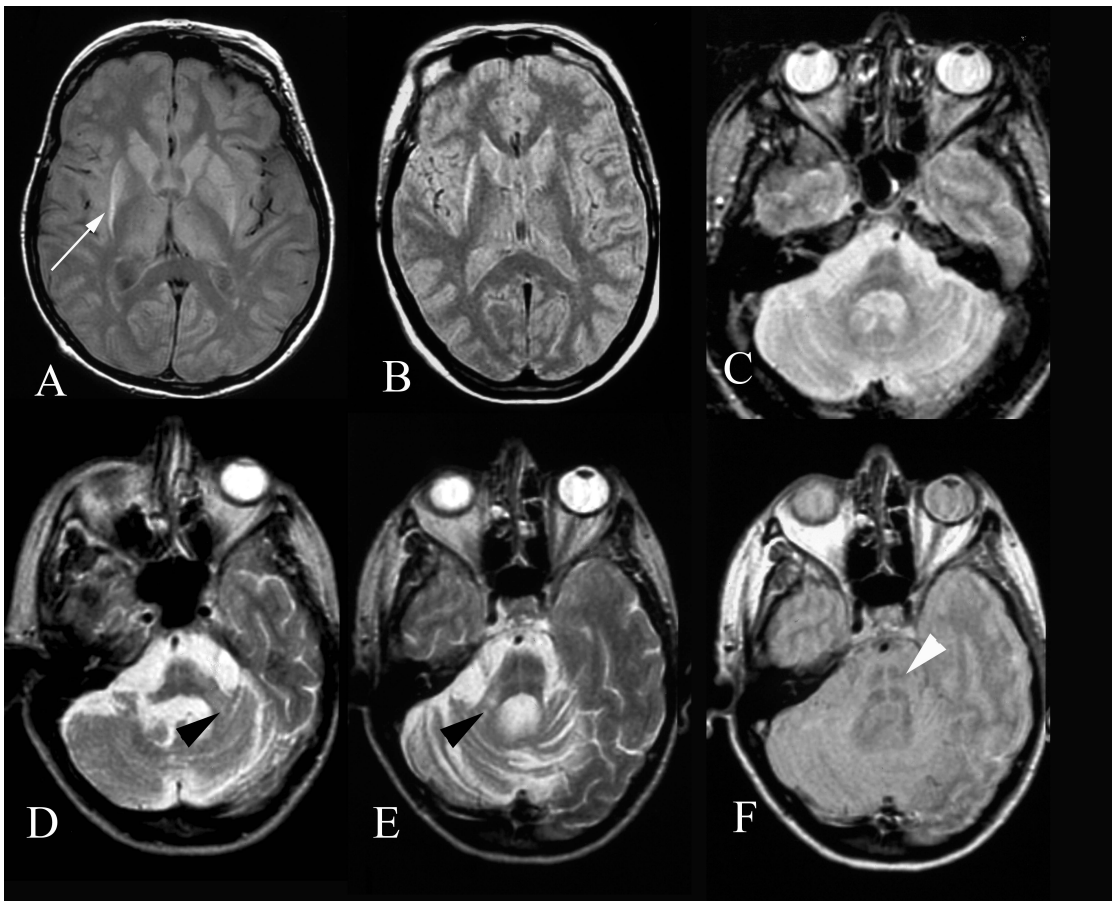

Figure 4.2: Putaminal atrophy, hyperintense putaminal rim (HPR), hot cross bun (HCB) and middle cerebellar peduncle (MCP) signs in MSA. Axial Proton density weighted images [A] & [F] and T2 weighted images [B-E] in pathologically confirmed MSA. [A] Right putaminal atrophy with HPR and early HPR on the left (white arrow) 4.8 years after disease onset; [B] bilateral putaminal atrophy and HPR 5.7 years after onset; [C] HCB sign in the pons 5.1 years after onset; [D-F] axial images from the same patient 6.3 years from onset showing a left MCP sign (black arrow head) [D], right MCP sign (black arrow head) and HCB [E] and the HCB on proton density image (white arrow head) [F] at the same level as [E].

Region	Abnormality	PSP	PD	MSA	CBD
Substantia Nigra	**Atrophy**	(Schrag, Good et al. 2000)	(Duguid, De La Paz et al. 1986; Drayer 1988; Braffman, Grossman et al. 1989; Pujol, Junque et al. 1992; Yagishita and Oda 1996)	(Drayer 1988; Schrag, Good et al. 2000; Savoiardo 2003)	(Schrag, Good et al. 2000)
	Smudging	(Savoiardo, Strada et al. 1989; Stern, Braffman et al. 1989; Yagishita and Oda 1996; Schrag, Good et al. 2000)	(Drayer 1988; Savoiardo, Girotti et al. 1994)	(Schrag, Good et al. 2000; Savoiardo 2003)	(Schrag, Good et al. 2000)
	Hyperintensity		(Braffman, Grossman et al. 1989)		
	Restoration of lateral signal	(Yekhlef, Ballan et al. 2003)	(Rutledge, Hilal et al. 1987; Stern, Braffman et al. 1989)		
Putamen	**Atrophy**	(Schrag, Good et al. 2000; Yekhlef, Ballan et al. 2003)	(Yekhlef, Ballan et al. 2003)	(Pastakia, Polinsky et al. 1986; Schrag, Kingsley et al. 1998; Schrag, Good et al. 2000; Bhattacharya, Saadia et al. 2002; Schocke, Seppi et al. 2002; Yekhlef, Ballan et al. 2003; Seppi and Schocke 2005)	(Savoiardo et al., 1994)
	Hypointensity	(Stern, Braffman et al. 1989; Savoiardo, Girotti et al. 1994; Kraft, Schwarz et al. 1999; Yekhlef, Ballan et al. 2003)	(Righini, Antonini et al. 2002)	(Drayer, Olanow et al. 1986; Pastakia, Polinsky et al. 1986; Drayer 1988; Savoiardo, Strada et al. 1990; Savoiardo, Girotti et al. 1994; Schulz, Klockgether et al. 1994; Schrag, Kingsley et al. 1998; Kraft, Schwarz et al. 1999; Schrag, Good et al. 2000; Bhattacharya, Saadia et al. 2002; Righini, Antonini et al. 2002; Savoiardo 2003; Yekhlef, Ballan et al. 2003; Seppi and Schocke 2005)	
	Hyperintensity			(Savoiardo, Strada et al. 1989; Savoiardo, Strada et al. 1990; Savoiardo, Girotti et al. 1994; Schrag, Kingsley et al. 1998)	
	Hyperintense putaminal rim	(Yekhlef, Ballan et al. 2003)		(Savoiardo, Girotti et al. 1994; Yagishita and Oda 1996; Schrag, Kingsley et al. 1998; Kraft, Schwarz et al. 1999; Schrag, Good et al. 2000; Bhattacharya, Saadia et al. 2002; Horimoto, Aiba et al. 2002; Schocke, Seppi et al. 2002; Watanabe, Saito et al. 2002; Savoiardo 2003; Seppi and Schocke 2005)	

Region	Abnormality	PSP	PD	MSA	CBD
Midbrain	**Midbrain atrophy (axial)**	(Rutledge, Hilal et al. 1987; Savoiardo, Strada et al. 1989; Savoiardo, Girotti et al. 1994; Yagishita and Oda 1996; Aiba, Hashizume et al. 1997; Schrag, Good et al. 2000; Savoiardo 2003; Yekhlef, Ballan et al. 2003)		(Stern, Braffman et al. 1989; Schulz, Klockgether et al. 1994; Schrag, Kingsley et al. 1998; Schrag, Good et al. 2000; Yekhlef, Ballan et al. 2003; Seppi and Schocke 2005)	(Yekhlef, Ballan et al. 2003)(Savoiardo, Girotti et al. 1994) (Schrag, Good et al. 2000; Tokumaru, Saito et al. 2009)
	Periaqueductal hyperintensity	(Rutledge, Hilal et al. 1987; Savoiardo, Strada et al. 1989; Savoiardo, Girotti et al. 1994; Yagishita and Oda 1996; Schrag, Good et al. 2000; Savoiardo 2003)		(Schrag, Good et al. 2000)	
	Tectal / tegmental hyperintensity	(Rutledge, Hilal et al. 1987; Yagishita and Oda 1996; Aiba, Hashizume et al. 1997; Schrag, Good et al. 2000; Savoiardo 2003)			
	Atrophy of quadrigeminal plate	(Rutledge, Hilal et al. 1987; Savoiardo, Strada et al. 1989; Savoiardo, Girotti et al. 1994; Aiba, Hashizume et al. 1997; Savoiardo 2003)			
	Dilatation of 3rd ventricle	(Rutledge, Hilal et al. 1987; Savoiardo, Girotti et al. 1994; Aiba, Hashizume et al. 1997; Schrag, Good et al. 2000; Savoiardo 2003)		(Schrag, Good et al. 2000; Yekhlef, Ballan et al. 2003)	(Schrag, Good et al. 2000)
	Superior colliculus hypointensity	(Savoiardo, Strada et al. 1989; Savoiardo, Girotti et al. 1994)			
	Hummingbird / Giant Penguin	(Kato, Arai et al. 2003; Oba, Yagishita et al. 2005)			
	Morning Glory Flower	(Adachi, Kawanami et al. 2004; Mori, Aoki et al. 2004)			
	Mickey Mouse	(Schott 2007)			
	SCP hyperintensity	(Kataoka, Tonomura et al. 2008)			
	SCP atrophy	(Paviour, Price et al. 2005; Slowinski, Imamura et al. 2008)			
	DSCP hyperintensity	(Oka, Katayama et al. 2001)			

Region	Abnormality	PSP	PD	MSA	CBD
Pons & Cerebellum	**Pontine atrophy**	(Aiba, Hashizume et al. 1997; Schrag, Good et al. 2000; Yekhlef, Ballan et al. 2003)		(Rutledge, Hilal et al. 1987; Savoiardo, Strada et al. 1990; Savoiardo, Girotti et al. 1994; Schrag, Kingsley et al. 1998; Bhattacharya, Saadia et al. 2002; Horimoto, Aiba et al. 2002; Savoiardo 2003; Yekhlef, Ballan et al. 2003)	
	Cerebellar atrophy	(Schrag, Good et al. 2000; Yekhlef, Ballan et al. 2003)		(Pastakia, Polinsky et al. 1986; Rutledge, Hilal et al. 1987; Savoiardo, Strada et al. 1990; Savoiardo, Girotti et al. 1994; Schulz, Klockgether et al. 1994; Yagishita and Oda 1996; Schrag, Kingsley et al. 1998; Schrag, Good et al. 2000; Bhattacharya, Saadia et al. 2002; Savoiardo 2003; Yekhlef, Ballan et al. 2003)	
	MCP atrophy	(Schrag, Good et al. 2000)		(Rutledge, Hilal et al. 1987; Savoiardo, Strada et al. 1990; Savoiardo, Girotti et al. 1994; Schrag, Kingsley et al. 1998; Schrag, Good et al. 2000; Savoiardo 2003)	
	Medullary atrophy			(Rutledge, Hilal et al. 1987; Bhattacharya, Saadia et al. 2002)	
	Inferior olivary atrophy			(Rutledge, Hilal et al. 1987)	
	Dilatation of 4th ventricle	(Aiba, Hashizume et al. 1997; Yekhlef, Ballan et al. 2003)		(Savoiardo, Girotti et al. 1994; Schrag, Good et al. 2000; Yekhlef, Ballan et al. 2003)	
	Pontocerebellar fibre hyperintensity			(Savoiardo, Strada et al. 1990; Savoiardo, Girotti et al. 1994; Schulz, Klockgether et al. 1994; Yagishita and Oda 1996; Schrag, Kingsley et al. 1998; Schrag, Good et al. 2000; Savoiardo 2003; Seppi and Schocke 2005)	
	MCP hyperintensity			(Savoiardo, Strada et al. 1990; Savoiardo, Girotti et al. 1994; Schrag, Kingsley et al. 1998; Schrag, Good et al. 2000; Bhattacharya, Saadia et al. 2002; Savoiardo 2003; Uchino, Sawada et al. 2004; Seppi and Schocke 2005)	

	Abnormality	PSP	PD	MSA	CBD
Pons & Cerebellum	**Cerebellar hyperintensity**			(Savoiardo, Strada et al. 1990; Savoiardo, Girotti et al. 1994; Savoiardo 2003)	
	Inferior olivary hyperintensity			(Savoiardo, Girotti et al. 1994)	
	Hot cross bun			(Schrag, Kingsley et al. 1998; Schrag, Good et al. 2000; Horimoto, Aiba et al. 2002; Watanabe, Saito et al. 2002; Uchino, Sawada et al. 2004)	
Cerebral Cortical Atrophy and Lateral Ventricle Dilatation	**Cortical atrophy**	frontotemporal (Schrag, Good et al. 2000; Savoiardo 2003); frontoparietal (Yekhlef, Ballan et al. 2003)		Frontal and parietal (Yekhlef, Ballan et al. 2003)	(frontal/parietal) (Tokumaru, Saito et al. 2009)(Savoiardo, Girotti et al. 1994; Savoiardo 2003; Koyama, Yagishita et al. 2007)(Hu, Josephs et al. 2005); global (Schrag, Good et al. 2000; Yekhlef, Ballan et al. 2003)
	Lateral ventricle dilatation	(Yekhlef, Ballan et al. 2003)		(Yekhlef, Ballan et al. 2003)	(Yekhlef, Ballan et al. 2003)
	Asymmetric atrophy	Symmetric (Savoiardo 2003)			Asymmetric (Tokumaru, Saito et al. 2009)(Koyama, Yagishita et al. 2007) (Savoiardo, Girotti et al. 1994; Savoiardo 2003); symmetric (Schrag, Good et al. 2000; Josephs, Tang-Wai et al. 2004)

Table 4.1: Abnormalities described in PSP, PD, MSA and CBD using conventional MRI

Imaging in CBD is complicated as the diagnostic accuracy rate is so low. In a series of 26 CBS patients frontal and parietal atrophy were the most common abnormalities, followed by dilatation of the lateral and third ventricles; asymmetric frontoparietal atrophy accompanied by lateral ventricular dilatation was the most reliable predictor of a clinical diagnosis of CBS when compared to PD, PSP and MSA (Yekhlef, Ballan et al. 2003). In CBD, cortical atrophy of the frontal and parietal regions on the side contralateral to the symptoms has been reported with associated enlargement of the lateral ventricle; no definite subcortical abnormalities are seen despite the presence of pathology within these structures (Soliveri, Monza et al. 1999; Savoiardo 2003). A more recent study reported that all CBS patients have cerebral atrophy, 81% asymmetry with the side contralateral to the affected limb most affected and atrophy was most severe in the anterior frontal and parietal lobes; 94% had corpus callosal atrophy (Koyama, Yagishita et al. 2007). Atrophy was also seen less frequently in the cerebral peduncles, pyramids and midbrain tegmentum. 88% had signal hyperintensity on FLAIR sequences in the frontal or parietal subcortical white

matter ipsilateral to the atrophic cortex with hyperintensities seen in the frontal lobes when there was motor aphasia or apraxia of speech, and parietal hyperintensities in 50% of those with parietal signs (Koyama, Yagishita et al. 2007). Furthermore, cMRI may show no significant patterns of regional atrophy or signal change enabling accurate identification of CBD (Schrag, Good et al. 2000; Josephs, Tang-Wai et al. 2004) [Table 4.1].

Although the specificity of some of these radiological signs is reported to be as high as 100% (Schrag, Kingsley et al. 1998; Schrag, Good et al. 2000; Kato, Arai et al. 2003; Yekhlef, Ballan et al. 2003; Adachi, Kawanami et al. 2004; Mori, Aoki et al. 2004; Oba, Yagishita et al. 2005), they are found in only a proportion of cases and are often absent in early disease when accurate clinical diagnosis is most difficult [Table 4.2].

An important weakness of published cMRI studies is that they use operational research criteria to define the disease under study; while these criteria may have high specificity for a pathological diagnosis there are significant misdiagnoses (in over 10%) (Hughes, Daniel et al. 2002) and cases with atypical clinical features are excluded by definition. Only very few studies have reported MR findings in pathologically confirmed cases (Yagishita and Oda 1996; Aiba, Hashizume et al. 1997; Slowinski, Imamura et al. 2008). This is particularly important in CBD where most cases presenting with CBS turn out to have alternative pathological diagnoses (Ling, O'Sullivan et al. 2010).

cMRI sign	Disease	Comparison	Sensitivity	Specificity	PPV	Reference
HB/GP	**PSP**	8 PSP, 12 PD, 10 controls	100%	100%	100%	(Kato, Arai et al. 2003)
HB/GP	**PSP**	21 PSP, 23 PD, 25 MSA-P, 31 controls	100%	100%	100%	(Oba, Yagishita et al. 2005)
HB/GP	**PSP**	8 PSP	100%	n/a	n/a	(Mori, Aoki et al. 2004)
MGF	**PSP**	5 PSP, 23 PD, 14 MSA	80%	97%	80%	(Adachi, Kawanami et al. 2004)
MGF	**PSP**	8 PSP	12.5%	n/a	n/a	(Mori, Aoki et al. 2004)
HPR	**MSA**	44 MSA, 47 IPD, 45 controls	40.6%	100%	100%	(Schrag, Kingsley et al. 1998)
HCB	**MSA**	54 MSA, 35 PSP	50%	97%	97%	(Schrag, Good et al. 2000)
HPR	**MSA**	54 MSA, 35 PSP	30%	91%	84%	(Schrag, Good et al. 2000)
MCP sign	**MSA**	54 MSA, 35 PSP	50%	94%	93%	(Schrag, Good et al. 2000)
Midbrain atrophy	**PSP**	54 MSA, 35 PSP	77%	37%	44%	(Schrag, Good et al. 2000)

Table 4.2: Accuracy of abnormalities reported in the literature for clinically-defined diagnosis. (HB/GP hummingbird/giant penguin sign; MGF morning glory flower sign; HPR hyperintense putaminal rim; HCB hot cross bun sign; MCP sign middle cerebellar peduncle hyperintensity sign)

Also, the sensitivity of MRI abnormalities has not been replicated in subsequent studies e.g. MGF in PSP (Mori, Aoki et al. 2004; Oba, Yagishita et al. 2005) or specific features have been described in other diseases e.g. MCP sign is seen in other diseases with pontocerebellar degeneration (Uchino, Sawada et al. 2004). Furthermore, not all published studies contain comparisons from all 4 disease groups mentioned in this study, meaning that a particular feature may be specific in one comparison but not another.

B. Aim

The aim of this study is to define the diagnostic accuracy of blinded radiological assessment of cMRI in PSP, MSA, PD and CBD where a histopathologically confirmed diagnosis has been made following post mortem brain donation, to report the sensitivity, and specificity of specific MR findings and compare cMRI abnormalities with macroscopic findings at post mortem examination.

C. Materials and Methods

1. Participant selection

Cases were selected from the Queen Square Brain Bank for Neurological Disorders (QSBB), UCL Institute of Neurology, where tissue is donated according to ethically approved protocols and stored under a licence from the Human Tissue Authority. Brains were sampled for histology using an established protocol (Trojanowski and Revesz 2007) and the diagnosis confirmed using standard neuropathological criteria (Ince, Clarke et al. 2008). Records were screened from 1997-2009, the availability of conventional MR imaging dictating whether a case could be included.

2. Clinical information

Most were assessed during life at either the National Hospital for Neurology and Neurosurgery, Queen Square, or the Regional Neurosciences centre, Newcastle General Hospital by a hospital specialist (neurologist or geriatrician). The final working clinical diagnosis during life was retrieved from available records. Included in the study were disease controls (pathologically confirmed PD and CBD) and a group of living healthy controls in whom no evidence of neurological disease was evident at time of imaging.

3. Image analysis

Conventional MR images were independently reviewed by two experienced neuroradiologists (Dr Caroline Micallef and Dr H Rolf Jager) blinded to the final clinical diagnosis although age at the time of imaging was taken into consideration and atrophy was considered significant when disproportionate to the general degree of atrophy. An independent radiological diagnosis was made by each rater, based on their experience and

knowledge of the imaging abnormalities described in the literature. When opinion differed images were reviewed jointly and a consensus reached. One rater (Dr Caroline Micallef) systematically screened MR images for a comprehensive list of abnormalities described in the literature [Table 4.1].

Macrosopic findings were retrospectively derived from macroscopic examination of the brain by two neuropathologists (Dr Janice L Holton and Professor Tamas Revesz) who were not blinded to clinical information according to the routine protocols of the QSBB.

4. Statistical Analysis

Group characteristics were compared between groups using multivariate analysis with post hoc Bonferroni correction or chi square test as appropriate. Cohen's kappa was used to assess inter-rater agreement. McNemar's chi square test was used to compare the proportion correctly identified using the clinical and radiological diagnosis. The chi square and exact tests were used to compare proportions with specific abnormalities. Sensitivity, specificity, positive and negative predictive values and likelihood ratios of positive and negative results were calculated in an Excel spreadsheet (Microsoft Office for Mac, 2004) using published formulae (Altman and Bland 1994; Altman and Bland 1994) and accuracy (true positives + true negatives / total of true and false positives and negatives) for clinical and radiological diagnoses. Statistical analysis was performed in PASW Statistics 18.0 for Mac except for deriving exact test values (SPSS for Windows version 17).

D. Results

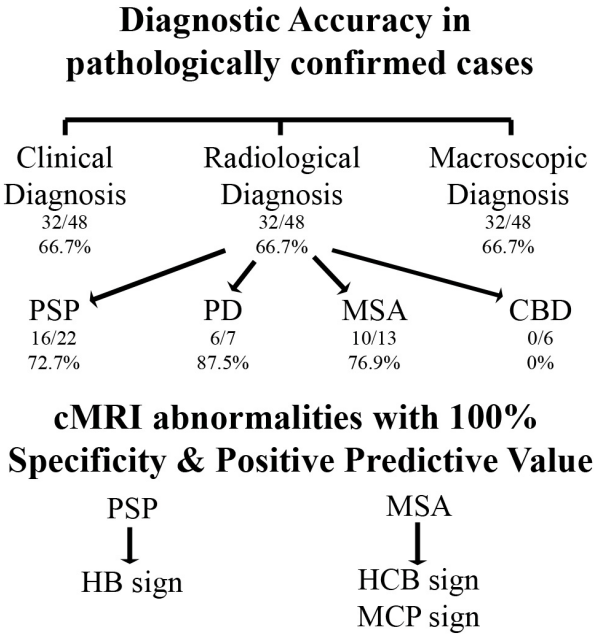

Figure 4.3: Overview of results of study

1. Group and MRI image characteristics

	Control	PSP	IPD	MSA	CBD	p value
n	9	22	7	13	6	
Gender (F)	3	4	1	6	3	NS
Mean age at Scan (SD)	67.3 (8.1)	69.4 (6.1)	65.6 (12.0)	58.0* (6.6)	71.0 (5.7)	< 0.001
Mean age at Onset (SD)	-	64.6 (6.7)	58.9 (12.1)	52.9** (7.4)	66.9 (5.8)	< 0.001
Mean age at death (SD)	-	71.6 (6.3)	68.4 (12.0)	60.3*** (6.4)	72.6 (5.4)	< 0.001
Mean disease duration at scan (SD)	-	4.8 (3.6)	6.7 (5.2)	5.1 (2.4)	5.1 (3.4)	NS
Mean total disease duration (SD)	-	7.0 (3.1)	9.5 (4.9)	7.4 (2.5)	5.7 (1.7)	NS

Table 4.3: Demographic features. Chi square test and Student's t test used as appropriate. *MSA versus PSP p = 0.001; MSA versus CBD p = 0.008; MSA versus control p = 0.055;

**MSA versus PSP p = 0.001; MSA versus CBD p = 0.004; ***MSA versus PSP p < 0.001; MSA versus CBD p = 0.008.

Group characteristics are summarised in Table 4.3. A total of 33 MR images were acquired digitally at the National Hospital for Neurology and Neurosurgery (NHNN), 9 were digitized films and 15 were viewed as 'hard copy' films. 51/57 (89.5%) were acquired on a 1.5T MRI system, 5 on 0.5T and 1 on a 1T system (1.5T scans were available in 9/9 control, 21/22 PSP, 5/7 PD, 11/13 MSA and 5/6 CBD cases). In 57/57 axial images were available, in 54/57 coronal and in 46/57 sagittal images; T2 images were available in 57/57, T1 images in 53/57, proton density images in 41/47, fluid attenuated inversion recovery images in 24/57.

2. Clinical Diagnosis

	Overall	PSP	IPD	MSA	CBD
Correct Clinical Diagnosis (%)	32/48 (66.7%)	20/22 (90.9%)	2/7 (28.6%)	8/13 (61.5%)	2/6 (33.3)
Correct Macroscopic Post Mortem Diagnosis (%)	32/48 (66.7%)	15/22 (68.2%)	7/7 (100%)	9/13 (69.2%)	1/6 (16.7%)
Correct Radiological Diagnosis (%)	32/48 (66.7%)	16/22 (72.7%)	6/7 (85.7%)	10/13 (76.9%)	0/6 (0%)

Table 4.4: Diagnostic accuracy of clinical diagnosis, macroscopic post mortem diagnosis and radiological diagnosis in pathologically confirmed disease (There was substantial inter-rater reliability for the radiological diagnosis (Cohen's kappa 0.733, p < 0.001).

Combined sensitivity for the PSP and MSA cases was 28/35 (80%): the clinical diagnosis of PSP was correct in 20/22 (90.9%) pathologically confirmed cases: They were sub-classified as Richardson's syndrome (PSP-RS) (n=14), PSP-Parkinsonim (n=1), PSP phenotype with late or no documented falls (n=3), PSP with unclassified subtype (n=1) and an encephalitic illness followed much later by a PSP phenotype (n=1). The two false negative cases were diagnosed with atypical parkinsonism and PD; there were 6 false positive diagnoses of PSP (MSA n=2, CBD n=2 and PD n=2). The sensitivity, specificity and accuracy of clinical diagnosis of PSP in the entire study cohort were 90.9%, 82.9% and 86.0% respectively

8/13 (61.5%) cases of pathologically confirmed MSA cases were correctly identified: 7 were classified as MSA-P and one MSA-C. Other clinical diagnoses included a cerebellar ataxia with autonomic features (n=1), atypical parkinsonism (n=1), PSP/CBS (n=2) and pure autonomic failure (n=1) – thus of the 13 cases 10 had a predominantly Parkinsonian presentation, 2 a predominantly cerebellar presentation and 1 purely autonomic. There was only one false positive MSA-P (PD histopathologically). The sensitivity, specificity and accuracy of clinical diagnosis of MSA in the entire study cohort were 61.5%, 97.7% and 89.5% respectively.

3. Radiological Diagnosis

In 45/48 (93.8%) cases images were reviewed by both raters with substantial inter-rater agreement for the radiological diagnosis (Cohen's kappa 0.708, $p < 0.001$).[25] Combined sensitivity for the PSP and MSA cases was 26/35 (74.3%). The radiological diagnosis of PSP was correct in 16/22 (72.7%) and of MSA in 10/13 (76.9%) cases. The sensitivity, specificity and accuracy of radiological diagnosis of PSP were 72.7%, 94.3% and 86.0% respectively. The sensitivity, specificity and accuracy of radiological diagnosis of MSA were 76.9%, 100% and 94.7% respectively. After consensus no cases of PSP were classified as MSA, and no cases of MSA as PSP. In one living control case a morning glory flower sign was seen on axial images of the midbrain but no other specific abnormality and one CBD case had evidence of midbrain atrophy compatible with PSP based on axial images only.

4. Comparison of clinical and radiological diagnostic sensitivity and specificity

Although the clinical diagnosis was more sensitive in PSP, the radiological diagnosis was more specific; the radiological diagnosis was more sensitive in MSA and slightly more specific. However, differences in the proportion correctly identified using radiological or clinical diagnoses did not reach statistical significance (McNemar's chi square test; $p > 0.05$).

5. Sensitivity and specificity of reported abnormalities

The frequency, sensitivity, specificity, positive and negative predictive values and likelihood ratios of specific abnormalities are displayed in Tables 4.5 and 4.6. The HB sign had 100% specificity and PPV for a pathological diagnosis of PSP; The MCP and HCB signs had 100% specificity and PPV for a pathological diagnosis of MSA. When PD was compared to PSP the HB sign, MGF sign, SCP atrophy and dilatation of the 4th ventricle had 100% specificity and

PPV for PSP ($p < 0.05$); when PD was compared to MSA 4th ventricle dilatation, the MCP sign and HCB sign had 100% specificity and PPV for MSA ($p < 0.05$). When compared to CBD the HB sign, and the MCP and HCB signs had 100% specificity and PPV for PSP and MSA respectively ($p < 0.05$).

Table 4.5 (overleaf): Frequency of abnormalities seen on conventional MRI by group. The abnormalities listed are those that have been reported in the literature and formed a checklist for the blinded systematic screen of cMRI images. In agreement with published studies very few abnormalities were seen on cMRI in our clinically atypical PD group (5/7 clinically atypical) and there were no specific findings in CBD.

Region	Abnormality	Frequency by Group									
		Control		PSP		PD		MSA		CBD	
Substantia Nigra	Atrophy	1/9	11.1%	7/19	36.8%	1/7	14.3%	2/12	16.7%	0/6	0%
	Smudging	1/9	11.1%	7/19	36.8%	1/7	14.3%	3/12	25%	0/6	0%
	Hyperintensity	0/9	0%	2/19	10.5%	0/7	0%	0/12	0%	0/6	0%
	Restoration of lateral signal	0/9	0%	1/19	5.3%	0/7	0%	0/12	0%	0/5	0%
Putamen	Atrophy	1/9	11.1%	10/18	55.6%	1/5	16.7%	6/12	50%	1/5	20%
	Hypointensity	2/9	22.2%	5/19	26.3%	0/7	0%	1/12	8.3%	1/6	16.7%
	Hyperintensity	0/9	0%	0/19	0%	0/7	0%	1/11	8.3%	2/4	33.3%
	Hyperintense putaminal rim	2/9	22.2%	4/19	21.1%	0/7	0%	3/12	25%	0/5	0%
Midbrain	Midbrain atrophy (axial)	3/9	33.3%	19/22	86.4%	2/7	28.6%	4/12	33.3%	4/6	66.7%
	Periaqueductal hyperintensity	3/9	33.3%	6/19	31.6%	1/7	14.3%	5/12	41.7%	3/6	50%
	Tectal hyperintensity	0/9	0%	0/20	0%	0/7	0%	0/12	0%	0/6	0%
	Atrophy of quadrigeminal plate	3/9	33.3%	17/22	77.3%	2/7	28.6%	3/12	25%	4/6	66.7%
	Dilatation of 3rd ventricle	3/9	33.3%	17/22	77.3%	4/7	57.1%	4/12	33.3%	5/6	83.3%
	Superior colliculus hypointensity	0/9	0%	0/19	0%	1/7	14.3%	0/12	0%	0/6	0%
	Hummingbird / Giant Penguin	0/9	0%	13/19	68.4%	0/5	0%	0/11	0%	0/4	0%
	Morning Glory Flower	1/9	11.1%	11/22	50%	0/7	0%	0/12	0%	0/6	0%
	Mickey Mouse	0/9	0%	1/22	4.5%	0/7	0%	0/12	0%	0/6	0%
	SCP hyperintensity	1/9	11.1%	3/20	15.0%	0/7	0%	1/12	8.3%	2/6	33.3%
	Dentate hypointensity	0/9	0%	1/20	4.8%	0/7	0%	1/12	8.3%	0/6	0%
	SCP atrophy	1/9	11.1%	12/21	57.1%	0/7	0%	2/12	16.7%	2/6	33.3%
	DSCP hyperintensity	0/9	0%	2/20	10%	0/7	0%	0/12	0%	0/6	0%
Pons & Cerebellum	Pontine atrophy	0/9	0%	5/22	22.7%	0/7	0%	4/12	33.3%	1/6	16.7%
	Cerebellar atrophy	2/9	22.2%	9/22	40.9%	1/7	14.3%	7/12	58.3%	1/6	16.7%
	MCP atrophy	0/9	0%	3/22	13.6%	0/7	0%	4/12	33.3%	0/6	0%
	Medullary atrophy	0/9	0%	2/22	9.1	0/7	0%	1/12	8.3%	0/6	0%
	Inferior olivary atrophy	0/9	0%	4/22	18.4%	0/7	0%	2/12	16.7%	0/6	0%
	Dilatation of 4th ventricle	0/9	0%	12/22	54.5%	0/7	0%	8/12	66.7%	1/6	16.7%
	Pontocerebellar fibre hyperintensity	0/9	0%	3/20	15.0%	0/7	0%	4/12	33.3%	1/6	16.7%
	MCP hyperintensity	0/9	0%	0/21	0%	0/7	0%	6/12	50.0%	0/6	0%
	Pontine hyperintensity	0/9	0%	2/20	10.0%	0/7	0%	1/11	8.3%	1/6	16.7%
	Cerebellar hyperintensity	0/9	0%	0/21	0%	0/7	0%	0/12	0%	0/6	0%
	Inferior olivary hyperintensity	0/9	0%	0/21	0%	0/7	0%	0/12	0%	0/6	0%
	Hot cross bun	0/9	0%	0/20	0%	0/7	0%	7/12	58.3%	0/6	0%
Cerebral Cortical Atrophy & Lateral Ventricle Dilatation	Cortical atrophy	3/9	33.3%	15/21	71.4%	4/7	57.1%	4/12	33.3%	4/6	66.7%
	Lateral ventricle dilatation	6/9	66.7%	16/19	84.2%	7/7	100%	8/12	66.7%	6/6	100%
	Asymmetric atrophy	0/9	0%	2/21	9.5%	1/7	14.3%	0/12	0%	0/6	0%
	Global atrophy	1/9	11.1%	10/21	47.6%	1/7	14.3%	2/12	16.7%	3/6	50.0%
	Frontal atrophy	1/9	11.1%	12/21	57.1%	1/7	14.3%	2/12	16.7%	4/6	66.7%
	Parietal atrophy	3/9	33.3%	14/21	66.7%	3/7	42.9%	2/12	16.7%	4/6	66.7%
	Temporal atrophy	1/9	11.1%	11/21	52.4%	1/7	14.3%	2/12	16.7%	3/6	50.0%

	Region	Abnormality	Sensitivity	Specificity	PPV	NPV	LR+	LR-	p
PSP vs Ctrl	Putamen	Atrophy	55.6	88.9	90.9	50.0	5.0	0.5	0.042
	Midbrain	Atrophy (axial)	86.4	66.7	86.4	66.7	2.6	0.2	0.007
		Atrophy of quadrigeminal plate	77.3	66.7	85.0	54.5	2.3	0.3	0.038
		Dilatation of 3rd ventricle	77.3	66.7	85.0	54.5	2.3	0.3	0.038
		Hummingbird / Giant Penguin	68.4	100.0	100.0	60.0	∞	0.3	0.001
		SCP atrophy	57.1	88.9	92.3	47.1	5.1	0.5	0.042
	Pons & Cerebellum	Dilatation of 4th ventricle	54.5	100.0	100.0	47.4	∞	0.5	0.005
	Supratentorial	Frontal atrophy	57.1	88.9	92.3	47.1	5.1	0.5	0.042
		Temporal atrophy	52.4	88.9	91.7	44.4	4.7	0.5	0.049
PSP vs PD	Midbrain	atrophy (axial)	86.4	71.4	90.5	62.5	3.0	0.2	0.003
		Atrophy of quadrigeminal plate	77.3	71.4	89.5	50.0	2.7	0.3	0.030
		Hummingbird / Giant Penguin	68.4	100.0	100.0	45.5	∞	0.3	0.011
		MGF	50.0	100.0	100.0	38.9	∞	0.5	0.026
		SCP atrophy	57.1	100.0	100.0	43.8	∞	0.4	0.010
	Pons & Cerebellum	Dilatation of 4th ventricle	67.7	100.0	100.0	41.2	∞	0.3	0.023
	Supratentorial	Frontal atrophy	57.1	85.7	92.3	40.0	4.0	0.5	0.084
PSP vs MSA	Midbrain	Atrophy (axial)	86.4	66.7	82.6	72.7	2.6	0.2	0.005
		Atrophy of quadrigeminal plate	77.3	75.0	85.0	64.3	3.1	0.3	0.003
		Dilatation of 3rd ventricle	77.3	66.7	81.0	61.5	2.3	0.3	0.025
		Hummingbird / Giant Penguin	68.4	100.0	100.0	64.7	∞	0.3	0.000
		MGF	50.0	100.0	100.0	52.2	∞	0.5	0.003
		SCP atrophy	57.1	83.3	85.7	52.6	3.4	0.5	0.024
	Supratentorial	Frontal atrophy	57.1	83.3	85.7	52.6	3.4	0.5	0.024
		Parietal atrophy	66.7	83.3	87.5	58.8	4.0	0.4	0.006
		Temporal atrophy	52.4	83.3	84.6	50.0	3.1	0.6	0.067
PSP vs CBD	Midbrain	Hummingbird / Giant Penguin	68.4	100.0	100.0	40.0	∞	0.3	0.024
		MGF	50.0	100.0	100.0	35.3	∞	0.5	0.055

Table 4.6: Sensitivity, Specificity, Positive Predictive Value (PPV), Negative Predictive Value (NPV) Likelihood ratio for a positive result (LR+) and likelihood ratio for a negative result (LR-) in pathologically confirmed PSP.

Comparison	Region	Abnormality	Sensitivity	Specificity	PPV	NPV	LR+	LR-	p
MSA vs Ctrl	Pons & Cerebellum	MCP atrophy	33.3	100.0	100.0	52.9	∞	0.7	0.104
		Dilatation of 4th ventricle	66.7	100.0	100.0	69.2	∞	0.3	0.005
		MCP hyperintensity	50.0	100.0	100.0	60.0	∞	0.5	0.019
		Pontocerebellar firbre hyperintensity	33.3	100.0	100.0	52.9	∞	0.7	0.104
		HCB	58.3	100.0	100.0	64.3	∞	0.4	0.007
MSA vs PSP	Midbrain	Atrophy (axial)	33.3	13.6	17.4	27.3	0.4	4.9	0.005
		Atrophy of quadrigeminal plate	25.0	22.7	15.0	35.7	0.3	3.3	0.003
		Dilatation of 3rd ventricle	33.3	22.7	19.0	38.5	0.4	2.9	0.025
		SCP atrophy	16.7	42.9	14.3	47.4	0.3	1.9	0.024
	Pons & Cerebellum	MCP hyperintensity	50.0	100.0	100.0	77.8	∞	0.5	0.001
		HCB	58.3	100.0	100.0	80.0	∞	0.4	0.000
	Supratentorial	Frontal atrophy	16.7	42.9	14.3	47.4	0.3	1.9	0.024
		Parietal atrophy	16.7	33.3	12.5	41.2	0.3	2.5	0.006
MSA vs PD	Pons & Cerebellum	Dilatation of 4^{th} ventricle	66.7	100.0	100.0	63.6	∞	0.3	0.013
		MCP hyperintensity	50.0	100.0	100.0	53.8	∞	0.5	0.044
		HCB	58.3	100.0	100.0	54.5	∞	0.4	0.038
MSA vs CBD	Pons & Cerebellum	MCP hyperintensity	50.0	100.0	100.0	50.0	∞	0.5	0.054
		HCB	58.3	100.0	100.0	54.5	∞	0.4	0.038

Table 4.7: Sensitivity, Specificity, Positive Predictive Value (PPV), Negative Predictive Value (NPV) Likelihood ratio for a positive result (LR+) and likelihood ratio for a negative result (LR-) in pathologically confirmed MSA.

6. Macroscopic examination of the brain at post mortem

The sensitivity of macroscopic examination in predicting the histopathological diagnosis was 24/35 (68.6%) for combined PSP and MSA and individually (15/22 (68.2%) for PSP and 9/13 (69.2 %) for MSA. External examination of the brain revealed prominent cortical atrophy in PSP [Table 4], dilatation of the lateral ventricles and atrophy of the deep cortical white matter. STN atrophy and discolouration, atrophy of the midbrain and pontine tegmentum, SCP and blurring of the dentate nucleus were frequent but not universal in PSP. In MSA there was putaminal atrophy and discolouration, and atrophy of the pontine base, cerebellar cortex and atrophy and discolouration of cerebellar white matter. In MSA the distribution of pathology was classified as striatonigral degeneration (SND) predominant in 4, 4 had equal SND and olivopontocerebellar atrophy (OPCA) pathology, 3 were OPCA predominant, 1 had minimal change MSA and 1 was not further classified.

	Macroscopic Abnormality	PSP		MSA		PD		CBD	
External appearance	Cortical Atrophy	16/22	(72.7%)	1/10	(10%)	2/4	(50%)	5/6	(83.3%)
	Frontal atrophy	12/22	(54.5%)	1/10	(10%)	2/4	(50%)	4/6	(66.7%)
	Frontoparietal atrophy	4/22	(18.2%)	0/10	(0%)	0/4	(0%)	1/6	(16.7%)
Brain slices	Lateral ventricle dilatation	19/23	(82.6%)	6/13	(46.2%)	3/7	(42.9%)	5/6	(83.3%)
	Focal cortical atrophy	3/23	(13.0%)	0/13	(0%)	0/7	(0%)	1/6	(16.7%)
	Deep WM atrophy	13/22	(59.0%)	1/12	(8.3%)	1/7	(14.3%)	4/6	(66.7%)
	Global WM atrophy	2/22	(9.1%)	0/12	(0%)	1/7	(14.3%)	1/6	(16.7%)
	Frontal WM atrophy	11/22	(50.0%)	1/12	(14.3%)	0/7	(0%)	3/6	(50.0%)
	Corpus callosum atrophy	3/18	(16.7%)	0/13	(0%)	0/6	(0%)	0/3	(0%)
	Caudate atrophy	1/23	(4.3%)	1/13	(7.7%)	0/7	(0%)	1/5	(20.0%)
	Putaminal atrophy	0/22	(0%)	7/13	(53.8%)	0/7	(0%)	0/5	(0%)
	Putaminal discolouration	0/22	(0%)	5/13	(38.5%)	0/7	(0%)	0/5	(0%)
	Pallidal atrophy	5/23	(21.7%)	1/12	(8.3%)	0/7	(0%)	0/6	(0%)
	Thalamus atrophy	5/21	(23.8%)	0/12	(0%)	0/7	(0%)	1/4	(25%)
	STN atrophy	16/20	(80.0%)	0/10	(0%)	0/7	(0%)	0/4	(0%)
	STN discolouration	17/20	(85.0%)	0/10	(0%)	0/7	(0%)	2/4	(50.0%)
	Amygdala atrophy	1/18	(5.6%)	0/12	(0%)	0/7	(0%)	0/6	(0%)
	Hippocampal atrophy	1/18	(5.6%)	1/11	(9.1%)	1/7	(14.3%)	2/6	(33.3%)
	SN pallor	21/21	(100%)	13/13	(100%)	6/6	(100%)	5/5	(100%)
	LC pallor	18/19	(94.7%)	11/11	(100%)	7/7	(100%)	5/6	(83.3%)
	Midbrain tegmental atrophy	13/17	(76.5%)	2/5	(40.0%)	0/4	(0%)	0/3	(0%)
	Pontine tegmental atrophy	13/20	(65.0%)	1/8	(12.5%)	0/5	(0%)	1/5	(20.0%)
	SCP atrophy	8/10	(80.0%)	0/2	(0%)	0/5	(0%)	1/4	(25.0%)
	Pontine base atrophy	0/7	(0.0%)	7/10	(70.0%)	0/5	(0%)	0/4	(0.0%)
	Medulla atrophy	1/20	(5.0%)	0/9	(0%)	0/5	(0%)	0/6	(0%)
	Inferior olive atrophy	1/10	(10.0%)	3/5	(60.0%)	0/3	(0%)	0/5	(0%)
	Cerebellar cortical atrophy	0/23	(0%)	4/11	(36.4%)	0/7	(0%)	0/6	(0%)
	Cerebellar vermis atrophy	0/20	(0%)	4/10	(40.0%)	0/6	(0%)	0/6	(0%)
	Cerebellar white matter atrophy	0/23	(0%)	7/13	(53.8%)	0/7	(0%)	0/6	(0%)
	Cerebellar white matter discolouration	0/20	(0%)	9/13	(69.2%)	0/7	(0%)	0/6	(0%)
	Dentate blurring	13/22	(59.1%)	3/9	(33.3%)	0/7	(0%)	1/5	(20.0%)
	Dentate discolouration	4/22	(18.2%)	0/9	(0%)	0/7	(0%)	0/5	(0%)

Table 4.8: Frequency of macroscopic findings at post mortem examination of the brain. Routine assessment of the post mortem brain was undertaken unblinded to clinical information.

E. Discussion

This is the first systematic radiological-pathological study in the neurodegenerative parkinsonian syndromes PSP and MSA. We report the sensitivity and specificity of the radiological diagnosis in a cohort including disease controls (pathologically confirmed PD and CBD) and healthy controls, the accuracy of cMRI abnormalities for the pathological diagnosis and directly compare cMRI with macroscopic findings at post mortem. cMRI included standard T1-weighted, T2-weighted and FLAIR images and not advanced MRI imaging techniques, such as diffusion tensor imaging or susceptibility weighted imaging which are still not commonly available in many centres. Our pragmatic evaluation of the routine diagnostic value of cMRI and the substantial inter-rater reliability for diagnosis, suggest that our results may be applicable in standard clinical environments.

1. Accuracy of clinical and radiological diagnosis using cMRI

We found that the clinical diagnosis was more sensitive in PSP (90.9% in PSP compared with 72.7% in MSA) and the radiological diagnosis more sensitive in MSA (61.5% in PSP compared with 76.9% in MSA) although these differences did not reach statistical significance. The radiological diagnosis was more specific than the clinical diagnosis in both PSP and MSA and radiologically no case of MSA was classified as PSP or vice versa (i.e. the consensus radiological diagnosis had 100% specificity).

2. cMRI in pathologically confirmed PSP

The most clinically useful abnormalities seen in PSP were signs of midbrain atrophy, SCP atrophy and frontal and parietal cortical atrophy [Tables 4.5 & 4.6]. Midbrain atrophy was seen in 86.4% and third ventricular enlargement in 77.3%, which is comparable to other reports (Schrag, Good et al. 2000; Yekhlef, Ballan et al. 2003; Righini, Antonini et al. 2004). The MGF sign was very specific but with a sensitivity of only 50%. This is lower than the original description (80%) (Adachi, Kawanami et al. 2004) but higher than a subsequent report (12.5%) (Mori, Aoki et al. 2004). Although the HB sign was found in only 68.4% (in contrast to published studies where it was seen in all cases (Kato, Arai et al. 2003; Oba, Yagishita et al. 2005)), our study supports the high specificity of this finding. When compared to CBD the presence of the HB sign was the only significant finding for PSP [Table 4.6]. The higher sensitivity of the HB sign than the MGF sign [Table 4.6] is concordant with Mori and colleagues where mid sagittal rather than axial images were more reliable in the

assessment of midbrain atrophy (Mori, Aoki et al. 2004). This is due to variability in the angle of the axial plane both used in routine practice and in our heterogenous group which was not optimised for assessment of axial midbrain atrophy (Oba, Yagishita et al. 2005).

Atrophy of the STN, the most characteristic pathological finding of PSP, was seen in only 80% at post mortem [Table 4.8]. The fact that regional atrophy of structures reported to be very specific for PSP may not even be present after death indicates that assessment of regional atrophy on cMRI during life will never enable identification of all cases of PSP.

3. cMRI in pathologically confirmed MSA

In MSA significant cMRI findings were centred in the pons and cerebellum [Tables 4.5 & 4.7]. It may seem surprising that putaminal abnormalities are not more frequent in this group, with only 50% of MSA having putaminal atrophy and 25% the HPR sign on cMRI, particularly given the fact that 8/13 (61.5%) were clinically MSA-P, and 10/13 (76.9%) had a parkinsonian clinical phenotype. The relative lack of putaminal findings in our collection of MSA using cMRI [Table 4.5] is borne out at macrocopic examination of the brain [table 4.8]: only 53.8% of MSA cases had putaminal atrophy, and 38.5% putaminal discolouration.

Overlap between the clinical, radiological and pathological involvement of SND and OPCA pathology is well known. Work in pathologically confirmed cases suggests that SND-predominant cases have more severe parkinsonism clinically and OPCA-predominant cases more severe cerebellar signs (Ozawa, Paviour et al. 2004). However, neuroradiological studies suggest evidence for OPCA radiologically in MSA-P which is in agreement with our findings – in one study 50% of MSA-C had putaminal atrophy (Schrag, Good et al. 2000) and conversely in MSA-P cerebellar findings on cMRI can be highly specific for a diagnosis of MSA-P when compared to PD (90-100%) if less sensitive (14-71%) (Osaki, Wenning et al. 2002). Our cohort has a bias towards parkinsonian conditions and further studies of more purely cerebellar MSA phenotypes are important to study the relationship between the relative distribution of pathology (which is not evident from clinical studies), MRI and clinical findings.

We also found putaminal atrophy and the HPR in PSP in our study, as reported elsewhere (Yekhlef, Ballan et al. 2003) and putaminal atrophy was seen in one PD case with a disease duration of 6.8 yrs - although previous reports suggest that this is either absent in PD (Schrag, Kingsley et al. 1998) or found in up to 38.89% (Yekhlef, Ballan et al. 2003).

Interestingly, there was no putaminal atrophy identified in PSP, CBD or PD at macroscopic examination of the brain [Table 4.8].

The pontine and cerebellar features were more robust MRI findings in MSA – with MCP hyperintensity in 6/12 (50.0%) and the HCB sign in 7/12 (58.3%): only pontine base atrophy in 7/10 (70.0%) and discolouration of the deep cerebellar white matter in 9/13 (69.2%) were more common at macroscopic post mortem examination. These figures are in accordance with published studies (Schrag, Kingsley et al. 1998; Schrag, Good et al. 2000; Bhattacharya, Saadia et al. 2002; Seppi and Schocke 2005). However, the MCP sign has been described in Wilson's disease, hepatic encephalopathy, extrapontine myelinolysis, acute disseminated encephalomyelitis, wallerian degeneration of the pontocerebellar tracts after pontine insult, leukodystrophy and toluene abuse (Uchino, Sawada et al. 2004) and is a characteristic of Fragile X tremor ataxia syndrome (Brunberg, Jacquemont et al. 2002). The HCB sign is also seen in parkinsonism secondary to vasculitis (Muqit, Mort et al. 2001), spinocerebellar ataxias (including SCA-2 (Burk, Skalej et al. 2001), SCA-3 (Murata, Yamaguchi et al. 1998), SCA-7 and SCA-8 (Lee, Liu et al. 2009)) and variant CJD (Soares-Fernandes, Ribeiro et al. 2009). Nonetheless, in the context of the differential diagnosis of atypical Parkinsonism the high specificity and PPV can be clinically useful (Osaki, Wenning et al. 2002) [table 4.7]. Not all MSA cases had either putaminal or cerebellar abnormalities at macroscopic post mortem examination and the frequency of findings such as pontine and cerebellar atrophy were very similar to that seen using cMRI.

4. cMRI in pathologically confirmed PD

Very few abnormalities were seen on cMRI in the PD group [table 4.5], despite the atypical clinical features in our study. This is in accordance with the literature, which suggests that MRI changes in PD are too subtle to be reliably detected by cMRI (Savoiardo 2003; Yekhlef, Ballan et al. 2003; Seppi and Schocke 2005; Sitburana and Ondo 2009). Macroscopic post mortem findings are restricted to the SN and locus coeruleus (LC) both of which are not reliably assessed on cMRI. Our very atypical group of PD likely represents a referral bias to the QSBB. In addition to this it has not been routine in the UK for patients with a clinical diagnosis of PD to have routine imaging unless there are atypical features or if deep brain stimulation is being considered (NICE, 2006). This also explains the relatively low number of cases of PD identified with available imaging.

5. cMRI in pathologically confirmed CBD

There were no cMRI specific findings in CBD and in no case was cortical atrophy felt to be asymmetric in CBD. Some of the literature suggests that frontoparietal hemispheric asymmetry is characteristic (Savoiardo 2003; Tokumaru, Saito et al. 2009) however in one study of pathologically confirmed cases this was not evident (Schrag, Good et al. 2000). The presence of midbrain atrophy, although not sufficient to be classified as the MGF or HB sign, is counter to some published work (Savoiardo 2003) although CBD is known to affect subcortical structures such as the SN and STN so midbrain atrophy and dilatation of the third ventricle are not unexpected findings. The HB and MGF signs indicate more severe midbrain atrophy and are found only in the PSP group. This is in keeping with published series with pathological confirmation where no distinguishing features were seen using cMRI in CBD (Schrag, Good et al. 2000; Josephs, Tang-Wai et al. 2004). The most common findings at macroscopic post mortem examination were cortical atrophy (particularly frontal) associated with deep white matter atrophy and dilatation of the lateral ventricle [Table 4.8]. CBD is particularly difficult to diagnose during life and studies using clinical diagnoses of CBD – the so-called corticobasal syndromes (CBS) – will be particularly susceptible to errors in predicting the underlying pathological diagnosis (Ling, O'Sullivan et al. 2010). Thus, interpretation of radiological studies of this very rare entity should be cautious in the absence of pathological confirmation.

6. Beyond cMRI

In this study cMRI enables the detection of regional atrophy in PSP and MSA that is found at macroscopic brain assessment. Smaller nuclei where pathological changes occur are reliably assessed at macroscopic brain examination but not on cMRI. Although some, e.g. the STN may be more clearly identified at 3 Tesla (Slavin, Thulborn et al. 2006) there is very little published data on the diagnostic accuracy with pathological confirmation. Microstructural abnormalities in the substantia nigra such as those found using DTI (Vaillancourt, Spraker et al. 2009) or differences in the deposition of iron in nuclei such as the SN (Martin, Wieler et al. 2008) are interesting new MR imaging techniques that have not been studied systematically in PSP and MSA. Objective measurements of conventional images have been shown to improve accuracy in predicting the clinical diagnosis (Quattrone, Nicoletti et al. 2008), and voxel-based morphometry (Josephs, Whitwell et al. 2008) and automatic segmentation (Messina, Cerasa et al. 2011) are promising techniques which may increase sensitivity of detecting regional atrophy during life.

7. Strengths and limitations of the study

There are limitations of this study. We included a few CBD and clinically atypical PD cases and did not include other neurodegenerative diseases which may be clinically confused (including frontotemporal dementia, FTDP-17, spinocerebellar ataxias) which may have an effect on specificity and predictive values. The retrospectively collected cMRI images were heterogeneous. However, 89.5% of all studies were performed at 1.5 T and images could be successfully assessed for a comprehensive checklist of abnormalities with only a few cases where some of the signs could not be assessed; the effect of including a few cases with lower field strength may have led to under-reporting of signal change abnormalities. The results obtained provide, therefore, a 'real-world' assessment of the diagnostic value of routine radiological practice. The use of working clinical diagnoses and inclusion of clinically atypical cases is important in studies of MRI as many cases are often excluded from clinical studies. Furthermore, the key strength of this study lies in the neuropathological confirmation of the diagnosis, detailed blinded assessment of cMRI images and comparison with macroscopic abnormalities at post mortem.

F. Conclusion

In a cohort of pathologically proven parkinsonian illnesses some cMRI findings are highly specific in MSA and PSP but lower sensitivity means a significant proportion of cases will not have diagnostic abnormalities. However, a consensus radiological diagnosis did not misclassify PSP as MSA or vice versa. Using subjective assessment most regional atrophy found at macrocopic examination is detected using cMRI although it may not enable accurate diagnosis of these conditions in all cases even in experienced hands; the use of more advanced and novel MRI techniques will be needed to improve accurate prognostication in the clinic and in the development of specific biomarkers for the monitoring of disease progression.

Chapter 5: The midbrain to pons ratio - A simple and specific MRI sign of progressive supranuclear palsy

A. Introduction

Neurodegenerative diseases presenting with Parkinsonism including idiopathic Parkinson's disease (PD), Progressive Supranuclear Palsy (PSP) and Multiple System Atrophy (MSA) can be difficult to differentiate clinically, particularly early in the disease course (Hughes, Daniel et al. 2002). Characteristic midbrain atrophy in PSP and pontine atrophy in MSA can be assessed on MRI (Massey, Micallef et al. 2012); however many MR-based measurements proposed as diagnostic for PSP or MSA lack pathological verification and are often not easy to apply routinely (Asato, Akiguchi et al. 2000; Schrag, Good et al. 2000; Warmuth-Metz, Naumann et al. 2001; Kato, Arai et al. 2003; Righini, Antonini et al. 2004; Oba, Yagishita et al. 2005; Quattrone, Nicoletti et al. 2008). A summary of published methods is described in Table 5.1.

Measurement	Method	Reference
Axial SN measurement	Axial T2w MRI 5mm slice thickness 0-20 degrees positive to inferior orbitomeatal line cut off 50% hyperintensity of SNC	(Duguid, De La Paz et al. 1986; Tohgi, Takahashi et al. 2001)
	Axial T2w MRI 0-20 degrees positive to inferior orbitomeatal line cut off 50% hyperintensity 2 parallel lines either side mean of 3 measurements	(Braffman, Grossman et al. 1989)
	Axial T2w MRI Plane is through superior colliculus and orbital surface of frontal lobe Intensity values measured across a line perpendicular to the SN and passing through the middle of the RN using 50% maximum intensity value as cut off	(Pujol, Junque et al. 1992)
Axial midbrain measurements	Axial T2w MRI Axial midbrain diameter < 17mm in PSP	(Schrag, Good et al. 2000)
	Axial T2w MRI Axial perpendicular to axis of midbrain / ACPC line; AP diameter of midbrain at the level of the superior colliculus < 17mm for all PSP but significant overlap	(Righini, Antonini et al. 2004)
	Axial T2w MRI Maximum midsagittal AP diameter	(Warmuth-Metz, Naumann et al. 2001)

Measurement	Method	Reference
Axial pontine measurements	Axial T2w MRI Maximum AP diameter midline**;** Level of the MCP	(Warmuth-Metz, Naumann et al. 2001)
Sagittal measurements	Sagittal T1WI Pons: maximal perpendicular at midpontine level**;** Midbrain: maximal diameter in plane along axis of aqueduct**;** Tectal plate: maximal diameter	(Warmuth-Metz, Naumann et al. 2001)
	Sagittal T1WI Rostral midbrain at level of PC**;** Caudal midbrain at level of superior pontine notch**;** Pontine: fastigium of fourth ventricle**;** Medulla: obex	(Asato, Akiguchi et al. 2000)
	Sagittal T1w MRI Segmentation of the midbrain parallel to inferior transverse plane of splenium and genu**.** First division at intercollicular space**;** second division at superior border of pons**.** third division at inferior border of pons**;** fourth division transverse plane through the posterior mammillary body Measurements of Area: Rostral midbrain tegmentum**;** Caudal midbrain tegmentum**;** Superior colliculus**;** Inferior colliculus**;** Pontine base**;** Pontine tegmentum**;** Diameter**;** Interpeduncular fossa behind mammillary body**;** Midbrain tegmentum	(Kato, Arai et al. 2003)
	Sagittal T1WI Segmentation of the pons and midbrain and comparison of areas to make ratio	(Oba, Yagishita et al. 2005)
	Sagittal T1WI Segmentation of CC, and measurements of the cingulate cortex	(Arai 2006)
	T1W MRI Pons area and midbrain area in mid sagittal slice; MCP and SCP width in parasagittal and coronal slices respectively; Ratio of pons to midbrain did not distinguish PSP from MSA-P or PD completely; Ratio of MCP to SCP did not distinguish PSP from MSA-P or PD complete; However the MRPI completely distinguished the groups	(Quattrone, Nicoletti et al. 2008)

Table 5.1: Published studies of measurements on conventional MRI in PSP and related conditions.

Three factors determined the development of the ratio:

1. The need for a simple measurement that is easy to perform even by non-specialists, easy to explain, not time-consuming or needing special software and reproducible.

2. The pattern of pathology and atrophy in PSP and MSA: involvement of the midbrain tegmentum PSP leading to a concave superior profile (Righini, Antonini et al. 2004; Oba, Yagishita et al. 2005) and flattening of the pontine base in MSA (Oba, Yagishita et

al. 2005).

3. Midsagittal images were felt to be more reliable than axial images for assessing midbrain volume loss subjectively and less variable than axial images in terms of the plane commonly acquired (Mori, Aoki et al. 2004; Massey, Micallef et al. 2012).

B. Aim

Our hypothesis was that simple measurements of the midbrain and pons (or their ratio) on midsagittal MRI would identify confirmed PSP and MSA.

C. Materials and Methods

1. Participant Selection

A pathologically confirmed cohort of PSP, PD and MSA subjects (Table 1) was selected from the Queen Square Brain Bank (QSBB) at UCL Institute of Neurology; brains were donated following ethically approved protocols under licence from the Human Tissue Authority. A cohort of PSP, PD, MSA and healthy subjects was prospectively recruited at the National Hospital for Neurology and Neurosurgery, as part of an ethically approved study with written informed consent.

In the pathologically confirmed group the diagnosis was determined using standard neuropathological criteria (Ince, Clarke et al. 2008). In the clinically diagnosed group participants fulfilled operational criteria (Gibb and Lees 1988; Litvan, Agid et al. 1996; Gilman, Low et al. 1999) and were assessed with clinimetric scales including Hoehn & Yahr, (Hoehn and Yahr 1967) the unified Parkinson's disease rating scale (UPDRS) (Fahn, Elton et al. 1987), Folstein's Mini-mental State Examination (MMSE) (Folstein, Folstein et al. 1975), the frontal assessment battery (FAB) (Dubois, Slachevsky et al. 2000), Golbe's PSP rating scale (PSPRS) (Golbe and Ohman-Strickland 2007) or the unified MSA rating scale (UMSARS) (Wenning, Tison et al. 2004). Healthy controls had no history of neurological illness at time of imaging [Figure 1].

In the pathologically confirmed group cases were selected where conventional 1.5T midsagittal T1-weighted images were electronically available. In the clinically diagnosed group all had 3T MRI with volumetric T1-weighted images.

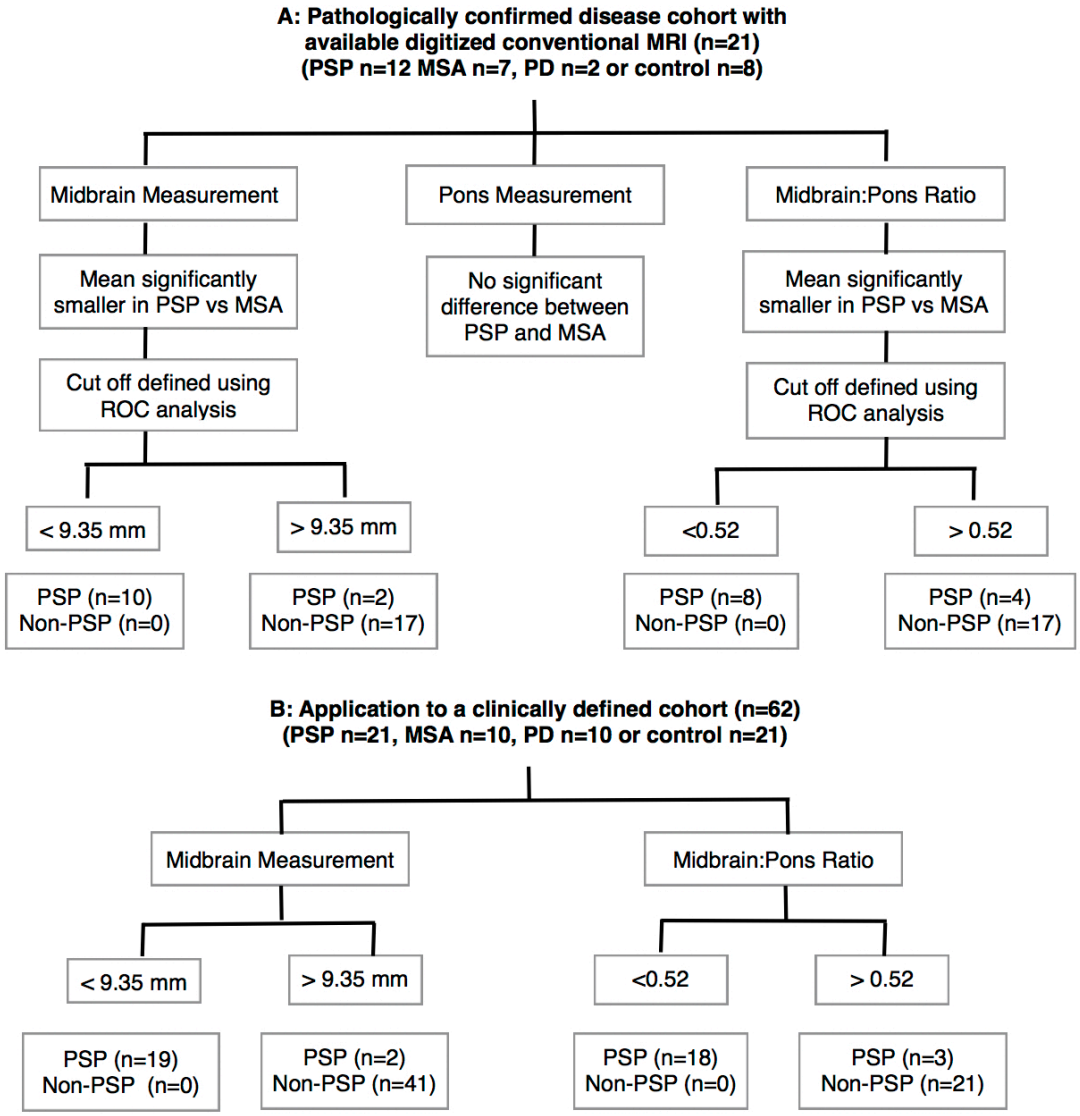

Figure 5.1: Flow diagram in the pathologically confirmed group (A) and application of cut off values to the clinically defined group (B).

2. Midbrain and pons measurements and the midbrain:pons ratio

Elliptical regions of interest were placed over the pons and the midbrain in the midsagittal slice [Figure 2]. Two lines were drawn to define the major axes of the ellipses, corresponding to oblique superior-inferior axes (thin white lines). The maximal measurement perpendicular to the major axis was taken (thick white lines). In all cases the posterior border of the pons was clearly identifiable and did not include the pontine tegmentum; the midbrain measurement did not include the collicular plate and was chosen to maximise the chance of detecting atrophy of this region in PSP as exhibited by the concave appearance in the midsagittal plane (Righini, Antonini et al. 2004).

The midbrain/pons ratio was derived by dividing the midbrain by the pons measurements. In the pathologically-confirmed group (n=29), measurements were made blinded to clinical and pathological information (CM - neuroradiologist); a randomly chosen subset (n=8) was measured by another rater (NF - neurologist) for inter-rater assessment. In the clinically-diagnosed group (n=62) a third rater (LM - neurology trainee) performed all measurements.

3. Statistical Analysis

Group characteristics were compared using multivariate analysis with post-hoc Bonferroni correction. An intraclass correlation coefficient was used to assess inter-rater agreement and ROC curve analysis to define cut off values (maximal sum of sensitivity and specificity) in the pathologically-confirmed group that were subsequently applied to the clinical group. Pearson's correlation coefficient was used to assess correlation of the midbrain measurement and ratio with age at onset, age at scan and disease duration in the pathologically confirmed group, and in the clinically diagnosed group clinical scores. SPSS 20.0 for Mac was used for statistical analysis.

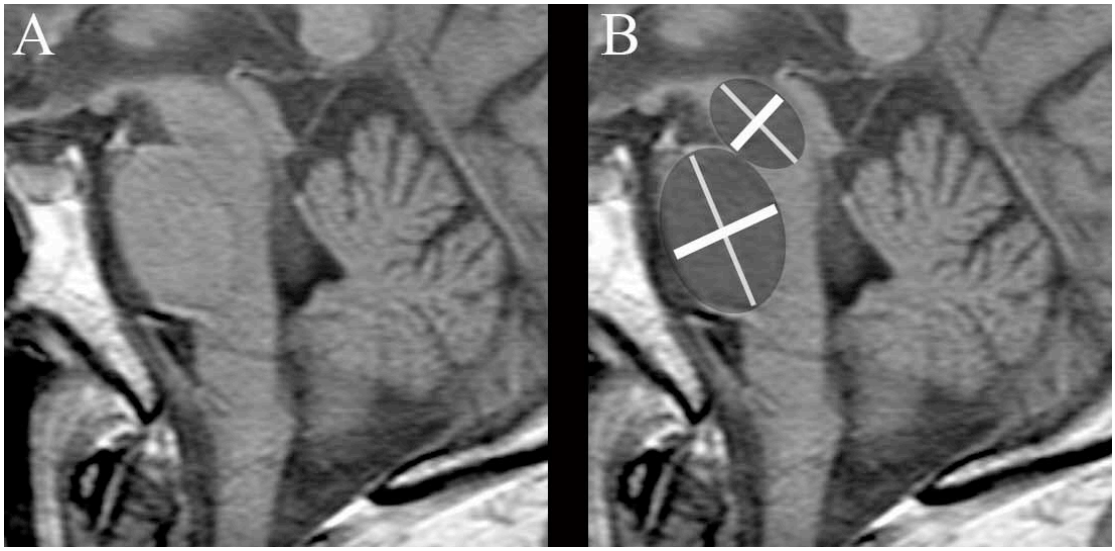

Figure 5.2: Measuring the anterior-posterior distance of the pons and midbrain. For details of see text.

D. Results

1. Demographic features

The demographic features of both cohorts are described in table 5.2.

2. Measurement values

In pathologically confirmed PSP the mean midbrain measurement and the midbrain:pons ratio were significantly smaller than controls and MSA; in the MSA group there was a trend for the pons measurement to be smaller than controls Additionally in the clinically diagnosed group the pons was significantly smaller and the midbrain:pons ratio was significantly increased in MSA relative to PSP, to PD and to controls [Table 5.3; Figure 5.3]. Single measure intraclass correlation coefficients were 0.97 for the midbrain measurement and 0.94 for the pontine measurement ($P<0.001$ for both). In the clinically diagnosed PSP group a threshold of 9.35mm for midbrain diameter had 100% specificity and positive predictive value for PSP and only 2 cases are not classified as PSP (2/21=9.5%). Outliers included one probable PSP with a disease duration of 3.7 years and one possible PSP with a disease duration of 4.7 years. For a diagnosis of PSP using a threshold of 0.52 for the midbrain:pons ratio there was a specificity and positive predictive value of 100% and

sensitivity of 85.7%. No correlation was found between age, disease duration or clinimetric scores with the midbrain or pons measurements or ratio.

Group		Control	PSP	PD	MSA	ANOVA
Pathologically confirmed group	n	8	12	2	7	
	Age at scan (SD)	66.8 (8.5)	69.5 (5.0)	70.5 (6.2)	58.4 (5.2)	MSA < PSP (p<0.001) MSA < PD (p<0.05)
	Disease duration at scan (SD)		3.9 (2.4)	10.7 (9.4)	5.6 (2.9)	ns
Clinically diagnosed group	n	21	21	10	10	
	Age at scan	65.9 (5.6)	69.4 (6.5)	66.6 (6.0)	63.4 (8.2)	ns
	Disease duration		4.6 (3.1)	7.3 (4.1)	4.9 (2.1)	ns
	H&Y		3.8 (0.8)	2.2 (0.8)	4.1 (0.7)	PSP & MSA > PD (p<0.001)
	UPDRS I		3.5 (1.9)	2.6 (1.6)	3.4 (1.7)	ns
	UPDRS II		20.5 (7.5)	10.2 (4.7)	26.7 (6.1)	PSP & MSA > PD (p<0.001)
	UPDRS III		38.6 (12.0)	23.9 (9.3)	52.0 (9.4)	PSP > PD (p=0.003); MSA > PD (p<0.001); MSA>PSP (p=0.008)
	MMSE		27.5 (2.3)	28.9 (1.2)	28.8 (1.0)	ns
	FAB		12.5 (4.3)	17.0 (0.9)	16.0 (1.7)	PSP<PD (p=0.003); PSP<MSA (p=0.025)
	PSPRS		38.5 (11.7)			
	UMSARS				54.9 (12.4)	

Table 5.2: Demographic and clinimetric features of the pathologically confirmed and clinically diagnosed groups. Statistically significant differences (ANOVA) in bold. In the clinical cohort 17/21 were probable and 4/21 possible PSP and 7/10 MSA were probable and 3/10 possible by research criteria. 8/10 MSA cases were of the parkinsonian-predominant phenotype (MSA-P) in the clinically diagnosed group.

Group	Measurement	Control	PSP	PD	MSA	ANOVA
Pathologically Confirmed Group	Midbrain	11.5 (0.4)	8.1 (1.2)	10.1 (0.8)	10.7 (0.7)	PSP<Control & MSA (p<0.001)
	Pons	18.2 (0.9)	17.4 (1.8)	17.8 (0.0)	15.5 (2.4)	MSA < Control (p=0.061)
	Midbrain:Pons ratio	0.63 (0.03)	0.47 (0.08)	0.57 (0.05)	0.70 (0.11)	PSP<Control & MSA (p<0.001)
Clinically Diagnosed Group	Midbrain	11.1 (0.8)	7.55 (1.12)	11.4 (0.7)	10.8 (0.8)	PSP<Control, PD, MSA (p<0.001)
	Pons	17.8 (1.4)	17.1 (1.4)	18.3 (1.1)	14.8 (3.3)	MSA<PSP (p<0.001); MSA<PD & Control (p<0.05)
	Midbrain:Pons ratio	0.62 (0.05)	0.44 (0.08)	0.63 (0.05)	0.77 (0.18)	PSP<Control, PD, MSA (p<0.001); MSA>PSP (p<0.001); MSA>PD & Control (p<0.05)

Table 5. 3: Mean (SD) measurements (mm) in the pathologically confirmed and clinically diagnosed groups. Statistically significant differences (ANOVA) in bold. Defined by the maximum sum of sensitivity and specificity from the ROC curve in pathologically confirmed cases, a midbrain measurement of less than 9.35mm had 83% sensitivity, 100% specificity and positive predictive value for PSP (area under the curve 0.94; p = 0.002) and a ratio of less than 0.52 had 67% sensitivity and 100% specificity and positive predictive value for PSP (area under the curve 0.95; p=0.001) when compared to MSA [Figure 3].

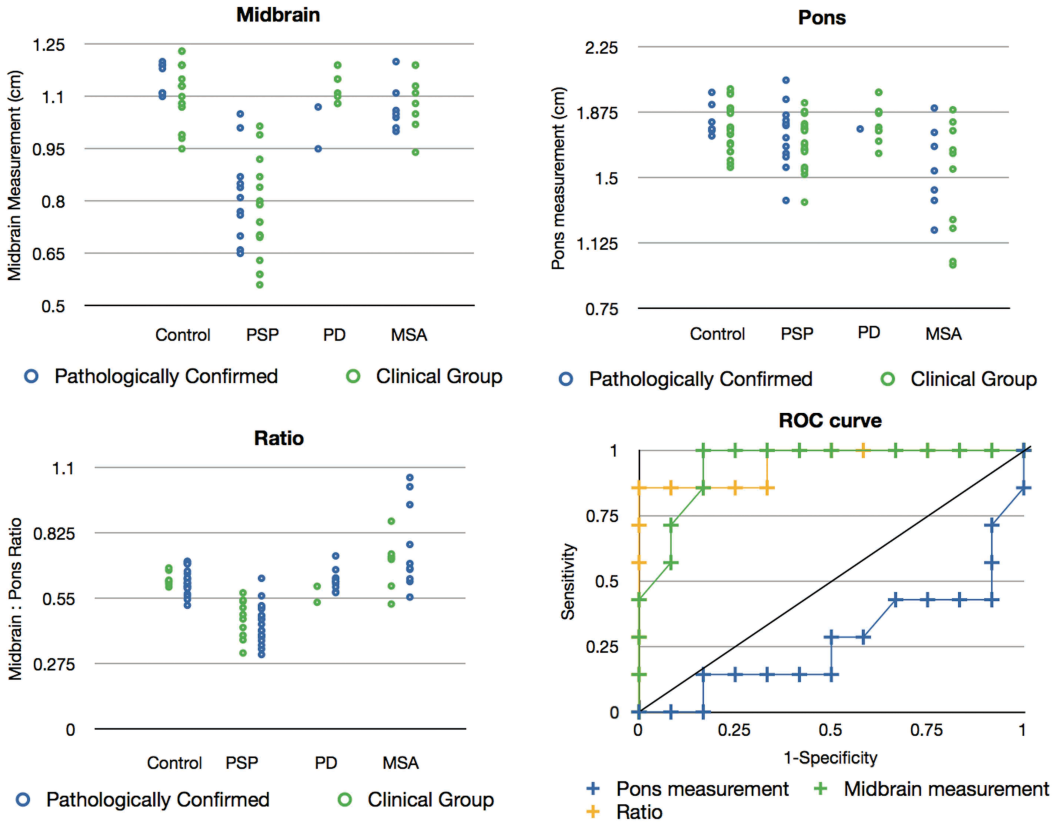

Figure 5.3: Scatterplots of the midbrain and pons measurements showing both pathologically confirmed and clinically diagnosed groups and Receiver Operating Curve analysis in the pathologically confirmed group comparing PSP and MSA.

E. Discussion

In pathologically confirmed disease there was support for our hypothesis that there is a significantly smaller midbrain tegmental measurement and a reduced midbrain tegmentum:pontine base ratio in PSP compared to controls and MSA. Conversely, in MSA there was a trend towards an increased midbrain:pontine base measurement. Put simply, in normal controls the midbrain tegmentum was approximately 2/3 of the pontine base, whereas in PSP it is less than 50% and in MSA it is greater than 2/3 [Table 5.2; Figure 5.3] - all non-PSP subjects had a midbrain:pons ratio greater than 52%; 67% (pathologically confimed PSP) and 85.7% (clinically diagnosed PSP) had a ratio of less than 52%. There was excellent inter-rater reliability in the measures.

Using ROC analysis a cut-off value of 9.35mm midbrain tegmental measurement had 100% specificity and 83% sensitivity for a pathological diagnosis of PSP and a midbrain

tegmentum: pontine base ratio of 0.52 or less had a 67% sensitivity and 100% specificity for PSP when compared to MSA. When applied to the clinically diagnosed group the cut-off values were still 100% specific for PSP, with sensitivities of 90.5% and 87.5%, respectively.

1. Comparison with visual assessment and other published measurements

The maximal midsagittal midbrain tegmentum measurement and ratio of midbrain tegmentum to pontine base are approximately equivalent in terms of area under the curve in predicting the diagnosis: while the midbrain tegmentum measurement has higher sensitivity for the diagnosis, the ratio controls for head size which is a confounding factor of simpler measurements. Visual assessment of conventional MRI indicates that the most useful subjective feature of the routine radiological assessment of midbrain atrophy is the hummingbird sign (Kato, Arai et al. 2003; Massey, Micallef et al. 2012). Axial plane measurements often show overlap of PSP with other groups (Schrag, Good et al. 2000; Warmuth-Metz, Naumann et al. 2001; Righini, Antonini et al. 2004) and the variability in axial plane taken during routine MRI makes comparison difficult. It is more straightforward to obtain 'standard' mid sagittal images and both linear measurements (Asato, Akiguchi et al. 2000) and manual segmentation for measurement of area (Kato, Arai et al. 2003; Oba, Yagishita et al. 2005) have been used in clinically diagnosed cases.

Using our measurement the sensitivity for the diagnosis of PSP was high compared to that based on qualitative assessment alone where a hummingbird sign may be seen in only 67% (Massey, Micallef et al. 2012). This is promising as a measurement which can be derived rapidly with little training. Furthermore our results compare favourably with previous reports of linear measurements showing overlap between PSP and MSA but not control or PD groups (Warmuth-Metz, Naumann et al. 2001) and even more complex area measurements where overlapping values of midbrain and pons area are still found (Oba, Yagishita et al. 2005; Groschel, Kastrup et al. 2006) as have more detailed analysis of midsagital area of the rostral and caudal midbrain tegmentum (Kato, Arai et al. 2003).

Our results support the hypothesis that because of differential patterns of atrophy (PSP with greater midbrain loss and MSA with greater pontine loss) a simple ratio measurement of midbrain:pons helps in differentiating PSP and MSA. [Figure 5.3 – the spread of MSA values to be greater for the ratio hence potentially increasing the distinction between the two]. This is part of the rationale employed in the MR Parkinson Index (MRPI) measurement (Quattrone, Nicoletti et al. 2008).

2. Correlation with disease duration and severity

We did not, however, find a correlation between disease duration or severity measured using clinimetric scales. A previous study has been reported a correlation of disease severity with the area of the midbrain in sagittal section, and a midbrain to pons area ratio (Oba, Yagishita et al. 2005) but other studies using linear measurements and the MRPI do not report on this (Schrag, Good et al. 2000; Kato, Arai et al. 2003; Righini, Antonini et al. 2004; Quattrone, Nicoletti et al. 2008). A clear problem with these studies is the reliance on clinical criteria which by definition restrict the spectrum of cases studied, particularly early in the disease course when the clinical diagnosis is most uncertain. In order to address this issue, prospective studies of subsequently pathologically confirmed disease will be necessary. In the case of a simple linear measurement it may be too much to expect correlation with measurements of disease severity. Indeed, area measurements of the midbrain in the mid-sagittal plane in two dimensions although useful for making a diagnosis of PSP do not correlate with disease severity although a three-dimensional volumetric technique has shown correlation between midbrain volume and clinical severity (Groschel, Hauser et al. 2004; Groschel, Kastrup et al. 2006).

3. Strengths and limitations of the study

The strengths of our study lie in the pathological validation of the diagnosis and the rationalised approach to developing simple measurement based on knowledge of the pathological topography. However, there was a relatively small sample size of the pathologically confirmed group although our findings were confirmed in a larger clinically diagnosed cohort.

A strength of our study is that the clinically diagnosed group of MSA (8/10 MSA-P, 2/10 MSA-C) were clinically relevant in that we selected those with largely Parkinsonian features who are more likely to cause diagnostic difficulty. Those with cerebellar predominant disease might be expected to have greater pontine atrophy - in effect our inclusion of a high proportion of MSA-P patients is a sterner test for our proposed measure. Post Mortem studies confirm a relationship between the relative distribution of pathology in the striatonigral and olivopontocerebellar regions correlating with MSA-P and MSA-C respectively, although there is overlap (Ozawa, Paviour et al. 2004).

F. Conclusion

Many methods are described in the literature for distinguishing between PSP and other conditions based on measurements of conventional imaging. However, often the method is not straight-forward, axial images are used (which are less reliable than sagittal images at least in part due to more intrinsic variation in angle of acquisition (Mori, Aoki et al. 2004)) or relatively complicated measurements of areas or ratios are advocated. These are outside of the bounds of everyday practice and not feasible particularly in the non-specialist setting.

Our method is simple, robust and, in a clinical setting, suitable for use without the need for specialist training, time consuming procedures or software that is not already available in most basic imaging systems. It affords a histopathologically supported and clinically feasible rapid assessment of midbrain and pontine base atrophy which may help in the diagnosis and differential diagnosis of PSP and MSA.

Chapter 7: High resolution MR anatomy of the subthalamic nucleus: Imaging at 9.4 T with histological validation

A. Introduction

The subthalamic nucleus (STN) was first described by Jules Bernard Luys (1828-1897) in 1865 (Parent 2002). In the early 20th century Purdon Martin identified vascular lesions in the subthalamic region in cases of hemiballism (Purdon Martin 1927). More recent studies demonstrate that improvement in Parkinsonian symptoms in the 1-methyl-4-phenyl-1,2,3,6-tetrahydropyridine (MPTP) monkey model of Parkinsonism is found after placement of lesions (Bergman, Wichmann et al. 1990; Aziz, Peggs et al. 1991) or high-frequency stimulation of the STN (Benazzouz, Gross et al. 1993). As a consequence the STN has become the target of choice for deep brain stimulation in advanced Parkinson's Disease (PD) (Limousin, Pollak et al. 1995; Limousin, Krack et al. 1998).

The oblique orientation and small size of this structure contribute to the difficulties in its identification using conventional MRI. In planning placement of deep brain electrodes, standard brain atlases are commonly used to derive the coordinates of the STN in relation to the patient's ventricular landmarks obtained by ventriculography (Benabid, Krack et al. 2000) or T1-weighted MR (Starr 2002). Clinical and electrophysiological surrogates are used to confirm electrode placement (Gross, Krack et al. 2006). However, the anatomical accuracy of this approach has been challenged by pathological reports of inaccuracies in electrode placement (Counelis, Simuni et al. 2003; Hariz, Blomstedt et al. 2004; McClelland, Vonsattel et al. 2007) and by demonstration of the inter-individual variability in the shape, size and position of the STN (den Dunnen and Staal 2005; Ashkan, Blomstedt et al. 2007). Direct visualisation of the STN is reported using reproducible MRI methods (Zonenshayn, Rezai et al. 2000; Hariz, Krack et al. 2003; Hariz, Blomstedt et al. 2004; Foltynie, Zrinzo et al. 2011). However, a further study has suggested that the STN is only partially visualised on conventional MRI at 1.5T (Dormont, Ricciardi et al. 2004).

The accuracy of MR in visualising structures such as the STN is best assessed by comparing its characteristics on MR directly with those revealed histologically. Thus far there has been no direct comparison between the STN visualisation on MRI and its histological characteristics in the same specimen.

B. Aim

We aimed to validate directly the anatomical definition of the STN using high field MRI with histological examination of the same tissue, and to determine the anatomical variability of this nucleus.

C. Materials and Methods

1. Preparation of post mortem tissue

Post mortem brain tissue was obtained from the Queen Square Brain Bank for Neurological Disorders (QSBB), UCL Institute of Neurology, where tissue is donated according to ethically approved protocols and is stored under a licence from the Human Tissue Authority. Eight specimens were used in this study [Table 1].

No	Gender	Side fixed	Age at death	DOF (days)	Pathological diagnosis	Cause of death
1	F	Both	94	4149	Tissue not examined pathologically	"Old age"
2	M	Right	94	51	1. Small vessel disease (severe) 2. Braak & Braak stage IV	Broncho-pneuomonia
3	M	Right	38	56	1. No diagnosis made	Metastatic disease
4	M	Left	78	78	1. Cerebral amyloid angiopathy (moderate)	Metastatic carcinoma of the lung
5	M	Right	79	1029	1. No diagnosis made	1. Bilateral broncho-pneumonia 2. Possible metastatic disease
6	F	Left	82	366	1. Pathological ageing 2. Moderate cerebral amyloid angiopathy 3. Mild small vessel disease	
7	F	Right	82	302	1. Control 2. Pathological Ageing 3. Parietal Infarct	1. Broncho-pneumonia
8	F	Right	72	67	1. Amyotropic lateral sclerosis	1. Metastatic disease

Table 7.1: Characteristics of cases studied

Formalin-fixed tissue was dissected to produce a tissue block that included the subthalamic nucleus. The MR axis was aligned perpendicular to the axis of the brainstem and, after imaging, the specimen was divided along this midline sagittal axis before embedding in paraffin.

2. MRI Protocol

Samples were imaged at room temperature in perfluoropolyether (Fomblin, Solvay Selexis) at 9.4T (Varian NMRS MRI) with a 40mm quadrature volume RF coil.

1. Parameters for high-resolution spin-echo (SE) images were: TE 15-22ms, TR 2000-2200ms, scan averages 24-32, interleaved slices, slice thickness 0.5-1mm, slice gap 0.5-1mm, matrix 512x512, field of view (FOV) 45x45mm (in-plane resolution 88 µm) and imaging time up to 10 hours.
2. Superior in-plane resolution was obtained in one case: 1024x1024 matrix (in plane resolution 44 µm), 132 averages; other parameters as above, imaging time 72 hours.
3. Three-dimensional gradient echo (ge3d) sequences had the following parameters: TR 12ms, TE 3.2ms, flip angle 10°, FOV 45mm x 45mm x 90mm, Matrix 256 x 256 x 512, 14 averages, acquisition time 3 hours 4 minutes.

These parameters were chosen on the basis of pilot acquisitions to yield optimal image contrast for the structures of interest; due to the reduced T2 relaxation times in fixed tissue at 9.4T (unpublished data) the SE sequence parameters produced predominantly T2-weighted image contrast. Images were viewed and processed in ImageJ (version 1.43h, US National Institutes of Health, Bethesda, Maryland)(Rasbrand, 2009).

3. Histological Protocol

After imaging, tissue blocks were cut and embedded in paraffin wax and serially sectioned at 20 um. Every 20th section was stained with the Luxol Fast Blue and Cresyl Violet (LFB/CV) method in 4 cases, and in 3 of these further sections were stained with Perls stain for iron. Macroscopic images were obtained at 20-40x magnification using Image Pro Plus (Mediacybernetics, Bethseda, MD www.mediacy.com).

4. Image segmentation, orientation, dimensions and volume calculations

MR images were segmented manually in ITK-SNAP (version 1.8.0) (Yushkevich, Piven et al. 2006) with reference to neuroanatomical atlases (Schaltenbrand and Wahren 1977; Carpenter and Sutin 1983; Nieuwenhuys, Voogd et al. 1988). After manual segmentation the STN volume was calculated using the volume and statistics function. Segmentation-mask measurements of the STN width (maximum distance in the axial plane from medial to lateral tip) and depth (maximum distance in the axial plane between the anterior and posterior borders perpendicular to the width measurement) in the axial plane were obtained with ImageJ; the height was calculated with reference to the number of 1-1.5mm axial slices in which the STN appeared. The higher-contrast SE images were used for calculation of volume and measurements. Ge3d images were used to demonstrate the relationship of structures in three dimensions due the their intrinsic higher resolution in all 3 orthogonal planes.

5. Position relative to internal markers

The position of the STN was determined in relationship to three arbitrary lines in the axial plane [See figure 7.1]:

1. The midline
2. A line connecting the anterior border of the fornix with the posterior border of the mamillothalamic tract (the FMT line)
3. A line parallel to the axis of the myelinated fibres separating the substantia nigra (SN) and red nucleus (RN) (the RN line) through the maximum diameter of the red nucleus

The position of the STN itself was represented by a line connecting the posterolateral and the anteromedial tip of the STN (the STN line). The FMT line and STN line were used as reference at all levels. The RN line was not used at levels above the RN, the transverse myelinated fibres have a more circular shape at this level and are thus less amenable to being used as a reliable marker of axis. SPSS 16.0 for Mac (Microsoft, Redmond, WA) was used for statistical analysis.

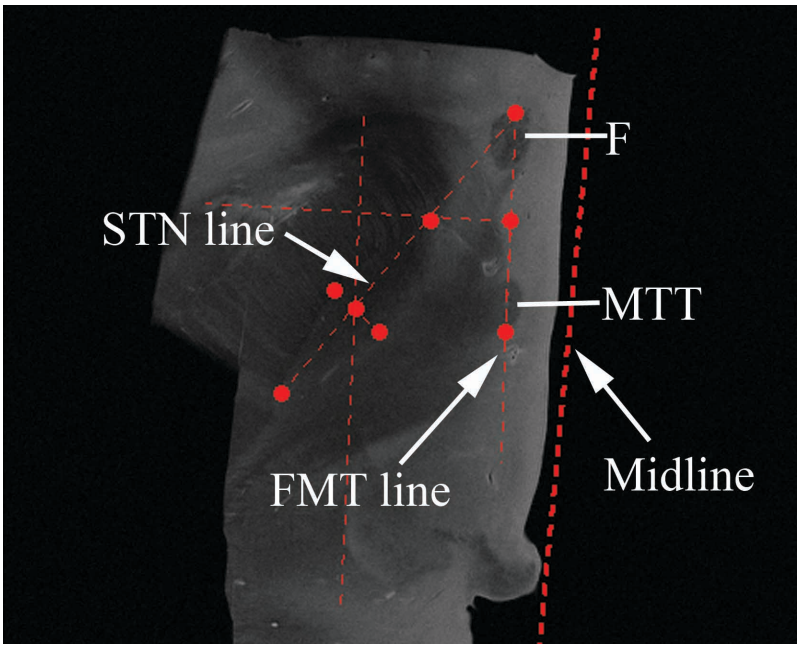

Figure 7.1: Assessing the anatomical variability of the STN at 9.4T. SE axial image through a superior level of the STN with the MTT and F clearly identifiable. Reference points are the midline, and the midpoint between the F and MTT. Measured points are marked as red dots and included the medial and lateral tips, the anterior and posterior borders of the STN. See text.

D. Results

1. Shape and Signal Characteristics of the STN on SE Images

Excellent contrast between white and grey matter allowed clear definition of the STN boundaries on SE images in all cases. In the axial plane, the STN was almond-shaped and lay at an oblique angle to the anteroposterior (AP) axis of the brainstem [Figure 7.2]. In 5/8 cases studied (6/9 nuclei) the STN was of intermediate signal intensity, similar to that of the internal capsule and between that of grey matter structures such as the pulvinar and hypothalamus which appeared hyperintense, and that of the pallidum, ansa lenticularis (AL), RN and SN which were hypointense [Figure 7.2]. In 2 cases (long duration fixation) the signal arising from the STN was higher and in one the STN was relatively hypointense and comparable to other iron-laden nuclei. The anteromedial portion of the STN was relatively hypointense in 6/8 cases compared to the posterolateral portion [Figure 7.2A-D short white arrow].

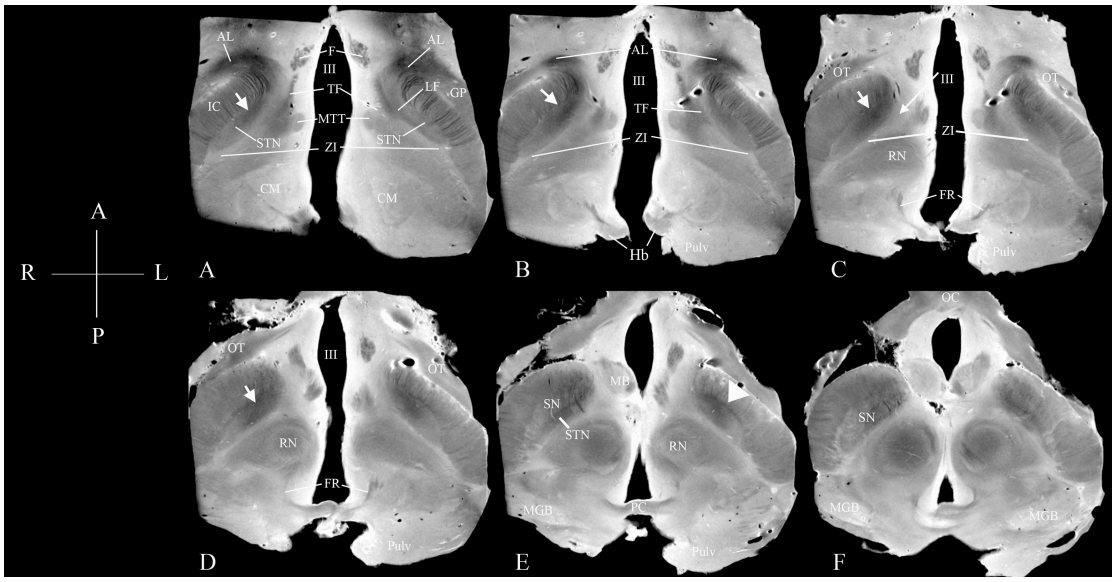

Figure 7.2: Axial Plane. The anatomy of the STN on SE MRI at 9.4T showing both halves of the midbrain in serial axial sections from superior to inferior levels [A-F]. Long white arrow: anteromedial border of the STN defined by the confluence of the ZI and posterior border of the hypothalamus. Short white arrow: medial hypointensity of the STN (seen in 6/9 subthalamic nuclei studied). Arrow head in 2E identifying the hypointense band forming the anterior border of the STN and enabling discrimination from the SN at more inferior levels. Acquired with an in-plane resolution of 88µm. Orientation: A - anterior, P - posterior, M - medial, L - lateral.

2. Position of the STN

Axial SE images were available in all cases; additional coronal and sagittal SE images were available in one [Figures 7.3 & 7.4]. The STN lay obliquely in all three planes. In the axial plane, the STN was approximately 40 degrees oblique to the midline: at the more superior level studied the mean angle was 42.8 degrees (SD 7.3) and at the inferior level studied 38.1 degrees (SD 3.8) [table 7.4b]; in the sagittal plane 35 degrees oblique to the vertical axis [Figure 7.3] and in the coronal plane 50 degrees oblique to the midline [Figure 7.4].

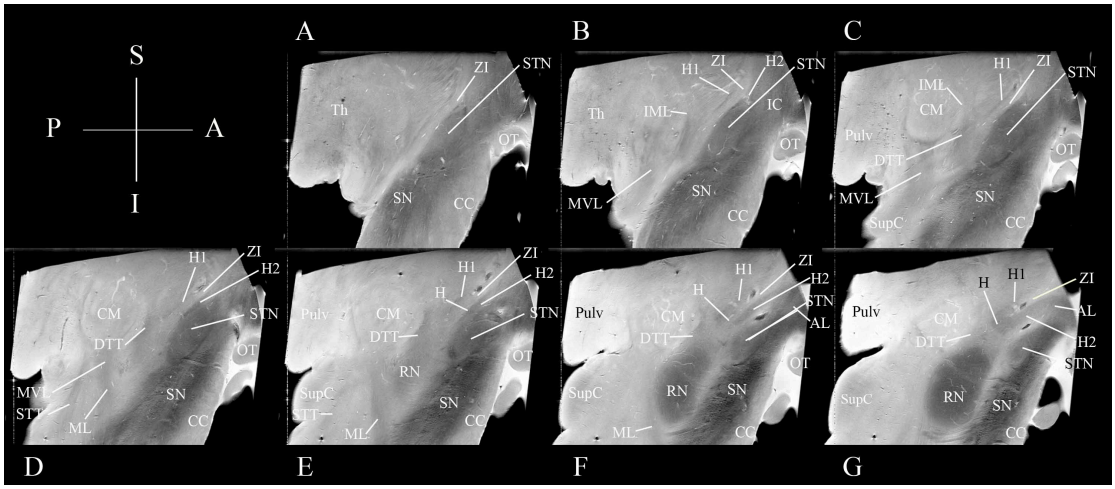

Figure 7.3: Sagittal Plane. The STN in serial 1mm sagittal sections from lateral to medial [A-G]. Acquired with an in-plane resolution of 88µm. Orientation: S – superior, I – inferior, P – posterior, A – anterior.

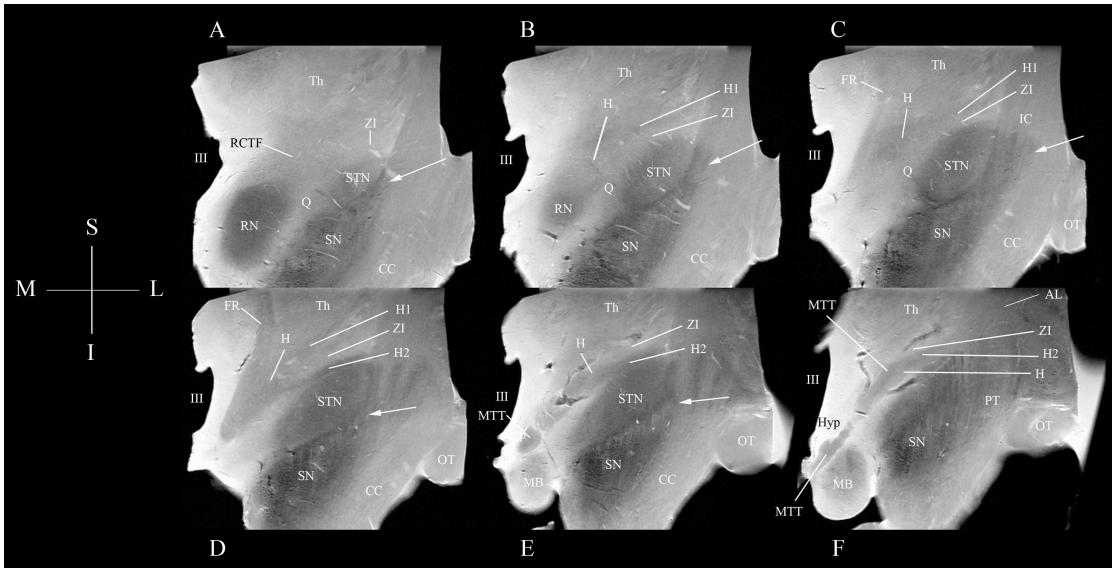

Figure 7.4: Coronal Plane: The STN in serial 1mm coronal sections in a control case from posterior to anterior [A-F]. The SN can be seen enveloping the inferolateral border of the STN (white arrow). Acquired with an in-plane resolution of 88µm. Orientation: S – superior, I – inferior, M – medial, L- lateral.

3. Borders of the STN

The anterior border of the STN was formed by the internal capsule superiorly [Figures 7.2 A-D, 7.3B, 7.4C] and the substantia nigra inferiorly [Figure 7.2E, 7.3C-G, 7.4A-E arrowed]. The STN was outlined by a rim of hypointensity, particularly at more inferior levels, in all cases [Figure 7.2D-F]. The SN enveloped the anterior and inferior aspect of the STN at the level of

the optic tract [Figure 7.3 A-G], with the zona incerta (ZI) running along the posterior and superior surface [Figure 7.3 C-E] and the lenticular fasciculus (LF, H2 field of Forel) at the most superior aspect of the STN [Figure 7.3 D-F]. In more medial sagittal slices, the ansa lenticularis (AL) was seen sweeping around the medial internal capsule [Figure 7.3 F&G] forming part of the medial and anterior border of the STN. The AL was also seen joining H2 to form the H Field of Forel [Figure 7.3 F-G] and the thalamic fasciculus (H1) [Figure 7.3 B-F]. The anterior and medial border was clearly defined, bounded by the ZI, and the posterior aspect of the hypothalamus. [Figure 7.2C long arrow](Hamani et al., 2004). The LF also formed the most medial 1/3 of the anterior border of the STN at the most superior level.

The superior border of the STN was formed by the LF, seen as a region of hypointensity in all cases in axial sections but best appreciated in the sagittal and coronal planes [Figures 7.3D-F, 7.4D-E]. The LF was seen as a slightly lower intensity structure in MR slices above the STN in the axial, coronal and sagittal planes.

The posterior border was formed by a hyperintense band that corresponds to the grey matter of the zona incerta above the level of the RN [Figure 7.2A&B]. At lower levels the hyperintense signal arose from tissue between the STN and more caudally the SN and the RN: this is the site of myelinated fibres orientated in the axial plane in a posterolateral-anteromedial axis (Adachi et al., 1999) of the nigrostriatal tract(Adachi et al., 1999; Moore et al., 1971) or the pallidoreticular bundle (bundle Q) (Schaltenbrand and Wahren, 1977).

The inferior border of the STN is formed by the SN, which is wrapped around the most inferolateral aspect [Figure 7.3 A-F, Figure 7.4 A-E white arrow]. It is more difficult to accurately define this boundary in the axial plane [Figure 7.2E where the most inferior part of the right STN is seen and 7.2F where the most inferior part of the left STN is seen]. The STN returns a slightly higher signal than the SN in 4/8 cases. More importantly, a relatively hypointense signal band was found in all cases enabling separation of STN from SN [Figure 7.2 C-E, arrow head 2E].

In the cases where higher resolution images acquired with an in-plane resolution of 44μm) were available this also enabled accurate identification of fibres of the subthalamic fasciculus as they pass through the internal capsule [Figure 7.5].

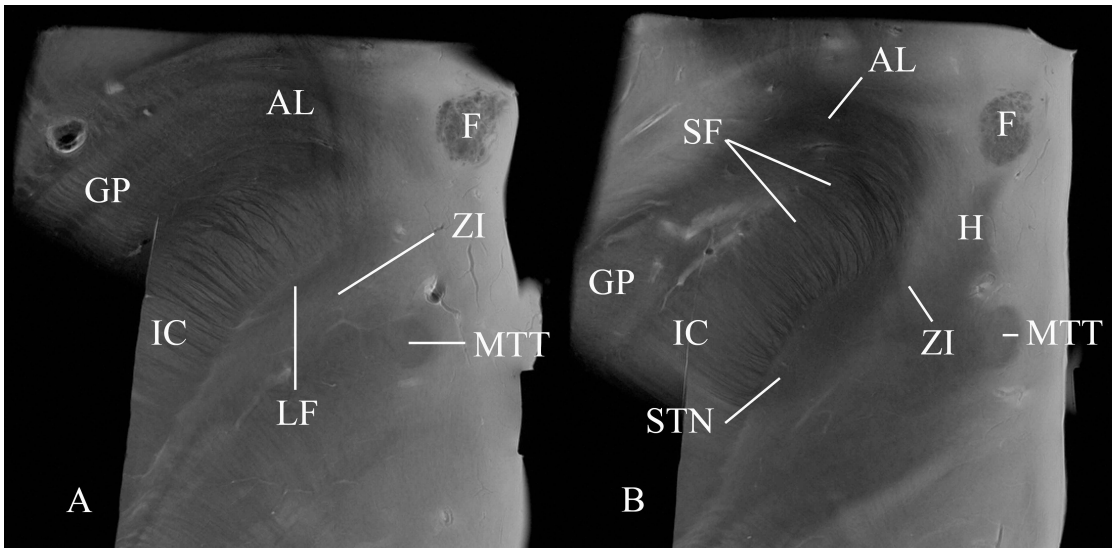

Figure 7.5: The STN in the axial plane using SE MRI with image resolution acquired at 44 µm in plane. 5A just above the level of the STN, 5B at a superior level of the STN above the RN. The resolution of these images allows clear identification of fibres of the subthalamic fasciculus radiating through the internal capsule.

4. Comparison of MR images with LFB/CV stain and Perl stain

MR images with corresponding LFB/CV stained sections were available in 4 cases. Comparison of the SE MR images with the histological sections confirmed a good anatomical correspondence [Figure 7.6 and legend].

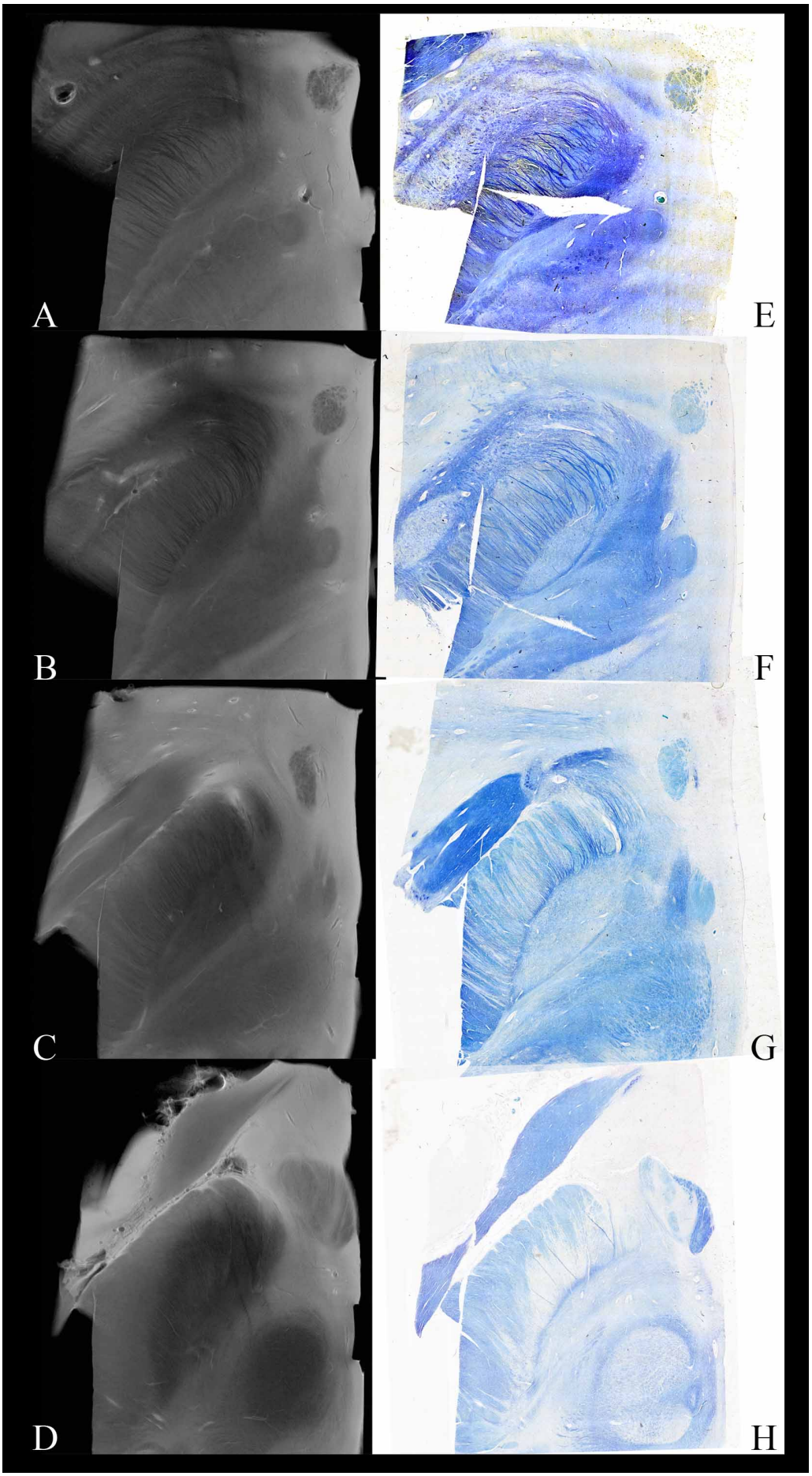
A
B
C
D
E
F
G
H

Figure 7.6 (previous page): Comparison of 9.4T SE MRI images [A-D] and histological sections stained using the LFB/CV method [E-G]. MRI in plane resolution 88 μm. Images are unlabelled to make comparison easier. For anatomical labels see figure 3. The STN is identified clearly as an almond shaped structure surrounded by white matter tracts (blue stain on LFB/CV images). LFB/CV staining within the STN was uniform in 4/4 cases with no particular anteromedial/posterolateral gradient evident. Structures corresponding to the borders of the STN can be clearly identified: at superior levels the LF can be seen as a dark blue myelinated structure corresponding to a region of hypointensity on T2w images [A&E]. One step inferiorly [B&F] the STN is clearly demarcated by a rim of dark blue staining and the fibres of the subthalamic fasciculus are seen radiating through the internal capsule – corresponding to the hypointensity seen on the anterolateral border of the STN on T2w/PDw images. The posteromedial border is clearly defined on the LFB/CV images as white matter tracts but on the MR images there is a relatively hyperintense signal arising from the region of the zona Incerta [B&F]. A region densely staining for myelin is seen separating the STN anteromedially from the superior SN posterolaterally on the LFB/CV image - this corresponds to a relatively hypointense region on the MR image [D&H]. It can be seen that the medial border of the STN is less clearly defined on the LFB/CV image at this level near the posterior aspect of the anteromedial tip on the LFB/CV image but this remains well defined on the 9.4T SE MR image [H].

Perls stain for iron was performed in 3 cases. At superior levels the most intense staining was seen in the globus pallidus and the AL as it courses around the internal capsule and comes to lie adjacent to the anteromedial tip of the STN [Figure 7.7A-C]. The SN was seen at lower levels with intense Perl-positive staining particularly in the most anterior and medial portion [Figure 7.7D-F]. The STN itself stained less intensely and the more lateral and posterior portions were least heavily stained in 2/3 cases, particularly in the more inferior sections [Figure 7.7B-E]. By comparison the most hypointense signal, correlating to the distribution of most intense Perl staining, was seen in the superior, anterior and medial STN [Figure 7.2]. In one case, Perl stain was uniform in the STN and corresponded to uniform hypointensity on high field MR images.

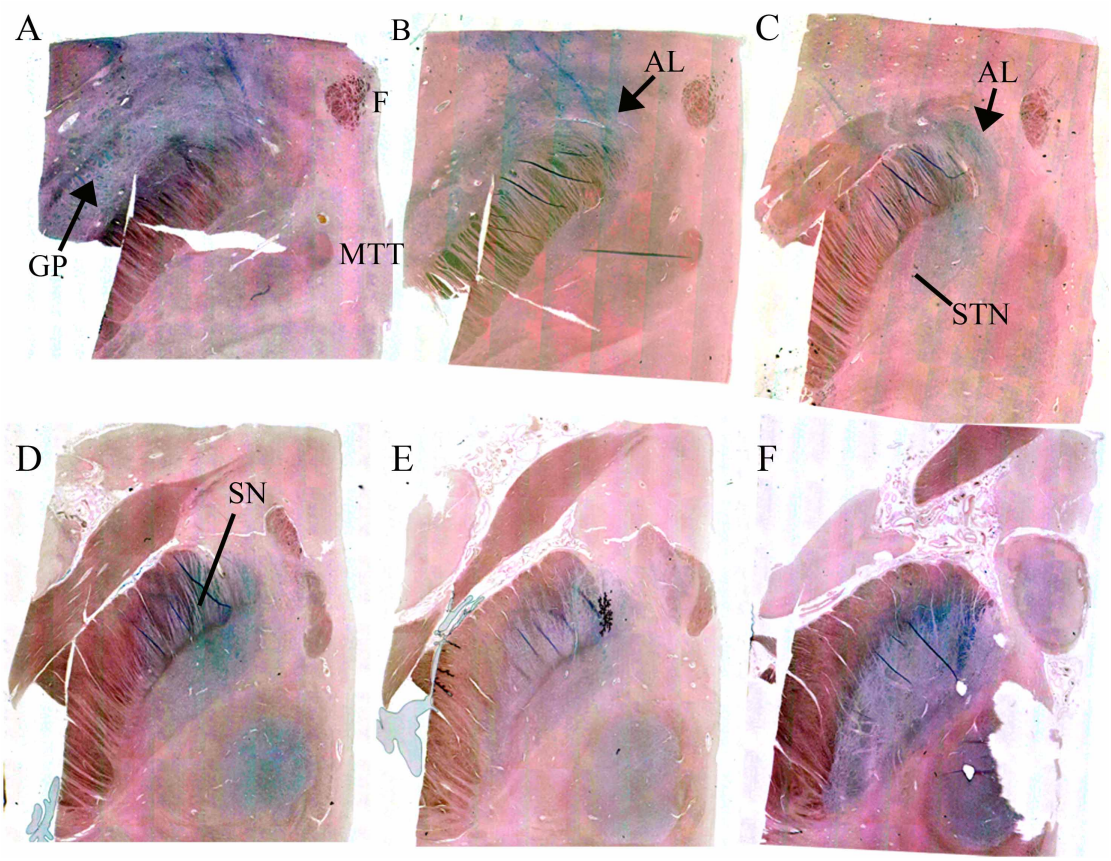

Figure 7.7: Perl stain of the STN and environs. Serial axial sections through the subthalamic nucleus [A-F] from just above the STN [A] showing Prussian blue staining in the GP; in the STN Prussian blue staining is evident mostly in the medial half of the STN [B-D] and in the lower levels [D-F] intense staining of the SN pars reticulata is seen [D and E] just anterior to the STN.

5. Demonstration of three dimensional relationships of the STN

We have reconstructed the anatomy of the STN and surrounding structures by manually segmenting the ge3d images. This allowed us to display the relationship of the STN to surrounding structures in three dimensions (Figure 7.8).

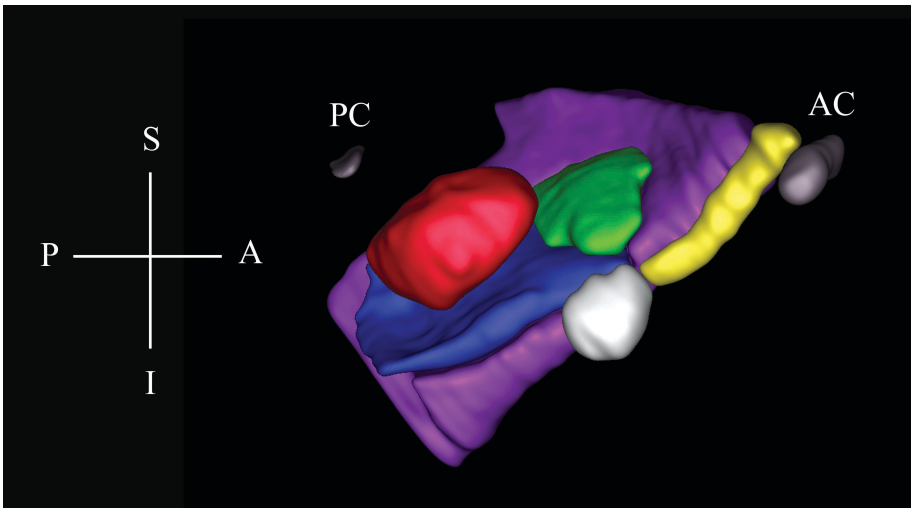

Figure 7.8: Three-dimensional reconstruction viewed from the midline showing the relationship of the STN (green) to the internal capsule (purple), RN (red), SN (dark blue), MB (light grey), Fornix (yellow), AC and PC (dark grey, labelled) orientated so that the AC-PC line is horizontal. Orientation: S – superior, I – inferior, A – anterior, P- posterior.

6. Measurements of the STN and its landmarks

The volume of the STN was 106 mm^3 on average (range 87-126 mm^3), the maximum width 12 mm, the maximum depth 3.2 mm and the height 6.6 mm [table 7.2].

Case number	Max Width (mm)	Max Depth (mm)	Max Height (mm)	Volume (mm^3)
1 (R)	12.0	3.3	6	120
1 (L)	11.4	3.2	6	103
2 ^	12.6	3.3	4.5	83
3	15.5	3.5	7.5	113
4	12.6	3.2	6	100
5	11.5	3.3	7.5	126
6	11	2.9	6	103
7	11.2	2.9	7	95
8	10	2.9	7	87
Mean	**12.0 (10-15.5)**	**3.2 (2.9-3.5)**	**6.6 (6-7.5)**	**106 (87-126)**

Table 7.2: Dimensions and volume of the STN. For mean values those quoted are mean (range). Mean height and volume calculation excludes case 2 where the imaging data did not cover the entire STN. ^ Incomplete STN measurement as MRI did not cover entire STN; hence for these cases the volume and height are underestimates. (R) right. (L) left.

Line/axis	Definition
'FMT Line'	Drawn between the Fornix and Mammillothalamic tract (FMT)
'STN line'	Drawn across the medial and lateral tips of the STN in the axial plane
'Midline'	Placed in the midline
'RN line'	Parallel to the high signal line running between the STN and RN at inferior levels

Table 7.3: Definition of axes used in studying the STN variability

The STN lies at a mean angle of approximately 40 degrees to the midline [Table 7.4; Figure 7.1]. The medial tip is 6mm, the lateral tip 13.5mm, the midpoint 10mm, the posterior boundary 9mm and the anterior boundary 11mm to the midline. The posterior boundary lies 4.3mm (range 3.3-5.2) and the anterior boundary 7.5mm (range 6.1-8.2) from the centre of the RN [Table 7.5]. The angle of the FMT line varies as the axial position becomes more inferior as it rotates to increase the angle between itself and the STN and midline. The midpoint of the FMT lies 3.3-3.5mm lateral to the midline. The medial tip of the STN lies approximately 3mm lateral to the FMT and within 1 mm of it in the AP axis. The lateral tip and midpoint measurements are more discrepant between the superior and inferior levels based on the FMT line, as one might expect given the difference in angle of the FMT with axial position [Table 7.4].

	FMT-STN Angle	Medial tip		Lateral tip		Mid point		Dorsal midpoint		Ventral midpoint	
		X	Y	X	Y	X	Y	X	Y	X	Y
Sup	42.3 (9.7)	2.9 (1.6)	0.2 (0.6)	10.3 (1.2)	8.6 (1.9)	6.5 (1.2)	4.3 (1.3)	5.3 (0.8)	5.1 (1.2)	7.5 (1.4)	3.6 (1.3)
Inf	57.6 (10.4)	3.2 (1.1)	0.2 (0.7)	12.6 (1.3)	6.6 (2.2)	7.9 (1.3)	3.6 (1.2)	7.1 (0.9)	4.4 (1.2)	8.4 (0.9)	1.9 (1.3)

Table 7.4a: Measurements relative to the midpoint between the mamillothalamic tract and the Fornix

	STN-midline Angle	Medial tip	Lateral tip	Mid point	Dorsal mid point	Ventral mid point
		X	X	X	X	X
Sup	42.8 (7.3)	5.8 (1.9)	13.5 (2.0)	9.9 (1.8)	8.9 (1.6)	10.7 (2.0)
Inf	38.1 (3.8)	5.7 (1.3)	13.4 (1.4)	9.7 (1.0)	8.9 (1.2)	11.2 (1.1)

Table 7.4b: Measurements relative to the midline

Table 7.4: Measurements: angles (SD) in degrees, otherwise linear measurements mean (SD) in mm. x is distance medial-lateral; y is distance anterior-posterior.

Distance from mid point of RN	Dorsal STN border	Ventral STN border	STN depth
Mean (Range)	4.3 (3.3-5.2)	7.5 (6.1-8.2)	3.6 (2.7-4.0)

Table 7.5: Distance in mm from the midpoint of the RN

The position of the STN relative to a midpoint between the fornix and MTT at superior and inferior levels can be seen in 7/8 cases [Figure 7.9]. These scatter plots demonstrate visually the anatomical variability. No significant association was found between the position of the STN and age at death. However, with duration of fixation there was a trend towards an increase in distance for the lateral, anterior and posterior borders and a statistically significant increase in distance of the midpoint of the STN from the midline (Pearson correlation coefficient -0.769, $p = 0.043$ for the STN midpoint). However, this relationship is no longer significant when the outlier with very long fixation time is excluded from the analysis.

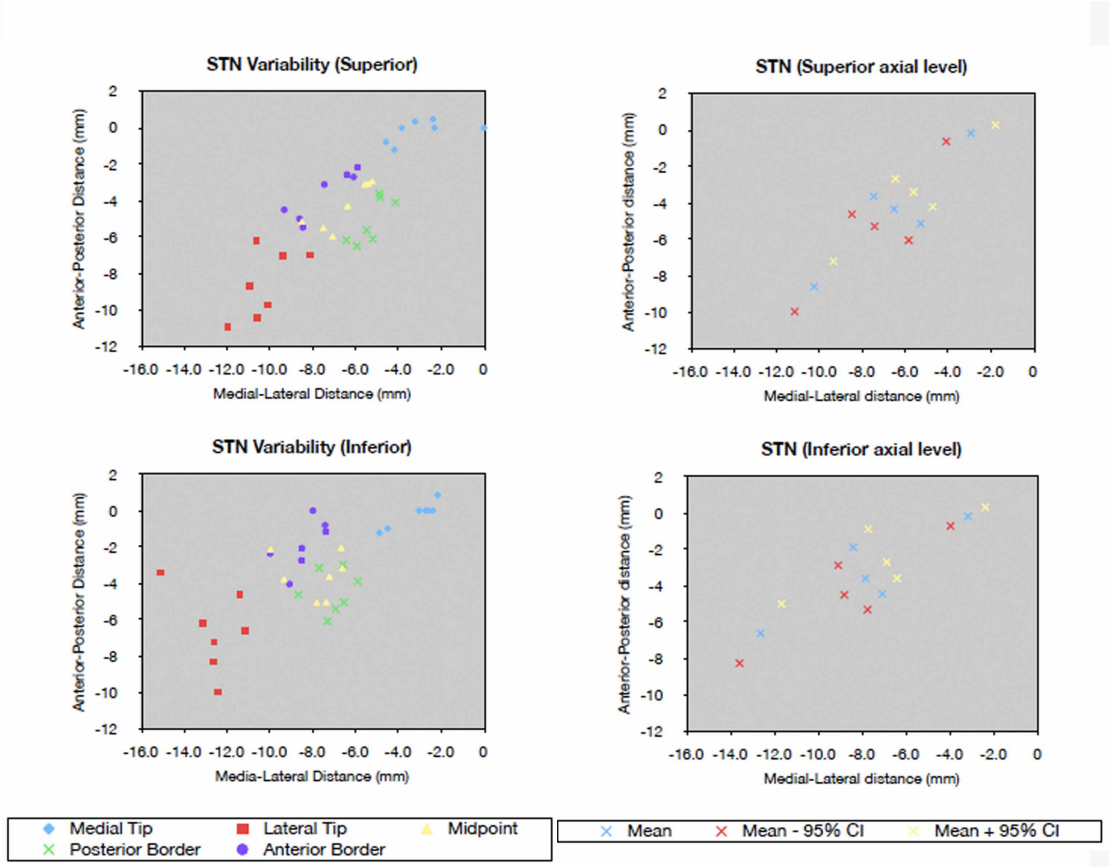

Figure 7.9: Variability of the position of the STN. Scatter plots on the left include the measured locations of points for all available cases for superior and inferior levels examined. Scatter plots on the right show the mean position relative to the midpoint between the fornix and mamillothalamic tract in the axial plane. The upper and lower 95% confidence intervals are also plotted using coordinates in the x- and y-axis. Points plotted to give the profile of the STN are the medial and lateral tip, the anterior and posterior midpoints and the midpoint of the STN. See figure 11. All samples were reoriented such that the midpoint between the MTT and fornix is at position 0 in the x- and y-axis. See table 3 for mean values and standard deviation.

E. Discussion

We have described the anatomy of the STN, its internal structure and anatomic variability seen using high field MRI, with histological validation. On 9.4T MRI, a variable signal was distinguished within the STN in 75%, reflecting differences in iron deposition as confirmed by Perls stain. This anatomical variability confirms the importance of direct STN visualisation when targeting it for stereotactic surgical procedures.

High field MRI of post mortem tissue has been used to define the anatomy of structures difficult to visualise on clinical MRI (Silver, Djalilian et al. 2002; Lane, Witte et al. 2005) including the STN (Rijkers, Temel et al. 2007). The main advantages of MR microscopy are increased signal-to-noise ratio (SNR), minimisation of movement artefacts and the ability to image in orthogonal planes with multiple averages. This enables a significant increase in spatial resolution and reduced partial volume effects. We obtained in-plane resolution comparable to macroscopic post-mortem examination - with clear demarcation of the boundaries of the STN and visualisation of small structures such as the subthalamic fasciculus, the lenticular fasciculus and the zona incerta.

1. STN borders and internal signal on high field MRI

The borders of the STN were clearly visualised in all specimens allowing straightforward differentiation from the SN. At 1.5T, the STN returns an apparently homogeneously distributed hypointense signal on T2-weighted MRI (Bejjani, Dormont et al. 2000; Hariz, Krack et al. 2003; Coenen, Prescher et al. 2008). This hypointense area may only represent one component of the STN; another smaller component may not be visible on MRI or with Perls stain on histology (Dormont, Ricciardi et al. 2004). In our study at 9.4T, we identified areas of signal variability within the STN in 75% of cases: a relatively hypointense area was located anteromedially and a relatively hyperintense area was located posterolaterally [Figure 7.2]. The anatomic location of the latter suggests that it corresponds to the area not consistently visualised at 1.5T. Perls stain confirmed the difference in iron deposition suggesting that the difference in T2 signal is related to a difference in tissue iron content. Some have attributed the hypointense signal in the STN to iron (Rutledge, Hilal et al. 1987) although others have suggested that the high neuronal density of the STN may contribute (Hamani, Richter et al. 2005). The signal heterogeneity we observed may be related to the functional subdivision of the STN into three separate territories – the limbic anteromedial part, the associative mid-part and the sensorimotor posterolateral part. These functional

subdivisions are based on extrapolation from animal work (Parent and Hazrati 1995; Karachi, Yelnik et al. 2005; Yelnik, Bardinet et al. 2007) but have not, to our knowledge, been specifically shown in humans. It may be this posterolateral or "sensorimotor" portion that is difficult to visualise on lower field conventional MRI. The homogeneous signal in 25% (2/8) of our cases, with histological validation, highlights the degree of variability that can be encountered. It is, however, important to note that it is not clear whether the STN as visualized clinically at 1.5T represents a component of the STN or the complete nucleus and this will have a bearing on targeting strategies in functional neurosurgery. However, we would also argue that direct visualisation of a portion of the surgical target is superior to estimating its location based on indirect landmarks.

We have previously studied anatomical accuracy in context of stereotactic targeting of the pedunculopontine nucleus (PPN) for deep brain stimulation (Zrinzo, Zrinzo et al. 2011). We were able to validate a method of targeting the PPN by comparing its position as seen on both conventional 1.5T MRI and high field 9.4T post mortem MRI, with macroscopic histological images in the same tissue. A similar study comparing conventional and high resolution images with histological material to validate methods for targeting the STN has not yet been undertaken.

2. STN Volume on MRI

In our study, the STN mean volume of 106 mm^3 (range 83-126) is comparable to previous measurements of around 127 mm^3 post mortem in controls (the quoted measurement of 254mm^3 is for both sides together) (Hardman, Halliday et al. 1997), 120 mm^3 (assuming that both left and right STN volumes were used in this paper also)(Hardman, Henderson et al. 2002) and 158mm^3 (Yelnik 2002). In a further study the reported STN volume was 174.5mm^3 but these individuals were younger at the time of death and duration of fixation at the time of measurement shorter (Levesque and Parent 2005). After formalin fixation and processing into paraffin wax there is marked potentially non-uniform tissue shrinkage (Quester and Schroder 1997). This has implications when comparing ante mortem with post mortem measurements of volume and linear dimensions, which may be significantly affected by the fixation process.

3. Anatomical variability

Significant anatomical variability of the STN was found on our histologically validated high resolution MRI in relation to the midline and other internal structures. At the more inferior level studied, the position of the lateral tip was most variable– this level includes the RN and is close to the target slice used on conventional 1.5T imaging used for surgical STN planning (Bejjani, Dormont et al. 2000). This is the region of the STN not so clearly seen on conventional MRI and likely to be a sensorimotor portion of the nucleus. Even small variations in the position of the STN in a region where the maximal depth of the STN in the axial plane is only 3.2mm are likely to be significant. On conventional MRI the medial STN is 8.6mm +/- 4.3 lateral to the midline and the lateral STN 13mm +/- 6 (Hamani, Richter et al. 2005). In this study the midpoint of the STN at superior levels is found 9.9 mm lateral to the midline at superior levels and 9.7mm lateral to the midline more inferiorly. This is comparable to other post mortem data (den Dunnen and Staal 2005). Although it is important to note that our samples were not studied in a plane parallel to the AC-PC line, this variability again highlights the importance of direct visualisation of the STN for accurate localisation. Furthermore, increasing the MRI spatial resolution may improve the accuracy of STN localisation compared to current conventional approaches.

4. Advantages of MR microscopy and advances in MRI

Like others we found MR microscopy to be an excellent tool to display and study anatomy in three dimensions (Rijkers, Temel et al. 2007) – a feat which cannot be performed with standard histological techniques [Figure 7.8]. This study lays the groundwork for future imaging of this region as high field MRI is becoming more widely available with clinical 3T (Slavin, Thulborn et al. 2006) and 7T machines enabling detailed study of the STN during life (Cho, Min et al. ; Abosch, Yacoub et al. 2010). Furthermore, newer MR methodologies are improving our ability to accurately identify the STN during life (for review see (Massey and Yousry 2010)) including added susceptibility (T2*) contrast using multiple gradient echoes (Elolf, Bockermann et al. 2007), susceptibility weighted imaging (Vertinsky, Coenen et al. 2009) and fast grey matter acquisition T1 inversion recovery (Suhyadhom, Haq et al. 2009). However none of these methodologies have thus far been validated by comparison with histological material. The ability to image the STN during life at spatial resolutions similar to those reported post mortem herein would provide significant progress in both localisation accuracy for stereotactic surgery and the assessment of pathological changes in this nucleus.

Chapter 8: Histologically validated Substantia Nigra anatomy in controls and parkinsonism using spin echo MR Microscopy at 9.4T

A. Introduction

Many studies have tried to define the substantia nigra (SN) using conventional MRI. This complicated nucleus is difficult to define histologically and so it is not surprising that there has been some difficulty using conventional MRI given the intricate structure of this nucleus at a resolution not yet accessible in standard MR imaging.

Early MRI studies suggested that the distribution of iron in the midbrain determined the T2 signal hypointensity within the SN (Drayer, Burger et al. 1986; Drayer, Olanow et al. 1986; Rutledge, Hilal et al. 1987; Drayer 1988; Drayer 1988). An anterior and medial region of signal hypointensity was attributed to the SNr, and the lateral posterior region with higher signal intensity to the SNc (Drayer, Olanow et al. 1986). Only a few studies performed direct comparison of early MR and histological images (Flannigan, Bradley et al. 1985; Hirsch, Kemp et al. 1989; Solsberg, Fournier et al. 1990) and there are none using more recent techniques. The basis for the study of the anatomy of the SN comes from a paper in 1986 determined by knowledge of the relative distribution of iron – it being higher in the SNr than SNc (Duguid, De La Paz et al. 1986).

As already discussed, not all agree with this anatomical definition of the SN on conventional MRI (Savoiardo, Girotti et al. 1994; Gorell, Ordidge et al. 1995; Adachi, Hosoya et al. 1999; Martin, Wieler et al. 2008; Massey and Yousry 2010). Very promising however, has been high field MR imaging. At 7.0T the SN is much more clearly demarcated and there are even some morphological differences between controls and PD but without pathological confirmation (Cho, Oh et al. 2011; Kwon, Kim et al. 2012).

B. Aim

The aim of this study was to produce an accurate and validated description of the anatomy of the SN based on histological staining including immunohistochemistry and Perl stain of the same tissue studied with high field spin echo MRI at 9.4 Tesla – so called MR microscopy and describe anatomical changes based on histological findings in disease including PD and PSP.

C. Materials and Methods

Post mortem brain tissue was obtained from the Queen Square Brain Bank for Neurological Disorders (QSBB), UCL Institute of Neurology, where tissue is donated according to ethically approved protocols and is stored under a licence from the Human Tissue Authority. Brains were sampled for histology using an established protocol (Trojanowski and Revesz 2007) and the diagnosis confirmed using standard neuropathological criteria (Ince, Clarke et al. 2008).

1. Tissue preparation

Formalin-fixed tissue was dissected to produce a tissue block that included the substantia nigra. The MR axis was aligned perpendicular to the axis of the brainstem and, after imaging, the specimen was divided along this midline sagittal axis before embedding in paraffin.

2. MRI Protocol

Samples were imaged at room temperature in perfluoropolyether (Fomblin, Solvay Selexis) at 9.4T (Varian NMRS MRI) with a 40mm quadrature volume RF coil as previously described (Massey, Miranda et al. 2012).

1. Parameters for high-resolution spin echo (SE) images were: TE 15-22ms, TR 2000-2200ms, scan averages 24-32, interleaved slices, slice thickness 0.5-1mm, slice gap 0.5-1mm, matrix 512x512, field of view (FOV) 45x45mm (in-plane resolution 88 µm) and imaging time up to 10 hours.
2. Superior in-plane resolution was obtained in one case: 1024x1024 matrix (in plane resolution 44 µm), 132 averages; other parameters as above, imaging time 72 hours.

These parameters were chosen on the basis of pilot acquisitions to yield optimal image contrast for the structures of interest. Images were viewed and processed in ImageJ (version 1.43h, US National Institutes of Health, Bethesda, Maryland).(Rasbrand 2009)

3. Histological Protocol

After imaging the tissue blocks were embedded in paraffin and serially sectioned at 20 microns. Every 20th section was stained with Luxol Fast Blue and Cresyl Violet (LFB). MR images and LFB slides were visually compared and once the best match between histology and MRI was chosen, further sections were stained with Perls stain for iron and immunohistochemistry for substance P (SP) and calbindin (CB). Sections were dewaxed and taken to absolute alcohol, blocked in H_2O_2 / methanol for 10 minutes and washed in running tap water. All antibodies were pretreated by pressure cooking for 10 minutes in citrate buffer PH 6 and washed well in running tap water before being transferred to PBS. Substance P was blocked in 10% normal swine serum for 10 minutes. All antibodies were incubated for 1 hour at room temperature and then washed 3x 5mins in PBS. Polyclonal antibodies were incubated in swine anti rabbit 1:200 for 30 mins. Monoclonal antibodies were incubated in rabbit anti mouse 1:200 for 30 mins and then washed 3x 5mins in PBS. All sections were incubated in Vector ABC for 30 mins and washed 3x 5mins in PBS. Next, the colour was developed with glucose oxidase nickel dab solution and then washed well in running tap water. Sections were counterstained in Mayers Haematoxylin for 1 min and washed in running tap water. Finally they were dehydrated and mounted. The following antibodies were used: Substance P (Invitrogen Polyclonal; 1:50); Calbindin (Abcam Monoclonal; 1:400). Macroscopic images were obtained at 20-40x magnification using Image Pro Plus (Mediacybernetics, Bethesda, MD www.mediacy.com) and microscopic images using Leica biosystems digital image hub.

4. Image segmentation

MR images were segmented manually in ITK-SNAP (version 1.8.0) (Yushkevich, Piven et al. 2006). Reconstructions were then made using the mesh function, and measurement of volume was performed on manually segmented regions . Linear measurements of SN breadth and width were performed in Image J.

5. Approach to Analysis

The anatomy of the SN was demonstrated in a single case with LFB, Perl stain, SP and CB immunohistochemistry and high field SE MR Microscopy at multiple serial axial levels through the SN.

The anatomy was defined by overlying LFB, SP, CB, Perl and SE MRI images level by level. A cartoon of the anatomy was developed to confirm the borders and internal anatomy of the SN.

Once the anatomy was demonstrated the volume, dimensions and variability in borders, landmarks and internal anatomy was studied in control and disease cases (PD, PSP) at the level of the exit of the IIIrd cranial nerve and RN which is the most studied level in the pathological and radiological literature.

D. Results

1. Characteristics of cases studied

Twenty three cases were included in the study including 10 controls, 8 PSP and 5 PD. The key case features and pathological diagnoses are shown in table 1 and group data and measurements in table 2.

No	Gender	Side fixed	Age	DOF (days)	Category	Pathological diagnosis
1	F	Both	94	4149	Control	n/a
2*	M	right	94	51	Control	Small vessel disease (severe), Braak & Braak stage IV
3*	M	right	38	56	Control	minimal abeta deposition
4*	M	left	78	78	Control	CAA (moderate)
5	M	both	79	1029	Control	pathological ageing, mild cvd
6	F	Left	82	366	Control	pathological ageing, mild svd, mod caa
7	F	Right	82	302	Control	Pathological ageing, right parietal infarct
8	F	Right	72	67	Control	MND
9	F	Right	99	26	Control	B&B IV NFT pathology
10	M	Left	89	18	Control	n/a
11*	M	Left	68	54	PSP	PSP, Lewy Body Pathology, Pathological Ageing
12*	M	Right	69	89	PSP	PSP, Pathological Ageing
13	M	RIght	66	315	PSP	PSP
14	M	Right	86	165	PSP	PSP, Pathological Ageing, Small haemorrhagic frontal focus
15	M	Whole	68	88	PSP	PSP, Pathological Ageing
16	M	Right	71	51	PSP	PSP
17	F	Right	75	85	PSP	PSP
18	M	Left	67	51	PSP	PSP, Acute MCA infarct
19*	M	Left	79	260	PD	PD
20*	M	Right	83	28	PD	PD
21	M	Right	70	31	PD	PD, Limbic Lewy Body Pathology
22	F	Left	62	45	PD	PD, neocortical Lewy Body Pathology
23	M	Left	71	31	PD	PD, Limbic Lewy Body Pathology, Neocortical Lewy Body Pathology, Pathological Ageing, mild CAA, focal hippocampal infarction

Table 8.1: Characteristics of individual cases studied including pathological diagnoses.

		Control	PSP	PD	ANOVA
n		10	8	5	-
Gender		5F; 5M	1F; 7M	1F; 4M	NS
Side		7R; 5L	6R; 3L	2R; 3L	NS
Age (yrs)		81 (38-94)	71 (67-75)	73 (62-83)	NS
DOF (days)		935 (18-4149)	112 (51-315)	79 (31-260)	NS
SN Volume (ml)		211.3 (172.2 - 288.5)	**120.8** (105.7 - 147.6)	180.6 (155.0 - 238.5)	PSP<Ctrl p < 0.001 PSP<PD p = 0.008 PDvsCtrl NS
DSCP	**Width**	8.4 (5.5 - 11.2)	6.8 (5.5 - 10.8)	8.6 (7.5 - 10.3)	NS
	Depth	2.1 (1.1 - 3.4)	**1.24** (0.7 - 1.8)	2.3 (1.8 - 2.6)	PSP<Ctrl p = 0.01 PSP<PD p = 0.01 PDvsCtrl NS
III/RN	**Width**	11.7 (10.3 - 14.7)	**8.6** (6.9 - 10.4)	10.8 (10.3 - 11.2)	PSP<Ctrl p < 0.001 PSP<PD p = 0.007 PDvsCtrl NS
	Depth	3.0 (2.2 - 4.0)	**1.6** (0.8 - 2.4)	2.2 (1.5 - 2.9)	PSP<Ctrl p < 0.001 PSPvsPD NS PDvsCtrl NS
STN	**Width**	9.1 (6.1 - 11.3)	7.5 (6.0 - 9.2)	7.4 (6.2 - 9.0)	NS
	Depth	2.1 (0.9 - 3.8)	1.6 (1.2 - 2.1)	1.8 (1.6 - 2.0)	NS

Table 8.2: Characteristics of cases studied by group including measurement of volume and breadth and width. Measurements in the axial plane are reported at three levels: the decussation of the superior cerebellar peduncle (DSCP), the level of the IIIrd nerve fascicles and red nucleus (III/RN), and the level of the STN (STN).

2. Defining the anatomy of the SN on SE MRI in serial axial sections

The substantia nigra as defined by SP and CB immunohistochemsitry was studied from the level of the STN [level 1] to the level of the brachium conjunctivum [level 7] in serial 0.5mm thick axial sections spaced by 1.0 mm [Fig 8.1A-E].

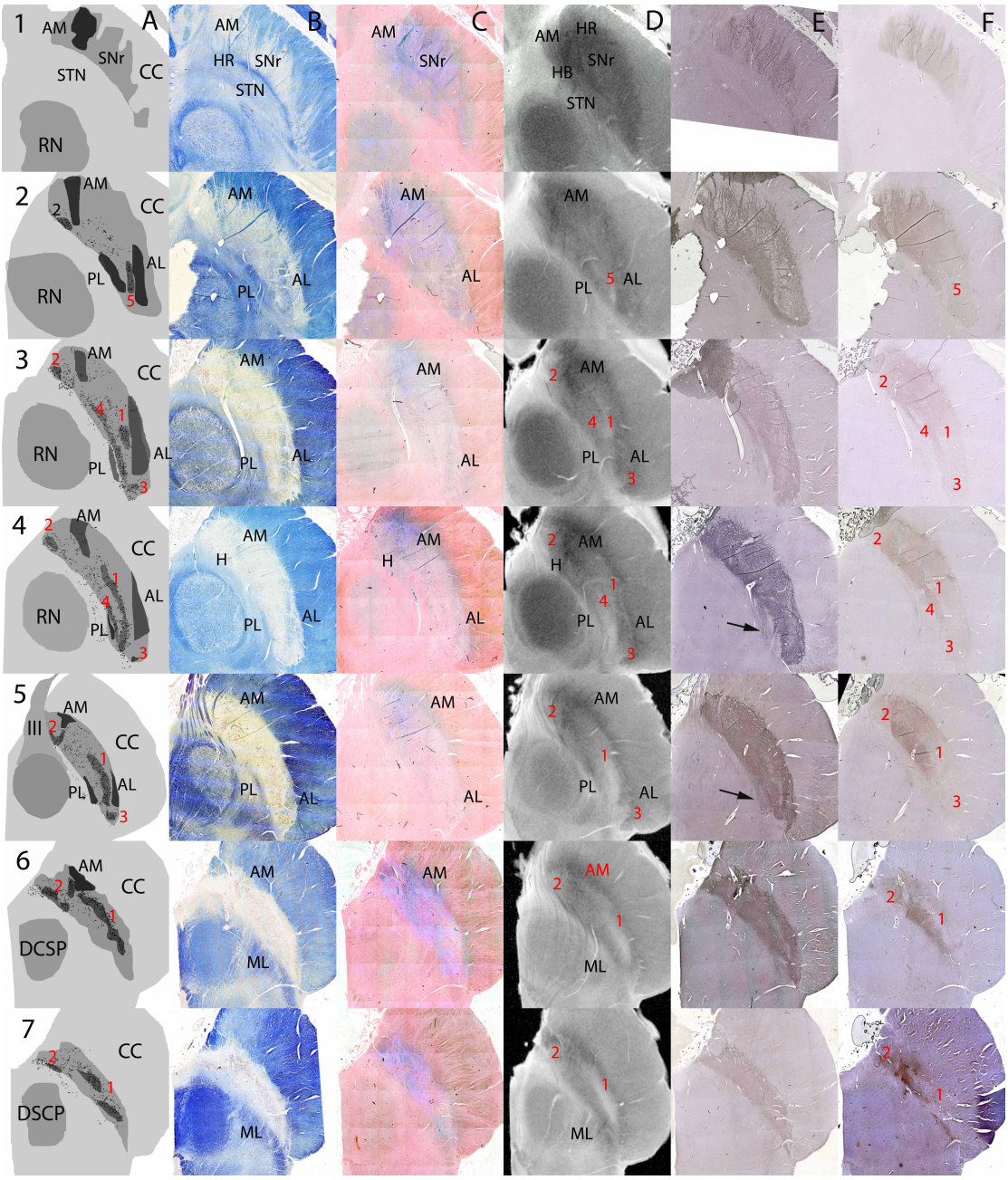

Figure 8.1: The anatomy of the SN on serial axial sections using LFB, Perl stain, high field SE MRI, and SP and CB immunohistochemistry. Case 2 was a 36 yr old male. Serial axial sections at 1.5 mm through a single SN A: cartoon showing key anatomical structures based on SP and LFB for borders, LFB for location of pigmented neurons on SNc and CB for nigrosomes. Pigmented neurons are shown as black dots and it is notable that not all of these fall within the CB-defined nigrosomes. B: LFB. C: Perl stain. D: High field SE MRI. E: SP. F: CB. Anatomical landmarks are in black. Nigrosomes (1-5) are labelled in red. See text for a detailed description of the anatomy and comparison of images.

3. Borders

a) Anterior Border

The anterior SN was bordered by the crus cerebri.

LFB: The border was clear except superior and medially [Fig 8.1B levels 1&2] where there were 'interdigitations' of blue-staining myelinated fibres and regions of low LFB staining [Fig 8.2A&B]. In the most medial portion there is white matter clustering which has the appearance of a 'hook' (see below) [Fig 8.1B levels 2-4]. On the lateral border encroaching into the SN there is a myelinated cluster which forms a triangular shape (anteromedial (AM) white matter see below) [Fig 8.1B levels 2-5].

Perl: There is staining throughout the anterior border but particularly anteromedially [Fig 1C all levels]. This encroached on the myelinated fibres of the corticospinal tracts and AM [Fig 8.2B&E] (see below).

Immunohistochemistry: SP stain defines the anterior border by staining the striatonigral innervating fibres and is in agreement with the LFB stain with fibres seen radiating into the CC [Fig 8.1E, Fig 8.2C&F]. This gives rise to a linear appearance which interdigitates with the crus cerebri [Fig 8.1E levels 1-3]. CB also has a serrated appearance at this level but gives a more uniform appearance with more dense staining medially.

Spin echo MRI: The medial part of the anterior border is more diffuse but lacks the interdigitating/serrated appearance of the anatomical and immunocytochemistry [Fig 8.1D levels 1-7]. There is a hypointense rim (HR) which corresponds to the anterior border but is more prominent superomedially.

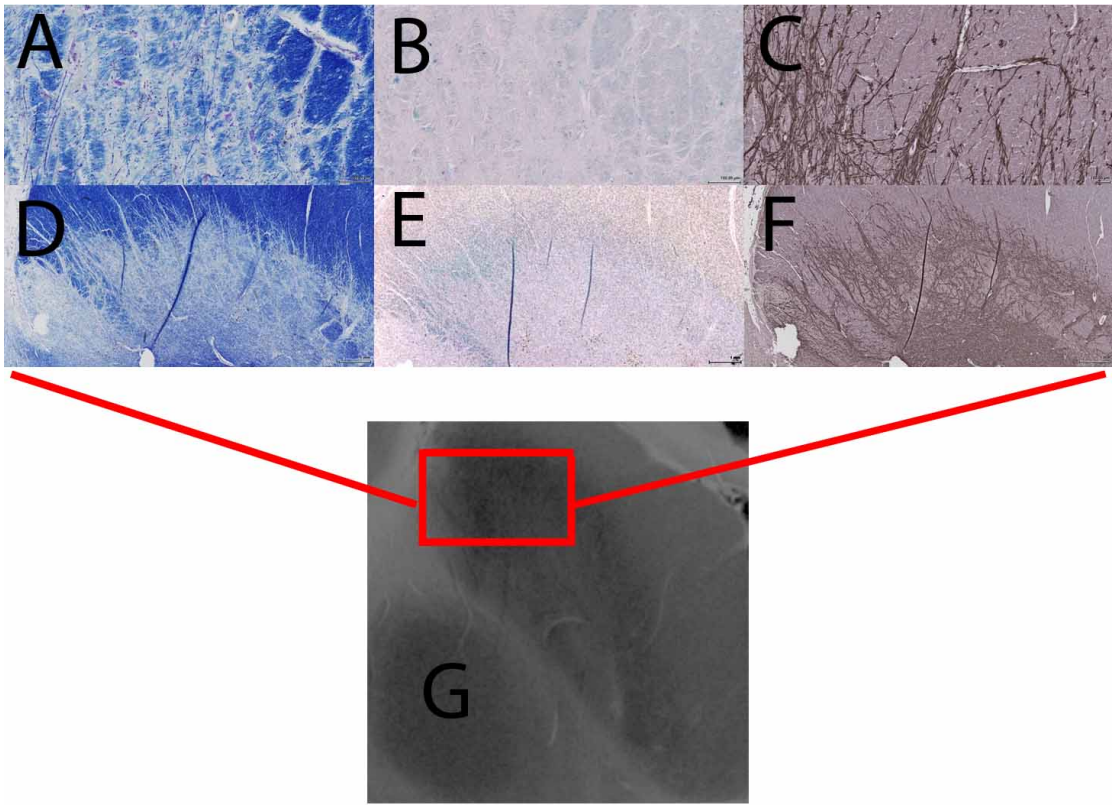

Figure 8.2**:** The anteromedial border of the SN at superior levels. A-C 10x magnification; D-F 2x magnification. A & D LFB, B & E Perl stain, C & F SP. G high field SE MRI image show region represented by histological sections. Lower and higher field histological sections using LFB and SP show the interdigitation of white matter with the anteromedial border of the SN. Perl stain can be seen blurring the boundary of the SN in B & E and appears to stain both white matter in the border and within the anterior SN itself - the anteriomedial white matter (AM) landmark; see text.

b) Posterior Border

The posterior border of the SN is somewhat controversial in the literature. Using SP immunohistochemistry the parabrachial nucleus (Halliday 2004) or gamma group of Olzewski (Olzewski 1954) are excluded and this definition has been used for this study.

LFB: the posterior border is defined by myelinated fibres which appear to run in a posterolateral to anteromedial axis (Gorell, Ordidge et al. 1995; Adachi, Hosoya et al. 1999) seen at superior levels separating the SN from the STN [Fig 8.1B level 1] or the RN/BC [Fig 8.1B level 2-7]. Laterally at lower levels this is formed by the medial lemniscus (ML) which is more heavily myelinated [Fig 8.1B level 6-7]. At mid-levels there is a small group of myelinated fibres which we have termed posterolateral white matter (PL) [Fig 8.1B levels 2-5]. The medial posterior border is less clearly defined but at its most medial aspect is bounded by fibres of the third nerve in the mid-level section [Fig 8.1B level 5].

Perl: At the most superior levels Perl stain for iron reveals dense staining on the medial posterior border [Fig 8.1C level 1]. Below this relatively less iron is deposited in the posterior border than the anterior border of the SN [Fig 8.1C levels 2-5] until at the lower levels there is more intense Perl staining, particularly medially [Fig 8.1C levels 6-7].

Immunohistochemistry: SP defines the border in correspondance with LFB except in the mid-levels lateral portion where there is a small posterior protrusion not seen on LFB [Fig 8.1E levels 3-4 arrowed]. CB stains as per LFB although the medial-lateral gradient makes the lateral portion less evident.

Spin echo MRI: At the most superior level a hypointense band (HB) separates the STN and SN [Fig 8.1D level 1] (Massey, Miranda et al. 2012). At lower levels the border is defined by a high signal intensity band. At mid-levels it is less clear and medially comprised of both a thin high intensity band adjacent to the RN and a region of hypointensity bordering on the relative hyperintensity of the SN itself. At lower levels the hypointense band is more prominent corresponding to the increased Perl staining, and the border is formed by a hyperintense band separating the SN from the ML laterally [Fig 8.1C&D levels 6-7].

c) Lateral Border

LFB: The lateral border of the SN is bounded by the crus cerebri wrapping around the SN [Fig 8.1B level 1-4] and the abutting of the CC and ML at lower levels [Fig 8.1B level 5-7].

Perl: There is less iron staining at the most lateral portion of the border of the SN than medially but it is still evident at the most lateral portion.

Immunohistochemisty: The border is clearly defined, although less so on CB than SP due to the medial-lateral gradient.

Spin echo MRI: The border is clearly defined corresponding to the distribution of myelinated fibres with some iron on the anterior aspect of the lateral border.

d) Medial Border

This is most clearly defined at the level of the exit of the fascicles of the third nerve.

LFB: At levels where fascicles of the third nerve are found this defines the medial border [Fig 8.1 level 5]. At other levels the medial border is determined by the medial edge of the tissue specimen.

Perl: The anterior medial SN has high iron staining.

Immunohistochemsity: These clearly define a medial border

Spin echo MRI: The medial border is defined by a hyperintense rim formed by the bundles containing fascicles of the third nerve [Fig 8.1 level 5].

4. Three useful landmarks

We identified three internal landmarks within the substance of the SN:

1. Anterior Medial White Matter (AM): in the anterior and medial SN there are myelinated fibres appearing in the shape of a 'hook' (H) [Fig 8.1A&B levels 1-6]. Clusters of fascicles of WM staining blue on LFB and with Perl stain are seen within the SN, indicating that they are a site of iron deposition. [Fig 8.1C levels 1-6]. On spin echo MRI there is corresponding signal hypointensity [Fig 8.1D levels 1-6]. Higher field images demonstrate Perl staining as both pigment in the neuropil and in clusters of white matter [Figure 8.2B&E].
2. Anterior Lateral White Matter (AL): in the anterolateral portion of the SN there is a triangular region containing myelinated fibres [Fig 1B levels 2-5]. These fibres have higher Perl staining [Fig 8.1C levels 2-5] and are seen as hypointense on MRI [Fig 8.1D levels 2-5].
3. Posterior Lateral White Matter (PL): in the posterolateral SN there are myelinated fibres found just medial to the medial border of the SN [Fig 8.1A&B levels 2-5]. At the most inferior levels these correspond the the medial lemniscus [Fig 8.1B levels 6-7]. In contrast to the AL these do no appear to stain strongly for Perl but are still signal-hypointense [Fig 8.1D levels 2-5] on SE MRI.

5. Substantia Nigra pars reticularis (SNr)

The SNr was found anteriorly and superiorly to the SNc [Fig 8.1A levels 1-3] and was thus clearer at superior levels - pigmented cells were found from level 2-7 [Fig 8.1A levels 2-7]. It is defined by non-pigmented cells on the LFB [Fig 8.3]. It corresponds topographically to the region of high iron staining anteriorly and medially at more superior levels [Fig 8.1]. On high field SE MRI it appears heterogeneously with a hypointense rim (HR) and relatively hyperintense core, and is not immediately distinguishable from the SNc using SP or CB immunohistochemistry or by signal characteristics on SE MRI.

6. Substantia Nigra pars compacta (SNc) internal anatomy

The SNc is defined by the presence of cells pigmented with neuromelanin [Fig 8.1A all levels & Fig 8.3]. These are visible on the LFB and Perl stained sections and can be defined by location (Hassler 1937; Gibb, Fearnley et al. 1990) or by using calbindin immunohistochemistry to delineate so-called 'nigrosomes' where there is relatively reduced calbindin staining of the neuropil (Damier, Hirsch et al. 1999)[Fig 8.1A&E levels 2-7; Fig 8.3]. Not all pigmented cells are found in nigrosomes (Damier, Hirsch et al. 1999) and this is demonstrated in the cartoon [Fig 8.1A levels 2-7]. On Perl stain there is less intense staining within the nigrosomes, particularly seen at lower levels [Figure 8.1C levels 4-7] and Perl staining is less intense in nigrosomes [Fig 8.1C level 6 & 7].

Nigrosome 1 (N1 - the 'ventrolateral tier') was seen in levels 3-7. It was closely apposed to the posterior border of AL [Fig 8.1A&E levels 3-5] and formed a solitary band in lower levels [Fig 8.1 A&E levels 6-7]. On spin echo MRI it appears as a hyperintense band radiating across from the posterolateral border towards the anteromedial border defined by hypointensity of the AL on the anterior border and a hypointense band on the posterior border particularly medially where the 'hook' formed by the AM was seen [Fig 8.1A&D levels 3-7].

Nigrosome 2 (N2 - the pars medialis) was seen at all levels where pigmented cells were found [Fig 8.1A&E levels 2-7] at the most posterior and medial tip of the SN. This was not so clearly seen on spin echo MRI. There is relative signal hyperintensity at the most medial and posterior tip but this does not directly correspond to the size and shape of the region identified by calbindin immunohistochemistry, although the cluster of pigmented cells clearly extends beyond this region [Fig 8.1A&E all levels].

Nigrosome 3 (N3 - the 'pars lateralis') was seen in levels 4-6. It is bounded by the AL and the CC as it wraps around the lateral border of the SN [Fig 8.1A&B levels 3-5]. N3 was identified on spin echo MRI by signal hyperintensity bounded by the low signal intensity of AL and the CC [Fig 8.1 A&D levels 3-5].

Nigrosome 4 (N4 - the 'dorsolateral tier') was seen in levels 3 & 4. It abutted the posterior border of the SN and the PL [Fig 8.1 levels 3&4]. On spin echo MRI it appeared as a hyperintense band posterior to N1 and bounded by the signal hypointensity of the parabrachial nucleus immediately adjacent.

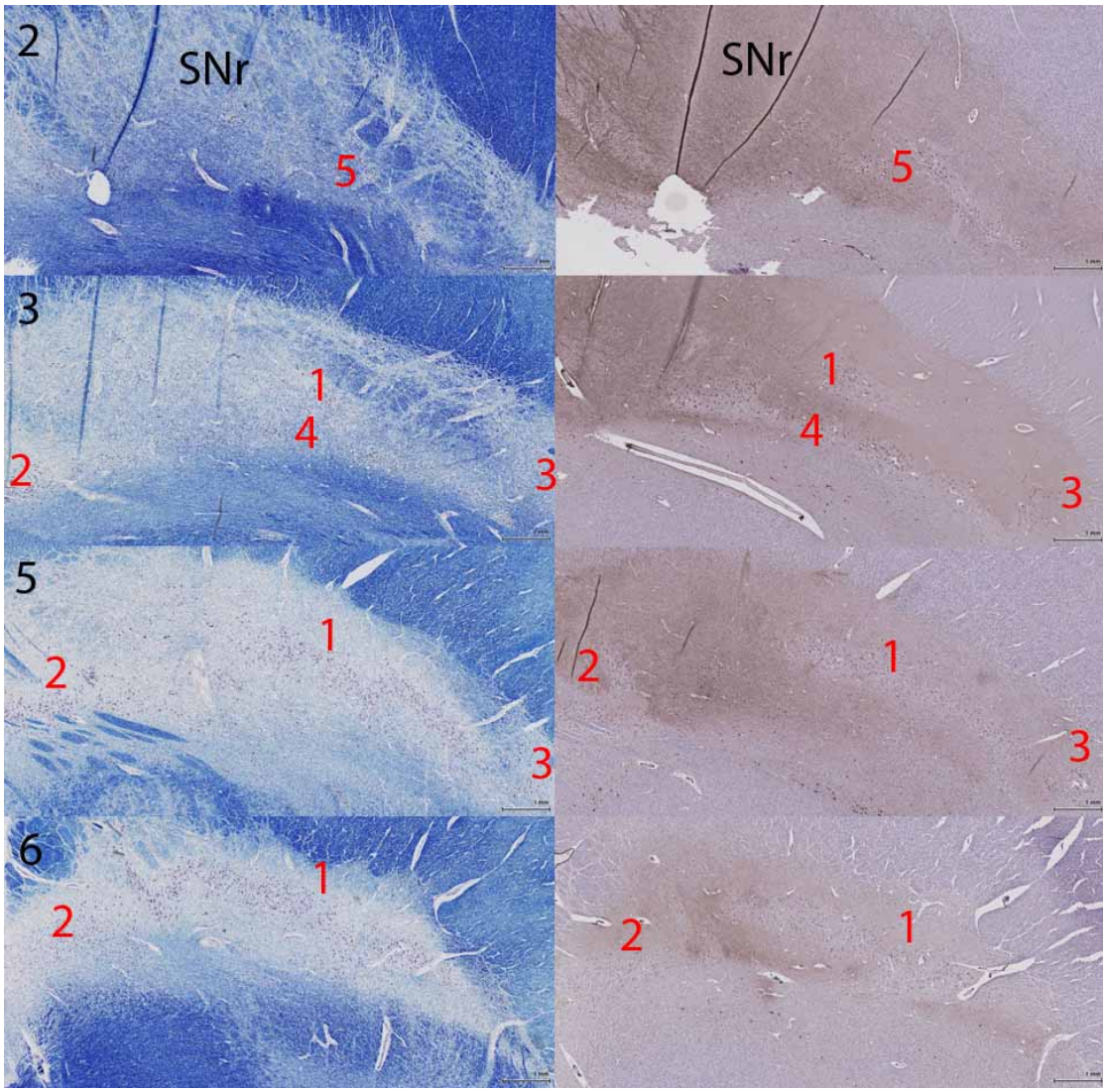

Figure 8.3: The internal anatomy of the SN using LFB and CB immunohistochemistry. LFB and CB stains delineating the anatomy of the nigrosomes within the SN at axial levels as per figure 1. At the `superior level (2) anterior and medial SN represents a regions without neuromelanin containing neurons and is the SNr. At the lower levels represented (3, 5, 6) clusters of neurons are seen both on LFB and CB immunohistochemistry. On CB stain regions of relative CB-poor stain are designated nigrosomes (Damier, Hirsch et al. 1999).

Nigrosome 5 (N5) was found at the most superior level where pigmented cells were found only [Fig 8.1A&E level 2]. This was seen on conventional MRI as a region of signal hyperintensity between the AL and PL.

On spin echo MRI N1 and N4 in the lateral SNc give the appearance of a spin echo signal hyperintense 'pincer' grasping a spin echo signal hypointense 'hook' corresponding to the Perl staining AM.

7. Sagittal and coronal plane images

In case 8 sagittal and coronal high field images were available. In the sagittal plane the superoposterior border of the SN is separated from the STN by a thin hypointense rim (HR); inferiorly SE MRI hyperintense signal white matter separates it from the RN including the region of the parabrachial nucleus. The inferoanterior border of the SN abuts the CC along the entire length of the nucleus [Fig 8.4 A-H].

In the coronal plane the superomedial border is defined by a hypointense rim (HR) separating it from the STN in the superior half; in the inferior half it is separated from the RN by the SE MRI hyperintense signal white matter. The inferolateral border is formed by the CC in the entire length of the SN [Fig 8.4 I-P].

8. Location, position and relations using SE MRI

The SN was clearly identified in all 10 control cases studied (11 half brains). It was found in the anterior portion of the midbrain posterior to the CC and anterior to the STN, RN and DSCP. It lay at an oblique angle in all three planes: in the axial plane the SN was approximately 40 degrees from the midline at the level of the STN and RN, and 30 degrees at the level of the DSCP; on sagittal images it lay at 35 degrees and in coronal images 45 degrees with reference to the axis of the brainstem; on these latter two images the SN was seen to lie mostly inferior and lateral to the RN and encase the STN's inferolateral aspect.

9. Volume and dimensions

The mean volume of the SN was 211.3 mm3 in controls, 120.8 mm3 in PSP and 180.8 mm3 in PD. In PSP the volume was significantly reduced compared to controls and PD, but there was no significant difference between PD and controls [Table 8.2]. The SN is most broad and deep at the level of the RN (mean width 11.72mm; mean depth 2.99mm), tapering at the superior extremity and resembling a tear in the sagittal and coronal planes [Fig 8.5]. Maximal length in the sagittal plane was 14.0 mm and in the coronal plane 14.4 mm. In PSP depth at the level of the RN and DSCP and width at the level of the RN were reduced in PSP [Table 8.2] but not in PD.

10. Borders at the level of the RN

The anterior border was more clearly defined laterally with haziness in the medial section with heavy deposition of iron and WM, SP+ fibres invaginating into the CC in controls, PD and PSP [Figs 8.2, 8.5-8.7, table 8.3]. This was also true on SE MRI in controls and PD [Fig 8.1, 8.5, 8.6] although in PSP [Fig 8.7] in some cases the lateral border was less distinct [table 8.4]

The posterior border was defined by white matter of the PBN medially and laterally by PL on histology in control and disease cases [table 3] and on SE MRI [table 8.4].

The medial border was clearly defined in all cases by fascicles of the IIIrd nerve and the medial CC and the lateral border were defined by the CC.

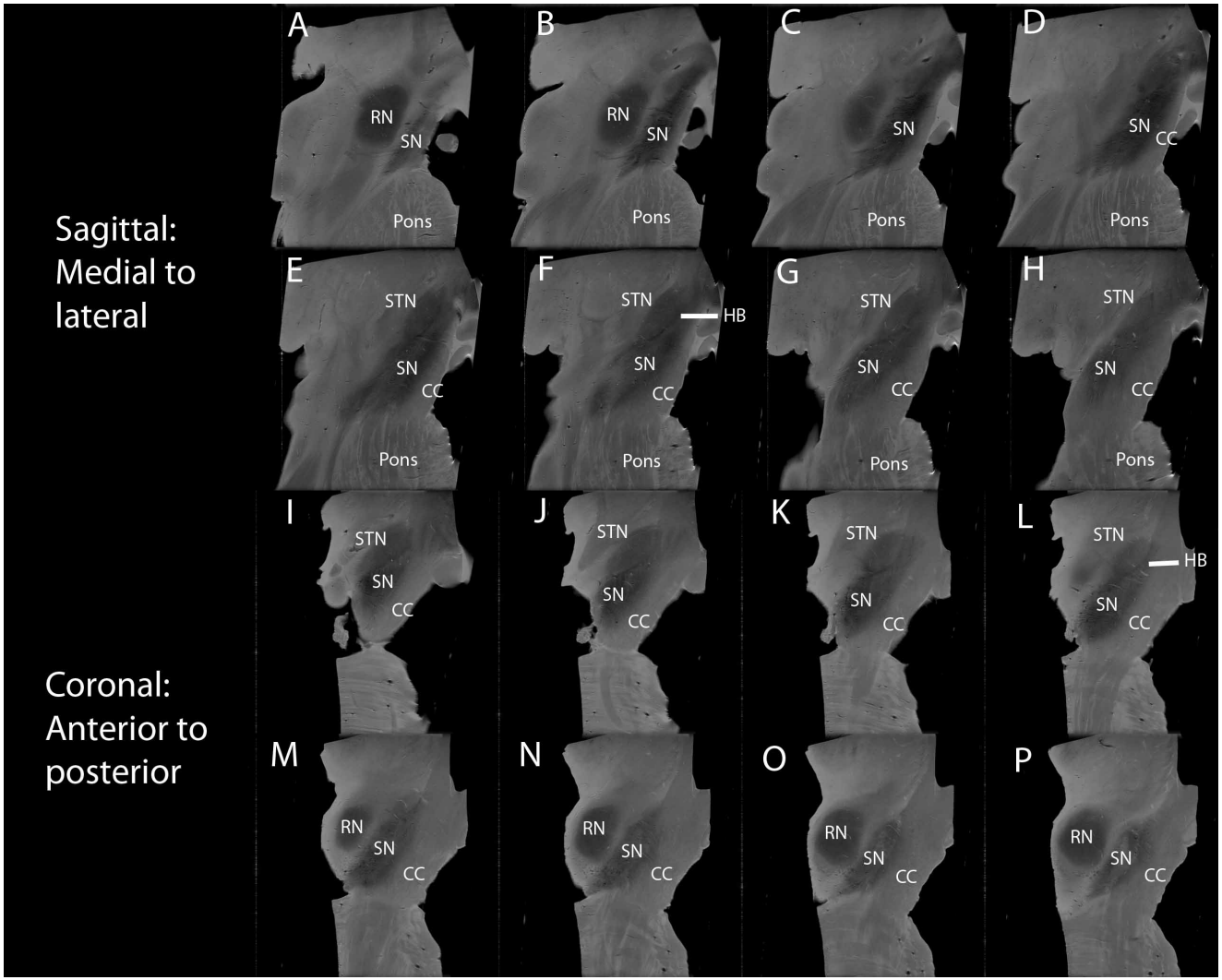

Figure 8.4: Sagittal and Coronal views using high field SE MRI. A-H serial sagittal views at 1mm from medial to lateral. SN inferior and anterior to the RN medially, and to the STN laterally. I-P serial coronal views at 1mm from anterior to posterior. The SN is inferior and tilted to the STN anteriorly and RN posteriorly. The CC forms the anterior border. Signal hypointensity ` greater more medially (B-D) and anteriorly (I-L) within the SN. The HB is seen separating the STN from the SN in both the sagittal (F) and coronal planes (L).

11. Landmarks at the level of the RN

AM, AL and PL were seen in all control and PD SNs at this level on histology and SE MRI, but were less frequent in the PSP group, particularly PL which was only seen in 1/8 PSP SNs [table 8.4].

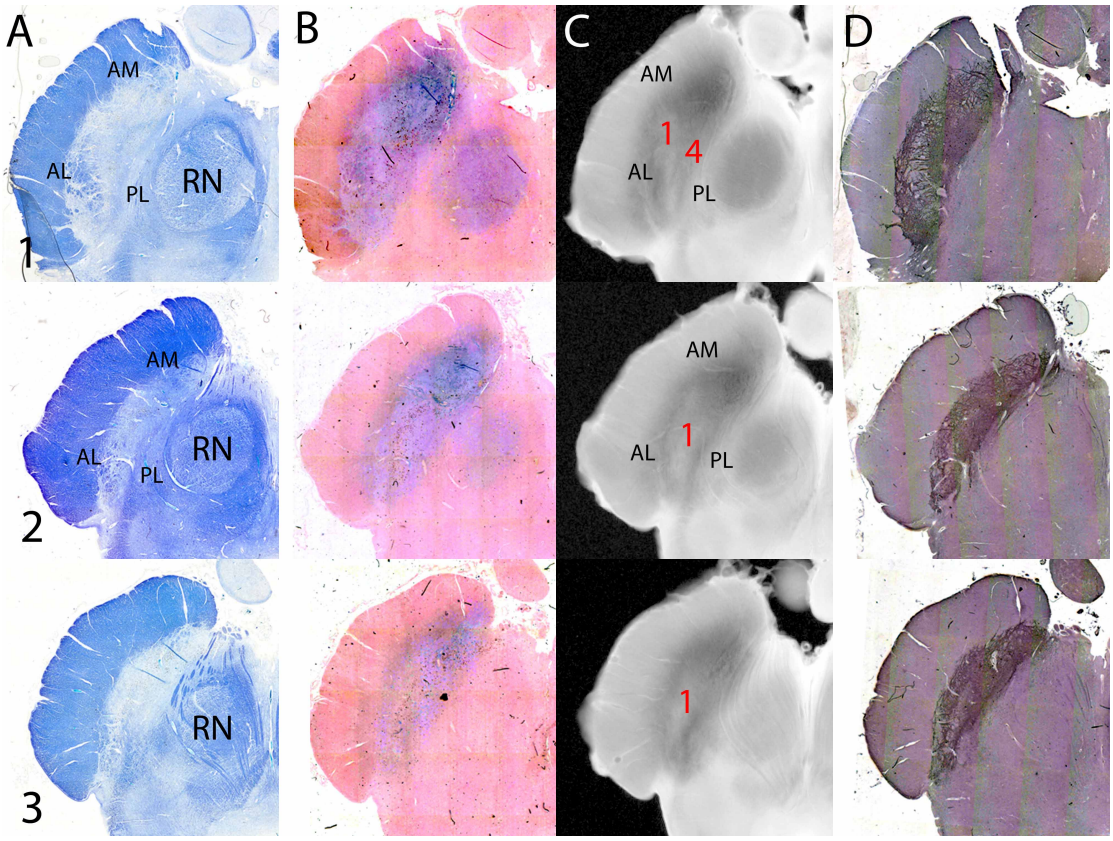

Figure 8.5: The anatomy of the SN in a further control case. Case 2 was a 94 yr old male. A: LFB. B: Perl stain. C: high field SE MRI. D: SP. 3 representative levels through the RN 1: just above the exit of the IIIrd nerve. 2: at the level of the exit of the IIIrd nerve fascicles. 3. below the level of the IIIrd nerve. The pigmented neurons of N1 are clearly seen within a region of reduced Perl staining and as a hyperintense band on SE MRI. The pincer and hook are clearly visualised, and the white matter andmarks AM, AL and PL.

12. Internal anatomy at the level of the RN

Overall and in keeping with the volume measurements [Tabl2 8.2] the SN appears similar in controls and PD [Fig 8.1, 8.5, 8.6] but is markedly thinned in PSP [Fig 8.7]. On histology N1, N3 and N4 were clearly visible and were associated with reduced Perl stain, whereas N2 was associated with increased Perl stain in controls. In the disease group the nigrosomes were

much less densely populated with pigmented neurons in PD [Fig 8.6 A & E] [Tabl3 8.3]. In PD the nigrosomes looked thick and pale [Fig 8.66 C & G]; in PSP thin and streaky with dense Perl staining [Fig 8.7 B & F]. On SE MRI, nigrosomes were paler in PD but still mostly identifiable [Fig 8.6 C & G; Table 8.4], and in PSP were more difficult to identify and had a stringy/streaky appearance when seen [Fig 8.6 C & G] [Table 8.4].

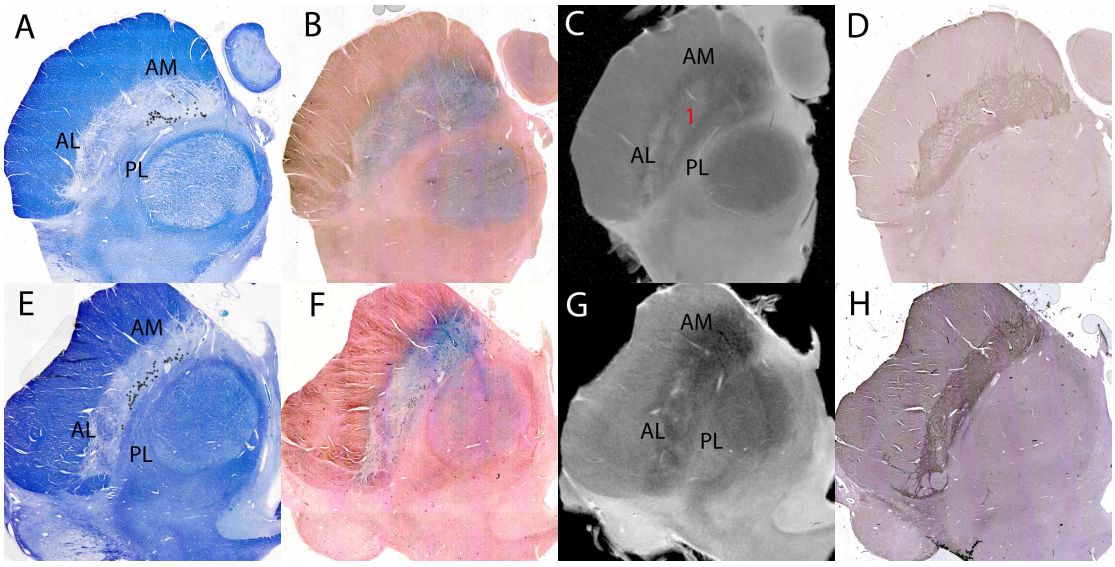

Figure 8.6: SN at the level of the RN and IIIrd nerve in PD. Images from a 79 yr old male [A-D] and 83 yr old male [E-H] with PD. A & E: LFB. B & F: Perl stain. C & G: high field SE MRI. D & H: SP. Borders and white matter landmarks are present and subjectively and objectively do not appear to have lost volume [Table 2]. SE MRI shows a high intensity band consistent with N1 when compared with control images. However, the remaining neuromelanin containing neurons (highlighted in black in A & E) are not within this structure.

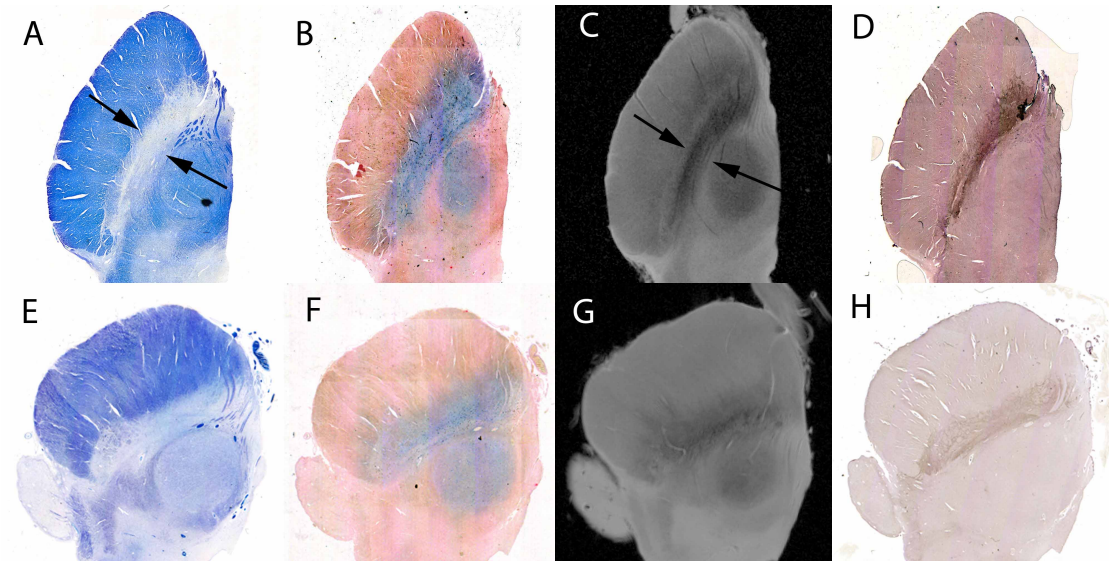

Figure 8.7: SN at the level of the RN and IIIrd nerve in PSP. Images from a 68 yr old male [A-D] and a 69 yr old male [E-H]. A & E: LFB. B & F: Perl stain. C & G: high field SE MRI. D & H: SP. The whole structure is markedly atrophic as exemplified by the reduced volume measurements and the reduced width and depth measurements [Table 8.2]. The borders, white matter landmarks and internal structure is much less distinct.

SNc at the level of the RN and IIIrd nerve exit			Control			PSP			PD		
HISTOPATHOLOGY			LFB	Perl	PV	LFB	Perl	PV	LFB	Perl	PV
Borders	Anterior	Medial blurring	3/3	3/3	3/3	2/2	2/2	2/2	2/2	2/2	2/2
		Lateral clarity	3/3	3/3	3/3	2/2	2/2	2/2	2/2	2/2	2/2
	Posterior	TMF	3/3	mild 3/3	0/3	1/2	mild 1/2	0/2	2/2	0/2	0/2
		ML	3/3	0/3	0/3	2/2	0/2	1/2 extn	2/2	0/2	0/2
	Medial	III	3/3	0/3	0/3	2/2	0/2	0/2	2/2	0/2	0/2
	Lateral	CC	3/3			3/3			3/3		
Landmarks	AM		3/3	2/3	2/3 hypo	2/2	2/2	hypo	2/2	2/2	2/2 hypo
	AL		3/3	3/3	3/3 hypo	2/2	2/2	hypo	2/2	2/2	hypo
	PL		3/3	1/3	3/3	2/2	2/2	hypo	2/2	2/2	hypo
Internal Anatomy	N1		3/3	3/3 hypo		sparse/absent	hyper++ 2/2		absent	2/2 hypo	
	N2		2/3	2/3 hyper		sparse/absent	hyper ++ 2/2		sparse/absent	2/2 hyper	
	N3		3/3	2/3 hypo		sparse/absent	hypo		absent	2/2 hypo	
	N4		3/3	3/3 hypo		sparse/absent	hyper++ 2/2		sparse/absent	2/2 hypo	
	N5										
	Pincer		3/3	3/3 hypo		0/2	0/2		0/2	2/2	
	Hook		3/3	2/3 hyper		1/2	0/2		2/2	2/2	
Comments						Thin, streaky, high Perl stain			Thick, pale nigrosomes		

Table 8.3: Anatomy of SNc at level of RN and exiting IIIrd nerve fascicles on histopathology

TMF - transverse myelinated fibres posterior to SN

SNc at the level of the RN and IIIrd nerve exit			Contol		PSP		PD	
SE MRI images			LFB	SE MRI	LFB	SE MRI	LFB	SE MRI
Borders	Anterior	Medial blurring	9/9	9/9	8/8	8/8	5/5	5/5
		Lateral clarity	9/9	9/9	7/8	6/8	4/5	5/5
	Posterior	TMF	7/9	7/9	3/8	7/8	4/5	5/5
		ML	9/9	9/9	8/8	8/8	4/5	5/5
	Medial	III	9/9	9/9	8/8	8/8	4/5	5/5
	Lateral	CC	8/9	8/9	8/8	8/8	4/5	5/5
Landmarks	AM		7/9	8/9	7/8	5/8	4/5	4/5
	AL		9/9	9/9	8/8	5/8	5/5	5/5
	PL		9/9	8/9	6/8	1/8	5/5	5/5
Internal Anatomy	N1		9/9	9/9	6/8 sparse	2/8 stringy	0/5	5/5 faint
	N2		9/9	0/9	6/8 sparse	0/8	4/5 sparse	0/5
	N3		9/9	7/9	6/8 sparse	1/8	3/5 sparse	3/5 faint
	N4		8/9	8/9	4/8 sparse	4/8 stringy	4/5 sparse	5/5 faint
	N5							
	Pincer		9/9	9/9	0/8	3/8	0/5	4/5
	Hook		6/9	9/9	5/8	2/8	5/5	5/5

Table 8.4: Anatomy of SNc at level of RN and exiting IIIrd nerve fascicles on high field SE MRI.

Case 1 never had pathological examination and so was excluded from this part of the analysis.

E. Discussion

1. Summary of findings

We have demonstrated the anatomy of the SN using high field SE MRI at 9.4T and validated this with post mortem histological tissue in the same specimens. The anterior border is more clearly delineated laterally and inferiorly and there is an intermingling of the SN and CC particularly anteriorly and medially at the most superior levels characterised by higher iron deposition on Perl staining and a serrated edge on SP immunohistochemistry. The posterior border is formed by white matter lying between the SN and RN in the medial aspect and the SL and ML in the lateral aspect and is mostly hypointense. The hyperintense band described in the literature is more posterior, abutting the RN and forms part of the PBN [Fig 8.1 B & D levels 3-5]. We describe three bundles of white matter on histopathology defined by position (AM, AL and PL) which are seen on high field MRI and are useful landmarks in the SN.

2. Internal Anatomy of the SN using high field MRI

Within the SN itself there is heterogenous signal. The region of the SNr is hypointense on SE MRI with a hypointense rim defining its anterior border, and a hypointense band defining its posterior border from the STN. The SNc is defined by the position of the pigmented neuromelanin positive neurons. By using immunohistochemistry for CB we are able to describe the accurate position of Damier's nigrosomes (Damier, Hirsch et al. 1999). These are seen on high field SE MRI as hyperintense regions whose position can be clarified by reference to the white matter landmarks AM, AL and PL. In controls the AM white matter landmark forms a hypointense hook appearance, and the combination of high signal from N1 and N4 at the level of the RN and IIIrd nerve fascicles form the appearance of a hyperintennse 'pincer'.

3. SN volume

We found no difference in SN volume between controls and PD, but in PSP the volume was markedly reduced [Table 8.2]. This was in accord with the markedly thinned appearance of the SN in axial sections on MRI and pathology and increased Perl staining for iron [Fig 8.6 & 8.7]. Furthermore, in PD the white matter landmarks and nigrosomes were still visible

although the latter appeared less clearly defined; in PSP the topographical destruction was far greater.

4. Strengths and weaknesses of the study

The major strength of our study is in the use of pathological materal to validate our findings on high field SE MRI. The consequence of this is that we have described the actual anatomy based on histopathological findings in the same tissue rather than the presumed anatomy based upon atlas comparisons. By using post mortem tissue we were not constrained by movement artifacts or problems with time such as heating and patient tolerability meaning that we could acquire multiple averages to increase signal-to-noise ratio and at high in-plane resolution. At the same time this is also a limitation in that the times we have used are not practical. Furthermore, there are significant differences between imaging post mortem tissue at room temperature when compared to imaging the brain in vivo at 37 degrees including differences in physical properties such as the relaxation times, and differences in measurements due to asymmetric tissue shrinkage during the fixation process. The histopathological protocol at the QSBB fixes half of the brain with the other frozen for biochemical studies so asymmetries and study of the side contralateral to the clinically worst affected side could not be undertaken. Additionally, our sample size is necessarily small due to the contraints of working with post mortem tissue and practical considerations in terms of time both in terms of imaging time available and the burden imposed for technical support for tissue processing, cutting and staining serial slides for analysis.

5. The intricate anatomy of the SN

The anatomy of the SN is highy complex: it is comprised not only of the SNr and SNc but the SNc is comprised of an intricate network of neurons segregated into functionally and anatomically distinct groups. Not only does it lie in a busy environment but as can be seen from the serial axial sections [Fig 8.1] it varies in its dimensions and the internal organisation throughout its course. The internal organisation has been the subject of debate in the literature for some time (Hassler 1937; Olzewski 1954; German, Manaye et al. 1989; Fearnley and Lees 1991; Gibb and Lees 1991; Gibb 1992; McRitchie, Halliday et al. 1995; McRitchie, Hardman et al. 1996; Damier, Hirsch et al. 1999) and differences in the angle of cut can have effects on the results, such is the variability. At the current time conventional imaging of the brainstem is too insensitive to pick up some of the subtleties

and this likely explains the heterogeneity of the results of clinical studies, along with the fact the the anatomy on MRI has not yet been clearly validated.

Inconsistencies in the description of the SN on conventional MRI has been noted before using conventional MRI (Savoiardo, Girotti et al. 1994; Gorell, Ordidge et al. 1995; Adachi, Hosoya et al. 1999; Martin, Wieler et al. 2008; Massey and Yousry 2010). Apart from the seminal paper of Oikawa et al there have been few studies looking at the pathological confirmation of the representation of the SN on MRI (Oikawa, Sasaki et al. 2002). As a consequence of this, may early studies have been based on a presumed understanding of the anatomy on conventional MRI (Duguid, De La Paz et al. 1986; Rutledge, Hilal et al. 1987; Drayer 1988; Drayer 1988; Pujol, Junque et al. 1992) (for review see (Massey and Yousry 2010)).

6. Advances in MRI of the SN

Other MRI techniques have been used more recently to image the SN and study it in disease but without pathological confirmation. High-resolution 3T imaging sensitive to the paramagnetic effects of neuromelanin shows signal hyperintensity in the SN (Sasaki, Shibata et al. 2006). Mulitshot diffusion-weighted MR imaging with a left to right diffusion direction gradient may define the borders of the SN better than T2 weighted imaging (Adachi, Hosoya et al. 1999). Other published techniques to delineate the SN include DESPOT1 (Menke, Jbabdi et al. 2010), relaxometry (Ordidge, Gorell et al. 1994; Gorell, Ordidge et al. 1995; Martin, Wieler et al. 2008; Peran, Cherubini et al. 2010), segmented inversion recovery imaging (SIRRIM) (Hutchinson, Raff et al. 2003; Raff, Hutchinson et al. 2006), GRASE and FFE (Eapen, Zald et al. 2011), susceptibility-weighted imaging (SWI) (Abosch, Yacoub et al. 2010) and magnetisation transfer ratio imaging (Helms, Draganski et al. 2009).

Recently published in vivo work at 7.0T has improved the resolution, contrast and signal-to-noise ratio of images of the SN using T2* (Cho, Oh et al. 2011; Kwon, Kim et al. 2012). The anatomical variability in the anterior border seen in PD, and the posterior border reduction in high signal intensity in PD are encouraging signs of detecting differences but the pathological correlate of this is not clear. While we did not study this particular feature in our work, using SE MRI we did not see dramatic differences between control and PD groups - in accordance with much of the literature. However, when compared to PSP there was a clear subjective difference in appearance of the SN which is not reliably evident on

conventional MRI, although differences have been reported. The undulation of the anterior border of the SN reported by Kwon et al does not have an obvious pathological correlate, particularly given that this is topographically likely to be part of the SNr as it is found in the most superior, anterior and medial part of the whole SN.

7. Imaging nigrosomes in the SN

CB immunohistochemistry has enabled us to define nigrosomes on our histological sections, which have a radiological correlate on our high field SE MRI images (Damier, Hirsch et al. 1999). We are not aware of this previously being reported. All 5 nigrosomes are seen in serial axial sections [Figure 8.1].

However, we do not appear to be imaging the pigmented neurons per se, as when they are absent in PD the SE MRI high signal remains [Figure 8.6]. This is in keeping with pathological work where the nigrosome structure is maintained even in the face of loss of pigmented SNc cells (Damier, Hirsch et al. 1999). This is interesting the context of much of the published literature on the SN in PD. Many studies have tried to detect differences in the traditionally defined SNc (Duguid, De La Paz et al. 1986) using conventional MRI. There are reports of reduced width (Duguid, De La Paz et al. 1986; Braffman, Grossman et al. 1989; Stern, Braffman et al. 1989; Pujol, Junque et al. 1992; Yagishita and Oda 1996) or smudging of the SNr hypointensity (Drayer 1988; Savoiardo, Strada et al. 1989; Savoiardo, Strada et al. 1990; Savoiardo, Girotti et al. 1994). However, only one study has found a correlation between the width of the SNc and a measure of clinical severity (Pujol, Junque et al. 1992).

8. Changes in disease

Using multishot diffusion-weighted MR imaging to define the borders of the SN more clearly also did not show a reduced SN width in PD (Adachi, Hosoya et al. 1999), or PD-weighted or fast SITR images (Oikawa, Sasaki et al. 2002). However, this is not greatly surprising as although there is clearly huge loss of neuromelanin containing pigmented cells in the SNc in PD (Fearnley and Lees 1991; Hardman, Halliday et al. 1997; Ma, Roytta et al. 1997) the pathological literature points to the fact that the volume of the SN does not reduce in PD (Ma, Roytta et al. 1997). In fact, pathological data in aging (Cabello, Thune et al. 2002) and a recent imaging study in PD (Kwon, Kim et al. 2012) suggest that it may paradoxically increase in size. The explanation for this is unclear but it seems fairly certain

that SN atrophy should not be expected in PD. Our data supports this idea - both in terms of the absolute measured volume not being significantly different from controls in PD [Table 8.2], and in the appearance of the SN in the axial plane having preserved width and depth both subjectively [Figure 8.6] and on formally measuring it [Table 8.2]. Therefore, other methods of determining ongoing Lewy body pathology are needed if we are to expect positive results in the SN. More recently, studies have shown a regional predilection of PD in the SN using DTI region of interest studies (Chan, Rumpel et al. 2007; Vaillancourt, Spraker et al. 2009; Peran, Cherubini et al. 2010) in agreement with the pathological topography (Fearnley and Lees 1991). However, subsequent studies have not confirmed this (Menke, Scholz et al. 2009).

In PSP the story is different in that far greater destruction of the borders and internal architecture of the SN is found with loss of the nigrosomal SE MRI hyperintensity [Figure 8.7, Table 8.3 & 8.4]. This is manifest as a reduced volume which is consistent with both the pathological literature where PSP affects both SNr and SNc (Hardman, Halliday et al. 1997), and imaging literature where a smaller SN has been described using multishot diffusion-weigthed imaging (Adachi, Hosoya et al. 1999). Many conventional MR imaging abnormalities have been described in the SN in PSP but none are of clinical utility currently (Massey, Micallef et al. 2012).

9. Suggestions for further work

There are many unanswered questions. There is very little information about the heterogeneity of iron deposition in the SN and the anterior border of the SN and the precise location of the iron, or its role in the pathogenesis. The precise anatomical correlate of signal hyperintensity on SE MRI in the region of the nigrosomes is not clear but it appears not to be the pigmented neurons of the SNc, as already discussed. The best method to study the anatomy of the SN is also unclear - iron is clearly important in the pathogenesis and so iron-sensitive techniques such as T2* and SWI should be employed; but we have shown that iron strays outside the SN proper and may be misleading in determining the boundary of the SN. Further studies are needed to answer some of these questions and in the absence of dramatic structural deficits in PD quantitative techniques such as relaxometry, DTI and MTI will need to be further evaluated with histopathological work to determine the correlate of any abnormalities detected.

F. Conclusions

We have demonstrated the anatomy of the SN histologically and applied this knowledge to understand the complex and heterogeneous high field SE MRI signals in the SN in the same tissue. The nigrosomes are seen using this technique and preserved in PD but not PSP, in accordance with pathological studies. Further work is needed to clarify the pathological correlates of MR imaging techniques in this protean nucleus so that it may become of use in the clinic during life.

Chapter 9: White matter disease in Progressive Supranuclear Palsy and Multiple System Atrophy using TBSS at 3T.

A. Introduction

Accurate clinical diagnosis of neurodegenerative diseases presenting with parkinsonism progressive supranuclear palsy (PSP) or multiple system atrophy (MSA) can be difficult. Post Mortem series show that only 84.2% of PSP cases and 88.2% of MSA cases may be correctly classified on clinical grounds even in experienced centres (Hughes, Daniel et al. 2002) and there is clinical heterogeneity in the presentation of these diseases (Williams, de Silva et al. 2005; Dickson, Ahmed et al. 2010) with regional pathological load determining the clinical phenotype.(Williams and Lees 2009).

Nevertheless, there is distinct neuropathological topography - the key features of PSP are atrophy and deposition of tau in the midbrain, subthalamic nucleus (STN), substantia nigra (SN), globus pallidus (GP), superior cerebellar peduncles (SCPs) and dentate nucleus (DN) which are most severely affected (Tsuboi, Slowinski et al. 2003; Williams, Holton et al. 2007); in MSA alpha synuclein containing glial cytoplasmic inclusions are found in the SN, dorsolateral putamen and pontine base, middle cerebellar peduncles (MCPs) and cerebellum (Ozawa, Paviour et al. 2004).

Conventional MRI findings in PSP and MSA are specific, but sensitivity is low (50-67%) (Massey, Micallef et al. 2012). Region-of interest (ROI)- based studies of quantitative MR techniques such as diffusion tensor imaging (DTI) have clinical utility (Stamelou, Knake et al. 2011) and may reveal abnormalities in the absence of changes on conventional MR images in MSA (Seppi, Scherfler et al. 2006; Seppi, Schocke et al. 2006). However, this approach only shows pathology in predefined regions of interest and may exclude changes in other affected regions.

Voxelwise analysis of MR data can demonstrate statistically significant differences between patient groups without requiring *a priori* assumptions regarding which regions are affected. Focal grey (GM) and white matter (WM) loss can be assessed with voxel-based morphometry (VBM) (Ashburner and Friston 2000) and microstructural disruption of WM tracts can be visualised using voxelwise diffusion-weighted imaging (DWI) data modelled

using a single diffusion tensor (DTI) in tract-based spatial statistics (TBSS) (Smith, Jenkinson et al. 2006).

Although VBM has been used in both PSP (Brenneis, Seppi et al. 2004; Price, Paviour et al. 2004; Cordato, Duggins et al. 2005; Padovani, Borroni et al. 2006; Josephs, Whitwell et al. 2008; Agosta, Kostic et al. 2010; Josephs, Whitwell et al. 2011) and MSA (Brenneis, Seppi et al. 2003; Specht, Minnerop et al. 2003; Hauser, Luft et al. 2006; Minnerop, Specht et al. 2007; Minnerop, Luders et al. 2010) and TBSS in PSP (Knake, Belke et al. ; Whitwell, Avula et al. 2011; Agosta, Pievani et al. 2012; Saini, Bagepally et al. 2012), there are no reports of the simultaneous use of both techniques in both conditions.

B. Aim

The aim of this study is to examine regional atrophy using VBM and the structural integrity of WM tracts using TBSS in patients with PSP and MSA. We assess whether these techniques provide complementary information and reflect clinical disease activity.

C. Materials and Methods

1. Participants

This study was approved by the local ethics committee and research and development department at UCL/UCLH Biomedical Research Centre. Written informed consent was obtained in 48 participants who had 3T MRI (Siemens Tim Trio; Siemens, Erlangen, Germany): 20 healthy controls, and 18 PSP and 10 MSA patients fulfilling research diagnostic criteria (Litvan, Agid et al. 1996; Gilman, Low et al. 1999). Twenty healthy controls had no significant neurological or psychiatric medical history [Table 1]. Patients were scored with Hoehn & Yahr,(Hoehn and Yahr 1967) UPDRS II and III (Fahn, Elton et al. 1987), Folstein's Minimental State Examination (MMSE) (Folstein, Folstein et al. 1975), the Frontal Assessment Battery (FAB) (Dubois, Slachevsky et al. 2000) and Golbe's PSP Rating scale (PSPRS) (Golbe and Ohman-Strickland 2007) or the unified MSA rating scale (UMSARS) (Wenning, Tison et al. 2004).

2. MRI Acquisition

Volumetric T1-weighted images (3D-MPRAGE; time to repetition (TR) / time to echo (TE) / inversion time 2200/2.9/900ms, flip angle 10°, 208 partitions, field of view (FoV) 28.2x28.2cm^2, matrix 256x256, isotropic spatial resolution 1.1mm) and echo-planar DWI (55 contiguous 2mm slices; b = 1000 s/mm^2 in 64 non-co-linear directions (2 averages) and b = 0 s/mm^2 (6 averages); TR/TE 6800/91ms, FoV 19.2x19.2cm, matrix 96x96, effective isotropic resolution 2mm) were acquired. Prior to analysis data were screened for movement artefact.

3. MRI Analysis

DARTEL-VBM analysis: T1 MPRAGE data were processed in SPM8. Firstly, they were manually reorientated and then underwent 'unified' segmentation which combines segmentation, bias correction and template normalisation in one step (Ashburner and Friston 2005). The resulting WM and GM tissue segments from all subjects were processed with DARTEL (Diffeomorphic Anatomical Registration Through Exponential Lie Algebra) (Ashburner 2007) to generate a cohort-specific template. Each subject's GM and WM segments were then warped to this template with signal intensities at each voxel 'modulated' to account for volume changes between original and warped spaces; data was smoothed with a 6mm Gaussian kernel and then analysed with an ANCOVA model in SPM8 using age and total intracranial volume (computed as the sum of GM, WM, cerebrospinal fluid segments) as covariates. Statistically significant group differences were visualised with multiple comparisons accounted for using uncorrected voxelwise p values at a threshold of 0.001 and a non-stationary correction for significant clusters ($p<0.05$) (Hayasaka, Phan et al. 2004).

TBSS: Voxelwise analysis of DTI data was carried out using TBSS (Tract-Based spatial statistics (Smith, Jenkinson et al. 2006), part of FSL (Functional MRI of the brain (FMRIB) Software Library) (Smith, Jenkinson et al. 2004). DWI data were processed using the FDT (FMRIB's Diffusion Toolbox) in FSL (Smith, Jenkinson et al. 2006). First, fractional anisotropy (FA) and mean diffusivity (MD) images were created by fitting a single tensor model to the raw diffusion data using FSL-FDT, and then brain-extracted using the brain extraction tool (FSL-BET). Radial diffusivity (RD) and axial diffusivity (AD) were calculated and then FA, MD, RD and AD data were aligned into a common space using the nonlinear registration tool FNIRT (FMRIB's non-linear image

registration tool) (Andersson, Jenkinson et al. 2007; Andersson, Jenkinson et al. 2007), which uses a b-spline representation of the registration warp field (Rueckert, Sonoda et al. 1999). Next, the mean FA image was created and thinned to create a mean FA skeleton which represents the centres of all tracts common to the group. Data was smoothed with a 6mm Gaussian kernel. Each subject's aligned FA data were then projected onto the mean FA skeleton and smoothed with a 6mm Gaussian kernel along the skeleton; the resulting data was fed into voxelwise cross-subject statistics with age as a covariate. Correction for multiple comparisons was done with threshold-free cluster enhancement (TFCE) (significance level of 0.05) (Smith and Nichols 2009).

4. Correlation with disease severity

When a statistically significant relationship was found between disease group and WM or GM loss, or FA or MD, it was tested for correlation with disease severity as measured by disease duration or clinimetric score. Age was used as a covariate in the analysis. Using SPM8 for DARTEL-VBM data the whole brain result was adjusted using a small-volume correction mask which was constructed using the significant association at the disease level. Using TBSS for FA and MD data a mask was made using significantly associated voxels and processed using the FEAT GUI in FSL.

D. Results

1. Group demographics

	Control	PSP	MSA	Statistical difference
n (gender)	20 (12F; 8M)	18 (6F; 12M)	10 (6F; 4M)	None
Age (SD)	66.1 (5.7)	69.8 (7.0)	63.4 (8.1)	None
Disease duration (SD)		4.3 (2.9)	4.9 (2.1)	None
Hoehn & Yahr (SD)		3.8 (0.7)	4.1 (0.7)	None
UPDRS II (SD)		20.2 (6.5)	26.7 (6.1)	*
UPDRS III (SD)		38.4 (8.5)	52.0 (9.4)	**
MMSE (SD)		27.6 (2.2)	28.8 (1.1)	None
FAB (SD)		13.1 (3.4)	16.0 (1.7)	***
PSPRS (SD)		37.6 (8.7)		
UMSARS (SD)			54.9 (12.44)	

Table 9.1: Demographic characteristics of participants. Age and Disease duration in years. *UPDRS II significantly greater in MSA than PSP ($p < 0.05$); **UPDRS III significantly greater in MSA than PSP ($p < 0.05$); ***FAB significantly lower in PSP than in MSA ($p < 0.05$).

Forty-eight cases were included in the analysis in 44 of which both VBM and TBSS were performed; in 2 artefact-free DTI data were unavailable for TBSS, and in a further 2 T1-volumetric data exhibited an unacceptable level of motion artefact leaving 46 in each group. Of the 18 PSP participants 15 were clinically classified as probable PSP, and 3 possible PSP. Of the 10 MSA participants 8 were of the MSA-P phenotype (1 possible MSA, 7 probable MSA), 2 of the MSA-C phenotype (1 possible MSA, 1 probable MSA). There were no significant between-group differences in age or disease duration at time of imaging. UPDRSII and III were greater in MSA than in PSP, and FAB less in PSP than MSA [table 9.1].

2. PSP versus controls

DARTEL-VBM: symmetrical GM loss was seen in the caudate nucleus and anterior putamen ($p < 0.001$) [table 9.2; figure 9.1C, G, I, K]. There was extensive volume loss in the following regions classified as WM: the dentate nucleus, SCPs, pontine and midbrain tegmentum, region of the SN and STN, crus cerebri, thalamus, and GP ($p < 0.001$)[table 9.2; figure 9.1A-C, F, I-K].

TBSS: extensive symmetrical WM FA reduction was found near the dentate nuclei, SCPs, decussation of the SCPs, the corpus callosum (sparing the splenium), the anterior limb of the internal capsule, and WM throughout the frontal, parietal and occipital lobes including the olfactory tracts, superior longitudinal fasciculi and forceps major and minor. There was relative sparing of the posterior limb of the internal capsule, the external capsule, the corticospinal tracts, the MCPs and the WM of the temporal lobes [Table 2; figure 1]. Symmetrical MD increase was found in the anterior 2/3 of the corpus callosum, anterior limb of the internal capsule, and frontal white matter. [Table 9.2; Figure 9.1] There were no statistically significant findings with AD and RD.

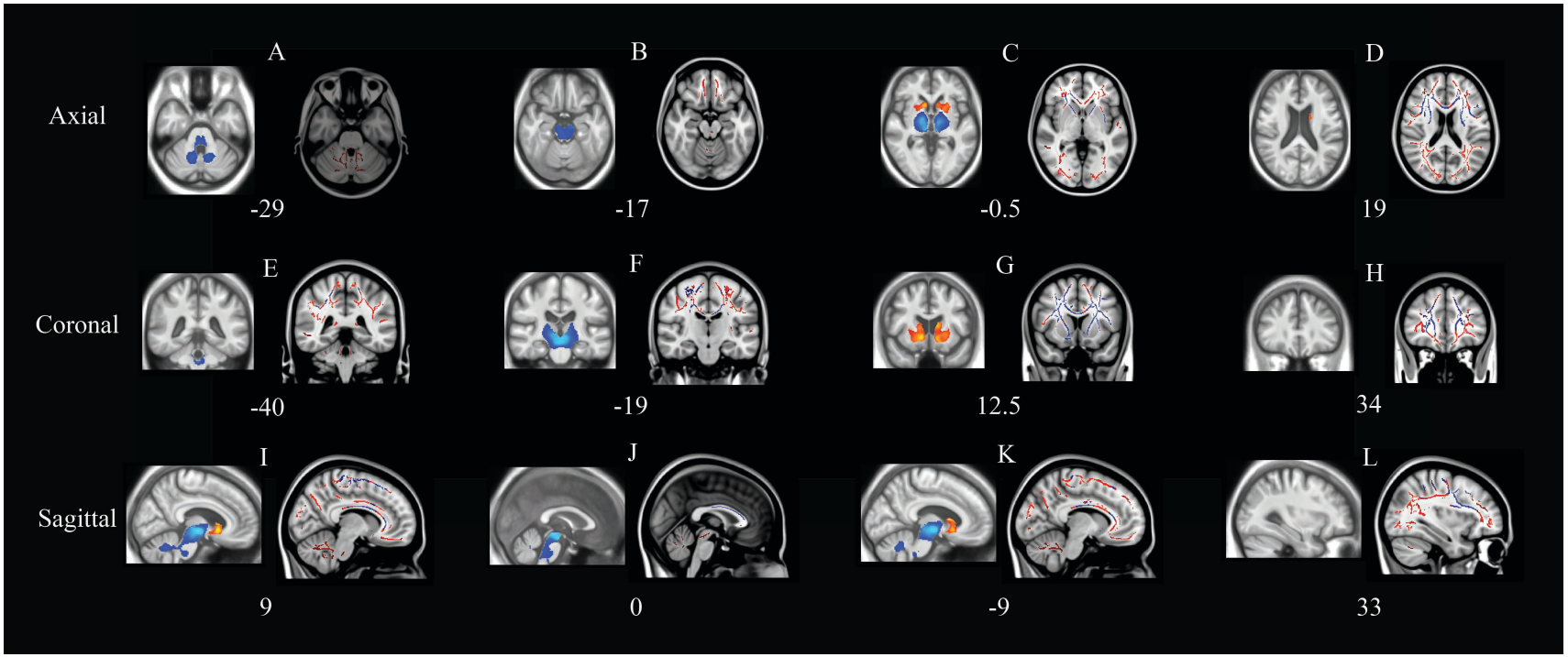

Figure 9.1: PSP compared to healthy controls – Axial, coronal and sagittal cuts in PSP vs controls. Paired images: the left image displays WM loss (blue) and GM loss (yellow) (Uncorrected p value <0.001 with cluster-level nonstationary correction p value < 0.05) and the right image shows reduced FA (red) or increased MD (blue) (TFCE p < 0.05). For anatomic details see tables 2 and 3. [A-D] axial, [E-H] coronal and [I-L] sagittal slices at specific MNI coordinates. VBM images displayed on average template from study group. TBSS images displayed on MNI 1mm template

3. MSA versus controls

DARTEL-VBM: GM loss was seen in the right caudate nucleus, anterior right putamen and inferior cerebellar hemispheres ($p < 0.001$) and there was a trend to GM loss in the left anterior putamen and caudate head ($p=0.052$) [table 2]; there was patchy cerebellar GM loss [table 2; figure 2A, B, E, I]. There was extensive symmetrical volume loss in the following regions classified as WM: the cerebellar WM, MCPs, pontine base (relative sparing of the tegmentum) [Figure 2A, B, E, F, I-K], and in the region of the posterolateral putamen and surrounding WM including the external capsule and the posterior limb of the internal capsule ($p < 0.001$) [Table 2; figure 2C, G].

TBSS: Reduced FA was found symmetrically in the deep cerebellar WM, inferior cerebellar peduncles, MCPs, pontocerebellar crossing fibres, corticospinal tracts (at the level of the pons), right SCP, body of the corpus callosum (mid-portion and forceps minor) and corticospinal tract in the precentral gyrus [Table 2; Figure 2]. There was no statistically significant MD increase in MSA, but there were trends suggestive of changes in the left MCP and deep cerebellar WM, the mid-portion of the corpus callosum, the external capsule, both limbs of the internal capsule and the corticospinal tract from the precentral gyrus to just above the internal capsule [Table 2]. There were no statistically significant findings with AD and RD.

4. MSA versus PSP

DARTEL-VBM: there were no significant clusters although a trend for putaminal atrophy in MSA and midbrain atrophy in PSP was observed when comparing regions classified as WM.

TBSS: no differences in FA, MD, AD, RD

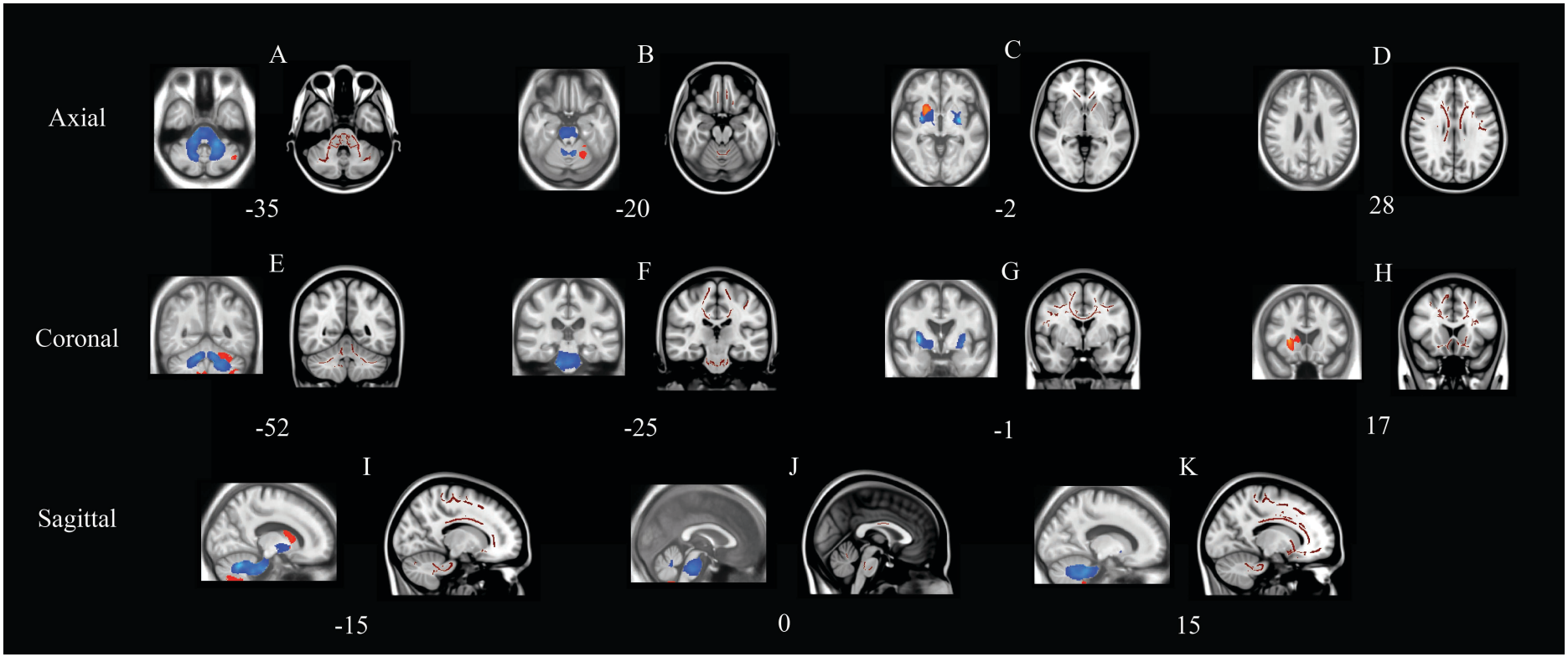

Figure 9.2: MSA compared to healthy controls – Axial, coronal and sagittal cuts in MSA vs controls. Paired images: the left image displays WM loss (blue) and GM loss (yellow) (Uncorrected p value <0.001 with cluster-level nonstationary correction p value < 0.05) and the right image shows reduced FA (red) or increased MD (blue) (TFCE p < 0.05). For anatomic details see tables 2 and 3. [A-D] axial, [E-H] coronal and [I-L] sagittal slices at specific MNI coordinates. VBM images displayed on average template from study group. TBSS images displayed on MNI 1mm template.

5. Correlation with Clinical Scores

Disease severity in PSP as measured by the PSPRS correlated with midbrain atrophy [Figure 9.3A] and disease duration with FA reduction in the parietal WM [Figure 3B]. The PSPRS score also correlated with MD increase in the frontal white matter and anterior corpus callosum [Figure 9.3C].

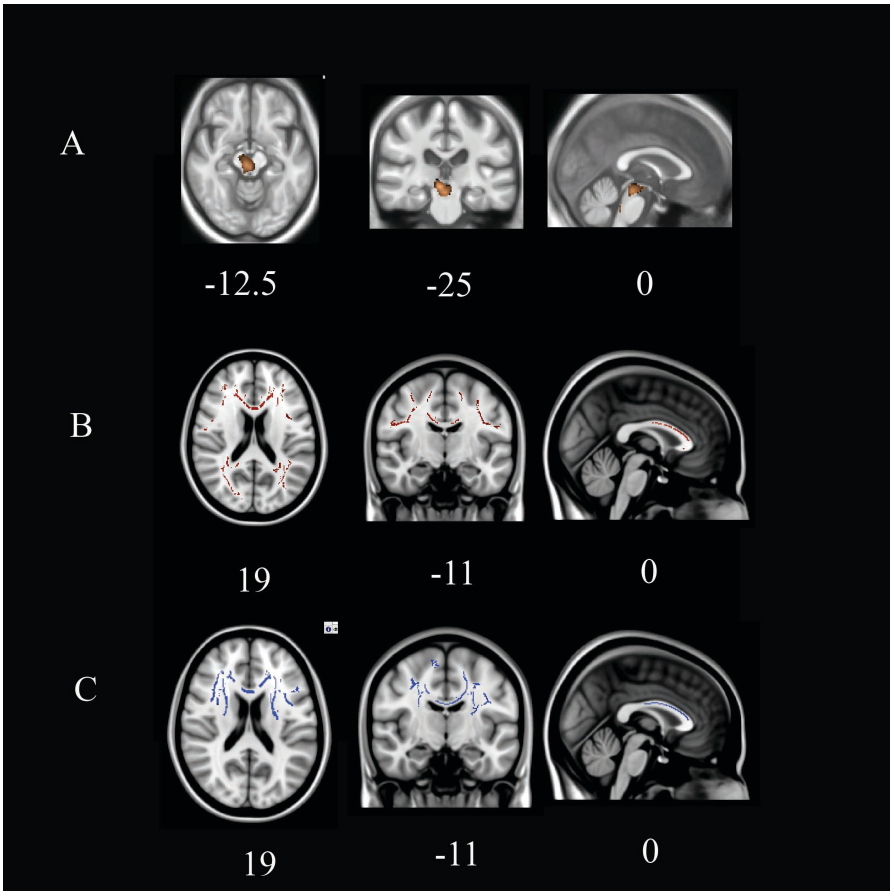

Figure 9.3: Correlation of quantitative MRI with clinimetric scores and disease duration. A: WM loss correlating with PSPRS in PSP (uncorrected p value <0.001 with cluster-level nonstationary correction p value < 0.05); B: significant reduction in FA in PSP correlating with PSPRS score (red) (TFCE p < 0.05); C: significant increase in MD in PSP (blue) correlating with PSPRS score (TFCE p < 0.05).

		PSP							MSA							
		Cluster p (corr)	Voxels	T value	Z	x	y	z	anatomical region	Cluster p (corr)	Voxels	T value	Z	x	y	z	anatomical region
VBM	GM	0.004	4668	5.03	4.49	-11	10	14	left caudate and anterior putamen	0.021	3929	6.88	5.73	20	9	4	right anterior putamen and head of caudate
		0.016	3526	4.98	4.46	11	14	-5	right caudate and anterior putamen	0.052	2217	6.26	5.34	-20	7	4	left anterior putamen and caudate head
										0.041	3801	4.89	4.39	-22	-42	-28	left inferior cerebellar grey matter
										0.067	4853	4.29	3.93	11	-57	-57	right inferior cerebellar grey mater
	WM	0.000	31600	8.5	6.63	-5	-12	-6	including regions of the thalamus, subthalamus, substantia nigra, cerebral peduncles, midbrain and pontine tegmentum and tectum, superior cerebellar peduncles and dentate nuclei	0.000	34983	7.21	5.92	31	-5	2	right posterolateral putamen including the external capsule and poterior limb of the internal capsule, and running down through the midbrain, substantia nigra, pontine base, middle cerebellar peduncles and cerebellar white matter
										0.006	3235	7.16	5.89	-31	-8	1	left posterolateral putamen including the external capsule and posterior limb of the internal capsule
		Index	Voxels	Zmax	x	y	z	anatomical region		Index	Voxels	Zmax	x	y	z	anatomical region
TBSS	FA	4	61787	0.998	27	28	-9	frontal WM including forceps minor including orbitofrontal regions, cingulum, anterior limb of the internal capsule, anterior external capsule,superior longitudinal fasciculus, from the body to the splenium of the corpus callosum sparing the genu but involving the lateral forceps major		3	14989	0.964	13	-7	31	body of corpus callosum sparing the genu and splenium, anterior corona radiata, and posteriolateral forceps minor, superior longitudinal fasciculus in the posterior frontal / anterior parietal regions, frontal and medial orbital cortex
		3	3072	0.972	8	-47	-30	right superior cerebellar peduncle, cerebellar white matter near the dentate and the left superior cerebellar peduncle		2	4240	0.966	11	-42	-40	pontine white matter, MCP, cerebellar white matter
		2	188	0.954	-2	-28	-16	decussation of the superior cerebellar peduncle		1	1115	0.954	-19	-15	48	left frontal WM including posterior forceps minor, anterior limb of internal capsule, external capsule and corticospinal tract
		1	83	0.952	10	-30	-40	pontine white matter								
	MD	1	23437	0.994	27	27	11	frontal white matter including posterior forceps minor, anterior limb of internal capsule, external capsule		2	14338	0.946	-32	-8	7	external capsule, posterior limb of internal capsule, body of the corpus callosum, posterior frontal and anterior parietal white matter extending up to the central sulcus
										1	280	0.902	-18	-38	-37	left middle cerebellar peduncle

Table 9.2: Left: DARTEL-VBM and TBSS in PSP vs Controls. Right: DARTEL-VBM and TBSS in MSA vs Controls. Significant clusters identified using DARTEL-VBM. Uncorrected p values with non-stationary correction at the 0.05 level or a trend is present ($p < 0.1$). Coordinates refer to standard MNI space. Significant clusters identified using TFCE in TBSS at the 0.05 level. Extensive changes are seen in FA in PSP although MD abnormalities are more restricted. Extensive posterior frontal and anterior parietal reduction in FA is seen in MSA, including increased MD in the external capsule and posterior limb of the internal capsule (trend). Coordinates refer to standard MNI space.

E. Discussion

VBM and TBSS detect disease-specific topography of PSP and MSA pathology during life. TBSS showed involvement of frontal white matter tracts and more extensive involvement of WM in the parieto-occipital lobes (in PSP) in areas where VBM did not show any differences compared to controls. DTI is sensitive to microstructural damage which may become evident before atrophy is significant enough to be detected either by standard clinical radiological assessment or VBM. In PSP midbrain atrophy and increased MD in frontal WM tracts correlated with increased Golbe's PSPRS score, and reduced FA in frontal WM with disease duration.

1. PSP

a) VBM in PSP

In PSP, our VBM findings [Table 9.2; figure 9.1] confirm those of others. Atrophy of the mesencephalon is the most common finding including the subthalamic region and inferior basal ganglia (Brenneis, Seppi et al. 2004; Price, Paviour et al. 2004; Cordato, Duggins et al. 2005; Boxer, Geschwind et al. 2006; Josephs, Whitwell et al. 2008; Agosta, Kostic et al. 2010; Focke, Helms et al. 2011). Other regions such as the cerebral peduncles are frequently atrophic (Brenneis, Seppi et al. 2004; Price, Paviour et al. 2004; Josephs, Whitwell et al. 2008; Agosta, Kostic et al. 2010; Focke, Helms et al. 2011) and WM loss in the SCP (Price, Paviour et al. 2004; Agosta, Kostic et al. 2010), external capsule (Josephs, Whitwell et al. 2008), and MCP and decussation of the SCP (Agosta, Kostic et al. 2010) are less commonly seen. The GP, SN and STN are affected particularly in the basal ganglia / brainstem variants of the disease (Steele, Richardson et al. 1964; Hauw, Daniel et al. 1994; Litvan, Hauw et al. 1996; Williams, Holton et al. 2007; Ahmed, Josephs et al. 2008). Atrophy of the SCP is found at post mortem and during life on MRI (Tsuboi, Slowinski et al. 2003; Paviour, Price et al. 2005; Slowinski, Imamura et al. 2008). GM loss in the head of the caudate nucleus and the anterior putamen has also been reported (Brenneis, Seppi et al. 2004; Price, Paviour et al. 2004; Cordato, Duggins et al. 2005; Josephs, Whitwell et al. 2008; Agosta, Kostic et al. 2010; Josephs, Whitwell et al. 2011). We did not find cortical GM loss in concordance with an earlier VBM study in PSP (Price, Paviour et al. 2004), although other investigators have variably found cortical volume loss in specific regions, including the insular cortex (Brenneis, Seppi et al. 2004; Agosta, Kostic et al. 2010), orbitofrontal cortex (Cordato, Duggins et al. 2005; Agosta, Kostic et al. 2010), hippocampus (Agosta, Kostic et al. 2010) and

parahippocampal gyrus,(Padovani, Borroni et al. 2006) premotor cortex,(Padovani, Borroni et al. 2006; Josephs, Whitwell et al. 2008; Focke, Helms et al. 2011) frontal operculum (Brenneis, Seppi et al. 2004; Cordato, Duggins et al. 2005; Boxer, Geschwind et al. 2006; Padovani, Borroni et al. 2006) and supplementary motor area (Brenneis, Seppi et al. 2004; Josephs, Whitwell et al. 2008; Whitwell, Avula et al. 2011).

Post mortem studies indicate that cortical involvement in PSP is commonly milder than subcortical frontal atrophy (Dickson 1999; Dickson, Rademakers et al. 2007; Williams, Holton et al. 2007). However, biochemical mapping using Western blot analysis of pathological tau has demonstrated widespread deposition in neocortical areas with a frontal predilection (Vermersch, Robitaille et al. 1994). Precentral gyrus involvement may lead to a primary lateral sclerosis phenotype, frontal and parietal association cortex involvement to a corticobasal syndrome and frontal tau deposition to the behavioural variant of fronto-temporal dementia (Dickson, Ahmed et al. 2010). This variability may explain differences in neuroradiological findings in the literature. Our study was not designed to detect the regional variations in the subtypes of PSP although others report differences between Richardson's syndrome and PSP-P (Agosta, Kostic et al. 2010) and cognitive and extrapyramidal predominant pathologically confirmed PSP (Josephs, Whitwell et al. 2008).

b) TBSS in PSP

ROI-based diffusion tensor tractography studies have shown degeneration in the SCP and its central projections (Nilsson, Markenroth Bloch et al. 2007) and reduced FA in the anterior corpus callosum, left arcuate fasciculus, posterior thalamic radiations, superior longitudinal fasciculus and internal capsule (Padovani, Borroni et al. 2006). The extensive involvement of frontal white matter tracts could provide an explanation for the 'subcortical' frontal-dysexecutive syndrome in PSP. A white matter process is supported by the fact that the tau protein is involved in axonal transport and abundant tau is found in WM using Western blot (Zhukareva, Joyce et al. 2006). An alternative explanation for WM loss is secondary Wallerian degeneration from areas of cortical or striatal atrophy. Either way, effects on WM may be detected only by measures of white matter integrity such as FA and MD.

Previous reports using TBSS in PSP show less frontal WM involvement but confirm involvement of posterior frontal white matter, anteriorcorpus callosum and the SCPs and connections (Whitwell, Avula et al. 2011), changes in FA, and also RD and AD in the corpus

callosum, olfactory cortex and SCP and connections but not the frontal subcortical WM (Knake, Belke et al. 2010), and extensive white matter disease consistent with our findings (Agosta, Pievani et al. 2012; Saini, Bagepally et al. 2012). Changes in FA were more widespread than changes of MD in our study and in contrast to others (Knake, Belke et al. 2010; Agosta, Pievani et al. 2012; Saini, Bagepally et al. 2012) we did not find statistically significant differences in radial (RD) or axial (AD) diffusivities in any of the affected anatomical locations. This is interesting in the context of the findings of a TBSS study in Alzheimer's disease, which found increased axial and radial diffusivities to be more sensitive than FA reductions (Acosta-Cabronero, Williams et al. 2010).

c) Potential Biomarker in PSP

Correlation of midbrain WM volume loss and increased MD in frontal WM with the PSPRS and frontal WM FA with disease duration support the potential role of these in the development of biomarkers.

2.MSA

a) VBM in MSA

VBM findings in MSA were centred on the striatum and pontocerebellar connections, as expected [Table 9.2; Figure 9.2] (Schott, Simon et al. 2003; Ozawa, Paviour et al. 2004; Hauser, Luft et al. 2006). In MSA WM loss has been reported in WM deep to the insula (Brenneis, Seppi et al. 2003), the corpus callosum (Brenneis, Seppi et al. 2003; Minnerop, Luders et al. 2010), the corticospinal tract (Minnerop, Luders et al. 2010) and the brainstem including the pons, MCP and cerebellar WM (Minnerop, Specht et al. 2007; Minnerop, Luders et al. 2010). We found bilateral patchy cerebellar GM atrophy and bilateral head of caudate and putaminal atrophy. Our cohort is a mixed cohort with 8/10 MSA-P which may explain the relative mildness of GM atrophy in the cerebellum. This region is more severely affected in MSA with a predominantly cerebellar phenotype (Ozawa, Paviour et al. 2004), although cerebellar GM loss is found in both MSA-P and MSA-C (Specht, Minnerop et al. 2003; Minnerop, Specht et al. 2007; Minnerop, Luders et al. 2010)(Chang, Chang et al. 2009), as is atrophy of the head of the caudate (Brenneis, Seppi et al. 2003; Specht, Minnerop et al. 2003; Hauser, Luft et al. 2006; Chang, Chang et al. 2009). Although putaminal atrophy is seen at post mortem examination of the brain (Ozawa, Paviour et al. 2004; Jellinger, Seppi

et al. 2005), it is not an invariable finding in vivo and has been reported in some MSA-P VBM studies only (Brenneis, Seppi et al. 2003; Minnerop, Specht et al. 2007).

b) TBSS in MSA

We are not aware of any published studies of voxelwise analysis of DTI data in MSA. ROI-based MR diffusion studies of the MCPs and Pons reveal selective reduction in FA and increased MD in the MCP in MSA.(Nilsson, Markenroth Bloch et al. 2007) (Paviour, Thornton et al. 2007) DTI studies of the pons showed a decreased FA in the transverse pontine fibers as the cross sign on conventional MR developed, preceding the FA reduction in the longitudinal pontine fibers.(Makino, Ito et al. 2011)

Our TBSS data confirm the involvement of the MCP and pontine and cerebellar WM tracts in MSA and add important information including involvement of the corpus callosum and posterior frontal (motor and premotor) deep WM tracts. This fits with emerging pathological and clinical evidence that MSA patients have cognitive deficits particularly in executive function and visuospatial skills (Kawai, Suenaga et al. 2008; Kao, Racine et al. 2009), and that these are more pronounced in MSA-P. Pathological studies indicate involvement with pathognomonic glial cytoplasmic inclusions found in the supplementary motor area, primary motor cortex,(Jellinger, Seppi et al. 2005) cingulate motor area and premotor cortex (Papp and Lantos 1994; Su, Yoshida et al. 2001).

3. Comparison of PSP and MSA groups

Direct comparison of the PSP and MSA group did not reveal any statistically significant differences with either VBM or TBSS . This may seem at first surprising given the specific regional differences between these two conditions and the control group, as described above. However, the lack of significant differences in the direct comparison is likely to be due to the fact that there will be greater differences between controls and disease (either PSP or MSA) than between PSP and MSA; these diseases show widespread pathology and so can be expected to show differences in measurements sensitive to pathological change from controls in many brain regions but not necessarily differences between PSP and MSA. We also used relatively small group sizes.

4. Advantages and limitations of the study

Advantages of vowel-wise techniques are that they are operator-independent, enable whole-brain exploration and do not require regions of interest to be placed *a priori*. We have used high field MRI at 3T with associated increase in signal-to-noise ratio, and the DARTEL addition to SPM8 to improve grey matter segmentation although this is still limited particularly in posterior regions. Our statistical analysis was devised to give few false positives, and thus homogenized our clusters into large regions which may have impacted on our correlative analysis. Others have taken another perspective (Josephs, Whitwell et al. 2008; Agosta, Kostic et al. 2010) making them more sensitive to the detection of subgroup differences. Although we do not have pathological confirmation of the clinical diagnosis, our cohort comes from a centre experienced in assessing parkinsonian disorders.

F. Conclusion

VBM and TBSS give complementary information about pathological processes in PSP and MSA during life. Systematic study of quantitative techniques sensitive to microstructural findings before atrophy has occurred is important not only for making an early diagnosis, but also in the context of our evolving understanding of clinical and pathological heterogeneity. Future studies should look at radiological signatures of these diseases using multimodal MRI. The role of these parameters as potential biomarkers for disease progression needs to be assessed in future longitudinal studies, ideally with pathological confirmation of the diagnosis.

Chapter 10: Summary of the thesis and Suggestions for future work

A. Summary of the thesis

1. Clinical studies

In a retrospective study of the natural history of PSP and MSA in a pathologically confirmed cohort the key findings were:

1. Patients with PSP had an older age of onset but similar disease duration to those with MSA.
2. Patients with PSP reached their first clinical milestone earlier than patients with MSA.
3. Regular falls, unintelligible speech and cognitive impairment also occurred earlier in PSP than in MSA.
4. In PSP an RS phenotype, male gender, older age of onset and a short interval from disease onset to reaching the first clinical milestone were all independent predictors of shorter disease duration to death.
5. Patients with RS also reached clinical milestones after a shorter interval from disease onset, compared to patients with PSP-P.
6. In MSA early autonomic failure, female gender, older age of onset, a short interval from disease onset to reaching the first clinical milestone and not being admitted to residential care were independent factors predicting shorter disease duration until death.
7. The time to the first clinical milestone is a useful prognostic predictor for survival. We confirm that RS had a less favourable course than PSP-P, and that early autonomic failure in MSA is associated with shorter survival.

In an objective study of bradykinesia and handwriting in PSP and PD using 3D movement analysis the main findings were:

1. Hypokinesia without decrement in patients with PSP, which differed from the finger tap pattern in PD.
2. We confirmed the sequence effect in PD (progressive bradykinesia and hypokinesia - 'true bradykinesia') which was not seen in PSP.

3. 'Hypokinesia' with 'absence of decrement' were identified in 87% of finger tap trials in the PSP group and only 12% in the PD OFF levodopa group.
4. In PSP, the mean amplitude was not correlated with disease duration or other clinimetric scores.
5. In PD smaller amplitude, slower speed and greater speed variability were all associated with a more severe UPDRS motor score.
6. Micrographia was present in 75% of patients with PSP and 15% of patients with PD.

Patients with PSP have a specific finger tap pattern of 'hypokinesia without decrement' and they do not have 'true' bradykinesia. Similarly, 'micrographia' and 'lack of decrement in script size' are also more common in PSP than in PD.

2. Conventional MRI in pathologically confirmed disease

In a study of 48 conventional MRI in neuropathologically confirmed cases assessed blinded to clinical details and systematically rated for reported abnormalities the key findings were:

1. Radiological assessment of MRI was correct in 16 /22 (72.7%) PSP cases and 10/13 (76.9%) MSA cases with substantial inter-rater agreement; no PSP case was misclassified as MSA or vice versa.
2. MRI was less sensitive but more specific than clinical diagnosis in PSP and both more sensitive and specific than clinical diagnosis in MSA.
3. The 'hummingbird' and 'morning glory' signs were highly specific for PSP, and 'the middle cerebellar peduncle sign' and 'hot cross bun' for MSA but sensitivity was lower (up to 68.4%) and characteristic findings may not be present even at autopsy.
4. No specific abnormalities in PD or CBD

Conventional MRI, clinical diagnosis and macroscopic examination at post mortem have similar sensitivity and specificity in predicting a neuropathological diagnosis. This study has validated specific radiological signs in pathologically confirmed PSP and MSA. However, the low sensitivity of these and macroscopic findings at autopsy suggest a need for imaging techniques sensitive to microstructural abnormalities without regional atrophy.

Simple linear measurements of the midbrain and pons and the midbrain to pons ratio on midsagittal MR images support the diagnosis of PSP in the clinic. This method was devised

in pathologically confirmed disease and corroborated in a clinically diagnosed cohort. The key findings were:

1. The mean midbrain measurement of 8.1mm was reduced in PSP ($p<0.001$) with reduction in the midbrain to pons ratio (PSP smaller than MSA; $p<0.001$).
2. In controls the mean midbrain to pons ratio was approximately 2/3 of the pontine base, in PSP it was less than 52% and in MSA the ratio was greater than 2/3.
3. A midbrain measurement of less than 9.35mm and ratio of 0.52 had 100% specificity for PSP. In the clinically defined group 19/21(90.5%) PSP cases had a midbrain measurement of less than 9.35 mm.

This is a simple and reliable measurement in pathologically confirmed disease based on the topography of atrophy in PSP with high sensitivity and specificity which may be a useful tool in the clinic.

3. The Anatomy of the STN and SN using high field MRI

These two small nuclei in the midbrain are key structures in Parkinsonian conditions. Review of the literature reveals that the STN has been difficult to identify accurately using conventional MRI and the SN is also not well defined. By using high field MRI of post mortem tissue with subsequently histologic and immunohistochemical study of the same tissue it was possible to define the anatomy of these structures more clearly.

Key findings in the STN include:

1. The anatomy of the STN and surrounding structures was demonstrated in all three anatomical planes using 9.4T MR images in concordance with LFB/CV stained histological sections.
2. Signal hypointensity was seen in 6/8 cases in the anterior and medial STN that corresponded with regions of more intense Perl staining.
3. There was significant variability in the volume, shape and location of the borders of the STN.

Using 9.4T MRI, the internal signal characteristics and borders of the STN are clearly defined and significant anatomical variability is apparent. Direct visualisation of the STN is

possible using high field MRI and this is particularly relevant, given its anatomical variability, for planning deep brain stimulation.

In the SN the key findings were:

1. The anterior border of the SN was defined by the crus cerebri. In the medial half it was less distinct due to the deposition of iron and the interdigitation of white matter and the SN. The posterior border was flanked by white matter bridging the red nucleus and SN and seen as hypointense on SE MRI.
2. Within the SN high signal structures corresponded to calbindin-confirmed nigrosomes.
3. Nigrosomes were still evident in PD but not in PSP.
4. The volume and dimensions of the SN were similar in PD and controls, but reduced in PSP

This enabled a histologically validated anatomical description of the SN on high field SE MRI at high resolution. The architecure of the pars compacta and the signal characteristics on MRI are influenced by iron deposition and white matter tracts running through the region. In accordance with the pathological literature we did not observe SN atrophy in PD and the nigrosome structure was maintained but in PSP there was microarchitectural destruction.

4. Multimodal high field MRI in PSP and related conditions

In a clincial study of PSP and MSA using multimodal 3.0T MRI and voxelwise analysis with VBM and TBSS the most important findings were:

1. In PSP atrophy of the striatum, dorsal thalamus, globus pallidus, subthalamus, midbrain tegmentum, the superior cerebellar peduncle (SCP) and its decussation, dentate nuclei and cerebellar white matter (WM) was seen.
2. In MSA the head of caudate, anterior and posterior putamen and the posterior limb of the internal capsule and external capsule, pontine base, middle cerebellar peduncle (MCP) and cerebellar WM were affected.
3. TBSS revealed reduced fractional anisotropy in the SCP and decussation of the SCP in PSP and the MCP and connections in MSA.
4. Extensive frontal and parieto-occipital WM changes in fractional anisotropy and mean diffusivity were found in PSP, which were more restricted in MSA.

5. Midbrain atrophy and frontal WM increased mean diffusivity (MD) were associated with increasing PSP rating scale score, and frontal WM reduced fractional anisotropy with disease duration.

Marked subcortical WM changes, particularly in PSP, were not evident on VBM indicating that more subtle findings may be detectable during life using TBSS analysis. Frontal WM tract disruption in PSP correlates with disease severity and duration and has potential as a biomarker.

B. Suggestions for future work

1. Clinical studies

There are significant differences in the clincial features and natural history of PSP-RS and PSP-P and the underlying pathology is of different severity. The natural history of other presentations (PSP-PAGF, PSP-PNFA etc) is not well described. Retrospective study of case notes has intrinsic limitations given the heterogeneity of physicians assessing patients under different clinical scenarios. Ideally a prospective study of PSP should be undertaken with subsequent pathological confirmation. This would require the entry criteria to the study to be very loose in order to increase the sensitivity and to identify early and atypical cases.

Now that it is clear in PSP-RS that true finger taps are manifestations of hypokinesia without decrement rather than true bradykinesia it would be interesting to assess whether PSP-P cases have true bradykinesia. This would again require prospective study with pathological confirmation of the diagnosis. Furthermore, the diagnostic utility of this finding could be assessed with a blinded video analysis of finger taps by a panel of movement disorders experts to confirm the clinical validity and reproducibility of the clinical finding. Given this finding other conditions including MSA, CBD and even pyramidal disorders may provide complementary findings given that one would expect pyramidal slowing but not necessarily hypokinesia - i.e. bradykinesia without decrement or hypokinesia.

2. Conventional MRI

Most studies of conventional imaging are in clinically diagnosed cases. While clinical research criteria predict the pathological diagnosis with high positive predictive values, there are still many misidentified and atypical cases that are excluded. It is this group in which imaging findings would have the greatest clinical utility. In seeking to address the question of how good conventional MRI is at predicting the pathological diagnosis in confirmed disease this work describes specific but subjective abnormalities. The second study in this section supports the use of simple linear measurements to increase the sensitivity of conventional MRI. However, it is still not clear at what stage these findings become apparent, although one anticipates that atrophy would take some time to develop. Studies of MRI techniques which may be present before atrophy is evident hold promise (for example, diffusion-weighted imaging in the putamen in MSA (Seppi, Schocke et al. 2006; Seppi, Schocke et al. 2006) but there are unresolved issues with quantitative MRI techniques including the use of different MRI techniques at different centres (standardisation).

3. Studying anatomy of high field MRI

High field MRI is becoming more readily available and the anatomy of smaller nuclei is starting to be more accurately defined as the resolution of imaging during life is improving. The accuracy of anatomical description is very important. In the STN there are no region of interest studies of clinical utility due to anatomical/resolution constraints. The ability to study this nucleus in disease would be very useful as it is a key nucleus pathologically in PSP and it is also very important in PD, where pathophysiological changes make it a key nucleus for targeting at DBS. High field MRI using post mortem tissue enables not only the identification of not only the STN but also many small surrounding structures. The challenge will be to reproduce this during life. Shorter acquisition times will be needed and these may be achieved using fast spin echo and other promisin techniques (MTR, SWI etc.).

The exact correlate of signal changes on MRI will need to be determined (gliosis, neuronal loss, protein deposition) if true markers of pathological progression in the STN and SN are to be determined during life. Studies correlating the pathological changes with quantitative MRI indices will help to clarify the correlation beyween these and whether more robust surrogates of pathology can be developed during life.

4. Multimodal MRI using volumetric techniques

Increasing use of high field 3T scanners and multiple MRI modalities may give complementary information during life not only about atrophy but also microstuctural integrity. Region of interest studies are labour-intensive and require a priori assumptions about the brain regions to be assessed. Volumetric techniques have advantages, but so far have been used to study disease groups rather than being useful for predicting disease in an individual case. Other techniques including automatic segmentation techniques may be useful in this regard, but use of such methods will require the development of individual disease signatures and a recognition of the heterogeneity of these within a pathologically defined disease and potential overlap with other diseases. Again, standardisation of techniques across sites will be important for reproducibiliy of results and in order to be of clinical utility a standard postprocessing protocol will be needed: many studies use different thresholds and smoothing, for example. Many of these ideas could be addressed with a single large prospective study of these techniques in carefully selected cases presenting to a movement disorders clinic. The protocol would involve standardised detailed clinical assessments, serial imaging with the same protocol and ultimately pathological confirmation of the diagnosis.

Acknowledgements

This work would not have been possible without the help of so many colleagues. In the first instance, thanks are due to Professor Andrew Lees, for allowing me to join the hallowed members of the Queen Square Brain Bank. Working for Professor Lees both in the clinic and in research has formed the basis for my clinical career in neurology and I can think of no better role model. Sean O'Sullivan, Laura Moriyama, Helen Ling, Atbin Djamshidian and Karen Doherty were constant companions and sources of encouragement and inspiration. Dominic Paviour introduced me to the royal toast and was instrumental in devising the ratio which formed part of chapter 5. Many others at QSBB were instrumental at key stages of these projects and I am particularly grateful to Susan Stoneham, Linda Parsons and Karen Shaw.

Much of this work was dependent on the neuropathological expertise of Professor Tamas Revesz and Dr Janice Holton, without whose patience and dedication the pathologically confirmed study and the high field post mortem study would not have been possible. Kate Strand was instumental in cutting thousands of slides and staining a significant proportion of them - a task for which I shall be eternally grateful to her. Many physicists have been crucial to different aspects of the studies described here including Harry Parkes, Po-Wah So, Mark White, Enrico de Vita, Laura Mancini, Chris Sinclair, John Thornton and Professor Xavier Golay. I am indebted to Caroline Micallef and Professor Nick Fox who spent many hours with me looking at MRI scans. Dr Mario Miranda and Dr Othman Al-Helli made the post mortem project possible by their enthusiasm and dedication, and also by helping coordinate our scanning slots and transporting specimens across London. Ludvic Zrinzo and Professor Marwan Hariz were instrumental in guiding me through the imaging and anatomy of the STN. Dr Rolf Jager has guided me in the clinical multimodal project and Professor Yousry has proved invaluable for his oversight and direction.

Of course none of this work would have been possible without the willing paricipation of the patients both donors to the QSBB and in the clinical studies whose enthusiasm for research was striking. This thesis has taken seven long years to put together during which a family of 6 has been formed. I am grateful for the tireless support, patience and encouragement of Laura, my long-suffering wife, particularly at the times when I started to doubt that it would come to completion. Finally, many thanks to my mother-in-law, Jane, for painstakingly proof-reading my draft thesis.

References

(1993). "Case records of the Massachusetts General Hospital. Weekly clinicopathological exercises. Case 46-1993. A 75-year-old man with right-sided rigidity, dysarthria, and abnormal gait." N Engl J Med **329**(21): 1560-1567.

Abosch, A., E. Yacoub, et al. (2010). "An assessment of current brain targets for deep brain stimulation surgery with susceptibility-weighted imaging at 7 tesla." Neurosurgery **67**(6): 1745-1756; discussion 1756.

Acosta-Cabronero, J., G. B. Williams, et al. (2010). "Absolute diffusivities define the landscape of white matter degeneration in Alzheimer's disease." Brain **133**(Pt 2): 529-539.

Adachi, M., T. Hosoya, et al. (1999). "Evaluation of the substantia nigra in patients with Parkinsonian syndrome accomplished using multishot diffusion-weighted MR imaging." AJNR Am J Neuroradiol **20**(8): 1500-1506.

Adachi, M., T. Kawanami, et al. (2004). "Morning glory sign: a particular MR finding in progressive supranuclear palsy." Magn Reson Med Sci **3**(3): 125-132.

Agosta, F., M. Pievani, et al. (2012). "Diffusion tensor MRI contributes to differentiate Richardson's syndrome from PSP-parkinsonism." Neurobiol Aging **33**(12): 2817-2826.

Agosta, F., V. S. Kostic, et al. (2010). "The in vivo distribution of brain tissue loss in Richardson's syndrome and PSP-parkinsonism: a VBM-DARTEL study." Eur J Neurosci **32**(4): 640-647.

Agostino, R., A. Berardelli, et al. (1994). "Analysis of repetitive and nonrepetitive sequential arm movements in patients with Parkinson's disease." Mov Disord **9**(3): 311-314.

Agostino, R., A. Berardelli, et al. (1998). "Clinical impairment of sequential finger movements in Parkinson's disease." Mov Disord **13**(3): 418-421.

Agostino, R., A. Curra, et al. (2003). "Impairment of individual finger movements in Parkinson's disease." Mov Disord **18**(5): 560-565.

Ahmed, Z., K. A. Josephs, et al. (2008). "Clinical and neuropathologic features of progressive supranuclear palsy with severe pallido-nigro-luysial degeneration and axonal dystrophy." Brain **131**(Pt 2): 460-472.

Aiba, I., Y. Hashizume, et al. (1997). "Relationship between brainstem MRI and pathological findings in progressive supranuclear palsy--study in autopsy cases." J Neurol Sci **152**(2): 210-217.

Aji, B. M., G. Medley, et al. (2013). "Perry syndrome: a disorder to consider in the differential diagnosis of Parkinsonism." J Neurol Sci **330**(1-2): 117-118.

Albert, M. L., R. G. Feldman, et al. (1974). "The 'subcortical dementia' of progressive supranuclear palsy." J Neurol Neurosurg Psychiatry **37**(2): 121-130.

Alonso-Canovas, A., P. Katschnig, et al. (2010). "Atypical parkinsonism with apraxia and supranuclear gaze abnormalities in type 1 Gaucher disease. Expanding the spectrum: case report and literature review." Mov Disord **25**(10): 1506-1509.

Altman, D. G. and J. M. Bland (1994). "Diagnostic tests 2: Predictive values." BMJ **309**(6947): 102.

Altman, D. G. and J. M. Bland (1994). "Diagnostic tests. 1: Sensitivity and specificity." BMJ **308**(6943): 1552.

Alvarez, L., R. Macias, et al. (2001). "Dorsal subthalamotomy for Parkinson's disease." Mov Disord **16**(1): 72-78.

Amarenco, P., E. Roullet, et al. (1991). "Progressive supranuclear palsy as the sole manifestation of systemic Whipple's disease treated with pefloxacine." J Neurol Neurosurg Psychiatry **54**(12): 1121-1122.

Andersson, J. L. R., M. Jenkinson, et al. (2007). "Non-linear optimisation." FMRIB Technical Report TR07JA1 **www.fmrib.ox.ac.uk/analysis/techrep**.

Andersson, J. L. R., M. Jenkinson, et al. (2007). "Non-linear registration, aka Spatial normalisation." FMRIB technical report TR07JA2 **www.fmrib.ox.ac.uk/analysis/techrep**.

Andrade-Souza, Y. M., J. M. Schwalb, et al. (2005). "Comparison of three methods of targeting the subthalamic nucleus for chronic stimulation in Parkinson's disease." Neurosurgery **56**(2 Suppl): 360-368; discussion 360-368.

Antonini, A., K. L. Leenders, et al. (1993). "T2 relaxation time in patients with Parkinson's disease." Neurology **43**(4): 697-700.

Aoki, S., Y. Okada, et al. (1989). "Normal deposition of brain iron in childhood and adolescence: MR imaging at 1.5 T." Radiology **172**(2): 381-385.

Arai, T., K. Ikeda, et al. (2001). "Distinct isoforms of tau aggregated in neurons and glial cells in brains of patients with Pick's disease, corticobasal degeneration and progressive supranuclear palsy." Acta Neuropathol **101**(2): 167-173.

Armstrong, M. J., I. Litvan, et al. (2013). "Criteria for the diagnosis of corticobasal degeneration." Neurology **80**(5): 496-503.

Asato, R., I. Akiguchi, et al. (2000). "Magnetic resonance imaging distinguishes progressive supranuclear palsy from multiple system atrophy." J Neural Transm **107**(12): 1427-1436.

Ashburner, J. (2007). "A fast diffeomorphic image registration algorithm." Neuroimage **38**(1): 95-113.

Ashburner, J. and K. J. Friston (2000). "Voxel-based morphometry--the methods." Neuroimage **11**(6 Pt 1): 805-821.

Ashburner, J. and K. J. Friston (2005). "Unified segmentation." Neuroimage **26**(3): 839-851.

Ashkan, K., P. Blomstedt, et al. (2007). "Variability of the subthalamic nucleus: the case for direct MRI guided targeting." Br J Neurosurg **21**(2): 197-200.

Aziz, T. Z., D. Peggs, et al. (1991). "Lesion of the subthalamic nucleus for the alleviation of 1-methyl-4-phenyl-1,2,3,6-tetrahydropyridine (MPTP)-induced parkinsonism in the primate." Mov Disord **6**(4): 288-292.

Bajaj, N. P., V. Gontu, et al. (2010). "Accuracy of clinical diagnosis in tremulous parkinsonian patients: a blinded video study." J Neurol Neurosurg Psychiatry **81**(11): 1223-1228.

Bardinet, E., M. Bhattacharjee, et al. (2009). "A three-dimensional histological atlas of the human basal ganglia. II. Atlas deformation strategy and evaluation in deep brain stimulation for Parkinson disease." J Neurosurg **110**(2): 208-219.

Bartzokis, G., J. L. Cummings, et al. (1999). "MRI evaluation of brain iron in earlier- and later-onset Parkinson's disease and normal subjects." Magn Reson Imaging **17**(2): 213-222.

Beck, A. T., C. H. Ward, et al. (1961). "An inventory for measuring depression." Arch Gen Psychiatry **4**: 561-571.

Bejjani, B. P., D. Dormont, et al. (2000). "Bilateral subthalamic stimulation for Parkinson's disease by using three-dimensional stereotactic magnetic resonance imaging and electrophysiological guidance." J Neurosurg **92**(4): 615-625.

Ben-Shlomo, Y., G. K. Wenning, et al. (1997). "Survival of patients with pathologically proven multiple system atrophy: a meta-analysis." Neurology **48**(2): 384-393.

Benabid, A. L., P. P. Krack, et al. (2000). "Deep brain stimulation of the subthalamic nucleus for Parkinson's disease: methodologic aspects and clinical criteria." Neurology **55**(12 Suppl 6): S40-44.

Benazzouz, A., C. Gross, et al. (1993). "Reversal of rigidity and improvement in motor performance by subthalamic high-frequency stimulation in MPTP-treated monkeys." Eur J Neurosci **5**(4): 382-389.

Berardelli, A., J. C. Rothwell, et al. (2001). "Pathophysiology of bradykinesia in Parkinson's disease." Brain **124**(Pt 11): 2131-2146.

Bergman, H., T. Wichmann, et al. (1990). "Reversal of experimental parkinsonism by lesions of the subthalamic nucleus." Science **249**(4975): 1436-1438.

Bergman, H., T. Wichmann, et al. (1994). "The primate subthalamic nucleus. II. Neuronal activity in the MPTP model of parkinsonism." J Neurophysiol **72**(2): 507-520.

Bhattacharya, K., D. Saadia, et al. (2002). "Brain magnetic resonance imaging in multiple-system atrophy and Parkinson disease: a diagnostic algorithm." Arch Neurol **59**(5): 835-842.

Boeve, B. F., A. E. Lang, et al. (2003). "Corticobasal degeneration and its relationship to progressive supranuclear palsy and frontotemporal dementia." Ann Neurol **54 Suppl 5**: S15-19.

Boeve, B., D. Dickson, et al. (2003). "Progressive nonfluent aphasia and subsequent aphasic dementia associated with atypical progressive supranuclear palsy pathology." Eur Neurol **49**(2): 72-78.

Borroni, B., C. Agosti, et al. (2011). "Genetic bases of Progressive Supranuclear Palsy: the MAPT tau disease." Curr Med Chem **18**(17): 2655-2660.

Bourekas, E. C., G. A. Christoforidis, et al. (1999). "High resolution MRI of the deep gray nuclei at 8 Tesla." J Comput Assist Tomogr **23**(6): 867-874.

Boxer, A. L., M. D. Geschwind, et al. (2006). "Patterns of brain atrophy that differentiate corticobasal degeneration syndrome from progressive supranuclear palsy." Arch Neurol **63**(1): 81-86.

Braak, H., K. Del Tredici, et al. (2003). "Staging of brain pathology related to sporadic Parkinson's disease." Neurobiol Aging **24**(2): 197-211.

Braffman, B. H., R. I. Grossman, et al. (1989). "MR imaging of Parkinson disease with spin-echo and gradient-echo sequences." AJR Am J Roentgenol **152**(1): 159-165.

Brenneis, C., K. Seppi, et al. (2003). "Voxel-based morphometry detects cortical atrophy in the Parkinson variant of multiple system atrophy." Mov Disord **18**(10): 1132-1138.

Brenneis, C., K. Seppi, et al. (2004). "Voxel based morphometry reveals a distinct pattern of frontal atrophy in progressive supranuclear palsy." J Neurol Neurosurg Psychiatry **75**(2): 246-249.

Brunberg, J. A., S. Jacquemont, et al. (2002). "Fragile X premutation carriers: characteristic MR imaging findings of adult male patients with progressive cerebellar and cognitive dysfunction." AJNR Am J Neuroradiol **23**(10): 1757-1766.

Bryant, M. S., D. H. Rintala, et al. (2010). "An investigation of two interventions for micrographia in individuals with Parkinson's disease." Clin Rehabil **24**(11): 1021-1026.

Burk, K., M. Skalej, et al. (2001). "Pontine MRI hyperintensities ("the cross sign") are not pathognomonic for multiple system atrophy (MSA)." Mov Disord **16**(3): 535.

Burn, D. J. and A. J. Lees (2002). "Progressive supranuclear palsy: where are we now?" Lancet Neurol **1**(6): 359-369.

Cabello, C. R., J. J. Thune, et al. (2002). "Ageing of substantia nigra in humans: cell loss may be compensated by hypertrophy." Neuropathol Appl Neurobiol **28**(4): 283-291.

Carpenter, M. and J. Sutin (1983). "Human Neuroanatomy 8th Edition

Castellani, R. J., S. L. Siedlak, et al. (2000). "Sequestration of iron by Lewy bodies in Parkinson's disease." Acta Neuropathol (Berl) **100**(2): 111-114.

Chan, L. L., H. Rumpel, et al. (2007). "Case control study of diffusion tensor imaging in Parkinson's disease." J Neurol Neurosurg Psychiatry **78**(12): 1383-1386.

Chang, C. C., Y. Y. Chang, et al. (2009). "Cognitive deficits in multiple system atrophy correlate with frontal atrophy and disease duration." Eur J Neurol **16**(10): 1144-1150.

Chaudhuri, K. R., D. G. Healy, et al. (2006). "Non-motor symptoms of Parkinson's disease: diagnosis and management." Lancet Neurol **5**(3): 235-245.

Chen, C. C., A. Pogosyan, et al. (2006). "Intra-operative recordings of local field potentials can help localize the subthalamic nucleus in Parkinson's disease surgery." Exp Neurol **198**(1): 214-221.

Cho, Z. H., H. K. Min, et al. (2008). "Direct visualization of deep brain stimulation targets in Parkinson disease with the use of 7-tesla magnetic resonance imaging." J Neurosurg **113**(3): 639-647.

Cho, Z. H., S. H. Oh, et al. (2011). "Direct visualization of Parkinson's disease by in vivo human brain imaging using 7.0T magnetic resonance imaging." Mov Disord **26**(4): 713-718.

Clark, A. W., H. J. Manz, et al. (1986). "Cortical degeneration with swollen chromatolytic neurons: its relationship to Pick's disease." J Neuropathol Exp Neurol **45**(3): 268-284.

Coenen, V. A., A. Prescher, et al. (2008). "What is dorso-lateral in the subthalamic Nucleus (STN)?--a topographic and anatomical consideration on the ambiguous description of today's primary target for deep brain stimulation (DBS) surgery." Acta Neurochir (Wien) **150**(11): 1163-1165; discussion 1165.

Cordato, N. J., A. J. Duggins, et al. (2005). "Clinical deficits correlate with regional cerebral atrophy in progressive supranuclear palsy." Brain **128**(Pt 6): 1259-1266.

Counelis, G. J., T. Simuni, et al. (2003). "Bilateral subthalamic nucleus deep brain stimulation for advanced PD: correlation of intraoperative MER and postoperative MRI with neuropathological findings." Mov Disord **18**(9): 1062-1065.

Damier, P., E. C. Hirsch, et al. (1999). "The substantia nigra of the human brain. I. Nigrosomes and the nigral matrix, a compartmental organization based on calbindin D(28K) immunohistochemistry." Brain **122 (Pt 8)**: 1421-1436.

Damier, P., E. C. Hirsch, et al. (1999). "The substantia nigra of the human brain. II. Patterns of loss of dopamine-containing neurons in Parkinson's disease." Brain **122 (Pt 8)**: 1437-1448.

Davie, C. A., G. J. Barker, et al. (1997). "Proton magnetic resonance spectroscopy in Steele-Richardson-Olszewski syndrome." Mov Disord **12**(5): 767-771.

Davies, K. G. and S. Daniluk (2008). "Stereotactic targeting of the subthalamic nucleus: relevance of magnetic resonance-based evaluation of interindividual variation in diencephalic anatomy." Stereotact Funct Neurosurg **86**(5): 330-331.

Davis, P. H., L. I. Golbe, et al. (1988). "Risk factors for progressive supranuclear palsy." Neurology **38**(10): 1546-1552.

Demirci, M., S. Grill, et al. (1997). "A mismatch between kinesthetic and visual perception in Parkinson's disease." Ann Neurol **41**(6): 781-788.

den Dunnen, W. F. and M. J. Staal (2005). "Anatomical alterations of the subthalamic nucleus in relation to age: a post mortem study." Mov Disord **20**(7): 893-898.

Derkinderen, P., S. Dupont, et al. (2002). "Micrographia secondary to lenticular lesions." Mov Disord **17**(4): 835-837.

Dexter, D. T., A. Carayon, et al. (1991). "Alterations in the levels of iron, ferritin and other trace metals in Parkinson's disease and other neurodegenerative diseases affecting the basal ganglia." Brain **114 (Pt 4)**: 1953-1975.

Dexter, D. T., F. R. Wells, et al. (1989). "Increased nigral iron content and alterations in other metal ions occurring in brain in Parkinson's disease." J Neurochem **52**(6): 1830-1836.

Dexter, D. T., P. Jenner, et al. (1992). "Alterations in levels of iron, ferritin, and other trace metals in neurodegenerative diseases affecting the basal ganglia. The Royal Kings and Queens Parkinson's Disease Research Group." Ann Neurol **32 Suppl**: S94-100.

Dickson, D. W. (1999). "Neuropathologic differentiation of progressive supranuclear palsy and corticobasal degeneration." J Neurol **246 Suppl 2**: II6-15.

Dickson, D. W., C. Bergeron, et al. (2002). "Office of Rare Diseases neuropathologic criteria for corticobasal degeneration." J Neuropathol Exp Neurol **61**(11): 935-946.

Dickson, D. W., R. Rademakers, et al. (2007). "Progressive supranuclear palsy: pathology and genetics." Brain Pathol **17**(1): 74-82.

Dickson, D. W., Z. Ahmed, et al. (2010). "Neuropathology of variants of progressive supranuclear palsy." Curr Opin Neurol **23**(4): 394-400.

Dormont, D., K. G. Ricciardi, et al. (2004). "Is the subthalamic nucleus hypointense on T2-weighted images? A correlation study using MR imaging and stereotactic atlas data." AJNR Am J Neuroradiol **25**(9): 1516-1523.

Drayer, B. P. (1988). "Imaging of the aging brain. Part I. Normal findings." Radiology **166**(3): 785-796.

Drayer, B. P. (1988). "Imaging of the aging brain. Part II. Pathologic conditions." Radiology **166**(3): 797-806.

Drayer, B. P., W. Olanow, et al. (1986). "Parkinson plus syndrome: diagnosis using high field MR imaging of brain iron." Radiology **159**(2): 493-498.

Drayer, B., P. Burger, et al. (1986). "MRI of brain iron." AJR Am J Roentgenol **147**(1): 103-110.

DSM-IV (1995). "Diagnostic and statistical manual of mental disorders." Washington: American Psychiatric Association.

Dubois, B., A. Slachevsky, et al. (2000). "The FAB: a Frontal Assessment Battery at bedside." Neurology **55**(11): 1621-1626.

Duguid, J. R., R. De La Paz, et al. (1986). "Magnetic resonance imaging of the midbrain in Parkinson's disease." Ann Neurol **20**(6): 744-747.

Eapen, M., D. H. Zald, et al. (2011). "Using high-resolution MR imaging at 7T to evaluate the anatomy of the midbrain dopaminergic system." AJNR Am J Neuroradiol **32**(4): 688-694.

Eckert, T., M. Sailer, et al. (2004). "Differentiation of idiopathic Parkinson's disease, multiple system atrophy, progressive supranuclear palsy, and healthy controls using magnetization transfer imaging." Neuroimage **21**(1): 229-235.

Elolf, E., V. Bockermann, et al. (2007). "Improved visibility of the subthalamic nucleus on high-resolution stereotactic MR imaging by added susceptibility (T2*) contrast using multiple gradient echoes." AJNR Am J Neuroradiol **28**(6): 1093-1094.

Enochs, W. S., W. B. Hyslop, et al. (1989). "Sources of the increased longitudinal relaxation rates observed in melanotic melanoma. An in vitro study of synthetic melanins." Invest Radiol **24**(10): 794-804.

Fahn, S., R. Elton, et al. (1987). "Recent Developments in Parkinson's Disease." Florham Park, NJ; Macmillan Health Care Information **2**.

Fearnley, J. M. and A. J. Lees (1990). "Striatonigral degeneration. A clinicopathological study." Brain **113 (Pt 6)**: 1823-1842.

Fearnley, J. M. and A. J. Lees (1991). "Ageing and Parkinson's disease: substantia nigra regional selectivity." Brain **114 (Pt 5)**: 2283-2301.

Fearnley, J. M., T. Revesz, et al. (1991). "Diffuse Lewy body disease presenting with a supranuclear gaze palsy." J Neurol Neurosurg Psychiatry **54**(2): 159-161.

Flannigan, B. D., W. G. Bradley, Jr., et al. (1985). "Magnetic resonance imaging of the brainstem: normal structure and basic functional anatomy." Radiology **154**(2): 375-383.

Focke, N. K., G. Helms, et al. (2011). "Individual voxel-based subtype prediction can differentiate progressive supranuclear palsy from idiopathic parkinson syndrome and healthy controls." Hum Brain Mapp.

Folstein, M. F., S. E. Folstein, et al. (1975). ""Mini-mental state". A practical method for grading the cognitive state of patients for the clinician." J Psychiatr Res **12**(3): 189-198.

Foltynie, T., L. Zrinzo, et al. (2011). "MRI-guided STN DBS in Parkinson's disease without microelectrode recording: efficacy and safety." J Neurol Neurosurg Psychiatry **82**(4): 358-363.

Forno, L. S. (1996). "Neuropathology of Parkinson's disease." J Neuropathol Exp Neurol **55**(3): 259-272.

Francois, C., J. Nguyen-Legros, et al. (1981). "Topographical and cytological localization of iron in rat and monkey brains." Brain Res **215**(1-2): 317-322.

Geddes, J. F., A. J. Hughes, et al. (1993). "Pathological overlap in cases of parkinsonism associated with neurofibrillary tangles. A study of recent cases of postencephalitic parkinsonism and comparison with progressive supranuclear palsy and Guamanian parkinsonism-dementia complex." Brain **116 (Pt 1)**: 281-302.

German, D. C., K. Manaye, et al. (1989). "Midbrain dopaminergic cell loss in Parkinson's disease: computer visualization." Ann Neurol **26**(4): 507-514.

Gibb, W. R. (1992). "Melanin, tyrosine hydroxylase, calbindin and substance P in the human midbrain and substantia nigra in relation to nigrostriatal projections and differential neuronal susceptibility in Parkinson's disease." Brain Res **581**(2): 283-291.

Gibb, W. R. and A. J. Lees (1988). "The relevance of the Lewy body to the pathogenesis of idiopathic Parkinson's disease." J Neurol Neurosurg Psychiatry **51**(6): 745-752.

Gibb, W. R. and A. J. Lees (1991). "Anatomy, pigmentation, ventral and dorsal subpopulations of the substantia nigra, and differential cell death in Parkinson's disease." J Neurol Neurosurg Psychiatry **54**(5): 388-396.

Gibb, W. R., J. M. Fearnley, et al. (1990). "The anatomy and pigmentation of the human substantia nigra in relation to selective neuronal vulnerability." Adv Neurol **53**: 31-34.

Gibb, W. R., P. J. Luthert, et al. (1989). "Corticobasal degeneration." Brain **112 (Pt 5)**: 1171-1192.

Gilman, S., P. A. Low, et al. (1999). "Consensus statement on the diagnosis of multiple system atrophy." J Neurol Sci **163**(1): 94-98.

Gilman, S., R. Little, et al. (2000). "Evolution of sporadic olivopontocerebellar atrophy into multiple system atrophy." Neurology **55**(4): 527-532.

Godeiro-Junior, C., R. J. Inaoka, et al. (2006). "Mutations in NPC1 in two Brazilian patients with Niemann-Pick disease type C and progressive supranuclear palsy-like presentation." Mov Disord **21**(12): 2270-2272.

Goetz, C. G., B. C. Tilley, et al. (2008). "Movement Disorder Society-sponsored revision of the Unified Parkinson's Disease Rating Scale (MDS-UPDRS): scale presentation and clinimetric testing results." Mov Disord **23**(15): 2129-2170.

Golbe, L. I. and P. A. Ohman-Strickland (2007). "A clinical rating scale for progressive supranuclear palsy." Brain **130**(Pt 6): 1552-1565.

Golbe, L. I., P. H. Davis, et al. (1988). "Prevalence and natural history of progressive supranuclear palsy." Neurology **38**(7): 1031-1034.

Gorell, J. M., R. J. Ordidge, et al. (1995). "Increased iron-related MRI contrast in the substantia nigra in Parkinson's disease." Neurology **45**(6): 1138-1143.

Graham, J. M., M. N. Paley, et al. (2000). "Brain iron deposition in Parkinson's disease imaged using the PRIME magnetic resonance sequence." Brain **123 Pt 12**: 2423-2431.

Griffiths, P. D., B. R. Dobson, et al. (1999). "Iron in the basal ganglia in Parkinson's disease. An in vitro study using extended X-ray absorption fine structure and cryo-electron microscopy." Brain **122 (Pt 4)**: 667-673.

Groschel, K., A. Kastrup, et al. (2006). "Penguins and hummingbirds: midbrain atrophy in progressive supranuclear palsy." Neurology **66**(6): 949-950.

Groschel, K., T. K. Hauser, et al. (2004). "Magnetic resonance imaging-based volumetry differentiates progressive supranuclear palsy from corticobasal degeneration." Neuroimage **21**(2): 714-724.

Gross, R. E., P. Krack, et al. (2006). "Electrophysiological mapping for the implantation of deep brain stimulators for Parkinson's disease and tremor." Mov Disord **21 Suppl 14**: S259-283.

Hallett, M. (2011). "Bradykinesia: why do Parkinson's patients have it and what trouble does it cause?" Mov Disord **26**(9): 1579-1581.

Halliday, G. M. (2004). "Chapter 14: Substantia Nigra and Locus Coeruleus " in Paxinos, G and Mai, JK The Human Nervous System 2nd Edition 2004

Hamani, C., E. O. Richter, et al. (2005). "Correspondence of microelectrode mapping with magnetic resonance imaging for subthalamic nucleus procedures." Surg Neurol **63**(3): 249-253; discussion 253.

Hamani, C., J. A. Saint-Cyr, et al. (2004). "The subthalamic nucleus in the context of movement disorders." Brain **127**(Pt 1): 4-20.

Hardman, C. D., G. M. Halliday, et al. (1997). "Progressive supranuclear palsy affects both the substantia nigra pars compacta and reticulata." Exp Neurol **144**(1): 183-192.

Hardman, C. D., G. M. Halliday, et al. (1997). "The subthalamic nucleus in Parkinson's disease and progressive supranuclear palsy." J Neuropathol Exp Neurol **56**(2): 132-142.

Hardman, C. D., J. M. Henderson, et al. (2002). "Comparison of the basal ganglia in rats, marmosets, macaques, baboons, and humans: volume and neuronal number for the output, internal relay, and striatal modulating nuclei." J Comp Neurol **445**(3): 238-255.

Hardy, J., H. Cai, et al. (2006). "Genetics of Parkinson's disease and parkinsonism." Ann Neurol **60**(4): 389-398.

Hariz, M. I., P. Krack, et al. (2003). "A quick and universal method for stereotactic visualization of the subthalamic nucleus before and after implantation of deep brain stimulation electrodes." Stereotact Funct Neurosurg **80**(1-4): 96-101.

Hariz, M., P. Blomstedt, et al. (2004). "The myth of microelectrode recording in ensuring a precise location of the DBS electrode within the sensorimotor part of the subthalamic nucleus." Mov Disord **19**(7): 863-864.

Hassler, R. (1937). "Zur Normalanatomie der Substantia Nigra. Versuch einer architektonishen Gliederung." J Psychol Neurol **48**: 1-55.

Haug, A., P. Boyer, et al. (2013). "Diffuse lewy body disease presenting as corticobasal syndrome and progressive supranuclear palsy syndrome." Mov Disord **28**(8): 1153-1155.

Hauser, T. K., A. Luft, et al. (2006). "Visualization and quantification of disease progression in multiple system atrophy." Mov Disord **21**(10): 1674-1681.

Hauw, J. J., S. E. Daniel, et al. (1994). "Preliminary NINDS neuropathologic criteria for Steele-Richardson-Olszewski syndrome (progressive supranuclear palsy)." Neurology **44**(11): 2015-2019.

Hayasaka, S., K. L. Phan, et al. (2004). "Nonstationary cluster-size inference with random field and permutation methods." Neuroimage **22**(2): 676-687.

Helms, G., B. Draganski, et al. (2009). "Improved segmentation of deep brain grey matter structures using magnetization transfer (MT) parameter maps." Neuroimage **47**(1): 194-198.

Hely, M. A., J. G. Morris, et al. (2005). "Sydney Multicenter Study of Parkinson's disease: non-L-dopa-responsive problems dominate at 15 years." Mov Disord **20**(2): 190-199.

Hely, M. A., W. G. Reid, et al. (2008). "The Sydney multicenter study of Parkinson's disease: the inevitability of dementia at 20 years." Mov Disord **23**(6): 837-844.

Hirsch, W. L., S. S. Kemp, et al. (1989). "Anatomy of the brainstem: correlation of in vitro MR images with histologic sections." AJNR Am J Neuroradiol **10**(5): 923-928.

Hoehn, M. M. and M. D. Yahr (1967). "Parkinsonism: onset, progression and mortality." Neurology **17**(5): 427-442.

Houlden, H., M. Baker, et al. (2001). "Corticobasal degeneration and progressive supranuclear palsy share a common tau haplotype." Neurology **56**(12): 1702-1706.

Hu, M. T., C. Scherfler, et al. (2006). "Nigral degeneration and striatal dopaminergic dysfunction in idiopathic and Parkin-linked Parkinson's disease." Mov Disord **21**(3): 299-305.

Hu, M. T., S. J. White, et al. (2001). "A comparison of (18)F-dopa PET and inversion recovery MRI in the diagnosis of Parkinson's disease." Neurology **56**(9): 1195-1200.

Hughes, A. J., S. E. Daniel, et al. (1992). "Accuracy of clinical diagnosis of idiopathic Parkinson's disease: a clinico-pathological study of 100 cases." J Neurol Neurosurg Psychiatry **55**(3): 181-184.

Hughes, A. J., S. E. Daniel, et al. (2001). "Improved accuracy of clinical diagnosis of Lewy body Parkinson's disease." Neurology **57**(8): 1497-1499.

Hutchinson, M. and U. Raff (1999). "Parkinson's disease: a novel MRI method for determining structural changes in the substantia nigra." J Neurol Neurosurg Psychiatry **67**(6): 815-818.

Hutchinson, M. and U. Raff (2000). "Structural changes of the substantia nigra in Parkinson's disease as revealed by MR imaging." AJNR Am J Neuroradiol **21**(4): 697-701.

Hutchinson, M. and U. Raff (2008). "Detection of Parkinson's disease by MRI: Spin-lattice distribution imaging." Mov Disord **23**(14): 1991-1997.

Hutchinson, M., U. Raff, et al. (2003). "MRI correlates of pathology in parkinsonism: segmented inversion recovery ratio imaging (SIRRIM)." Neuroimage **20**(3): 1899-1902.

Iansek, R., F. Huxham, et al. (2006). "The sequence effect and gait festination in Parkinson disease: contributors to freezing of gait?" Mov Disord **21**(9): 1419-1424.

Ince, P. G., B. Clarke, et al. (2008). "Disorders of movement and system degenerations." In: Love S, Louis DN, Ellison DW, eds. Greenfield's Neuropathology **Vol. 1, 8th ed.**: 889-1030.

Iwasaki, Y., K. Ikeda, et al. (1999). "Micrographia in Huntington's disease." J Neurol Sci **162**(1): 106-107.

Jang, W., J. S. Kim, et al. (2012). "Reversible progressive supranuclear palsy-like phenotype as an initial manifestation of HIV infection." Neurol Sci **33**(5): 1169-1171.

Jellinger, K. A., K. Seppi, et al. (2005). "Grading of neuropathology in multiple system atrophy: proposal for a novel scale." Mov Disord **20 Suppl 12**: S29-36.

Jellinger, K., E. Kienzl, et al. (1992). "Iron-melanin complex in substantia nigra of parkinsonian brains: an x-ray microanalysis." J Neurochem **59**(3): 1168-1171.

Joel, D. and I. Weiner (1997). "The connections of the primate subthalamic nucleus: indirect pathways and the open-interconnected scheme of basal ganglia-thalamocortical circuitry." Brain Res Brain Res Rev **23**(1-2): 62-78.

Josephs, K. A. and D. W. Dickson (2003). "Diagnostic accuracy of progressive supranuclear palsy in the Society for Progressive Supranuclear Palsy brain bank." Mov Disord **18**(9): 1018-1026.

Josephs, K. A., B. F. Boeve, et al. (2005). "Atypical progressive supranuclear palsy underlying progressive apraxia of speech and nonfluent aphasia." Neurocase **11**(4): 283-296.

Josephs, K. A., D. F. Tang-Wai, et al. (2004). "Correlation between antemortem magnetic resonance imaging findings and pathologically confirmed corticobasal degeneration." Arch Neurol **61**(12): 1881-1884.

Josephs, K. A., J. L. Whitwell, et al. (2008). "Voxel-based morphometry in autopsy proven PSP and CBD." Neurobiol Aging **29**(2): 280-289.

Josephs, K. A., J. L. Whitwell, et al. (2011). "Gray matter correlates of behavioral severity in progressive supranuclear palsy." Mov Disord **26**(3): 493-498.

Kanazawa, M., M. Tada, et al. (2013). "Early clinical features of patients with progressive supranuclear palsy with predominant cerebellar ataxia." Parkinsonism Relat Disord.

Kang, S. Y., T. Wasaka, et al. (2010). "Characteristics of the sequence effect in Parkinson's disease." Mov Disord **25**(13): 2148-2155.

Kao, A. W., C. A. Racine, et al. (2009). "Cognitive and neuropsychiatric profile of the synucleinopathies: Parkinson disease, dementia with Lewy bodies, and multiple system atrophy." Alzheimer Dis Assoc Disord **23**(4): 365-370.

Karachi, C., J. Yelnik, et al. (2005). "The pallidosubthalamic projection: an anatomical substrate for nonmotor functions of the subthalamic nucleus in primates." Mov Disord **20**(2): 172-180.

Kataoka, H., Y. Tonomura, et al. (2008). "Signal changes of superior cerebellar peduncle on fluid-attenuated inversion recovery in progressive supranuclear palsy." Parkinsonism Relat Disord **14**(1): 63-65.

Kato, N., K. Arai, et al. (2003). "Study of the rostral midbrain atrophy in progressive supranuclear palsy." J Neurol Sci **210**(1-2): 57-60.

Kawai, Y., M. Suenaga, et al. (2008). "Cognitive impairments in multiple system atrophy: MSA-C vs MSA-P." Neurology **70**(16 Pt 2): 1390-1396.

Kempster, P. A., D. R. Williams, et al. (2007). "Patterns of levodopa response in Parkinson's disease: a clinico-pathological study." Brain **130**(Pt 8): 2123-2128.

Kertesz, A., P. Martinez-Lage, et al. (2000). "The corticobasal degeneration syndrome overlaps progressive aphasia and frontotemporal dementia." Neurology **55**(9): 1368-1375.

Kim, E. J., B. H. Lee, et al. (2005). "Micrographia on free writing versus copying tasks in idiopathic Parkinson's disease." Parkinsonism Relat Disord **11**(1): 57-63.

Kitajima, M., Y. Korogi, et al. (2008). "Human subthalamic nucleus: evaluation with high-resolution MR imaging at 3.0 T." Neuroradiology **50**(8): 675-681.

Klockgether, T., R. Ludtke, et al. (1998). "The natural history of degenerative ataxia: a retrospective study in 466 patients." Brain **121 (Pt 4)**: 589-600.

Knake, S., M. Belke, et al. "In vivo demonstration of microstructural brain pathology in progressive supranuclear palsy: a DTI study using TBSS." Mov Disord **25**(9): 1232-1238.

Kollensperger, M., F. Geser, et al. (2008). "Red flags for multiple system atrophy." Mov Disord **23**(8): 1093-1099.

Kosta, P., M. I. Argyropoulou, et al. (2006). "MRI evaluation of the basal ganglia size and iron content in patients with Parkinson's disease." J Neurol **253**(1): 26-32.

Koyama, M., A. Yagishita, et al. (2007). "Imaging of corticobasal degeneration syndrome." Neuroradiology **49**(11): 905-912.

Kraft, E., J. Schwarz, et al. (1999). "The combination of hypointense and hyperintense signal changes on T2-weighted magnetic resonance imaging sequences: a specific marker of multiple system atrophy?" Arch Neurol **56**(2): 225-228.

Kume, A., A. Takahashi, et al. (1993). "Neuronal cell loss of the striatonigral system in multiple system atrophy." J Neurol Sci **117**(1-2): 33-40.

Kuoppamaki, M., J. C. Rothwell, et al. (2005). "Parkinsonism following bilateral lesions of the globus pallidus: performance on a variety of motor tasks shows similarities with Parkinson's disease." J Neurol Neurosurg Psychiatry **76**(4): 482-490.

Kwon, D. H., J. M. Kim, et al. (2012). "Seven-Tesla magnetic resonance images of the substantia nigra in Parkinson disease." Ann Neurol **71**(2): 267-277.

Lane, J. I., R. J. Witte, et al. (2005). "Imaging microscopy of the middle and inner ear: Part II: MR microscopy." Clin Anat **18**(6): 409-415.

Lang, A. E. (2005). "Treatment of progressive supranuclear palsy and corticobasal degeneration." Mov Disord **20 Suppl 12**: S83-91.

Lannuzel, A., G. U. Hoglinger, et al. (2007). "Atypical parkinsonism in Guadeloupe: a common risk factor for two closely related phenotypes?" Brain **130**(Pt 3): 816-827.

Lantos, P. L. (1998). "The definition of multiple system atrophy: a review of recent developments." J Neuropathol Exp Neurol **57**(12): 1099-1111.

Larner, A. J. (2002). "Did Charles Dickens describe progressive supranuclear palsy in 1857?" Mov Disord **17**(4): 832-833.

Lee, C., B. Young, et al. (2006). "The role of the supramammillary commissure in MR localization of the subthalamic nucleus." Stereotact Funct Neurosurg **84**(5-6): 193-204.

Lee, S. E., G. D. Rabinovici, et al. (2011). "Clinicopathological correlations in corticobasal degeneration." Ann Neurol **70**(2): 327-340.

Lee, Y. C., C. S. Liu, et al. (2009). "The 'hot cross bun' sign in the patients with spinocerebellar ataxia." Eur J Neurol **16**(4): 513-516.

Lees, A. J., J. Hardy, et al. (2009). "Parkinson's disease." Lancet **373**(9680): 2055-2066.

Leiguarda, R., A. J. Lees, et al. (1994). "The nature of apraxia in corticobasal degeneration." J Neurol Neurosurg Psychiatry **57**(4): 455-459.

Lesage, S., I. Le Ber, et al. (2013). "C9orf72 repeat expansions are a rare genetic cause of parkinsonism." Brain **136**(Pt 2): 385-391.

Levesque, J. C. and A. Parent (2005). "GABAergic interneurons in human subthalamic nucleus." Mov Disord **20**(5): 574-584.

Limousin, P., P. Krack, et al. (1998). "Electrical stimulation of the subthalamic nucleus in advanced Parkinson's disease." N Engl J Med **339**(16): 1105-1111.

Limousin, P., P. Pollak, et al. (1995). "Bilateral subthalamic nucleus stimulation for severe Parkinson's disease." Mov Disord **10**(5): 672-674.

Limousin, P., P. Pollak, et al. (1995). "Effect of parkinsonian signs and symptoms of bilateral subthalamic nucleus stimulation." Lancet **345**(8942): 91-95.

Ling, H., R. de Silva, et al. (2013). "Characteristics of progressive supranuclear palsy presenting with corticobasal syndrome: a cortical variant." Neuropathol Appl Neurobiol.

Ling, H., S. S. O'Sullivan, et al. (2010). "Does corticobasal degeneration exist? A clinicopathological re-evaluation." Brain **133**(Pt 7): 2045-2057.

Litvan, I., C. A. Mangone, et al. (1996). "Natural history of progressive supranuclear palsy (Steele-Richardson-Olszewski syndrome) and clinical predictors of survival: a clinicopathological study." J Neurol Neurosurg Psychiatry **60**(6): 615-620.

Litvan, I., J. J. Hauw, et al. (1996). "Validity and reliability of the preliminary NINDS neuropathologic criteria for progressive supranuclear palsy and related disorders." J Neuropathol Exp Neurol **55**(1): 97-105.

Litvan, I., K. P. Bhatia, et al. (2003). "Movement Disorders Society Scientific Issues Committee report: SIC Task Force appraisal of clinical diagnostic criteria for Parkinsonian disorders." Mov Disord **18**(5): 467-486.

Litvan, I., Y. Agid, et al. (1996). "Clinical research criteria for the diagnosis of progressive supranuclear palsy (Steele-Richardson-Olszewski syndrome): report of the NINDS-SPSP international workshop." Neurology **47**(1): 1-9.

Lowe, J. G. L. and P. N. Leigh (1997). "Disorders of movement and system degeneration." In: Greenfield's Neuropathology. Graham PI, Lantos PL. 6 Edition. London, Arnold.: 297-399.

Ma, S. Y., M. Roytta, et al. (1997). "Correlation between neuromorphometry in the substantia nigra and clinical features in Parkinson's disease using disector counts." J Neurol Sci **151**(1): 83-87.

Magherini, A. and I. Litvan (2005). "Cognitive and behavioral aspects of PSP since Steele, Richardson and Olszewski's description of PSP 40 years ago and Albert's delineation of the subcortical dementia 30 years ago." Neurocase **11**(4): 250-262.

Magherini, A., R. Pentore, et al. (2007). "Progressive supranuclear gaze palsy without parkinsonism: a case of neuro-Whipple." Parkinsonism Relat Disord **13**(7): 449-452.

Mahapatra, R. K., M. J. Edwards, et al. (2004). "Corticobasal degeneration." Lancet Neurol **3**(12): 736-743.

Maher, E. R. and A. J. Lees (1986). "The clinical features and natural history of the Steele-Richardson-Olszewski syndrome (progressive supranuclear palsy)." Neurology **36**(7): 1005-1008.

Mai, J. K., P. H. Stephens, et al. (1986). "Substance P in the human brain." Neuroscience **17**(3): 709-739.

Makino, T., S. Ito, et al. (2011). "Involvement of pontine transverse and longitudinal fibers in multiple system atrophy: a tractography-based study." J Neurol Sci **303**(1-2): 61-66.

Manova, E. S., C. A. Habib, et al. (2009). "Characterizing the mesencephalon using susceptibility-weighted imaging." AJNR Am J Neuroradiol **30**(3): 569-574.

Maraganore, D. M., D. W. Anderson, et al. (1999). "Autopsy patterns for Parkinson's disease and related disorders in Olmsted County, Minnesota." Neurology **53**(6): 1342-1344.

Marsden, C. D. (1989). "Slowness of movement in Parkinson's disease." Mov Disord **4 Suppl 1**: S26-37.

Martin, W. R., M. Wieler, et al. (2008). "Midbrain iron content in early Parkinson disease: a potential biomarker of disease status." Neurology **70**(16 Pt 2): 1411-1417.

Massey, L. A. and T. A. Yousry (2010). "Anatomy of the substantia nigra and subthalamic nucleus on MR imaging." Neuroimaging Clin N Am **20**(1): 7-27.

Massey, L. A., C. Micallef, et al. (2012). "Conventional magnetic resonance imaging in confirmed progressive supranuclear palsy and multiple system atrophy." Mov Disord **27**(14): 1754-1762.

Massey, L. A., M. A. Miranda, et al. (2012). "High resolution MR anatomy of the subthalamic nucleus: imaging at 9.4 T with histological validation." Neuroimage **59**(3): 2035-2044.

Matej, R., G. G. Kovacs, et al. (2012). "Genetic Creutzfeldt-Jakob disease with R208H mutation presenting as progressive supranuclear palsy." Mov Disord **27**(4): 476-479.

McClelland, S., 3rd, J. P. Vonsattel, et al. (2007). "Relationship of clinical efficacy to post mortem-determined anatomic subthalamic stimulation in Parkinson syndrome." Clin Neuropathol **26**(6): 267-275.

McLennan, J. E., K. Nakano, et al. (1972). "Micrographia in Parkinson's disease." J Neurol Sci **15**(2): 141-152.

McRitchie, D. A. and G. M. Halliday (1995). "Calbindin D28k-containing neurons are restricted to the medial substantia nigra in humans." Neuroscience **65**(1): 87-91.

McRitchie, D. A., C. D. Hardman, et al. (1996). "Cytoarchitectural distribution of calcium binding proteins in midbrain dopaminergic regions of rats and humans." J Comp Neurol **364**(1): 121-150.

McRitchie, D. A., G. M. Halliday, et al. (1995). "Quantitative analysis of the variability of substantia nigra pigmented cell clusters in the human." Neuroscience **68**(2): 539-551.

Menke, R. A., J. Scholz, et al. (2009). "MRI characteristics of the substantia nigra in Parkinson's disease: a combined quantitative T1 and DTI study." Neuroimage **47**(2): 435-441.

Menke, R. A., S. Jbabdi, et al. (2010). "Connectivity-based segmentation of the substantia nigra in human and its implications in Parkinson's disease." Neuroimage **52**(4): 1175-1180.

Menuel, C., L. Garnero, et al. (2005). "Characterization and correction of distortions in stereotactic magnetic resonance imaging for bilateral subthalamic stimulation in Parkinson disease." J Neurosurg **103**(2): 256-266.

Messina, D., A. Cerasa, et al. (2011). "Patterns of brain atrophy in Parkinson's disease, progressive supranuclear palsy and multiple system atrophy." Parkinsonism Relat Disord **17**(3): 172-176.

Michaeli, S., G. Oz, et al. (2007). "Assessment of brain iron and neuronal integrity in patients with Parkinson's disease using novel MRI contrasts." Mov Disord **22**(3): 334-340.

Miller W. C., D. M. R. (1987). "Altered tonic activity of neurons in the globus pallidus and subthalamic nucleus in the primate MPTP model of Parkinsonism." Basal Ganglia II: Structure and Function Eds Carpenter and Jeyaranam 1987: 415-427.

Minati, L., M. Grisoli, et al. (2007). "Imaging degeneration of the substantia nigra in Parkinson disease with inversion-recovery MR imaging." AJNR Am J Neuroradiol **28**(2): 309-313.

Minnerop, M., E. Luders, et al. (2010). "Callosal tissue loss in multiple system atrophy--a one-year follow-up study." Mov Disord **25**(15): 2613-2620.

Minnerop, M., K. Specht, et al. (2007). "Voxel-based morphometry and voxel-based relaxometry in multiple system atrophy-a comparison between clinical subtypes and correlations with clinical parameters." Neuroimage **36**(4): 1086-1095.

Mizuno, T., K. Shiga, et al. (2005). "Discrepancy between clinical and pathological diagnoses of CBD and PSP." J Neurol **252**(6): 687-697.

Moore, D. J., A. B. West, et al. (2005). "Molecular pathophysiology of Parkinson's disease." Annu Rev Neurosci **28**: 57-87.

Mori, H., S. Aoki, et al. (2004). "Morning glory sign is not prevalent in progressive supranuclear palsy." Magn Reson Med Sci **3**(4): 215; author reply 216-217.

Morris, H. R., G. Gibb, et al. (2002). "Pathological, clinical and genetic heterogeneity in progressive supranuclear palsy." Brain **125**(Pt 5): 969-975.

Muqit, M. M., D. Mort, et al. (2001). ""Hot cross bun" sign in a patient with parkinsonism secondary to presumed vasculitis." J Neurol Neurosurg Psychiatry **71**(4): 565-566.

Murata, Y., S. Yamaguchi, et al. (1998). "Characteristic magnetic resonance imaging findings in Machado-Joseph disease." Arch Neurol **55**(1): 33-37.

Murialdo, A., R. Marchese, et al. (2000). "Neurosyphilis presenting as progressive supranuclear palsy." Mov Disord **15**(4): 730-731.

Nagao, S., O. Yokota, et al. (2012). "Progressive supranuclear palsy presenting as primary lateral sclerosis but lacking parkinsonism, gaze palsy, aphasia, or dementia." J Neurol Sci **323**(1-2): 147-153.

Nath, U., Y. Ben-Shlomo, et al. (2001). "The prevalence of progressive supranuclear palsy (Steele-Richardson-Olszewski syndrome) in the UK." Brain **124**(Pt 7): 1438-1449.

Nath, U., Y. Ben-Shlomo, et al. (2001). "The prevalence of progressive supranuclear palsy (Steele-Richardson-Olszewski syndrome) in the UK." Brain **124**(Pt 7): 1438-1449.

Nath, U., Y. Ben-Shlomo, et al. (2003). "Clinical features and natural history of progressive supranuclear palsy: a clinical cohort study." Neurology **60**(6): 910-916.

Nieuwenhuys, R., J. Voogd, et al. (1988). "The Human Central Nervous System: a synopsis and atlas 3rd Revised Edition."

Nieuwenhuys, R., J. Voogd, et al. (2008). "The Human Central Nervous System: a synopsis and atlas; Fourth Edition."

Nilsson, C., K. Markenroth Bloch, et al. (2007). "Tracking the neurodegeneration of parkinsonian disorders - a pilot study." Neuroradiology **49**(2): 111-119.

Oba, H., A. Yagishita, et al. (2005). "New and reliable MRI diagnosis for progressive supranuclear palsy." Neurology **64**(12): 2050-2055.

Oikawa, H., M. Sasaki, et al. (2002). "The substantia nigra in Parkinson disease: proton density-weighted spin-echo and fast short inversion time inversion-recovery MR findings." AJNR Am J Neuroradiol **23**(10): 1747-1756.

Oka, M., S. Katayama, et al. (2001). "Abnormal signals on proton density-weighted MRI of the superior cerebellar peduncle in progressive supranuclear palsy." Acta Neurol Scand **104**(1): 1-5.

Oldfield, R. C. (1971). "The assessment and analysis of handedness: the Edinburgh inventory." Neuropsychologia **9**(1): 97-113.

Oliveira, R. M., J. M. Gurd, et al. (1997). "Micrographia in Parkinson's disease: the effect of providing external cues." J Neurol Neurosurg Psychiatry **63**(4): 429-433.

Olzewski, J. a. B., D. (1954). "Cytoarchtecture of the Human Brain Stem."

Ordidge, R. J., J. M. Gorell, et al. (1994). "Assessment of relative brain iron concentrations using T2-weighted and T2*-weighted MRI at 3 Tesla." Magn Reson Med **32**(3): 335-341.

Osaki, Y., G. K. Wenning, et al. (2002). "Do published criteria improve clinical diagnostic accuracy in multiple system atrophy?" Neurology **59**(10): 1486-1491.

Ozawa, T., D. Paviour, et al. (2004). "The spectrum of pathological involvement of the striatonigral and olivopontocerebellar systems in multiple system atrophy: clinicopathological correlations." Brain **127**(Pt 12): 2657-2671.

Padovani, A., B. Borroni, et al. (2006). "Diffusion tensor imaging and voxel based morphometry study in early progressive supranuclear palsy." J Neurol Neurosurg Psychiatry **77**(4): 457-463.

Papapetropoulos, S., J. Gonzalez, et al. (2005). "Natural history of progressive supranuclear palsy: a clinicopathologic study from a population of brain donors." Eur Neurol **54**(1): 1-9.

Papp, M. I. and P. L. Lantos (1994). "The distribution of oligodendroglial inclusions in multiple system atrophy and its relevance to clinical symptomatology." Brain **117 (Pt 2)**: 235-243.

Papp, M. I., J. E. Kahn, et al. (1989). "Glial cytoplasmic inclusions in the CNS of patients with multiple system atrophy (striatonigral degeneration, olivopontocerebellar atrophy and Shy-Drager syndrome)." J Neurol Sci **94**(1-3): 79-100.

Parent, A. (2002). "Jules Bernard Luys and the subthalamic nucleus." Mov Disord **17**(1): 181-185.

Parent, A. and L. N. Hazrati (1995). "Functional anatomy of the basal ganglia. II. The place of subthalamic nucleus and external pallidum in basal ganglia circuitry." Brain Res Brain Res Rev **20**(1): 128-154.

Pastakia, B., R. Polinsky, et al. (1986). "Multiple system atrophy (Shy-Drager syndrome): MR imaging." Radiology **159**(2): 499-502.

Patel, N. K., S. Khan, et al. (2008). "Comparison of atlas- and magnetic-resonance-imaging-based stereotactic targeting of the subthalamic nucleus in the surgical treatment of Parkinson's disease." Stereotact Funct Neurosurg **86**(3): 153-161.

Paviour, D. C., J. S. Thornton, et al. (2007). "Diffusion-weighted magnetic resonance imaging differentiates Parkinsonian variant of multiple-system atrophy from progressive supranuclear palsy." Mov Disord **22**(1): 68-74.

Paviour, D. C., S. L. Price, et al. (2005). "Quantitative MRI measurement of superior cerebellar peduncle in progressive supranuclear palsy." Neurology **64**(4): 675-679.

Peran, P., A. Cherubini, et al. (2010). "Magnetic resonance imaging markers of Parkinson's disease nigrostriatal signature." Brain **133**(11): 3423-3433.

Petrovic, I. N., A. Martin-Bastida, et al. (2012). "MM2 subtype of sporadic Creutzfeldt-Jakob disease may underlie the clinical presentation of progressive supranuclear palsy." J Neurol.

Price, S., D. Paviour, et al. (2004). "Voxel-based morphometry detects patterns of atrophy that help differentiate progressive supranuclear palsy and Parkinson's disease." Neuroimage **23**(2): 663-669.

Pujol, J., C. Junque, et al. (1992). "Reduction of the substantia nigra width and motor decline in aging and Parkinson's disease." Arch Neurol **49**(11): 1119-1122.

Purdon Martin, J. (1927). "Hemichorea resulting from a local lesion of the brain. (The syndrome of the body of Luys)." Brain **50**: 637-651.

Quattrone, A., G. Nicoletti, et al. (2008). "MR imaging index for differentiation of progressive supranuclear palsy from Parkinson disease and the Parkinson variant of multiple system atrophy." Radiology **246**(1): 214-221.

Quester, R. and R. Schroder (1997). "The shrinkage of the human brain stem during formalin fixation and embedding in paraffin." J Neurosci Methods **75**(1): 81-89.

Raff, U., M. Hutchinson, et al. (2006). "Inversion recovery MRI in idiopathic Parkinson disease is a very sensitive tool to assess neurodegeneration in the substantia nigra: preliminary investigation." Acad Radiol **13**(6): 721-727.

Rafols, J. A. and C. A. Fox (1976). "The neurons in the primate subthalamic nucleus: a Golgi and electron microscopic study." J Comp Neurol **168**(1): 75-111.

Rasbrand, W. S. (2009). "Image J." U.S. National Institutes of Health, Bethseda, Maryland, USA **http://rsb.info.gov/ij/**.

Rebeiz, J. J., E. H. Kolodny, et al. (1968). "Corticodentatonigral degeneration with neuronal achromasia." Arch Neurol **18**(1): 20-33.

Reitblat, T., I. Polishchuk, et al. (2003). "Primary antiphospholipid antibody syndrome masquerading as progressive supranuclear palsy." Lupus **12**(1): 67-69.

Richter, E. O., T. Hoque, et al. (2004). "Determining the position and size of the subthalamic nucleus based on magnetic resonance imaging results in patients with advanced Parkinson disease." J Neurosurg **100**(3): 541-546.

Righini, A., A. Antonini, et al. (2004). "MR imaging of the superior profile of the midbrain: differential diagnosis between progressive supranuclear palsy and Parkinson disease." AJNR Am J Neuroradiol **25**(6): 927-932.

Rijkers, K., Y. Temel, et al. (2007). "The microanatomical environment of the subthalamic nucleus. Technical note." J Neurosurg **107**(1): 198-201.

Riley, D. E., A. E. Lang, et al. (1990). "Cortical-basal ganglionic degeneration." Neurology **40**(8): 1203-1212.

Rinne, J. O., M. S. Lee, et al. (1994). "Corticobasal degeneration. A clinical study of 36 cases." Brain **117 (Pt 5)**: 1183-1196.

Rippon, G. A., B. F. Boeve, et al. (2005). "Late-onset frontotemporal dementia associated with progressive supranuclear palsy/argyrophilic grain disease/Alzheimer's disease pathology." Neurocase **11**(3): 204-211.

Rivaud-Pechoux, S., M. Vidailhet, et al. (2000). "Longitudinal ocular motor study in corticobasal degeneration and progressive supranuclear palsy." Neurology **54**(5): 1029-1032.

Rueckert, D., L. I. Sonoda, et al. (1999). "Nonrigid registration using free-form deformations: application to breast MR images." IEEE Trans Med Imaging **18**(8): 712-721.

Rutledge, J. N., S. K. Hilal, et al. (1987). "Study of movement disorders and brain iron by MR." AJR Am J Roentgenol **149**(2): 365-379.

Saini, J., B. S. Bagepally, et al. (2012). "In vivo evaluation of white matter pathology in patients of progressive supranuclear palsy using TBSS." Neuroradiology **54**(7): 771-780.

Sanz, P., S. Nogue, et al. (2007). "Progressive supranuclear palsy-like parkinsonism resulting from occupational exposure to lead sulphate batteries." J Int Med Res **35**(1): 159-163.

Sasaki, M., E. Shibata, et al. (2006). "Neuromelanin magnetic resonance imaging of locus ceruleus and substantia nigra in Parkinson's disease." Neuroreport **17**(11): 1215-1218.

Sato, F., M. Parent, et al. (2000). "Axonal branching pattern of neurons of the subthalamic nucleus in primates." J Comp Neurol **424**(1): 142-152.

Savoiardo, M. (2003). "Differential diagnosis of Parkinson's disease and atypical parkinsonian disorders by magnetic resonance imaging." Neurol Sci **24 Suppl 1**: S35-37.

Savoiardo, M., F. Girotti, et al. (1994). "Magnetic resonance imaging in progressive supranuclear palsy and other parkinsonian disorders." J Neural Transm Suppl **42**: 93-110.

Savoiardo, M., L. Strada, et al. (1989). "MR imaging in progressive supranuclear palsy and Shy-Drager syndrome." J Comput Assist Tomogr **13**(4): 555-560.

Savoiardo, M., L. Strada, et al. (1990). "Olivopontocerebellar atrophy: MR diagnosis and relationship to multisystem atrophy." Radiology **174**(3 Pt 1): 693-696.

Scaravilli, T., E. Tolosa, et al. (2005). "Progressive supranuclear palsy and corticobasal degeneration: lumping versus splitting." Mov Disord **20 Suppl 12**: S21-28.

Schaltenbrand, G. and W. Wahren (1977). "Atlas for Stereotaxy of the Human Brain."

Schapira, A. H. (1999). "Science, medicine, and the future: Parkinson's disease." Bmj **318**(7179): 311-314.

Schenck, J. F. and E. A. Zimmerman (2004). "High-field magnetic resonance imaging of brain iron: birth of a biomarker?" NMR Biomed **17**(7): 433-445.

Schocke, M. F., K. Seppi, et al. (2002). "Diffusion-weighted MRI differentiates the Parkinson variant of multiple system atrophy from PD." Neurology **58**(4): 575-580.

Schott, J. M., J. E. Simon, et al. (2003). "Delineating the sites and progression of in vivo atrophy in multiple system atrophy using fluid-registered MRI." Mov Disord **18**(8): 955-958.

Schrag, A., C. D. Good, et al. (2000). "Differentiation of atypical parkinsonian syndromes with routine MRI." Neurology **54**(3): 697-702.

Schrag, A., D. Kingsley, et al. (1998). "Clinical usefulness of magnetic resonance imaging in multiple system atrophy." J Neurol Neurosurg Psychiatry **65**(1): 65-71.

Schrag, A., Y. Ben-Shlomo, et al. (1999). "Prevalence of progressive supranuclear palsy and multiple system atrophy: a cross-sectional study." Lancet **354**(9192): 1771-1775.

Schrag, A., Y. Ben-Shlomo, et al. (2000). "Cross sectional prevalence survey of idiopathic Parkinson's disease and Parkinsonism in London." Bmj **321**(7252): 21-22.

Schulz, J. B., T. Klockgether, et al. (1994). "Multiple system atrophy: natural history, MRI morphology, and dopamine receptor imaging with 123IBZM-SPECT." J Neurol Neurosurg Psychiatry **57**(9): 1047-1056.

Scolding, N. J. and A. J. Lees (1994). "Micrographia associated with a parietal lobe lesion in multiple sclerosis." J Neurol Neurosurg Psychiatry **57**(6): 739-741.

Seppi, K. and M. F. Schocke (2005). "An update on conventional and advanced magnetic resonance imaging techniques in the differential diagnosis of neurodegenerative parkinsonism." Curr Opin Neurol **18**(4): 370-375.

Seppi, K., C. Scherfler, et al. (2006). "Topography of dopamine transporter availability in progressive supranuclear palsy: a voxelwise [123I]beta-CIT SPECT analysis." Arch Neurol **63**(8): 1154-1160.

Seppi, K., M. F. Schocke, et al. (2006). "Progression of putaminal degeneration in multiple system atrophy: a serial diffusion MR study." Neuroimage **31**(1): 240-245.

Seppi, K., M. F. Schocke, et al. (2006). "Topography of putaminal degeneration in multiple system atrophy: a diffusion magnetic resonance study." Mov Disord **21**(6): 847-852.

Shibata, E., M. Sasaki, et al. (2006). "Age-related changes in locus ceruleus on neuromelanin magnetic resonance imaging at 3 Tesla." Magn Reson Med Sci **5**(4): 197-200.

Shink, E., M. D. Bevan, et al. (1996). "The subthalamic nucleus and the external pallidum: two tightly interconnected structures that control the output of the basal ganglia in the monkey." Neuroscience **73**(2): 335-357.

Silver, R. D., H. R. Djalilian, et al. (2002). "High-resolution magnetic resonance imaging of human cochlea." Laryngoscope **112**(10): 1737-1741.

Sitburana, O. and W. G. Ondo (2009). "Brain magnetic resonance imaging (MRI) in parkinsonian disorders." Parkinsonism Relat Disord **15**(3): 165-174.

Slavin, K. V., K. R. Thulborn, et al. (2006). "Direct visualization of the human subthalamic nucleus with 3T MR imaging." AJNR Am J Neuroradiol **27**(1): 80-84.

Slowinski, J., A. Imamura, et al. (2008). "MR imaging of brainstem atrophy in progressive supranuclear palsy." J Neurol **255**(1): 37-44.

Smith, S. M. and T. E. Nichols (2009). "Threshold-free cluster enhancement: addressing problems of smoothing, threshold dependence and localisation in cluster inference." Neuroimage **44**(1): 83-98.

Smith, S. M., M. Jenkinson, et al. (2004). "Advances in functional and structural MR image analysis and implementation as FSL." Neuroimage **23 Suppl 1**: S208-219.

Smith, S. M., M. Jenkinson, et al. (2006). "Tract-based spatial statistics: voxelwise analysis of multi-subject diffusion data." Neuroimage **31**(4): 1487-1505.

Smith, Y., L. N. Hazrati, et al. (1990). "Efferent projections of the subthalamic nucleus in the squirrel monkey as studied by the PHA-L anterograde tracing method." J Comp Neurol **294**(2): 306-323.

Soares-Fernandes, J. P., M. Ribeiro, et al. (2009). ""Hot cross bun" sign in variant Creutzfeldt-Jakob disease." AJNR Am J Neuroradiol **30**(3): E37.

Soliveri, P., D. Monza, et al. (1999). "Cognitive and magnetic resonance imaging aspects of corticobasal degeneration and progressive supranuclear palsy." Neurology **53**(3): 502-507.

Solsberg, M. D., D. Fournier, et al. (1990). "MR imaging of the excised human brainstem: a correlative neuroanatomic study." AJNR Am J Neuroradiol **11**(5): 1003-1013.

Specht, K., M. Minnerop, et al. (2003). "In vivo voxel-based morphometry in multiple system atrophy of the cerebellar type." Arch Neurol **60**(10): 1431-1435.

Spillantini, M. G. (1999). "Parkinson's disease, dementia with Lewy bodies and multiple system atrophy are alpha-synucleinopathies." Parkinsonism Relat Disord **5**(4): 157-162.

Stamelou, M., A. Alonso-Canovas, et al. (2012). "Dystonia in corticobasal degeneration: a review of the literature on 404 pathologically proven cases." Mov Disord **27**(6): 696-702.

Stamelou, M., S. Knake, et al. (2011). "Magnetic resonance imaging in progressive supranuclear palsy." J Neurol **258**(4): 549-558.

Starr, P. A. (2002). "Placement of deep brain stimulators into the subthalamic nucleus or Globus pallidus internus: technical approach." Stereotact Funct Neurosurg **79**(3-4): 118-145.

Steele, J. C., J. C. Richardson, et al. (1964). "Progressive Supranuclear Palsy. a Heterogeneous Degeneration Involving the Brain Stem, Basal Ganglia and

Cerebellum with Vertical Gaze and Pseudobulbar Palsy, Nuchal Dystonia and Dementia." Arch Neurol **10**: 333-359.

Steiger, M. J. and N. P. Quinn (1992). "Levodopa challenge test in Parkinson's disease." Lancet **339**(8795): 751-752.

Stern, M. B., B. H. Braffman, et al. (1989). "Magnetic resonance imaging in Parkinson's disease and parkinsonian syndromes." Neurology **39**(11): 1524-1526.

Su, M., Y. Yoshida, et al. (2001). "Primary involvement of the motor area in association with the nigrostriatal pathway in multiple system atrophy: neuropathological and morphometric evaluations." Acta Neuropathol **101**(1): 57-64.

Suhyadhom, A., I. U. Haq, et al. (2009). "A high resolution and high contrast MRI for differentiation of subcortical structures

Tada, M., O. Onodera, et al. (2007). "Early development of autonomic dysfunction may predict poor prognosis in patients with multiple system atrophy." Arch Neurol **64**(2): 256-260.

Tan, J. H., B. C. Goh, et al. (2005). "Paraneoplastic progressive supranuclear palsy syndrome in a patient with B-cell lymphoma." Parkinsonism Relat Disord **11**(3): 187-191.

Taoka, T., H. Hirabayashi, et al. (2009). ""Sukeroku sign" and "dent internal-capsule sign"--identification guide for targeting the subthalamic nucleus for placement of deep brain stimulation electrodes." Neuroradiology **51**(1): 11-16.

Temel, Y., A. Kessels, et al. (2006). "Behavioural changes after bilateral subthalamic stimulation in advanced Parkinson disease: a systematic review." Parkinsonism Relat Disord **12**(5): 265-272.

Testa, D., D. Monza, et al. (2001). "Comparison of natural histories of progressive supranuclear palsy and multiple system atrophy." Neurol Sci **22**(3): 247-251.

Thomas, D. L., E. De Vita, et al. (2004). "High-resolution fast spin echo imaging of the human brain at 4.7 T: implementation and sequence characteristics." Magn Reson Med **51**(6): 1254-1264.

Toda, H., N. Sawamoto, et al. (2009). "A novel composite targeting method using high-field magnetic resonance imaging for subthalamic nucleus deep brain stimulation." J Neurosurg.

Tokumaru, A. M., Y. Saito, et al. (2009). "Imaging-pathologic correlation in corticobasal degeneration." AJNR Am J Neuroradiol **30**(10): 1884-1892.

Tomlinson, C. L., R. Stowe, et al. (2010). "Systematic review of levodopa dose equivalency reporting in Parkinson's disease." Mov Disord **25**(15): 2649-2653.

Tremolizzo, L., F. Bertola, et al. (2011). "Progressive supranuclear palsy-like phenotype caused by progranulin p.Thr272fs mutation." Mov Disord **26**(10): 1964-1966.

Trojanowski, J. Q. and T. Revesz (2007). "Proposed neuropathological criteria for the post mortem diagnosis of multiple system atrophy." Neuropathol Appl Neurobiol **33**(6): 615-620.

Tsuboi, Y., J. Slowinski, et al. (2003). "Atrophy of superior cerebellar peduncle in progressive supranuclear palsy." Neurology **60**(11): 1766-1769.

Tsuboi, Y., K. A. Josephs, et al. (2005). "Increased tau burden in the cortices of progressive supranuclear palsy presenting with corticobasal syndrome." Mov Disord **20**(8): 982-988.

Uchino, A., A. Sawada, et al. (2004). "Symmetrical lesions of the middle cerebellar peduncle: MR imaging and differential diagnosis." Magn Reson Med Sci **3**(3): 133-140.

Vaillancourt, D. E., M. B. Spraker, et al. (2009). "High-resolution diffusion tensor imaging in the substantia nigra of de novo Parkinson disease." Neurology **72**(16): 1378-1384.

Vermersch, P., Y. Robitaille, et al. (1994). "Biochemical mapping of neurofibrillary degeneration in a case of progressive supranuclear palsy: evidence for general cortical involvement." Acta Neuropathol **87**(6): 572-577.

Vertinsky, A. T., V. A. Coenen, et al. (2009). "Localization of the Subthalamic Nucleus: Optimization with Susceptibility-Weighted Phase MR Imaging." AJNR Am J Neuroradiol.

Volz, S., E. Hattingen, et al. (2009). "Reduction of susceptibility-induced signal losses in multi-gradient-echo images: application to improved visualization of the subthalamic nucleus." Neuroimage **45**(4): 1135-1143.

Warmuth-Metz, M., M. Naumann, et al. (2001). "Measurement of the midbrain diameter on routine magnetic resonance imaging: a simple and accurate method of differentiating between Parkinson disease and progressive supranuclear palsy." Arch Neurol **58**(7): 1076-1079.

Watanabe, H., Y. Saito, et al. (2002). "Progression and prognosis in multiple system atrophy: an analysis of 230 Japanese patients." Brain **125**(Pt 5): 1070-1083.

Wenning, G. K., C. Colosimo, et al. (2004). "Multiple system atrophy." Lancet Neurol **3**(2): 93-103.

Wenning, G. K., F. Tison, et al. (1997). "Multiple system atrophy: a review of 203 pathologically proven cases." Mov Disord **12**(2): 133-147.

Wenning, G. K., F. Tison, et al. (2004). "Development and validation of the Unified Multiple System Atrophy Rating Scale (UMSARS)." Mov Disord **19**(12): 1391-1402.

Wenning, G. K., I. Litvan, et al. (1998). "Natural history and survival of 14 patients with corticobasal degeneration confirmed at post mortem examination." J Neurol Neurosurg Psychiatry **64**(2): 184-189.

Wenning, G. K., Y. Ben Shlomo, et al. (1994). "Clinical features and natural history of multiple system atrophy. An analysis of 100 cases." Brain **117 (Pt 4)**: 835-845.

Whitwell, J. L., R. Avula, et al. (2011). "Disrupted thalamocortical connectivity in PSP: A resting-state fMRI, DTI, and VBM study." Parkinsonism Relat Disord.

Wichmann, T., H. Bergman, et al. (1994). "The primate subthalamic nucleus. III. Changes in motor behavior and neuronal activity in the internal pallidum induced by subthalamic inactivation in the MPTP model of parkinsonism." J Neurophysiol **72**(2): 521-530.

Williams, D. R. (2006). "Tauopathies: classification and clinical update on neurodegenerative diseases associated with microtubule-associated protein tau." Intern Med J **36**(10): 652-660.

Williams, D. R. and A. J. Lees (2009). "Progressive supranuclear palsy: clinicopathological concepts and diagnostic challenges." Lancet Neurol **8**(3): 270-279.

Williams, D. R. and A. J. Lees (2010). "What features improve the accuracy of the clinical diagnosis of progressive supranuclear palsy-parkinsonism (PSP-P)?" Mov Disord **25**(3): 357-362.

Williams, D. R., A. Hadeed, et al. (2005). "Kufor Rakeb disease: autosomal recessive, levodopa-responsive parkinsonism with pyramidal degeneration, supranuclear gaze palsy, and dementia." Mov Disord **20**(10): 1264-1271.

Williams, D. R., J. L. Holton, et al. (2007). "Pathological tau burden and distribution distinguishes progressive supranuclear palsy-parkinsonism from Richardson's syndrome." Brain **130**(Pt 6): 1566-1576.

Williams, D. R., J. L. Holton, et al. (2007). "Pure akinesia with gait freezing: a third clinical phenotype of progressive supranuclear palsy." Mov Disord **22**(15): 2235-2241.

Williams, D. R., R. de Silva, et al. (2005). "Characteristics of two distinct clinical phenotypes in pathologically proven progressive supranuclear palsy: Richardson's syndrome and PSP-parkinsonism." Brain **128**(Pt 6): 1247-1258.

Winikates, J. and J. Jankovic (1994). "Vascular progressive supranuclear palsy." J Neural Transm Suppl **42**: 189-201.

Winter, Y., Y. Bezdolnyy, et al. (2010). "Incidence of Parkinson's disease and atypical parkinsonism: Russian population-based study." Mov Disord **25**(3): 349-356.

Yagishita, A. and M. Oda (1996). "Progressive supranuclear palsy: MRI and pathological findings." Neuroradiology **38 Suppl 1**: S60-66.

Yagishita, A. and M. Oda (1996). "Progressive supranuclear palsy: MRI and pathological findings." Neuroradiology **38 Suppl 1**: S60-66.

Yekhlef, F., G. Ballan, et al. (2003). "Routine MRI for the differential diagnosis of Parkinson's disease, MSA, PSP, and CBD." J Neural Transm **110**(2): 151-169.

Yelnik, J. (2002). "Functional anatomy of the basal ganglia." Mov Disord **17 Suppl 3**: S15-21.

Yelnik, J. and G. Percheron (1979). "Subthalamic neurons in primates: a quantitative and comparative analysis." Neuroscience **4**(11): 1717-1743.

Yelnik, J., E. Bardinet, et al. (2007). "A three-dimensional, histological and deformable atlas of the human basal ganglia. I. Atlas construction based on immunohistochemical and MRI data." Neuroimage **34**(2): 618-638.

Yoshikawa, K., Y. Nakata, et al. (2004). "Early pathological changes in the parkinsonian brain demonstrated by diffusion tensor MRI." J Neurol Neurosurg Psychiatry **75**(3): 481-484.

Yushkevich, P. A., J. Piven, et al. (2006). "User-guided 3D active contour segmentation of anatomical structures: significantly improved efficiency and reliability." Neuroimage **31**(3): 1116-1128.

Zecca, L., M. B. Youdim, et al. (2004). "Iron, brain ageing and neurodegenerative disorders." Nat Rev Neurosci **5**(11): 863-873.

Zhukareva, V., S. Joyce, et al. (2006). "Unexpected abundance of pathological tau in progressive supranuclear palsy white matter." Ann Neurol **60**(3): 335-345.

Zonenshayn, M., A. R. Rezai, et al. (2000). "Comparison of anatomic and neurophysiological methods for subthalamic nucleus targeting." Neurosurgery **47**(2): 282-292; discussion 292-284.

Zrinzo, L., L. V. Zrinzo, et al. (2011). "Targeting of the pedunculopontine nucleus by an MRI-guided approach: a cadaver study." J Neural Transm **118**(10): 1487-1495.